ADVANCED CONTROLLERS FOR BUILDING ENERGY MANAGEMENT SYSTEMS

Advanced controllers based on traditional mathematical methods (MIMO P + I, state-space, adaptive solutions with constraints) and intelligent solutions (fuzzy logic and genetic algorithms) are investigated for humidifying, ventilating and air-conditioning applications

by

Abu Bakar MHD. GHAZALI, MSc

A Thesis Submitted for the

Degree of Doctor of Philosophy

Department of Electronic and Electrical Engineering

University of Bradford

1996

ADVANCED CONTROLLERS FOR BUILDING ENERGY MANAGEMENT SYSTEMS

Abu Bakar MHD GHAZALI

Keywords: Building energy management systems; humidification, ventilation and air-conditioning; multi-input/multi-output (MIMO) systems; multivariable P + I controllers; state-space methods; modal control; constrained adaptive control; fuzzy logic controllers; genetic algorithms.

ABSTRACT

This thesis presents the design and implementation of control strategies for building energy management systems (BEMS). The controllers considered include the multi PI-loop controllers, state-space designs, constrained input and output MIMO adaptive controllers, fuzzy logic solutions and genetic algorithm techniques. The control performances of the designs developed using the various methods based on aspects such as regulation errors squared, energy consumptions and the settling periods are investigated for different designs. The aim of the control strategy is to regulate the room temperature and the humidity to required comfort levels.

In this study the building system under study is a 3 input/ 2 output system subject to external disturbances/effects. The three inputs are heating, cooling and humidification, and the 2 outputs are room air temperature and relative humidity. The external disturbances consist of climatic effects and other stochastic influences. The study is carried out within a simulation environment using the mathematical model of the test room at Loughborough University and the designed control solutions are verified through experimental trials using the full-scale BMS facility at the University of Bradford.

ACKNOWLEDGEMENTS

I wish to express my sincere thanks and gratitude to my supervisor Prof. G. S. Virk for his continued support, advice, and guidance throughout the duration of this work. My thanks are also extended to Prof. J. G. Gardiner, Head of the department, for his administrative support and Dr. D. Azzi for his help in setting the BEMS test room at the Bradford University.

I would also like to express my gratitude to the Malaysian Goverment and the Malaysian Institute of Nuclear Technology Research (MINT) in particular for the financial support throughout this period of study.

Last but not least, my gratitude goes to my parents, my wife and my childrens for their never ending support, patience and prayer.

TABLE OF CONTENTS

Chapter 1

Introduction

A modern building comprises many control loops which when combined, create an environment in which employees can work in safety and comfort, and provides a stable environment for storing valuable assets such as documents, plants and works of art. In addition other benefits to be derived from a well controlled building is the ability to save on the ever increasing operating costs by looking for ways in which to minimise energy consumption as well as addressing environmental concerns by minimising the release of carbon dioxide to the atmosphere since the built sector is a major consumer of energy. These facts are in agreement with the resolution from the 1992 Earth Summit in Rio on Climate Change where it was agreed that we should return emissions of CO_2 to their 1990 levels by the year 2000.

Other benefits to result from a well-operated building are that the improved conditions leads to greater occupant productivities, preventative maintenance can be employed thereby reducing maintenance cost because of the experience gain through the additional monitoring of components in the building environmental system, and enables the analyses of the data from all the control systems to aid decision making for future operation of the building. Moreover, there are a number of concepts in building

management systems (BMSs) which lead to the 'intelligent building' (Hamblin, 1995); the essential idea here is that the building (through its BMS) will be "intelligent" enough to respond and adapt automatically to the requirement of its users. This includes not only the working environment conditions but the systems concerning lighting, voice and data communications and security. When these buildings actually arrive they will provide the end user with greater functionality. One interesting example of this intelligence could be the use of solar blinds whose control based on whether it is more cost effective to use electrical energy to provide the additional cooling due to the increased heat generated by the increase in the internal lighting levels and 'intelligent' lighting systems have been suggested which are controlled by internal and external ambient light levels (Hamblin, 1995).

Intelligent control systems for buildings have a big market, especially in the developed countries. For example, the UK market for total value-added intelligent building controls (IBCs) in 1993 was £283 million (McHale, 1995) and is likely to be maintained for several years. So this fact justifies the investment in further research that is essential to improve IBC systems.

The main objectives in this field at the moment are to maintain comfortable internal working environments for the occupants in the building and to reduce overall building energy consumptions. These objectives have been satisfied in general by improving the insulation, since this is one of the most cost-effective measures. Other improvements which have been made are to the plant efficiency, to the design of the building and services systems, and an increased overall awareness of the need to conserve energy on the part of the occupants. Computer-assisted control in the form of building energy management systems is already widespread, but further research is needed to develop the

application of this modern technology to its full potential. These systems are not only able to control the heating, ventilating and air conditioning (HVAC) plant, but are also able to integrate lighting, fire detection, security, and energy tariffing features.

1.1. Building energy management systems

Intelligent building controls are also known as building energy management systems (BEMS) or building management systems (BMS) in general mean the use of digital computer technology for monitoring the status of buildings and their services systems, and then implementing appropriate control action based on the measured data (Loveday and Virk, 1992a). Such systems have been in existence since the early 1970s, and have evolved into distributed intelligence systems as shown in Figure 1.1 where we can see a number of outstations linked together to form a network which is connected to a central supervisory computer (usually a personal computer) via a data highway. Each outstation has its own processor to monitor and control the local zones (local loops), and the sensor's signals are sent to a local processor which then operate the inputs and actuators to control the operation. Sensors in these systems include thermisters to measure the temperature, flowmeters for measuring flows of air and/or water, and rh sensors for measuring relative humidity. The inputs and actuators consist of heaters, coolers and humidifiers as well as dampers which regulate the flow of air in and out of the occupied rooms. The remote outstations can be connected via modem links, if necessary, to form larger networks for controlling large buildings and complexes.

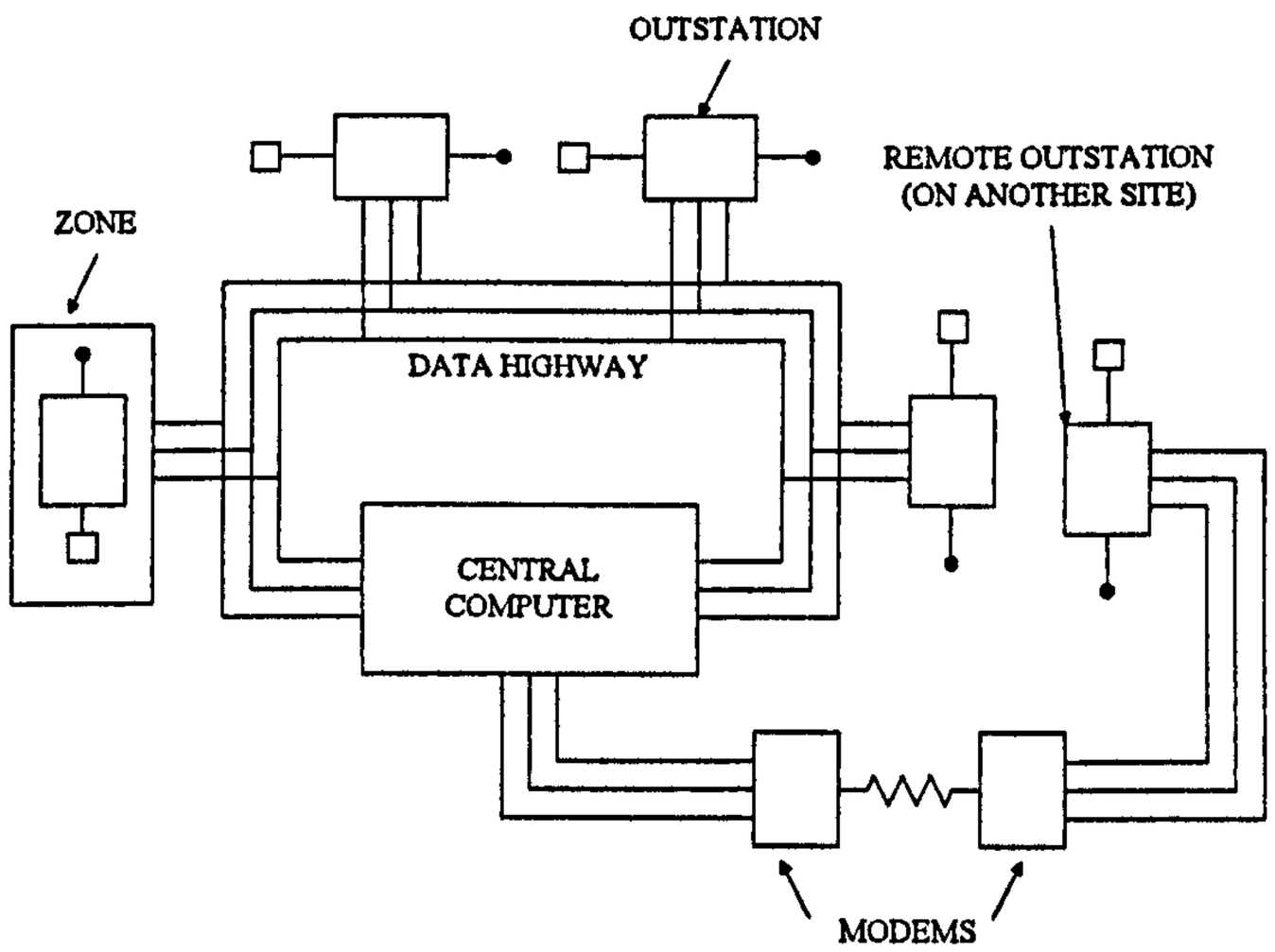

Figure 1.1: Distributed intelligence BEMS

1.2. Current control techniques

Although the analogue systems have been largely replaced by digital computer hardware, the actual control techniques currently employed in BEMS have changed little from the classical methods used for many years. Simple 'on/off', proportional, integral and derivative (PID) (Letherman, 1981) and optimum start/stop controls still form the most commonly used methods in commercial systems. The major change in the design is that the control strategies are now digitally implemented on the digital hardware in place. These three main classical control strategies are described next.

1.2.1. On/off control

In on/off control systems, sensors measure the instantaneous values of the relevant variable, such as temperature and these are compared with the desired setpoints so that the controlling unit can be switched on or off via an actuator so as to maintain the

required conditions. In practice, the on/off strategy is implemented by having two setpoints, one an upper and the other a lower. To explain the on/off operation we consider a temperature regulation system, and assume that the temperature is initially lower than both of these points. The strategy then is to keep the heater on until the measured temperature reaches the higher limit T_{upper}, at which point the heater is switched off; This causes the temperature to decay (normally), and when the measured temperature reaches the lower threshold T_{lower}, the heater is switched on again. This hytheresis (T_{upper} - T_{lower}) in the switching on and switching off points is useful in order to avoid continual on/off switching of the heater or whatever the controlling device is.

1.2.2. PID control

The PID controller is also known as the three-term controller, since its output is made up of three terms that are functions of its input; the first term is proportional to the input, the second is proportional to the integral of the input and the third is proportional to the derivative of the input. The function of each of these three terms can be explained by considering a simple unity feedback closed-loop system for controlling the temperature in a building zone, as illustrated in Figure 1.2.

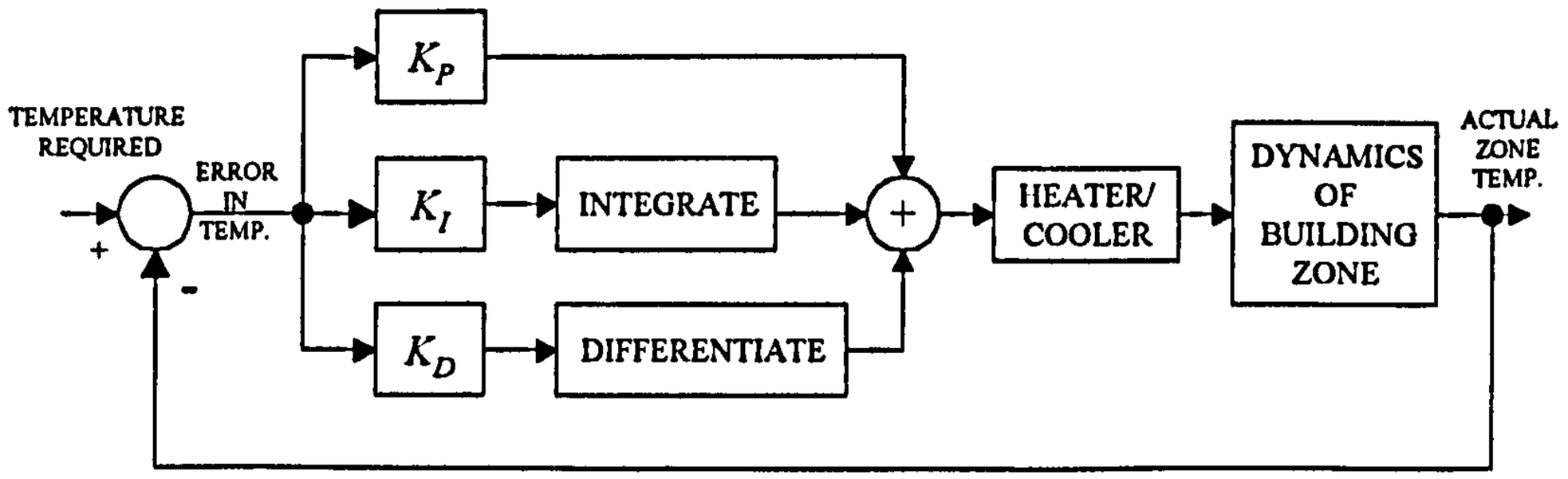

Figure 1.2: PID controller in a temperature control feedback loop

(i) Proportional term: This term acts as a baseline controller, since it takes the error and generates a signal proportional to it. The error here means the difference between the required temperature and the actual zone temperature at that time. For positive errors the actual temperature is lower than the required and hence heat is applied to the zone, whereas for negative signals, cooling is applied.

(ii) Integral term: This takes the error and sums (integrates) it over time, generating a signal proportional to the integrand. The effect of this term in the controlling signal is to drive steady-state errors to zero. In this way, we notice that although the error could be reducing, the integral term will still grow since the error is positive. The integration term reduces only when the error itself goes negative, and so can remain constant only when the error is zero. This corresponds to driving the error to zero.

(iii) Derivative term: This term produces a signal proportional to the rate of change of the error. It implies that if the error is increasing then a larger corrective action is needed and vice versa if the error is reducing. Here, the corrective action can be either heating or cooling to the system.

When these three terms are combined to form a PID controller, it produces an output $m(t)$ given by

$$m(t) = K_P e(t) + K_I \int_{t_0}^{t} e(t)\mathrm{d}t + K_D \frac{\mathrm{d}e(t)}{\mathrm{d}t} \tag{1.1}$$

where $e(t)$ is the instantaneous error at time t, t_0 is some initial time and K_P, K_I and K_D are the proportional, integration and derivative gains respectively.

In the commissioning phase of a BEMS, the PID controller in each zone is tuned by performing certain tests on the zone. Such tests are to determine the settings of K_P, K_I and K_D normally via a well known method due to Ziegler and Nichols (1942).

1.2.3. Optimal start/stop

Optimum start/stop strategies are a comparatively recent development (Jackson, 1971). The objective here is to start the controller (normally heating) of a building at such a time that the building just reaches its operational temperature when occupancy commences, normally at 9 am (i.e. optimal start). In a similar way, the heating can be stopped at such a time that the period at operational temperature ceases just when the occupants leave at say 5 pm (i.e. optimal stop). Such a controller is set up from the knowledge of the cooling/heating reaction curve, as shown in Figure 1.3.

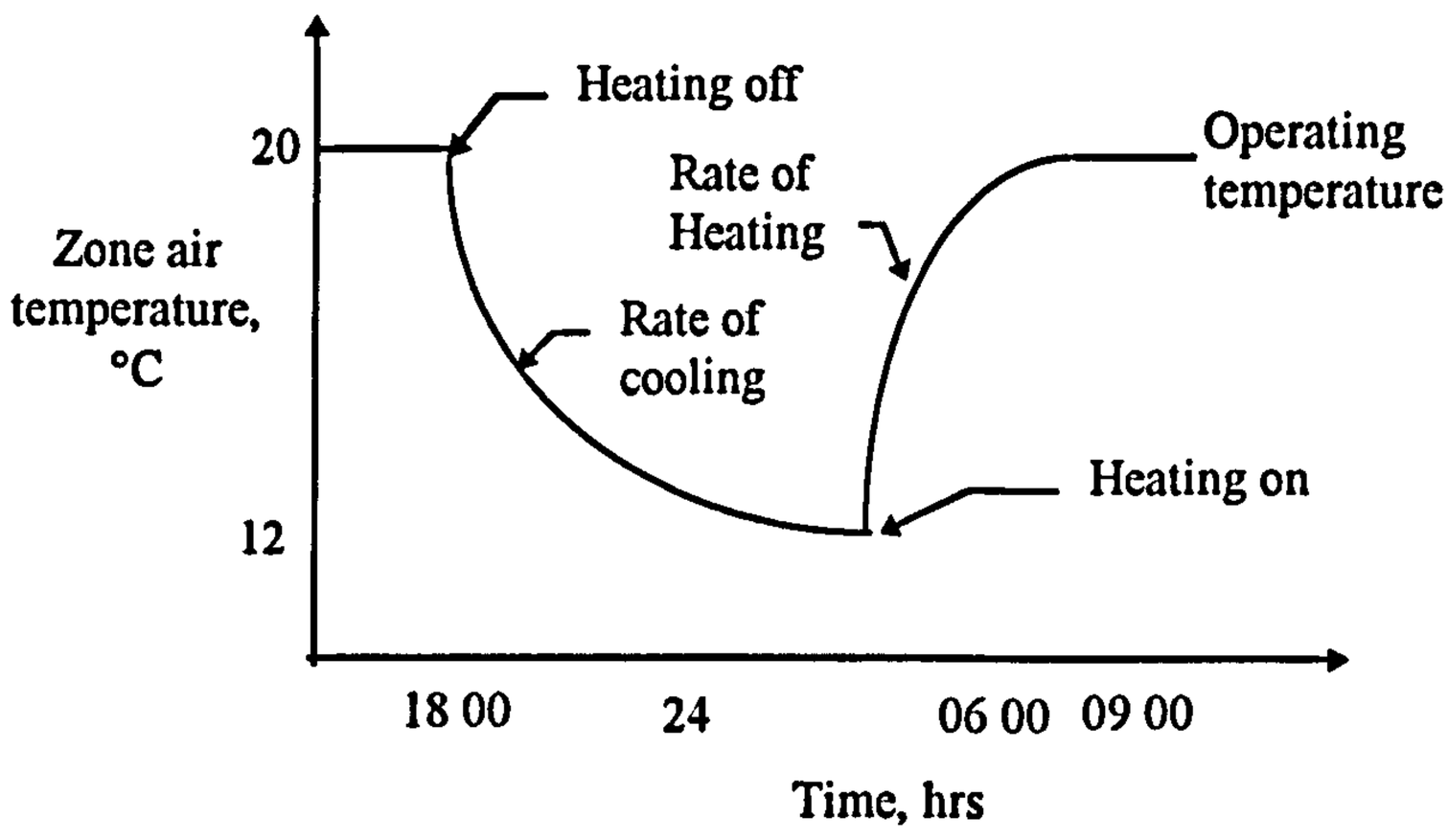

Figure 1.3: A typical cooling/heating curve for a zone

The controller can be programmed to ensure that the zone temperature reaches, for example, 20°C at 09.00 hours. Since heating/cooling reaction curves are influenced by

external temperature, some controllers have an external temperature sensor and its relation to the plant output rate can be programmed by the user.

1.3. The current status of BEMS

The development of BEMS or BMS has been closely allied to advances in the microelectronics technology (Rouse, 1990) and the stage has now been reached where direct digital control (DDC) techniques have displaced analogue technology as the most common methods for plant control in buildings. Advances in BMSs, likes other areas, have also faced difficulties and these can be identified into three major issues (Rouse, 1990):

a) Cabling difficulties: the increased quantities of cables and data place a larger burden on the existing methods used for ducting and networking. Optical fibre technology is likely to offer a solution.

b) Compatibility: at present, it is not possible to interface BEMS hardware from different manufacturers. A widespread adoption of the draft communication standard should solve this problem; however there is not much interest for BMS manufacturers to pursue this route.

c) Commissioning: this is an expensive and time-consuming process. Although dedicated controllers for individual plant items are designed and configured, this still leaves the final tuning of the control loops to be carried out on-site.

Current research might offer solutions to some of these problems, in particular that of commissioning. For example, Haves and Dexter (1991) have been investigating the use of simulation models to emulate the behaviour of the building/HVAC system; such models serve as a means for laboratory testing the performance of a BMS. Similar

emulators have been developed at the National Institute of Standards and Technology (NIST), USA and at Honeywell Controls, Wisconsin, USA. More recently, methods for developing self-tuning PID controllers for HVAC systems have been receiving attention (Dexter et al., 1990). The impact of artificial intelligence (AI), not only on commissioning, but also on system diagnostics and data management, is also being highlighted (Culp et al., 1990; Loveday and Virk, 1992a). However, the potential for improvement to the control algorithms has until now received limited attention. As already mentioned the control methods in BMS have mainly consisted of classical on/off or PID (Ziegler and Nichols, 1942) techniques. Optimum start/stop control (Jackson, 1971; Fielden and Ede, 1982; Murdoch et al., 1990) has been recently applied in digital form. Some fundamental prototyping of advanced controller strategies have also been investigated; Dexter and Trewhella (1990) have looked at the use of rule-based controllers employing fuzzy logic and its relevance to computer-based facilities management; Ling and Dexter (1994) have used a fuzzy rule-based supervisor to evaluate control performance and to adjust the temperature setpoint within a given comfort band. The full potential for advanced control in buildings via a BMS still remains to be investigated.

1.4. The potential for model-based control

The development of modelling and control techniques have traditionally been closely coupled; the main reason for this coupling is the need for a better understanding of the systems and processes before effective control can be designed and implemented. A mathematical model which describes a system's dynamical behaviour can be derived using stochastic identification techniques (see for example Ljung, 1987; Norton, 1986);

these are well known to many control system practitioners but have not been throughly applied to the building services sector. This is a great shame because model-based controls are deemed to be especially appropriate here; among the reasons for this are the following (Virk et al., 1992):

(i) Buildings possess slow dynamical effects and long dead times can also be present which give rise to large overshoots and undershoots in traditional PID controlled systems.

(ii) Buildings are multivariable in nature, since many inputs (causes such as climatic conditions, heat supplied and incidental gains) affect the many outputs (effects such as temperatures, humidities, and air flow rates in many zones).

(iii) Buildings can be subject to significant stochastic disturbance effects; these include fluctuations in occupancy levels, ventilation rate variations and climatic changes.

The model-based method has the capacity to improve the setpoint regulation as well as reduce the energy consumption because of the ability of the model to make accurate forecasts. Research on a laboratory-scale test system has shown that by employing a generalised minimum variance (GMV) controller design with an off-line model the air temperature can be regulated more effectively together with energy savings of 16% as compared to classical PID control (Virk et al., 1990). The potential of advanced control for the full-scale situations has also been investigated by other researchers (see for example Zaheer-Uddin, 1990; Athienitis, 1988; Penkan, 1990; Coley and Penkan, 1992). The main approach has been to derive the models of the air dynamics in the building using physical reasoning, and implement a model-based control strategy to improve the overall system performance. It is well known that a simple process model can be used for

in an on-line manner to tune a few parameters which are then used for control in an adaptive manner (Penman, 1990).

In a recent SERC report, Loveday and Virk (1992b) have demonstrated that multivariable stochastic identification techniques can be used to model a zone's thermal and moisture behaviour in a full-scale building. The model determined in this way can be used to accurately predict the air temperature and relative humidity in the zone over short term (10-20 minutes) and long term (several days) time horizons. Short term prediction errors have been shown to be well within ±0.25°C in 19°C and ±0.6%rh in 53 %rh whereas long term prediction errors have been found to be within ±0.8°C and 1.3% rh. Such accurate predictions clearly show that the modelling approach is suitable for this application area and that research effort should be utilised to assess the full potential of advanced modelling and subsequent model-based solutions for the building services sector.

1.5. Work in this thesis

The works presented in this thesis is the continuation of the efforts made by Loveday and Virk (1992b); as mentioned earlier, they have derived a multivariable model which accurately describes the dynamical behaviour within a typical office zone due to the effects of a heating, cooling and humidifying plant as well as climatic disturbances and other influences. The detailed explanation on the design and validation of this model is presented in chapter 2. By utilising this model, we will develop several advanced control strategies; some of these will be based on classical methods such as multi-input multi-output proportional and integration output (MIMO P+I) controllers, others will utilise modern mathematical modelling methods and are based on state-space and constrained

input adaptive controlled methods. In addition we will develop novel solutions based upon recent intelligent methods using fuzzy logic and genetic algorithmic techniques for humidifying, ventilating and air-conditioning applications. These methods and their solutions designed are tested within a simulation environment to regulate the air temperature and relative humidity form the main component in this thesis. These simulations of the solutions designed are carried out using MATLAB.

In addition to the simulation results the designed MIMO P+I and constrained input adaptive controllers and the fuzzy logic and GA based solutions are implemented upon the Bradford BMS research facility to yield encouraging results in term of output regulations and energy consumptions when compared with the commercial PI controller.

Chapter 2

The Simulation Environment

In this chapter the design and modelling of the office zone which is used in our studies is described. The office zone system and it's associated equipment were built, installed and commissioned at Loughborough University, United Kingdom, and the modelling work was funded by the Science and Engineering Research Council (SERC) under Research Contract GR/F/02014.

2.1. Office zone test system

In the study made by Loveday and Virk (1992b), the office zone and HVAC plant is modelled as a 3 input/2 output system subject to external disturbances/effects, as depicted in Figure 2.1. The three inputs are the heater, cooler and humidifier, and the two outputs are the test room air temperature and relative humidity. The external disturbances consist of climatic effects such as external air temperature and humidity, and solar gain and other stochastic influences include the number of occupants in the room and the frequency of the opening and closing of the door.

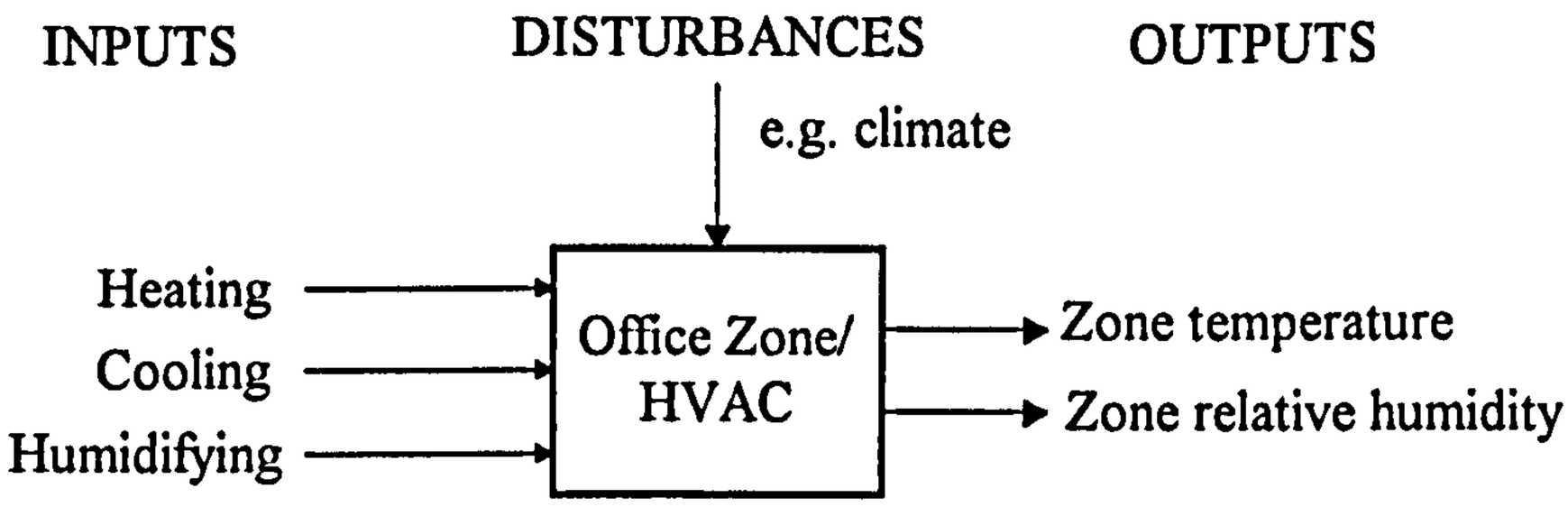

Figure 2.1: Block diagram of the Office-zone system

The office zone comprises a full-scale room and dedicated HVAC plant as shown in Figure 2.2. The room, of dimensions 5.4 metres long by 3.25 metres wide by 3 metres high, simulates an office comprising three internal walls and a fourth, outside, wall. The latter is south-west facing and contains a small doubled-glazed window. The chamber was equipped with a dedicated heating, ventilating and air-conditioning (HVAC) plant, comprising cooling coils, electrical heating elements and a humidifier. The heat output, of 5kW rating, is regulated by a phase control module driven by an analogue input of 0-5 volts. The cooling unit is of conventional direct expansion type with compressor rating of 2.6kW and the control of the cooling coils is via TTL on/off logic. The humidifier unit is of 2.7kW rating and again controlled by TTL on/off logic.

The methodology used to identify the multivariable model which describes the test room's air temperature and moisture behaviour follows the procedure advocated by many practitioners in this field (see for example Ljung, 1987; Norton, 1986; Virk et al, 1995). The procedure consists of the following sequential operations to be carried out on the system in question.

(i) single input step response tests;

(ii) single input pseudo random binary sequence (PRBS) response tests;

(iii) multi-input PRBS response tests;

(iv) modelling and model validation; and

(v) model robustness assessment.

The detailed aspects of this modelling procedure for this system can be found in Loveday and Virk (1992b).

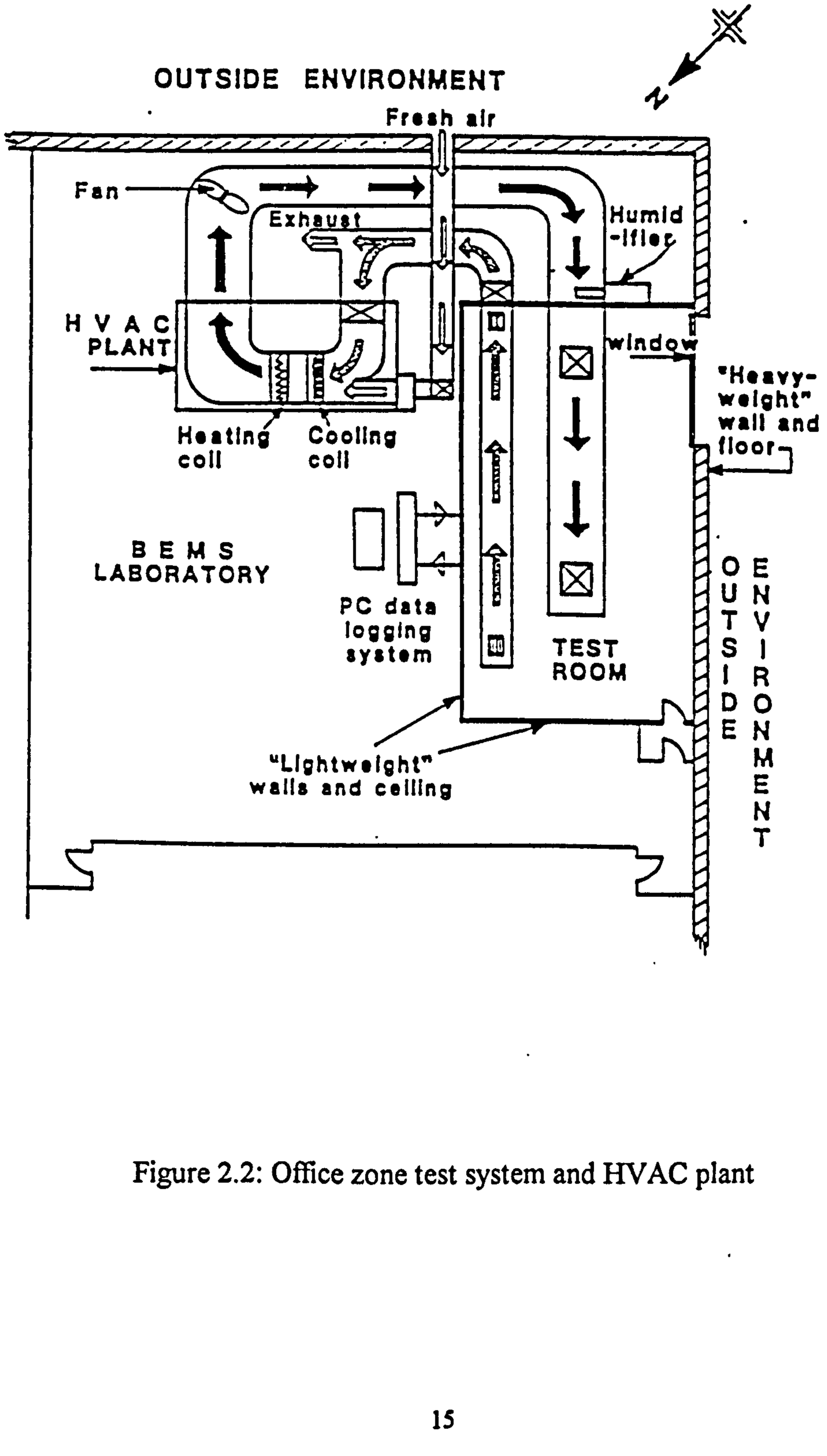

Figure 2.2: Office zone test system and HVAC plant

2.2. Discrete transfer function model

It is essential that the model should be derived for the zone in unfurnished and furnished conditions since commissioning of a BEMS normally takes place in unoccupied premises which is devoid of furnishings and fittings (Pike and Pennycook, 1992) so that the full effects of occupancy can be observed. Multivariable off-line predictive models have been determined and validated for both these conditions. For the unfurnished condition the room was totally empty, and the furnishings consisted of a three piece suite, a desk, a soft chair, two metallic cupboards and carpeting to the room. Using standard multivariable identification techniques, the following model was deduced for the zone in an unfurnished condition:

$$
\begin{aligned}
T_c(t) = {} & (1.61\, z^{-1} - 0.64\, z^{-2} + 0.02\, z^{-3})\, T_c(t) + (0.004\, z^{-1} - 0.006\, z^{-2}) H_c(t) \\
& + (0.22\, z^{-1} + 0.07 z^{-2} - 0.26\, z^{-3})\, W(t) + (-0.62\, z^{-1} + 0.36\, z^{-2} + 0.19 z^{-3})\, C(t) \\
& + 0.04\, z^{-1}\, H(t) + 0.001\, z^{-1}\, T_o(t) + 0.015\, z^{-1}\, S(t) \\
& + (1 - 1.36\, z^{-1} + 0.48\, z^{-2})\, V_1(t) + k_1 \qquad (2.1)
\end{aligned}
$$

$$
\begin{aligned}
H_c(t) = {} & (-0.04\, z^{-1} + 0.003\, z^{-2})\, T_c(t) + (1.54\, z^{-1} - 0.58\, z^{-2} + 0.02\, z^{-3}) H_c(t) \\
& + (-0.71\, z^{-1} + 0.37\, z^{-2} + 0.29\, z^{-3})\, W(t) + (-4.02\, z^{-1} + 3.73\, z^{-2})\, C(t) \\
& + (3.29\, z^{-1} - 2.42\, z^{-2} - 0.49\, z^{-3})\, H(t) + 0.01\, z^{-1}\, T_i(t) + 0.01 z^{-1}\, T_o(t) \\
& + 0.002\, z^{-1} H_o(t) - 0.09 z^{-1}\, S(t) + (1 - 1.24\, z^{-1} + 0.32\, z^{-2})\, V_2(t) + k_2 \qquad (2.2)
\end{aligned}
$$

for t = T, 2T, 3T,.., kT, ... where T_c is the office-zone air temperature in °C and H_c is the relative humidity in %rh, T_l is the temperature (in °C) of the laboratory which surrounds the office-zone, W is the heat input rate in kW, C is the cooling input rate in kW, H is the power input rate to produce moisture for the office-zone in kW, T_o is the outside air temperature in °C, H_o is the outside air relative humidity in %rh, S is the total solar irradiance in Wm^{-2} and V_1 and V_2 are white noise processes to represent unmodelled stochastic influences and k_1 and k_2 are constants. Here, the term z is the normal discrete operator, i.e. $z^{-1}f(t) = f(t\text{-T})$, where T is the sampling interval equal to 5 minutes.

For the furnished zone, the following model was deduced:

$$\begin{aligned} T_c(t) = {} & (1.66\,z^{-1} - 0.69\,z^{-2} + 0.031\,z^{-3})\,T_c(t) + (0.004\,z^{-1} - 0.003\,z^{-2})\,H_c(t) \\ & + (0.19\,z^{-1} + 0.09z^{-2} - 0.26\,z^{-3})\,W(t) + (-0.59\,z^{-1} + 0.29\,z^{-2} + 0.25z^{-3})\,C(t) \\ & + 0.004\,z^{-1}\,H(t) + 0.001\,z^{-1}\,T_o(t) + 0.021\,z^{-1}\,S(t) \\ & + (1 - 1.22\,z^{-1} + 0.30\,z^{-2})\,V_1(t) + k_1 \end{aligned} \tag{2.3}$$

$$\begin{aligned} H_c(t) = {} & (-0.011\,z^{-1} + 0.015\,z^{-2})\,T_c(t) + (-1.52\,z^{-1} + 0.56\,z^{-2} - 0.03\,z^{-3})\,H_c(t) \\ & + (-0.61\,z^{-1} + 0.16\,z^{-2} + 0.34\,z^{-3})\,W(t) + (-2.89\,z^{-1} + 2.98\,z^{-2})\,C(t) \\ & + (2.69\,z^{-1} - 2.37\,z^{-2} - 0.23\,z^{-3})\,H(t) + 0.004\,z^{-1}\,T_l(t) + 0.006z^{-1}\,T_o(t) \\ & + 0.002\,z^{-1}\,H_o(t) + (1 - 0.91\,z^{-1} + 0.03\,z^{-2})\,V_2(t) + k_2 \end{aligned} \tag{2.4}$$

Note that equations (2.1), (2.2), (2.3) and (2.4) are models for normalised values, that is, each term has had its mean value removed. The mean value of T_c, H_c, W, C, H, T_l, T_o,

H_o and S for these equations are 17.95°C, 53.26%rh, 2.52kW, 0.91kW, 1.08kW, 20.13°C, 1.53°C, 89.19%rh and 0.05 Wm^{-2} respectively.

2.3. Validation of the models

Both models have been validated and for completeness, we present two simple tests to compare the predictions from the model with data obtained through experiment. The first test is to simulate step responses and the second is to assess setpoint regulation using the on/off control strategy.

2.3.1. Step responses

Although the model relates to data obtained from the full-scale environmental chamber operating at some state and under certain climatic influences, it can be used, to an initial approximation, to simulate the room air temperature and relative humidity for any arbitrary condition. Since the simulated conditions will inevitably differ from those under which the data was collected it is necessary to let the model reach some nominal steady state condition before the simulation is carried out. This was done by making simplifying assumptions on the influencing terms, namely that the climatic effects T_i, T_o, H_o and S were constant at 20°C, 10°C and 70%rh, 0Wm^{-2} respectively and the other external influences V_1 and V_2, and the control inputs were assumed to be zero. The simulated results are shown in Figure 2.3 where it can be seen that the time needed to reach steady state conditions is approximately 30 hours and these values are 9.9°C and 69.5%rh for the temperature and the relative humidity respectively.

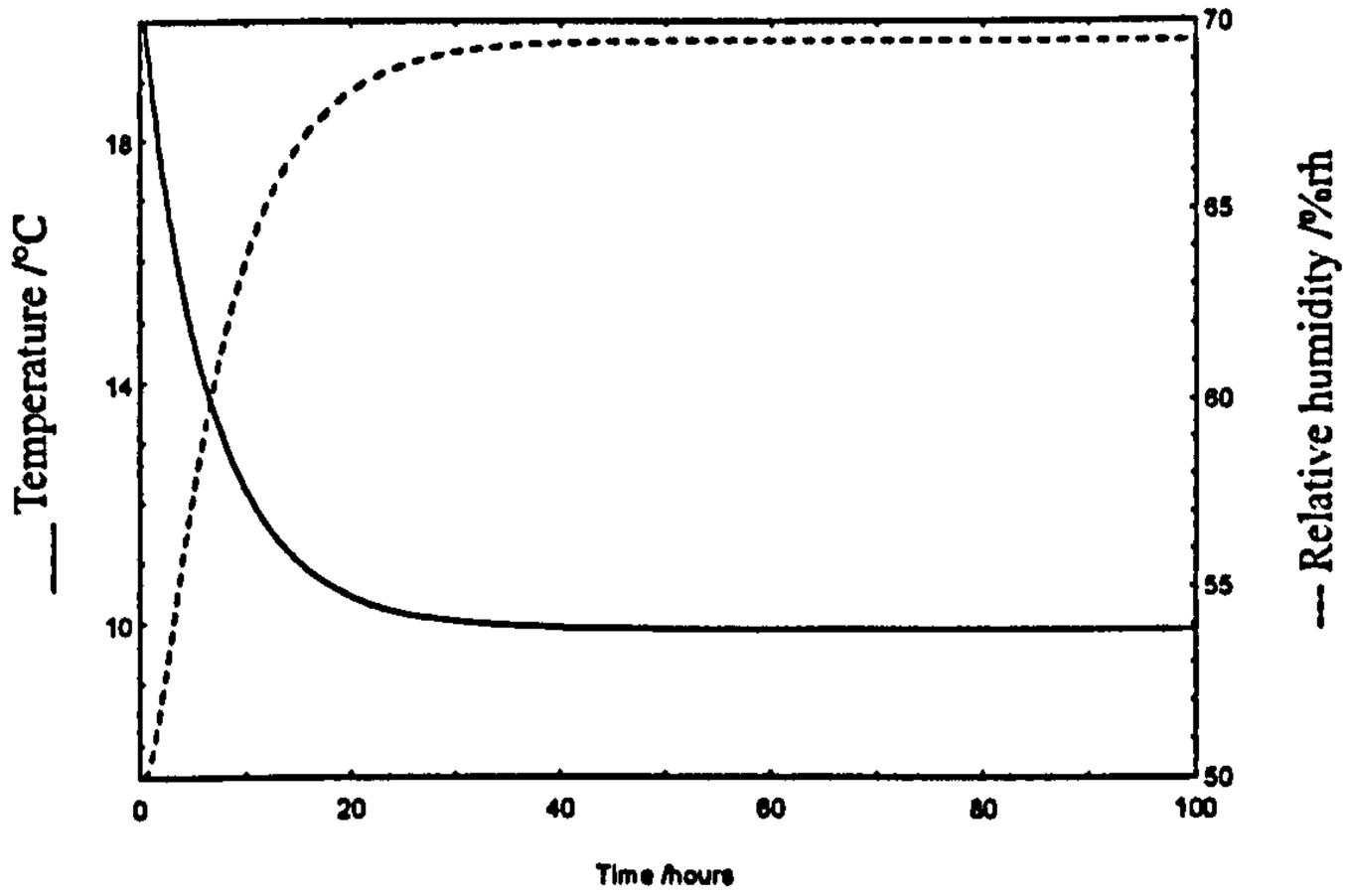

Figure 2.3: Convergence to steady-state conditions

After this time, $T_c(t)$ and $H_c(t)$ have nearly reached the values of outside temperature T_o and outdoor relative humidity H_o respectively. This is due to the physical thermodynamic and moisture behaviour of the air in the office. The values do not exactly equal the outdoor conditions because of the other influencing terms given in the equations (2.1) and (2.2).

After the steady-state conditions have been reached, step inputs to the heater W, cooler C and humidifier H were applied in turn to the system, and $T_c(t)$ and $H_c(t)$ responses calculated; these are plotted against time and are shown in Figures 2.4 - 2.6; the individual responses are for the heater, cooler and humidifier when they are all increased from 0 to 2.0, 1.0 and 1.0 respectively at $t = 54$ hours.

These simulation responses were compared with the actual step responses of the office system (Loveday and Virk,1992b) and the two were found to be in good agreement with each other. This shows that the effects of the inputs are dominant in comparison to other terms in the equations as well as showing that the model equations

(2.1) and (2.2) can be used to characterise the dynamic behaviour of the overall test system.

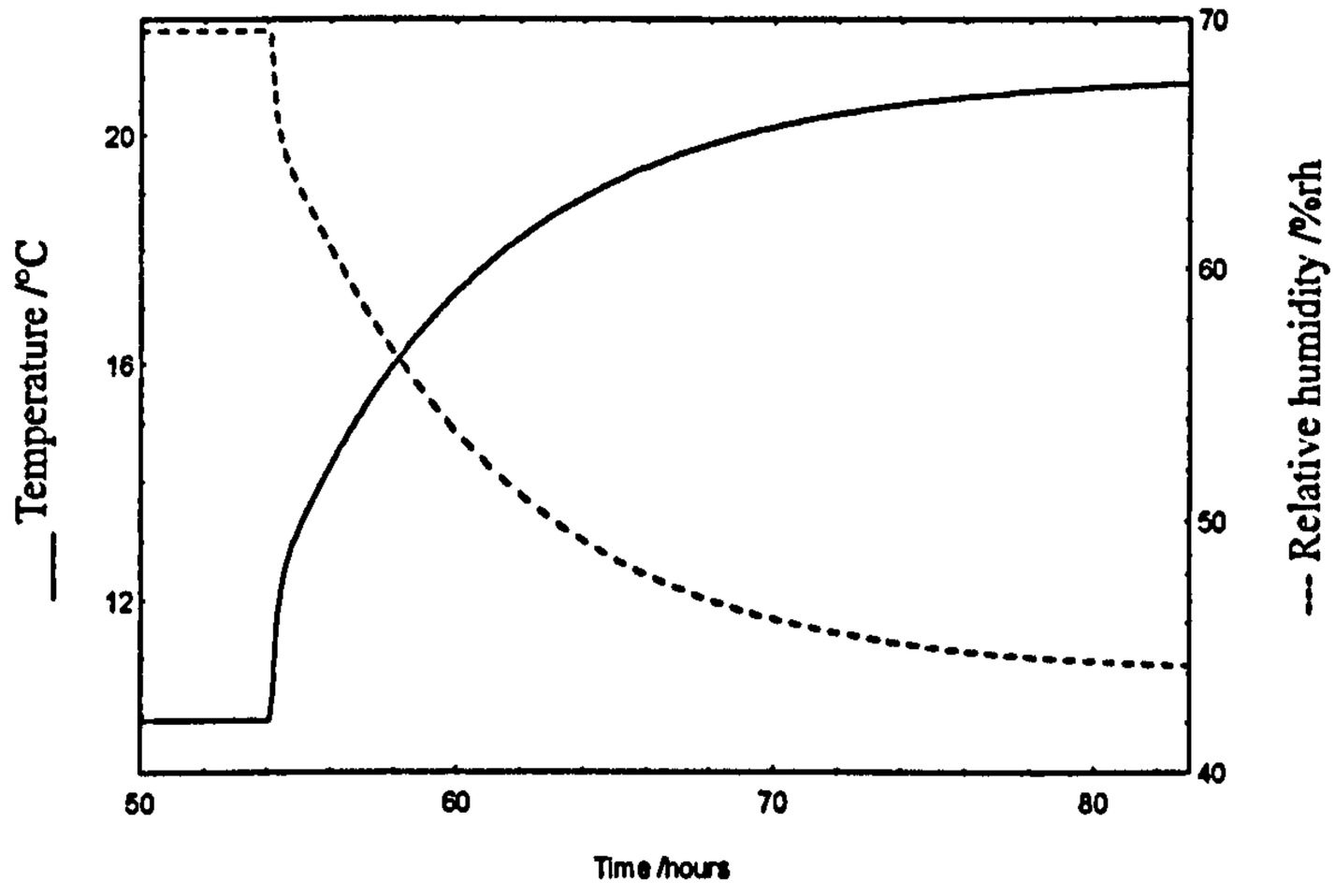

Figure 2.4: Simulation of heating step response

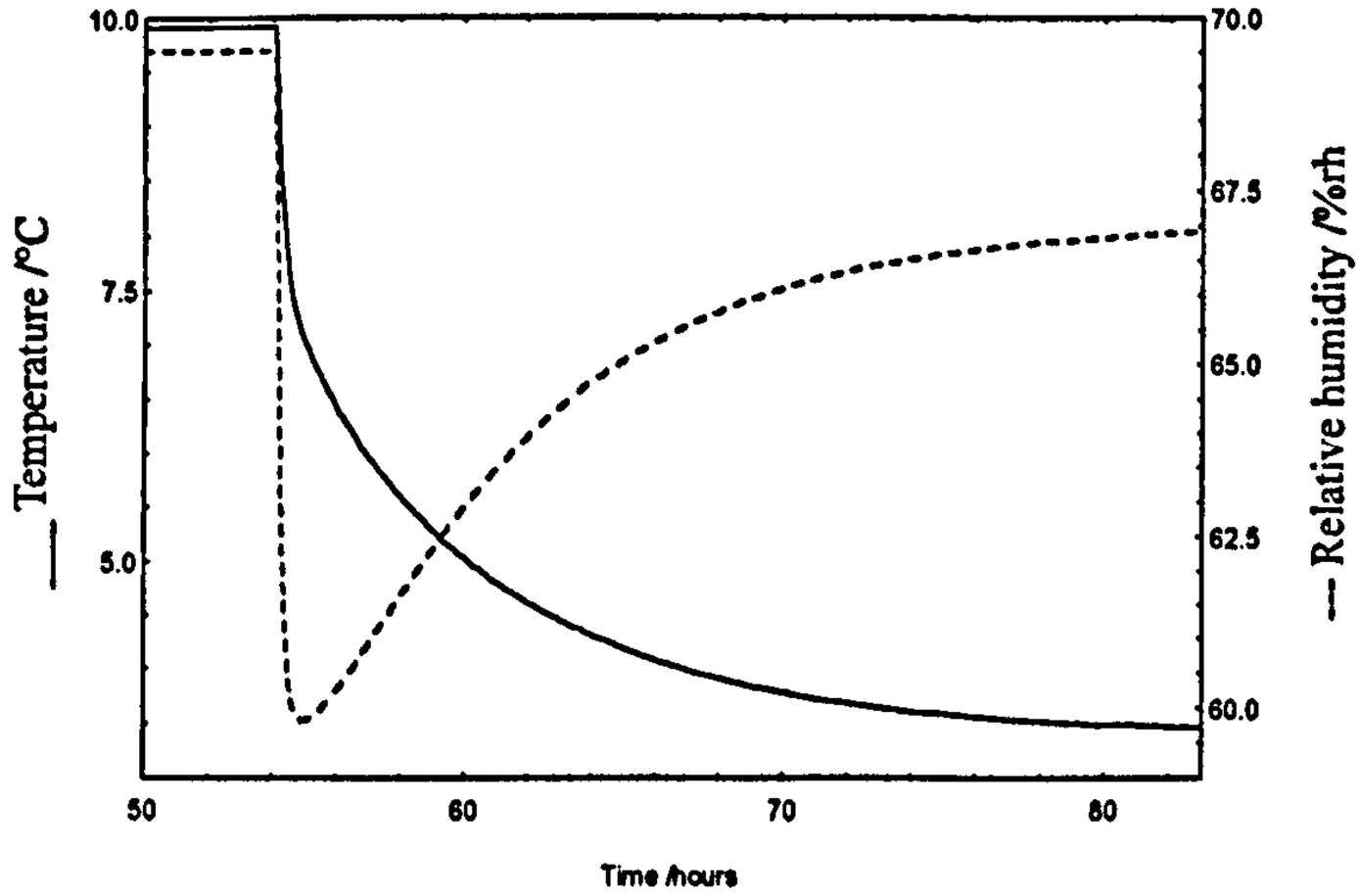

Figure 2.5: Simulation of cooling step response

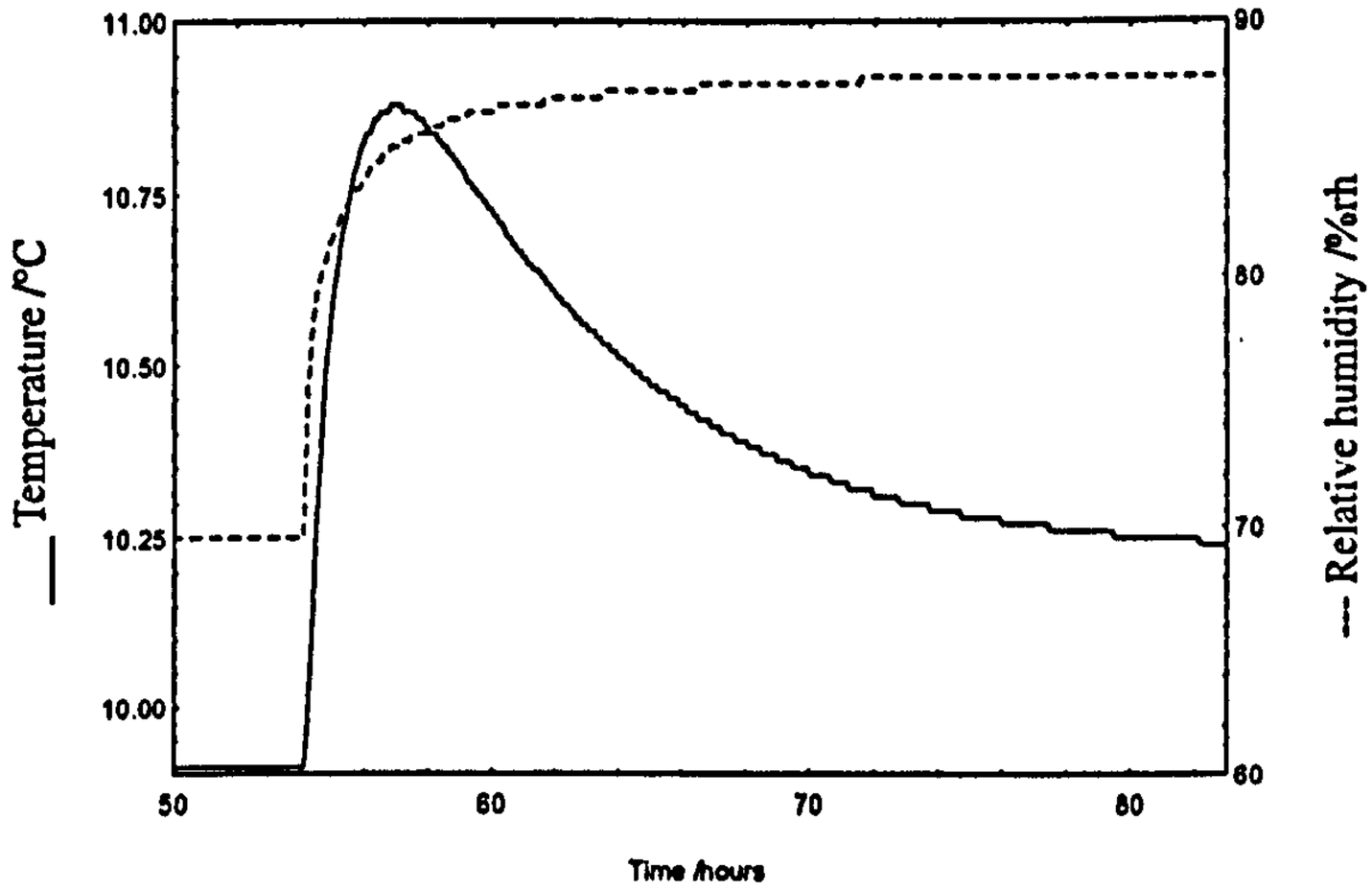

Figure 2.6: Simulation of humidifying step response

2.3.2. On/off control strategy

Two sets of actual data obtained from the Loughborough test facility when two simple control strategies were implemented for temperature regulation when the room was in an unfurnished condition. The two controllers implemented were:

1. conventional on/off control; and
2. predictive (model based) on/off control.

This data was obtained by assuming that the system was single input/single output (SISO) in nature, and it was the intention to regulate the room temperature by controlling the heater using an on/off control strategy. The other influences in equations (2.1) and (2.2) were also measured and recorded in the two data sets for further use in our investigations.

The actual temperature responses obtained from the on/off and model based on/off strategies are shown in Figures 2.7 and 2.8 respectively, where we can see that the predictive on/off method gives slightly better temperature regulation. A closer look at these comparisons are shown in Figures 2.9 and 2.10 where we concentrate on only the first 40 data points to study the temperature response as well as the heating power input. From these graphs, we can see that if we are at time *t*, then the next temperature reading at time *t*+T depends on the current condition of the heater, that is whether the heater is 'on' or 'off'; clearly this will mean that the temperature will either increase or decrease respectively after the heater has been on or off for a period of the sampling interval. This situation is in agreement with the heat input step response as shown in Figure 2.4. Note that in the actual data, the experiment was carried out in such a way that when the control law switches the heater to 'on' or 'off', it will then stay in that condition for a whole duration of the sampling interval T, i.e. 5 minutes. This procedure is identical to the implementation of the modelling equations (2.1), (2.2), (2.3) and (2.4).

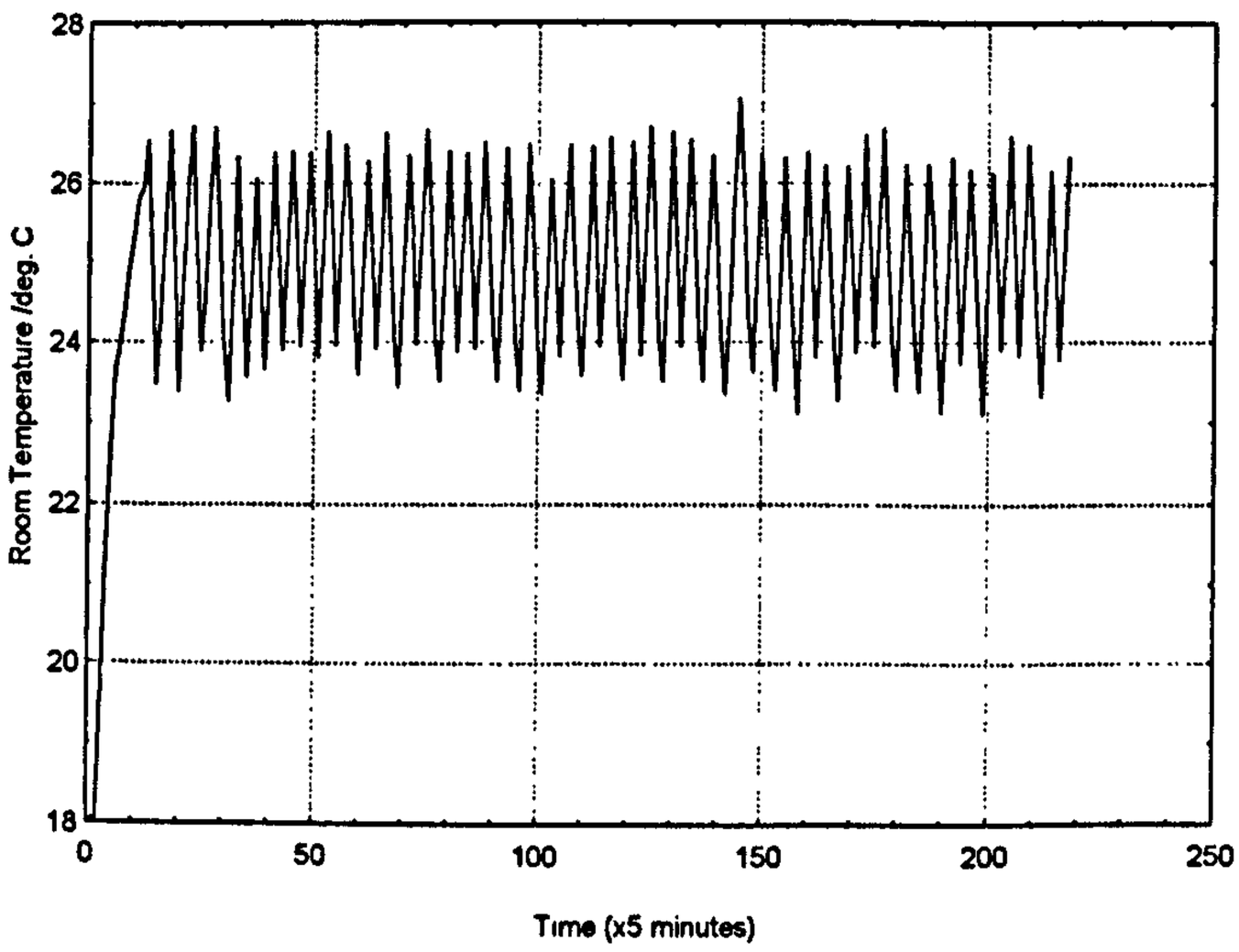

Figure 2.7: Measured temperature regulation using conventional on/off control

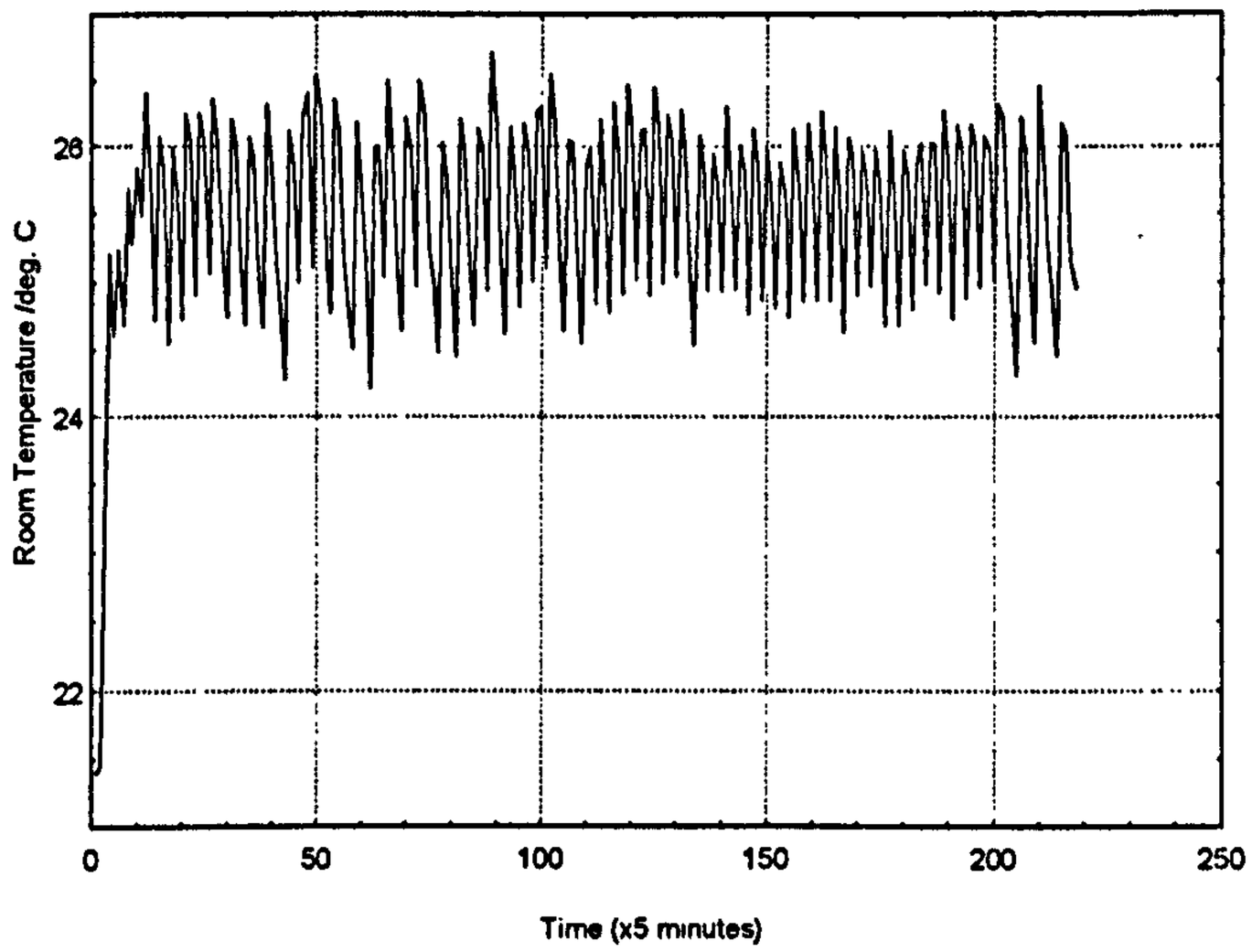

Figure 2.8: Measured temperature regulation using predictive on/off control

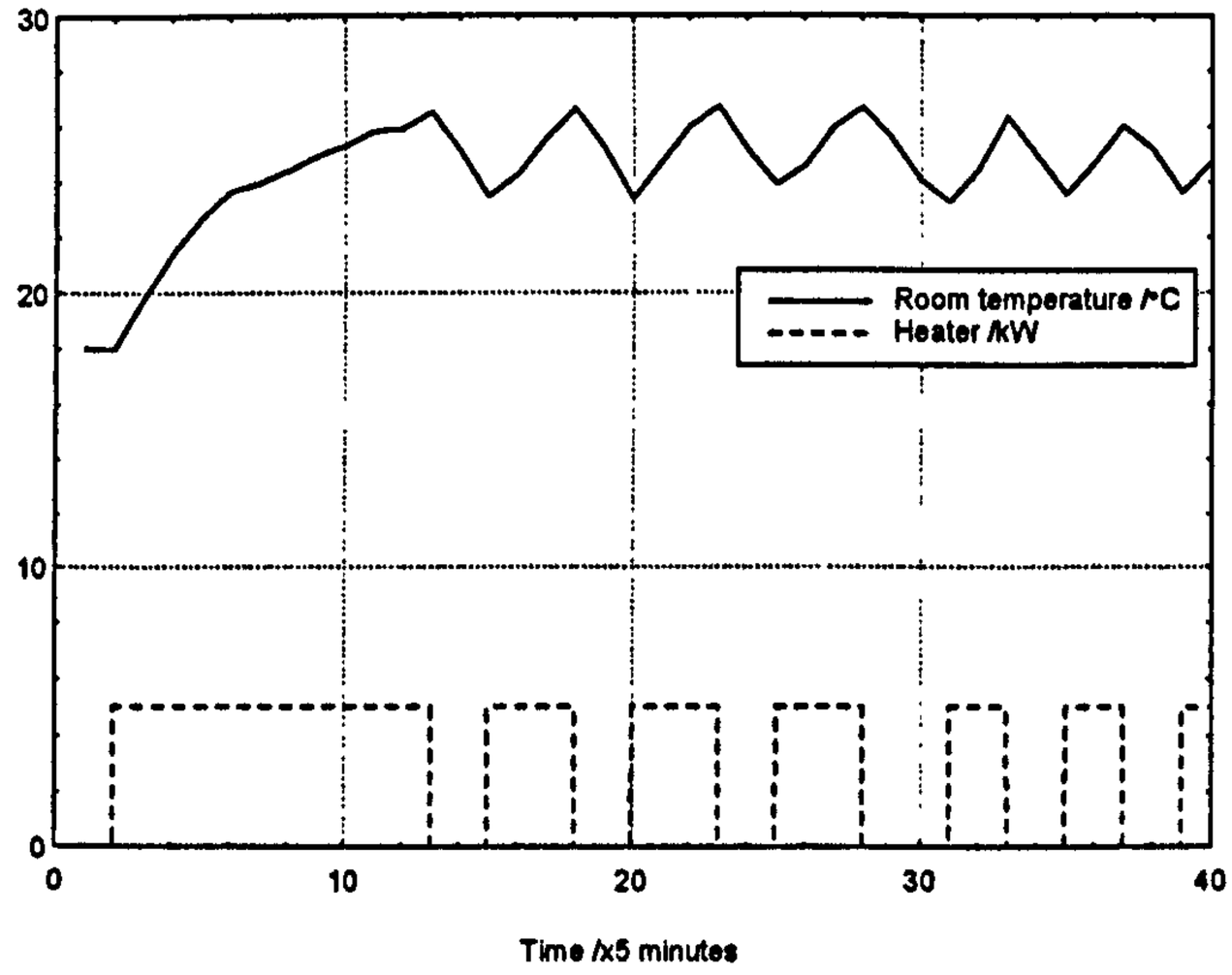

Figure 2.9: Measured output temperature - heater input relationship for on/off controller

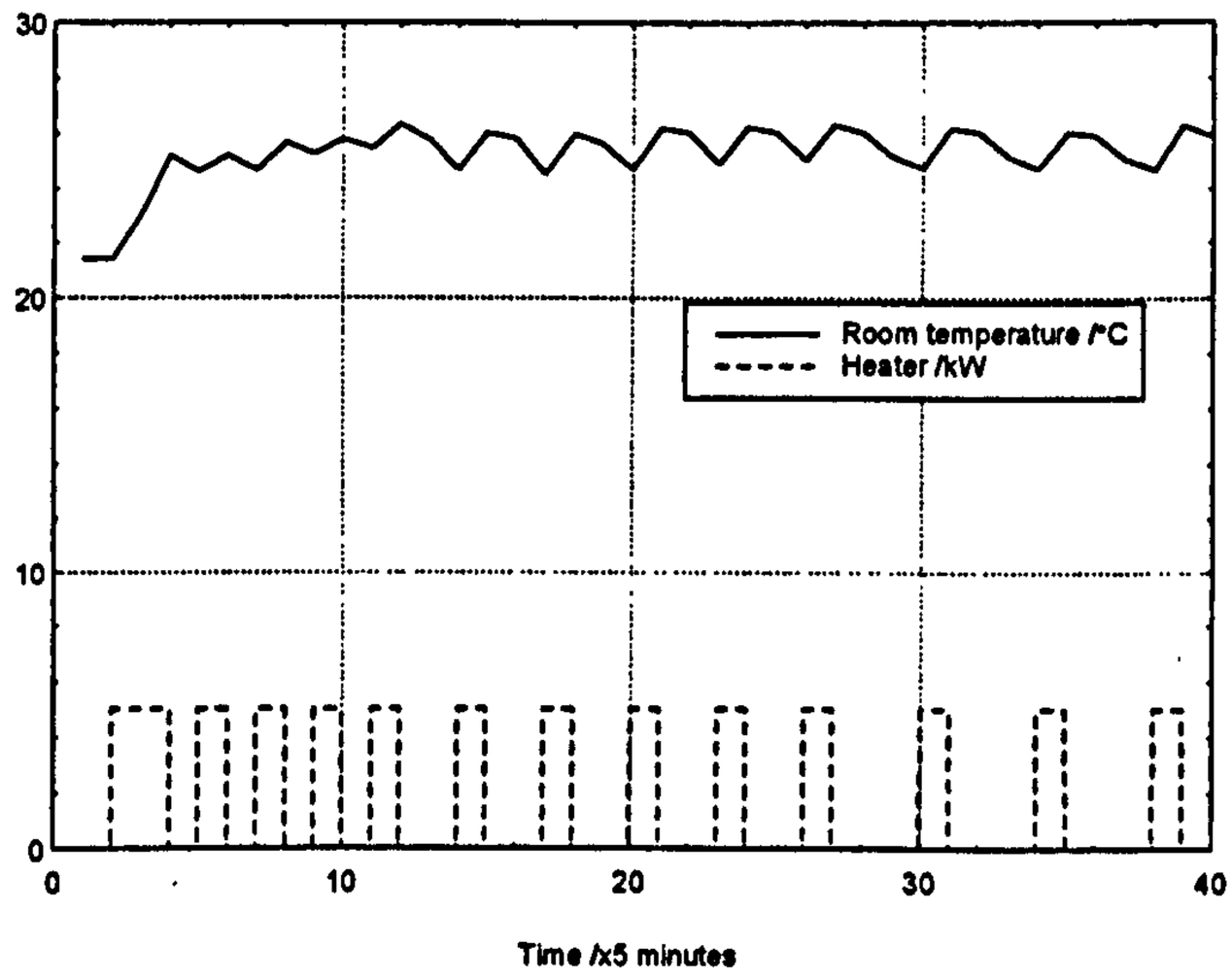

Figure 2.10: Measured output temperature - heater input relationship for predictive on/off controller

2.3.2.1. Simulation studies

In this section we implement the on/off and model-based on/off control strategies within a simulation environment to regulate the room temperature and compare the results with those obtained from the Loughborough chamber trials. We will assume here that equations (2.1) and (2.2) can be used to predict the thermal and moisture content of air in the office zone under unfurnished conditions. Algorithms 1 and 2 present the two control strategies.

Algorithm 1: Conventional on/off controller

Step 0: Set T_r, h, u_{on}, u_{off}, $t = 0$

Step 1: Measure $T_c(t)$ *and form error using*

$$e(t) = T_r - T_c(t)$$

Step 2: If $e(t) > h$, *set* $u(t) = u_{on}$

If $e(t) < -h$, *set* $u(t) = u_{off}$

If $abs(e(t)) \leq h$, *set* $u(t) = u(t-T)$

Step 3: Apply control u(t)

Step 4: Wait time T

Set $t = t + T$

Step 5: Goto Step 1

Algorithm 2: Model based on/off controller

Step 0: Set T_r, u_{on}, u_{off}, $t = 0$

Step 1: Measure $T_c(t)$

Step 2: Compute $\hat{T}_c(t + T)$ *for* u_{on} *and* u_{off} *using equation (2.1)*

Step 3: Calculate errors:

$e_{on} = abs(T_r - \hat{T}_c(t + T)(on))$

$e_{off} = abs(T_r - \hat{T}_c(t + T)(off))$

Step 4: If $e_{on} - e_{off} \geq 0$, *then* $u(t) = u_{off}$

If $e_{on} - e_{off} < 0$, *then* $u(t) = u_{on}$

Step 5: Apply control u(t)

Step 6: Wait time T

Set $t = t + T$

Step 7: Goto Step 1

In the experimental trials, the reference temperature T_r was set at 25°C, the on/off control hysteresis h was 1°C, when the heater is switched 'on' it outputs 5 kW (= u_{on})

and when it is 'off' it gives out 0 kW (= u_{off}) and the sampling interval T was 5 minutes. These conditions are utilised for the simulations as well where the control law decides whether the heater is 'on' or 'off', and the test room temperature is calculated via equations (2.1) and (2.2).

Obviously the measured temperatures in Step 1 of the algorithm need to be modified, for the simulation runs in that these temperatures are obtained via the model, rather than by measurement. The climatic terms in these equations are taken as these measured during the actual conventional on/off trials. For convenience, we assume that the white noise processes V_1 and V_2 have the form of pseudo random binary sequences (PRBS) (Godfrey, 1980) generated using 6 shift registers; the two levels of these PRBSs were assumed to equal 0.25 or -0.25 thus giving $V_1 = \pm 0.25°C$ and $V_2 = \pm 0.25\%rh$. These represent 25 percent of noise level into the system as discussed by Loveday and Virk (1992b).

For the initial conditions, we use the first 3 data points from the measured data, and the simulation trial commences at iteration $t = 4T$ to cater for the delayed terms in the model's equations. A simulation program was developed and a typical simulated trial is shown in Figure 2.11 where we can see that the overall system performance is slightly different from those obtained via the experimental trials (Figure 2.7). This is due to the fact that the accuracy of the model diminishes as the difference between the setpoint and the average room temperature grows significantly large. Moreover, the air dynamics in the room are nonlinear in nature (Loveday and Virk, 1992) but these nonlinearities are being approximated by the linear model equations (2.1) - (2.4). Consequenctly the model is a linearised approximation at a particular situation and model prediction will degraded when it is used away from this operating point. In Loveday and Virk (1992b), the

average temperature was measured to be 19.2°C and the mean error between predicted and measured temperatures for 25% noise level was ±0.86°C. Furthermore, the stochastic noise levels in the actual measurements was unknown and the 25% noise level used in the simulation environment is arbitrary. However, the result does show that the model can approximate the real life situation quite well and therefore can be used for determining the on/off control strategy for a real HVAC system.

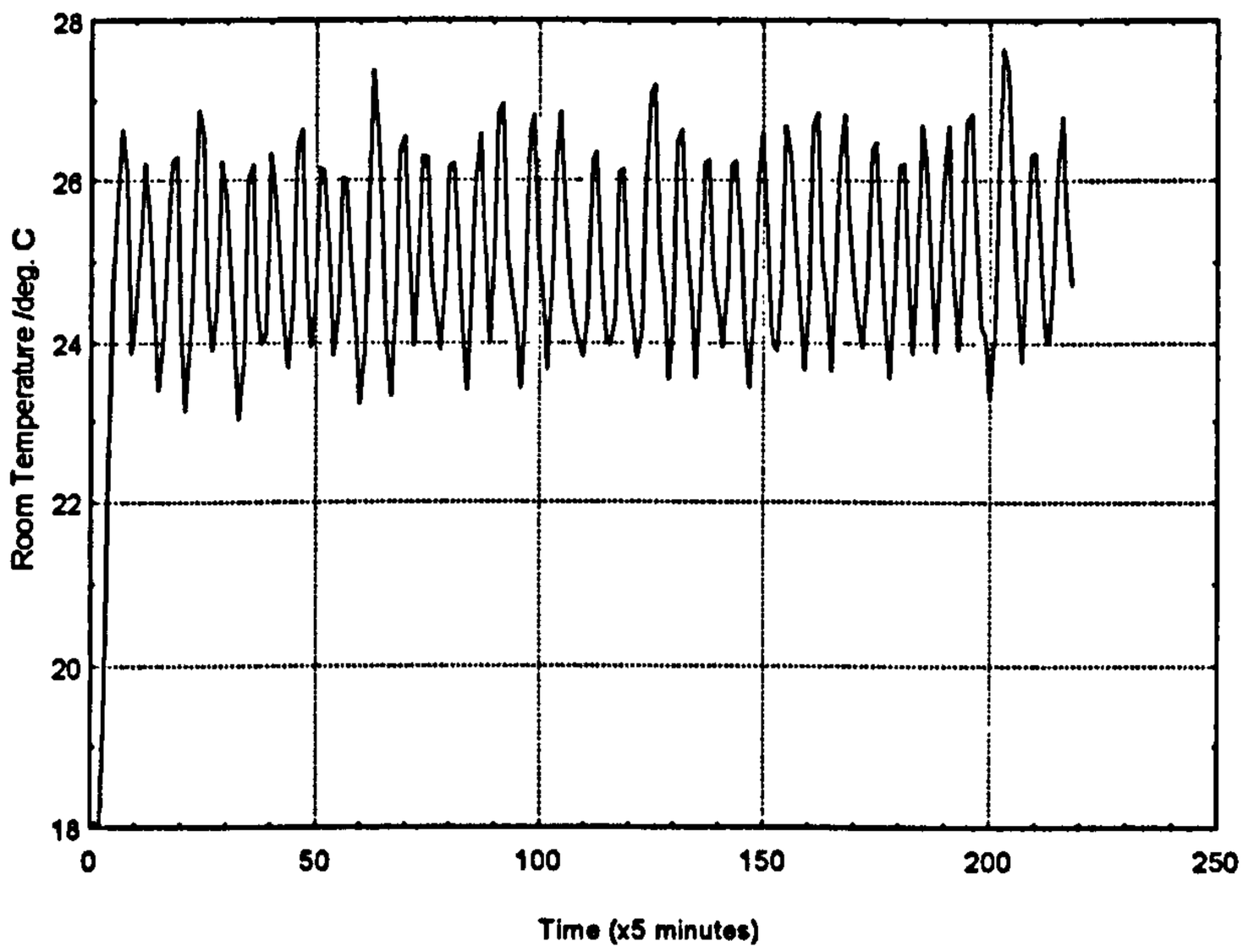

Figure 2.11: Simulated temperature regulation performance using on/off control

A similar approach as for the conventional on/off controller was applied for the predictive on/off control strategy; again $T_c(t)$ is calculated via equations (2.1) and (2.2). In Step 2, the predicted room temperature $\hat{T}_c(t+T)$ is computed for the heater turned on and off. Here, we use the model to predict the output if the heater was on ($u = u_{on}$) and if it was off (= u_{off}). The input which gives a smaller error at the next sampling instant is

chosen and applied into the system. The climatic terms in the model equations are those measured during the Loughborough chamber trials and similar V_1 and V_2 processes as applied for the conventional on/off simulations were used. The simulated results are shown in Figure 2.12 where we can see that the control performance is again a little different from the actual result (Figure 2.8) but there is considerable agreement; again for the same reasons as for the standard on/off strategy.

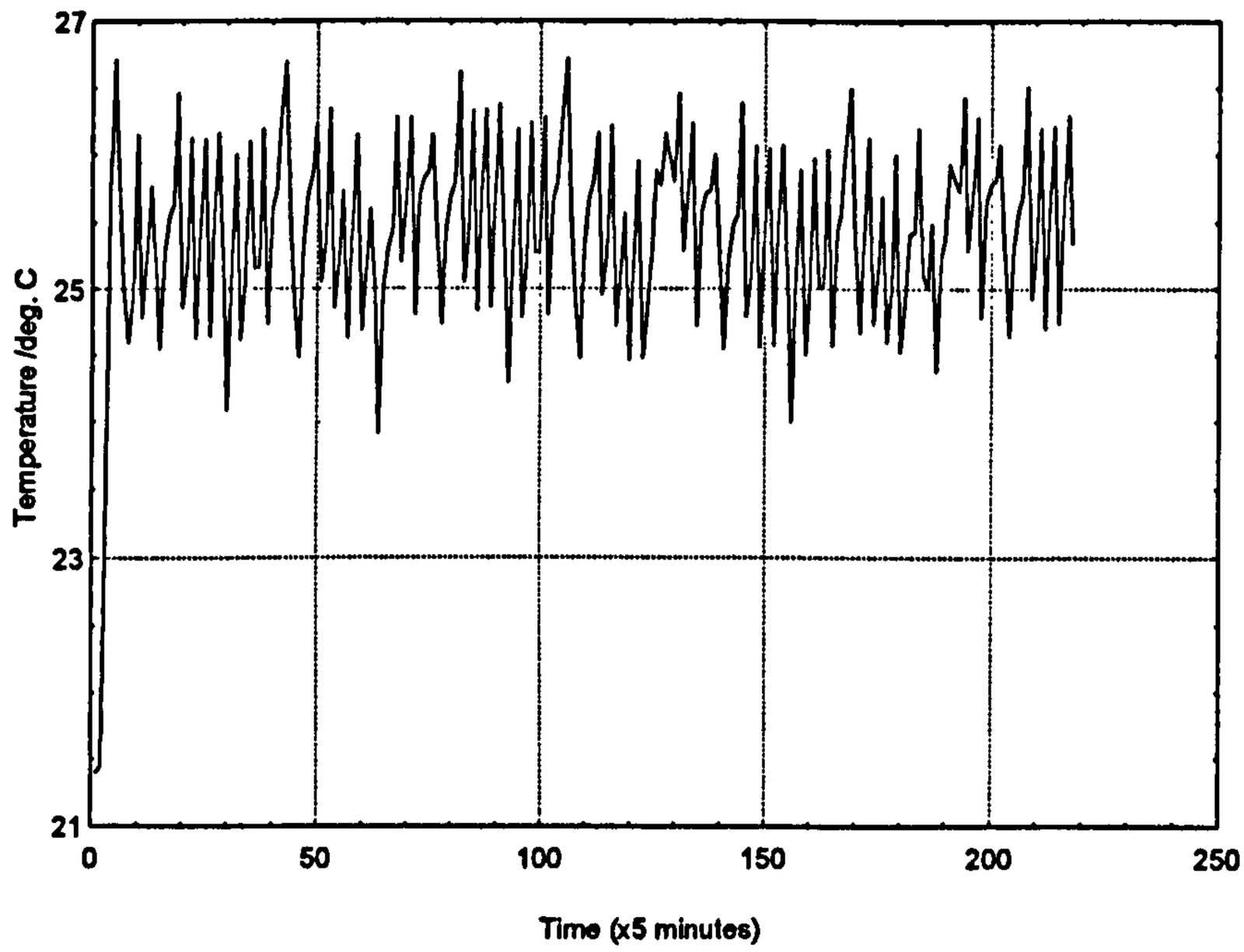

Figure 2.12: Simulated temperature regulation using the predictive on/off strategy

2.3.2.2. Model performance

The more objective assessment of the simulation studies can be obtained by calculating the squared errors of the temperatures as well as the energy used in attempting to maintain good regulation. These were calculated over the last 100 sample points for both

controllers and the results are summarised in Table 2.1. For an ideal case, the simulated result via the model would be identical to the experimental results obtained through measurements.

Table 2.1: Assessment of simulated and experimental studies

Control strategy	Methodology	Temp. errors squared, $°C^2$	Energy used, kWh
Conventional on/off	Experimental	107.36	18.75
	Simulation	123.89	18.17
Predictive on/off	Experimental	68.79	8.75
	Simulation	66.61	9.58

From Table 2.1, we can see that the simulation accuracies are quite acceptable since the regulation errors squared and the energies consumed for both control strategies calculated via the model are similar to the actual experimental results obtained from the Loughborough research chamber. The predictive on/off controller is superior in both the energy used and the regulation errors hence demonstrating the value of model-based control strategies even when very simple decision making is being carried out.

Our main conclusions here are that the performance of the unfurnished model used in the simulations imply that it can be used quite adequately to describe the temperature and relative humidity of the air in the test room due to heating inputs, as well as the climatic disturbances. The model's performance due to the cooling as well as the humidifying inputs were not analysed here because no experimental data was available

for comparative purposes, but the full model validation has been presented in Loveday and Virk (1992b). This model will be used in this thesis for the application of advanced controllers for building management systems. The furnished model (equations (2.3) and (2.4)) are not used for this purpose because the control law for this condition will be largely identical to that deduced using the unfurnished model. This is because both models have similar structure and the only difference is the coefficient for each term in the model; thus we would expect to give different magnitudes of the controller's tuning parameters.

2.4. Conclusions

This chapter has demonstrated that the use of the model can be used to assess model-based control strategies and the results achieved are very close to those obtained from carrying out experimental trials on the Loughborough test chamber. In view of the similarities we can conclude that the model can be used within a simulated environment to develop and test new advanced control algorithms and to assess their suitability for the BMS application area.

Chapter 3

Multi-input Multi-output P+I Controls

The three-term or PID (Proportional, Integral and Derivative) controller is the most widely used industrial controller, but in actual practice the gain for the derivative part in the PID device is usually zero, and so the unit reduces to a two term, or PI controller. This type of controller will be used in our design to regulate the system outputs. Since the office zone is a multi-input and multi-output (MIMO) system with 3 control inputs and 2 outputs, the PI tuning method for obtaining a good system performance is not straight forward to achieve, and this will be discussed in section 3.2. A solution for addressing this difficulty is to apply state-space methods where the dynamics of the system are formulated into state-space representation and the controller designed via state feedback and this is carried out in chapter 4. A robust multivariale PI tuning method was developed in Penttinen and Koivo (1980) where the matrix of proportional and integration gains are obtained by observing the outputs of the system subject to step inputs. This methodology was further improved by Koivo and Pohjolainen (1985). In this chapter, we propose a far simpler PI tuning methodology based on open-loop step responses and the performance of individual PI controllers when applied to our system; the overall control performance of the resulting closed-loop system is also studied here.

Since the dynamics of building zone are described by discrete modelling equations (2.1) and (2.2), this chapter, as well as the remainder of the thesis, will design several types of controller using the digital format. Our discussion commences with the design of a single PI-loop controller and this is followed by developing our multi PI-loop tuning methodology for the HVAC/office zone system.

3.1. Single PI-loop controller

In a controlled system, we require that the system output $y(t)$ tracks the setpoint $r(t)$ so that the error $e(t)$ reduces to zero at steady-state conditions. So the aim here is to find out the appropriate setting of the proportional, K_P, and integration, K_I, gains as well as the upper, I_M, and lower, $-I_M$, limits of the integral term so that the system output critically follows the setpoint. A well known method for obtaining the K_P and K_I is given by the tuning rules of Ziegler and Nichols (1942) which require closed-loop and/or open-loop step responses of the system. For the setting of I_M, we must ensure that the integral term does not grow too large thereby swamping the proportional term.

For our case, the open-loop system step response of each control input is carried out as explained in section 2.3.1 and the PI gains are given by

$$K_P = \frac{0.9U_s}{NL} \tag{3.1}$$

and

$$K_I = \frac{0.3K_P}{L} \tag{3.2}$$

where U_s, N and L can be obtained from the open-loop system step response of Figures 2.4, 2.5 and 2.6 and the terms are defined as in Figure 3.1.

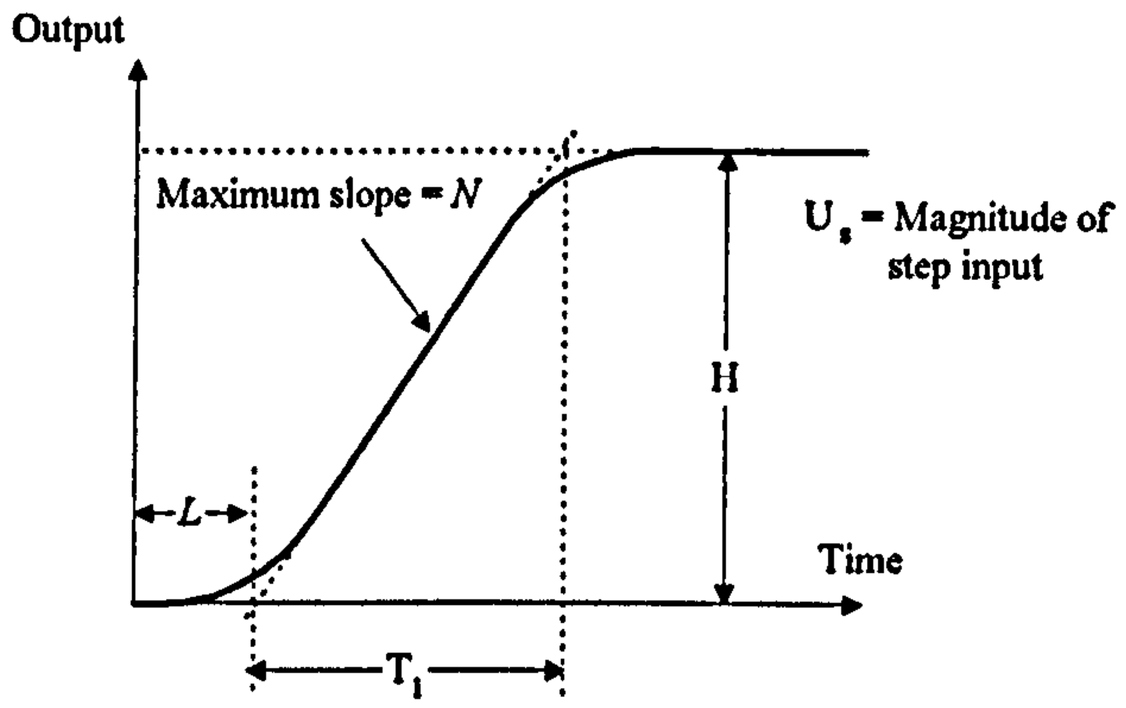

Figure 3.1: Open-loop system step response

As in the previous example of using PID controllers (section 1.2.2), here, the PI controller generates the control input $M(t)$ to the system by using the error signal $e(t)$ as shown in Figure 3.2 where $e(t)$ is the difference of the setpoint $r(t)$ and the system output $y(t)$.

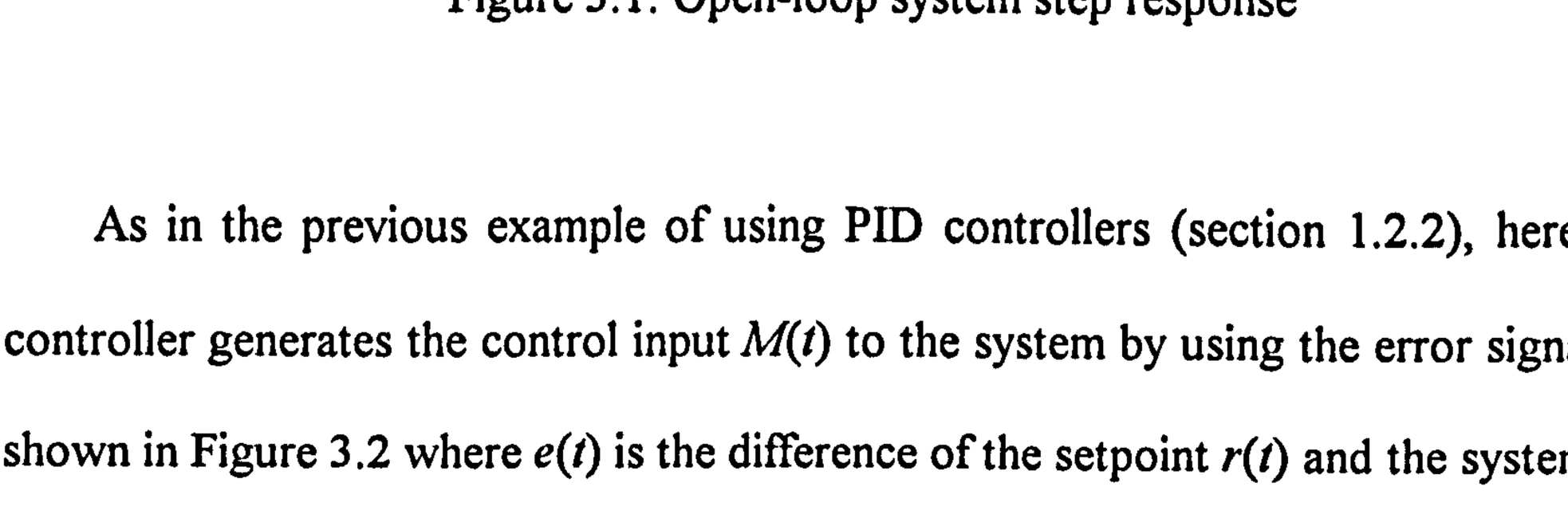

Figure 3.2: Single PI-loop controller

For example, considering that Figure 3.2 represents the temperature loop, then the temperature error, $e_T(t)$, is given by

$$e_T(t) = T_r(t) - T_c(t) \tag{3.3}$$

and the PI controller generates the control signal as

$$M(t) = K_P\, e_T(t) + K_I \int_0^t e_T(t)dt \tag{3.4}$$

where T_r is the desired setpoint for the room temperature. For a digital PI implementation, the integration term can be approximated by, for example the Euler method, which employs

$$\int_0^t e_T(t)dt \equiv I_T(t) = I_T(t\text{-T}) + \mathrm{T}e_T(t) \tag{3.5}$$

where T is the sampling interval. Equations (3.3) and (3.5) are also applied to the relative humidity loop controller by replacing $e_T(t)$ with

$$e_H(t) = H_r(t) - H_c(t) \tag{3.6}$$

and the relative humidity integration term becomes

$$I_H(t) = I_H(t\text{-T}) + \mathrm{T}e_H(t) \tag{3.7}$$

where H_r is the desired setpoint for the relative humidity in the room.

3.2. Multi PI-loop controller

As mentioned earlier, the office zone system has 3 inputs with which we can control the temperature and relative humidity at required set values, with minimum effect from the external disturbances. As shown in the step responses, each input has a strong effect on temperature and relative humidity, except for the humidifier which has little effect on the room temperature.

A classical method of feedback control for this situation can be to use two PI controllers for each input, one for the temperature loop and one for the relative humidity loop. The block diagram of the overall system for this configuration is shown in Figure

3.3 where PI#1, PI#2, ..., PI#6 are the six PI controllers and M_1, M_2, ..., M_6 are their respective outputs conbined as shown to drive the heater, cooler and humidifier controls.

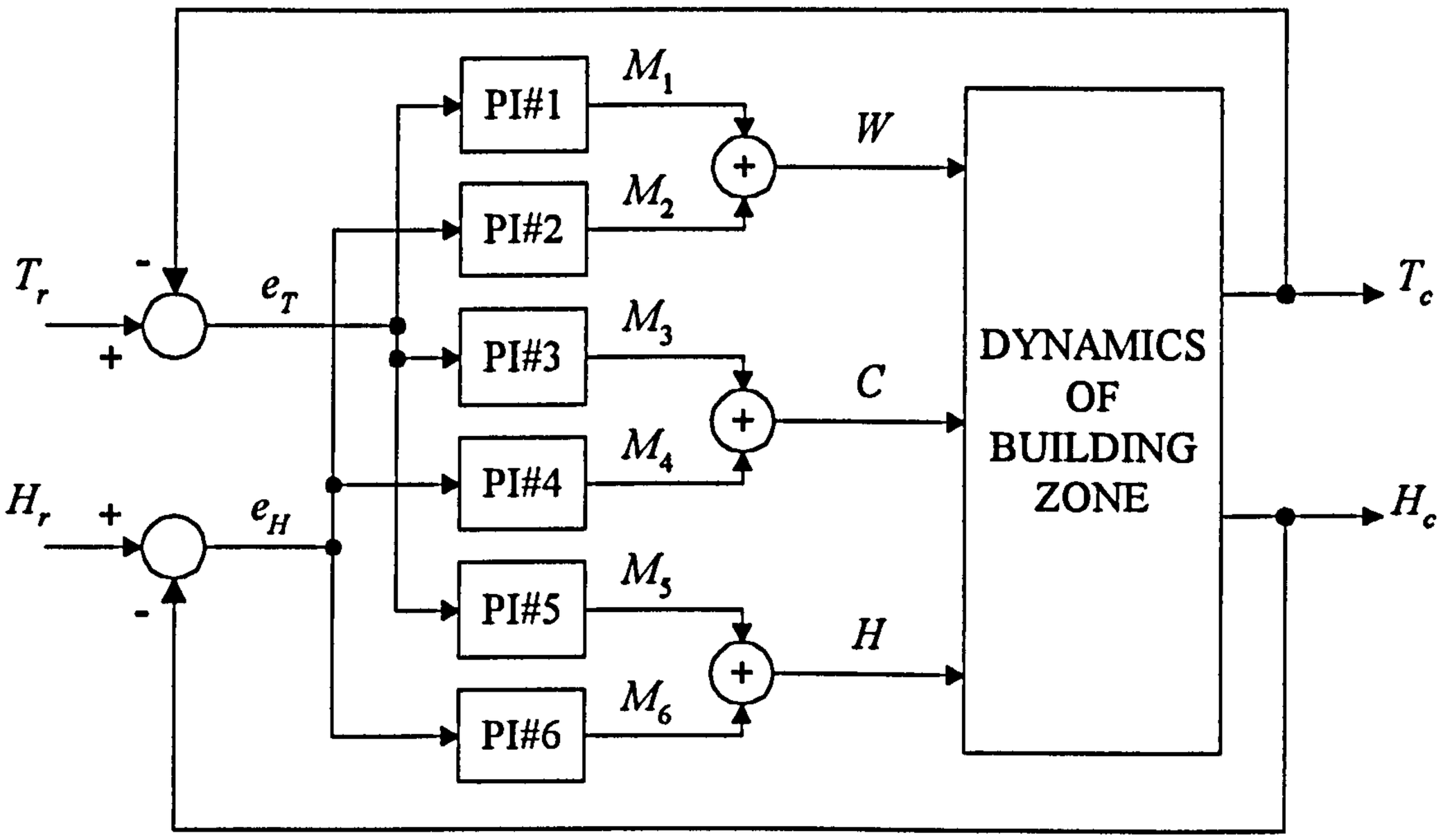

Figure 3.3: PI controller system structure

The objective here is to tune the K_P and K_I gains for optimum performance so that the temperature and relative humidity in the office-zone remain at required setpoints over a period of, say, one day. The performance of the tuned controller will be judged by looking at the regulation errors in the temperature and relative humidity as well as the overall energy consumed. Clearly a good controller design should have small errors and consume as little energy as possible.

During this 24 hours simulation period, we will assume the presence of external disturbances which effect the conditions in the room; these external disturbances will be assumed to take the following forms for convenience:

(i) Laboratory temperature: T_l is assumed to be constant at 20°C.

(ii) Outside temperature: $T_o = 15 + 6 \sin \omega t$, $0 \le t \le 12$ hours (day time)

$= 15 + 4 \sin \omega t$, $12 < t \le 24$ hours (night time).

(iii) Outside relative humidity: $H_o = 70 - 20 \sin \omega t$, $0 \le t \le 24$ hours.

(iv) Solar irradiance: $S = \sin \omega t$, $0 \le t \le 12$ hours (day time)

$= 0$, $12 < t \le 24$ hours (night time).

where $\omega = \pi/12$ and day time is deemed to be from 6 a.m. to 6 p.m. and night time from 6 p.m. to 6 a.m.

(v) White noise processes V_1 and V_2 were set to zero, that is, the system was assumed to have no stochastic effects.

In the system configuration as shown in Figure 3.3, the inputs to the heater, cooler and humidifier are equal to the sum of two terms arising from the proportional and integral controllers for the temperature and relative humidity loops. Therefore, at each iteration t, the PI output M_i , i =1, 2, ..., 6 is given by

$$\text{PI\#1:} \quad M_1(t) = K_{P1} e_T(t) + K_{I1} I_T(t) \tag{3.8}$$

$$\text{PI\#2:} \quad M_2(t) = K_{P2} e_H(t) + K_{I2} I_H(t) \tag{3.9}$$

$$\text{PI\#3:} \quad M_3(t) = K_{P3} e_T(t) + K_{I3} I_T(t) \tag{3.10}$$

$$\text{PI\#4:} \quad M_4(t) = K_{P4} e_H(t) + K_{I4} I_H(t) \tag{3.11}$$

$$\text{PI\#5:} \quad M_5(t) = K_{P5} e_T(t) + K_{I5} I_T(t) \tag{3.12}$$

$$\text{PI\#6:} \quad M_6(t) = K_{P6} e_H(t) + K_{I6} I_H(t) \tag{3.13}$$

and the control inputs W, C and H to the HVAC plant are obtained by summation of the two PI outputs, i.e. one for the temperature and one for the relative humidity, bearing in mind the limits on each control input, that is:

Heater: $W(t) = M_1(t) + M_2(t), \quad 0 \le W(t) \le 5.0$ (3.14)

Cooler: $C(t) = M_3(t) + M_4(t), \quad 0 \le C(t) \le 2.7$ (3.15)

Humidifier: $H(t) = M_5(t) + M_6(t), \quad 0 \le H(t) \le 2.6$ (3.16)

The Ziegler and Nichols (1942) tuning rules were followed using the open loop system step responses and applied to the system; however it was found that these tuning rules lead to poor control as shown in Figure 3.4, where we have assumed setpoints of 25°C and 50%rh for the temperature and relative humidity respectively. In the simulation of step responses, we assume that the climatic disturbances T_i, T_o, H_o and S are constant at 20°C, 10°C and 70%rh and 0Wm^{-2} respectively and the stochastic effects V_1 and V_2 are zero.

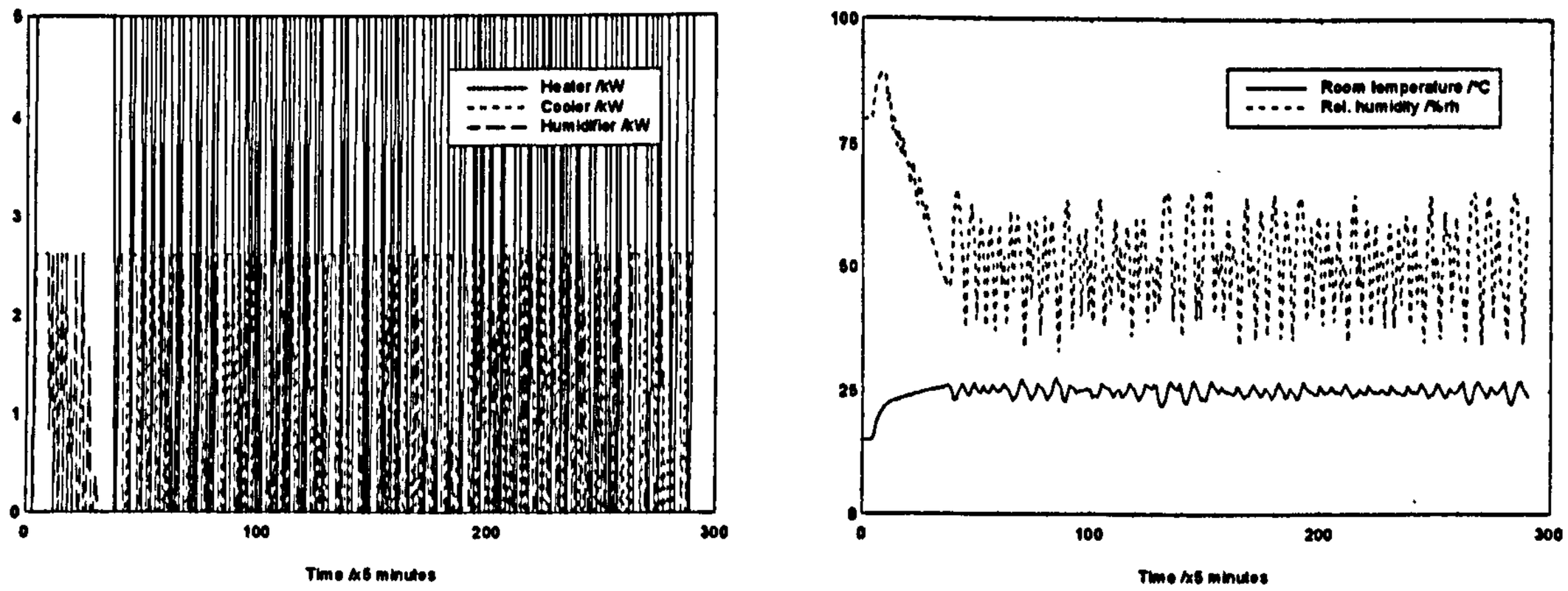

a) Control inputs

b) System outputs

Figure 3.4: Performance of 6 PIs tuned via the standard Ziegler-Nichols method (no noise)

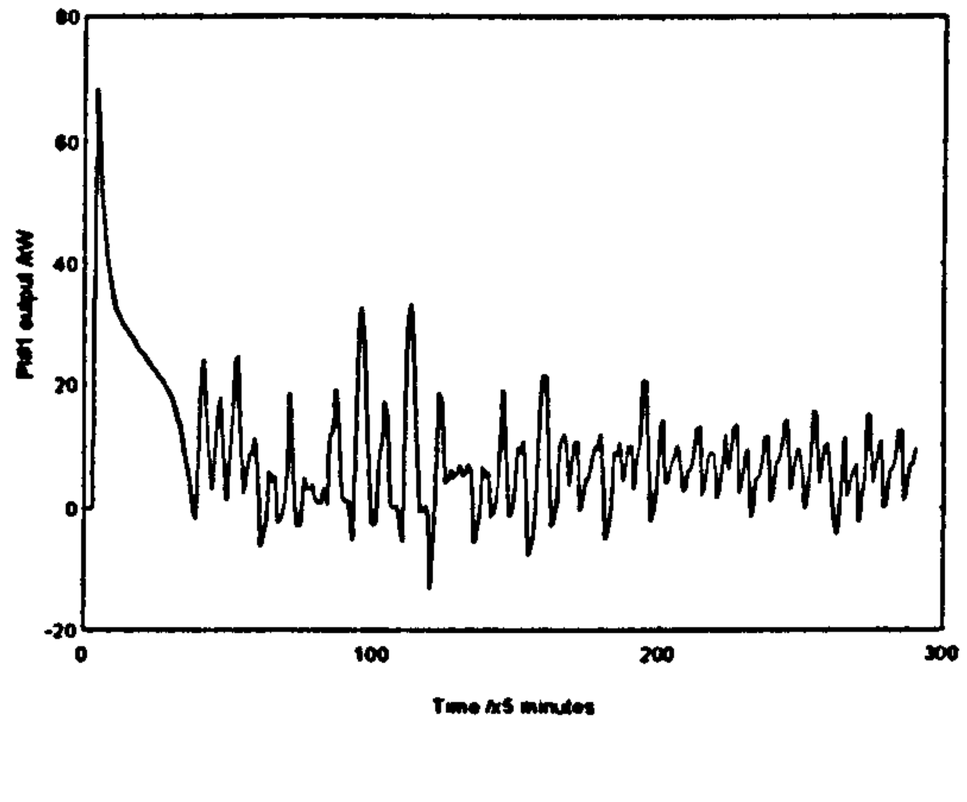

PI # 1

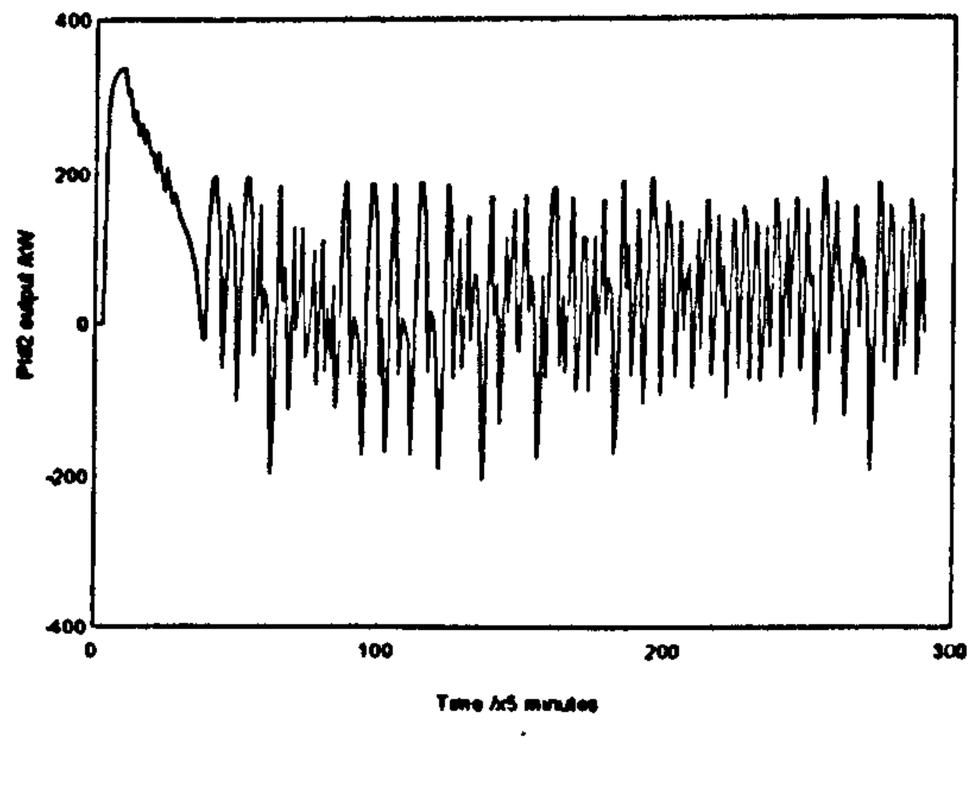

PI # 2

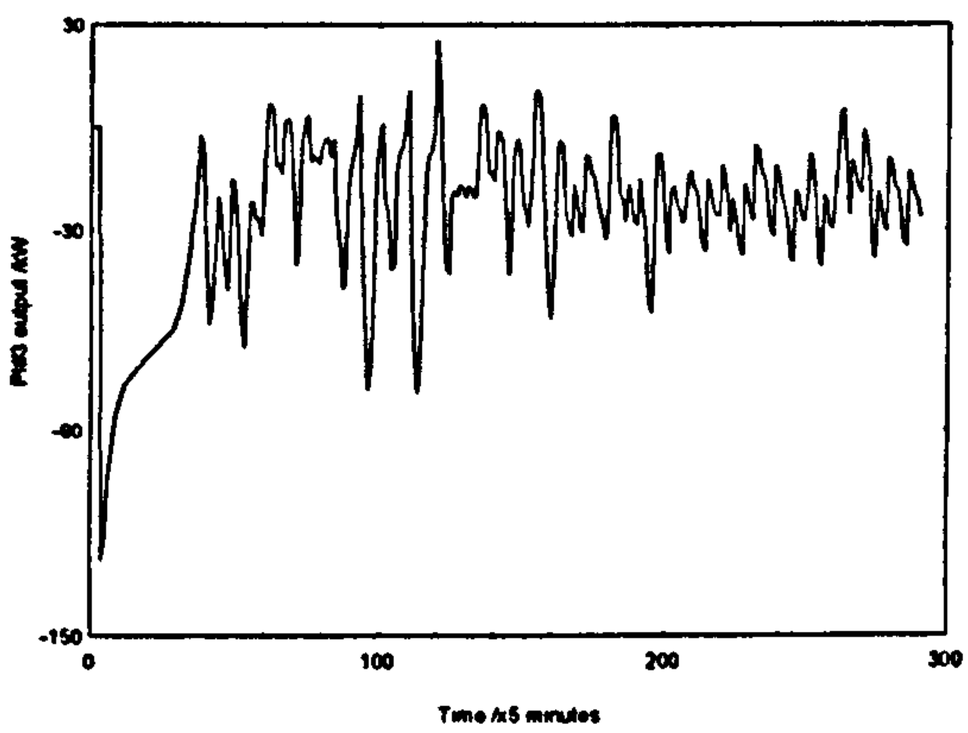

PI # 3

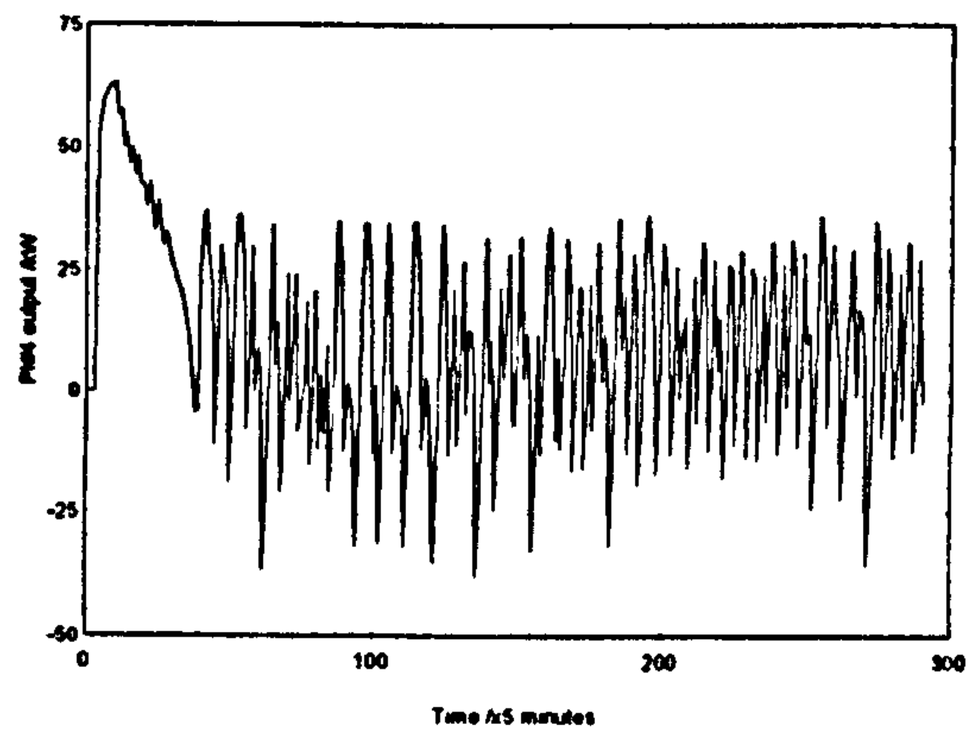

PI # 4

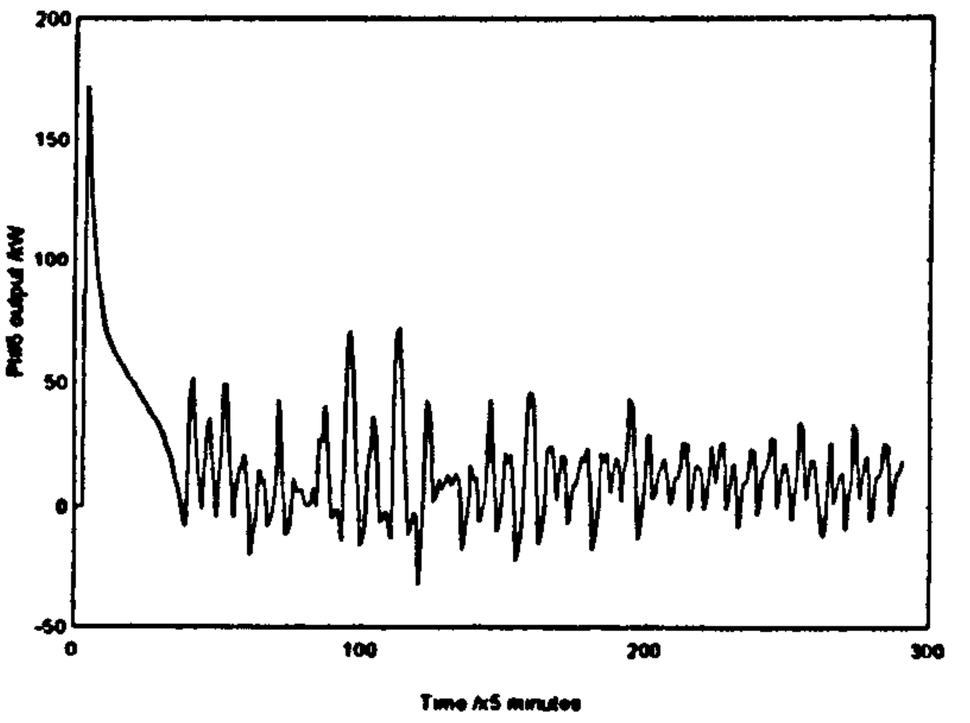

PI # 5

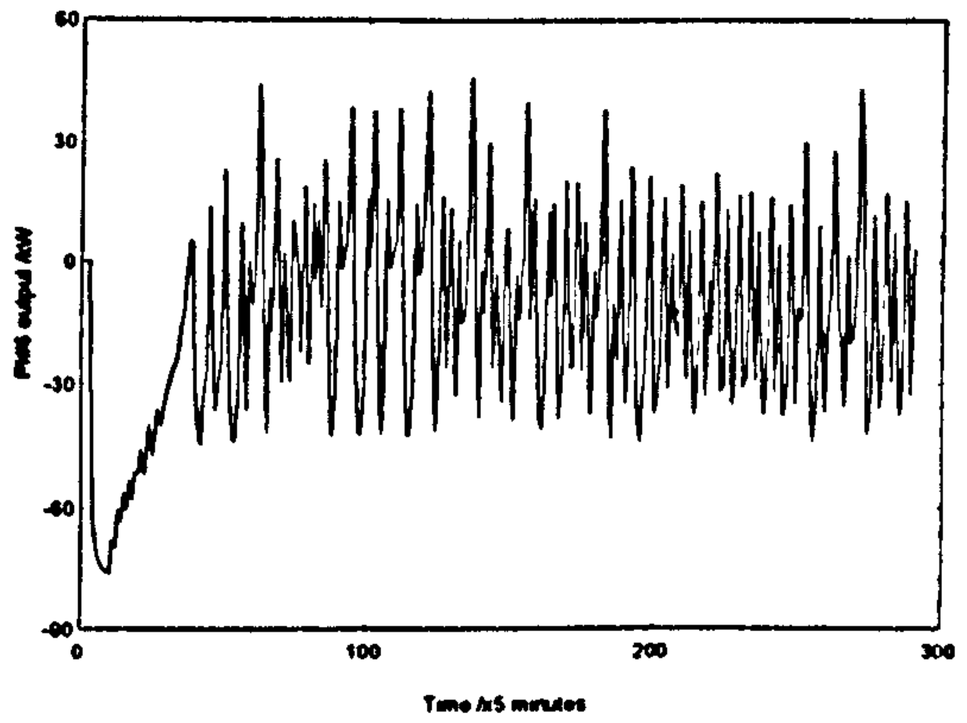

PI # 6

Figure 3.5: Performance of each PI controller tuned via the standard Ziegler-Nichols method (no noise)

PI Controller	N (°C/h)	L (h)	U_s (kW)	K_P (kW/°C)	K_I (kW/°C_h)
PI#1	6.16	0.038	1.250	4.81	38.0
PI#3	-5.27	0.017	0.675	-6.78	-119.7
PI#5	0.71	0.060	0.650	6.83	34.1

a). Temperature loop

PI Controller	N (%rh/h)	L (h)	U_s (kW)	K_P (kW/%rh)	K_I (kW/%rh_h)
PI#2	-11.20	0.017	1.250	-5.91	-104.2
PI#4	-33.90	0.017	0.675	-1.10	-19.4
PI#6	25.78	0.017	0.650	1.33	23.5

b). Relative humidity loop

Table 3.1: PI gains tuned by Zeigler-Nichols open-loop step response

It can be seen that the room temperature and the relative humidity have large fluctuations around the setpoints and the control inputs are switching excessively between the on and off states. Figure 3.5 shows the PI outputs for the situations in Figure 3.4 which are very large as compared to the limits of the control signals, and this explains the reason for the excessive switching of the control signals. The control performance over the last 100 sampling points are found to be as follows: the total squared error in the temperature and relative humidity were 88.8°C^2 and 7686.7 %rh^2 respectively and the energy

consumed by the heater, cooler and humidifier were 29.8, 5.9 and 11.7 kWh respectively.

Here, the K_P and K_I values of each loop for the three control inputs were obtained from equations (3.1) and (3.2) respectively by using the data from the individual step responses by increasing the controlled inputs from 50% to 75% of their maximum powers; the values are given in Table 3.1. The PI controllers obtained in this way lead to the poor performance shown in Figure 3.4 because the system is essentially multivariable in nature whereas the traditional Ziegler-Nichols method applies only to single input/single output systems. In other words, the K_P and K_I values given by the Ziegler-Nichols method is only valid if all the loops are independent of each other and do not apply to the multivariable case. In view of this it was decided to investigate an interactive methodology for tuning the PI gains in the multivariable situation so that the resulting controllers can yield better performances. However, we found that developing a multivariable PI loop tuning proved extremely difficult and the results were not acceptable due to large control input switchings. In view of this a more simpler detuning methodology to modify the Ziegler-Nichols gain was investigated and developed for the MIMO case. This is discussed next.

3.3. Multi PI-loop tuning methodology

Since our system has three control inputs, namely the heater, cooler and humidifier, and two outputs, namely the room temperature and the relative humidity, with the PI control structure as shown in Figure 3.3, then the tuning procedure which is suitable to our setup needs be developed so that the interaction effects are included in the tuning.

As shown in Figures 3.4 and 3.5, the PI output swings are very large as compared to their respective control limits but the controller is still able to regulate the air temperature and relative humidity in the room at their setpoints. This means that the Zeigler-Nichols tuning methodology is applicable in this multivariale system but it needs modification to improve the output regulations. It is straight forward to deduce that the large controller switchings are due to the large Ziegler-Nichols K_P and K_I gains for this system and thus, it indicates that a methodology should be developed to reduce these gains. Clearly, for a good control system, the output of individual PI controllers should not exceed the permitted control limit, namely, the output of the controllers PI#1 and PI#2, PI#3 and PI#4, and PI#5 and PI#6 should be regulating in the range of the heater, cooler and humidifier control limits respectively without any constraints implemented during the process controls. Based on these facts, we propose a simple method to recalculate the PI gains to improve the results obtained via Ziegler-Nichols methodology for this multivariable system and the method is given as follows:

First of all, we reduce the average individual PI output swings to within its control limit. This is done by reducing the output of controllers PI#1 and PI#2 to the range of 0 - 5 kW since they apply to the heater. Similarly, PI#3 and PI#4 outputs are reduced to 0 - 2.7 kW, and PI#5 and PI#6 outputs to 0 - 2.6 kW since they control the cooler and humidifier respectively. These reduction factors, of dimensionless units and positive sign, can be obtained by dividing the control limit with the average PI output swing at steady state condition of the individual PI controller and are used to modify the gains K_P and K_I so that the PI outputs fall into the control limits. The average PI output swings can be graphically estimated from Figure 3.5 and the

modified PI gains, namely, K_{PM} and K_{IM} are calculated by multiplying the Ziegler-Nichols PI gains K_P and K_I with their respective reduction factors.

The results are summarised in Table 3.2. As an example, let us calculate the modified Ziegler-Nichols gains, K_{PM} and K_{IM} for controller PI#1. The reduction gain equals the heater limit (5 kW) divided by the averaged PI#1 output swing (20 kW) at steady state condition which is equal to 0.25. Then, applying the above method, we calculate:

$K_{PM} = K_P$ x 0.25 = 1.2 kW/°C and $K_{IM} = K_I$ x 0.25 = 9.8 kW/°C_h.

A similar calculation can be performed to the remaining PI gains in the system in order to obtain their modified Ziegler-Nichols (Z-N) gains.

PI Controller	Ziegler-Nichols		Average output swing (kW)	Reduction factor	Modified Z-N	
	K_P (kW/°C)	K_I (kW/°C_h)			K_{PM} (kW/°C)	K_{IM} (kW/°C_h)
PI#1	4.81	38.0	20	0.2500	1.20	9.8
PI#3	-6.78	-119.7	40	0.0675	-0.46	-8.1
PI#5	13.73	68.7	40	0.0650	0.89	4.5

a) Temperature loop

PI Controller	Ziegler-Nichols		Average output swing (kW)	Reduction factor	Modified Z-N	
	K_P (kW/%rh)	K_I (kW/%rh_h)			K_{PM} (kW/%rh)	K_{IM} (kW/%rh_h)
PI#2	-5.91	-104.2	350	0.0140	-0.08	-1.5
PI#4	-1.10	-19.4	70	0.0386	-0.04	-0.75
PI#6	1.33	23.5	70	0.0371	0.05	0.87

b) Relative humidity loop

Table 3.2: Modified Zeigler-Nichols PI gains

3.3.1. Simulation results

In the simulation studies conducted, the following assumptions were made:

(i) The initial conditions assumed at the start time of 6 am are as follows:

T_c = 15°C, H_c = 80%rh, T_l = 20°C, T_o = 15°C, H_o = 70%rh, S = 0 Wm^{-2},

V_1 = 0°C and V_2 = 0%rh, and

(ii) The controlling inputs were all 'off' initially, i.e. $W(0) = C(0) = H(0) = 0$ kW.

A simulation trial was carried out for a desired room temperature T_r and relative humidity H_r of 25°C and 50%rh respectively, and the control performance over the last 100 sampling intervals are as follows:

- the total squared error of temperature and relative humidity are 0.0°C^2 and 0.002%rh^2 respectively;
- the energy required from the heater, cooler and humidifier are 28.3, 4.7 and 9.9 kWh respectively; and
- the required times to reach T_r and H_r are 3.3 and 3.4 hours respectively.

The simulation responses are shown in Figure 3.6 where we can see that an excellent control performance is achieved by using this simple tuning methodology as explained in Section 3.3. In this simulation, the closed-loop system commences at the sampling period t = 4T for the inclusion of delayed inputs and disturbances in the model regressions. It can be seen that the relative humidity has overshot to 90%rh during the settling period. This is due to the fact that maximum power for the humidifier is consumed in order to fight with the heater's effect on the relative humidity since the heater is also at full power. It can also see from Figure 3.6 a) that at the initial stages of the control trial, the heater is used at maximum power and the humidifier is reducing to speed up the settling

time for both outputs, and the heater is dominant in the control of the system at steady state condition.

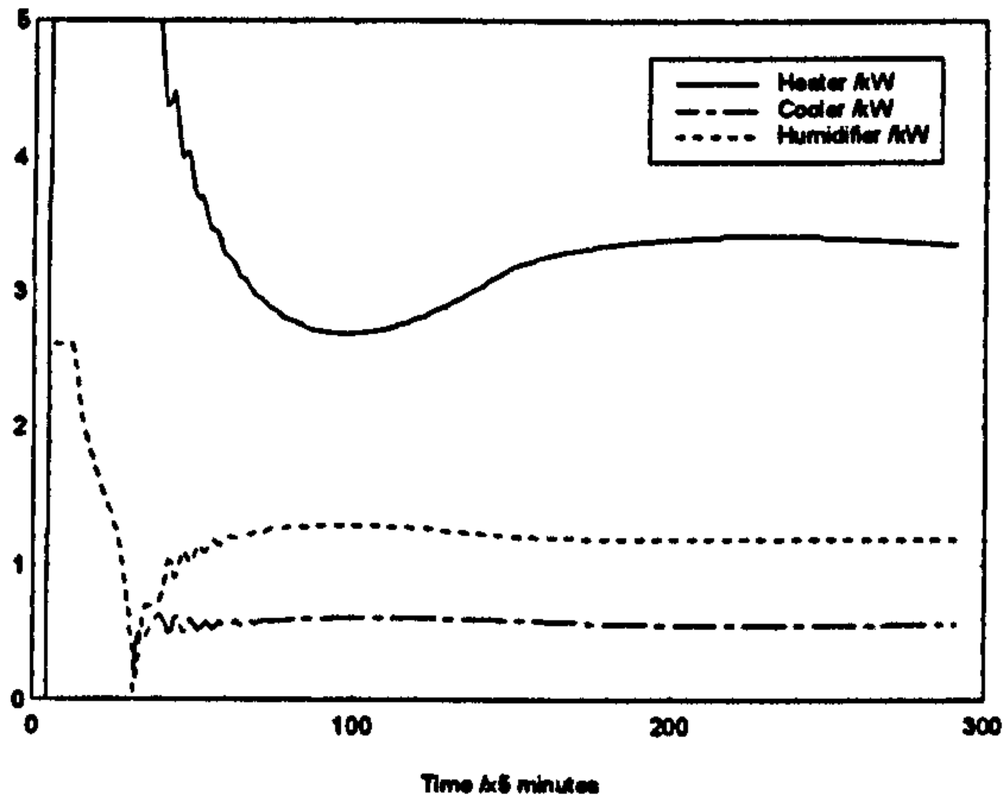

a) Control inputs b) System outputs

Figure 3.6: Performance of 6 well tuned PI controllers (no noise)

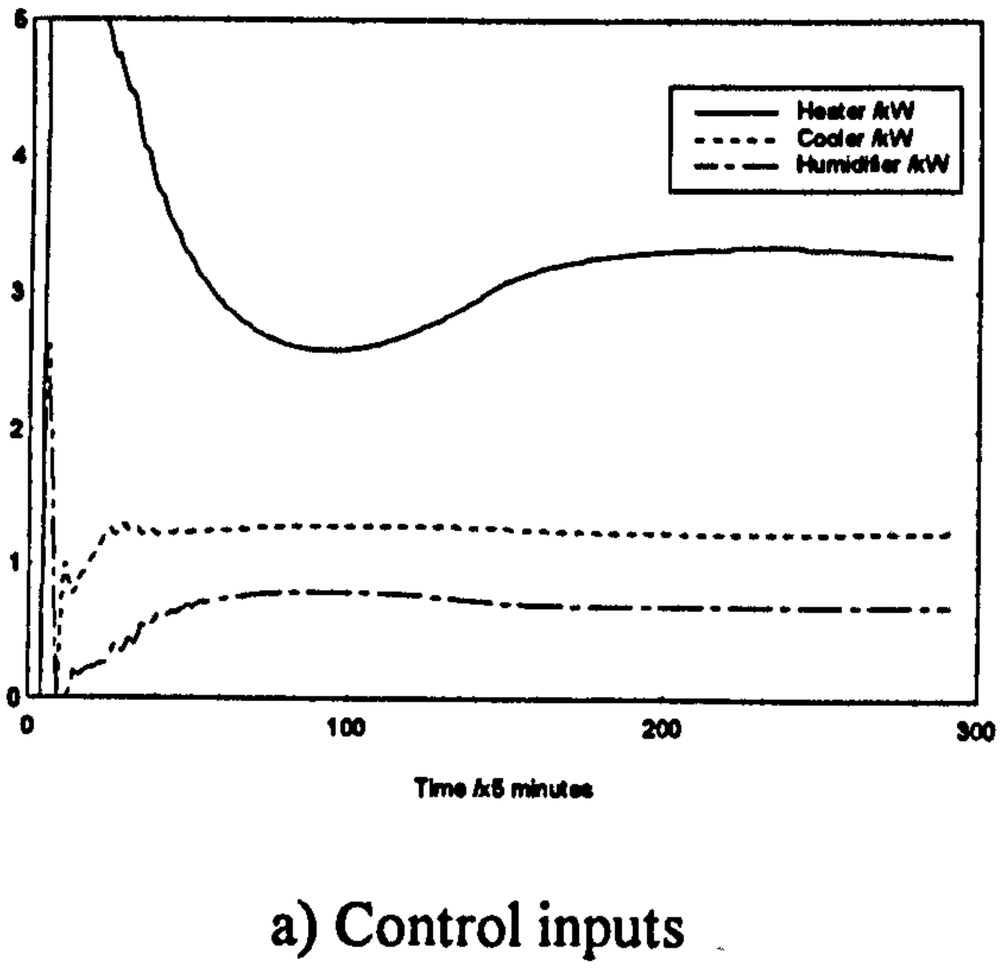

a) Control inputs b) System outputs

Figure 3.7: Control performance for setpoints of 20°C and 40%rh (no noise)

Figure 3.7 shows the performance for the temperature and relative humidity setpoints at 20°C and 40%rh respectively by using the same set of tuning parameters and

initial conditions. It was found that the control performances over the last 100 sampling points are as follows:

- the heater, cooler and humidifier consumed energies of 27.6, 10.3 and 5.6 kWh respectively;
- the total temperature and the relative humidity squared errors are $0.0°C^2$ and $0.002\%rh^2$ respectively; and
- the required times to reach T_r and H_r are 1.6 and 2.5 hours respectively.

To add a degree of realism into our simulation studies, we can insert some white noise processes V_1 and V_2 so that occupancy and other stochastic effects can be included in the analysis. For convenience pseudo random binary sequences (PRBS) generated using 6 shift registers with magnitudes $V_1 = \pm 0.5°C$ and $V_2 = \pm 0.5\%rh$, were used as the noise processes. These represent large disturbances and consequently should effect the dynamic behaviour of the system quite significantly. These terms were then included into the system of identical settings as used in Figure 3.6. The simulated result is shown in Figure 3.8 where the control performances for the last 100 sampling intervals are as follows:

- the heater, cooler and humidifier consumed 28.7, 5.7 and 10.8 kWh respectively; and
- the total temperature and the humidity squared errors are $81.0°C^2$ and $3098.5\%rh^2$ respectively.

These results show that the regulated errors have became sizeable as expected due to the disturbances which are not taken into account by the PI controllers. The situation can be improved by using an advanced model-based method such as a MIMO adaptive controller (Chapter 5) or a more intelligent solution such as a fuzzy logic controller

(Chapter 6) or a genetic algorithm optimisation technique (Chapter 7) which can attempt to correct for these stochastic effects.

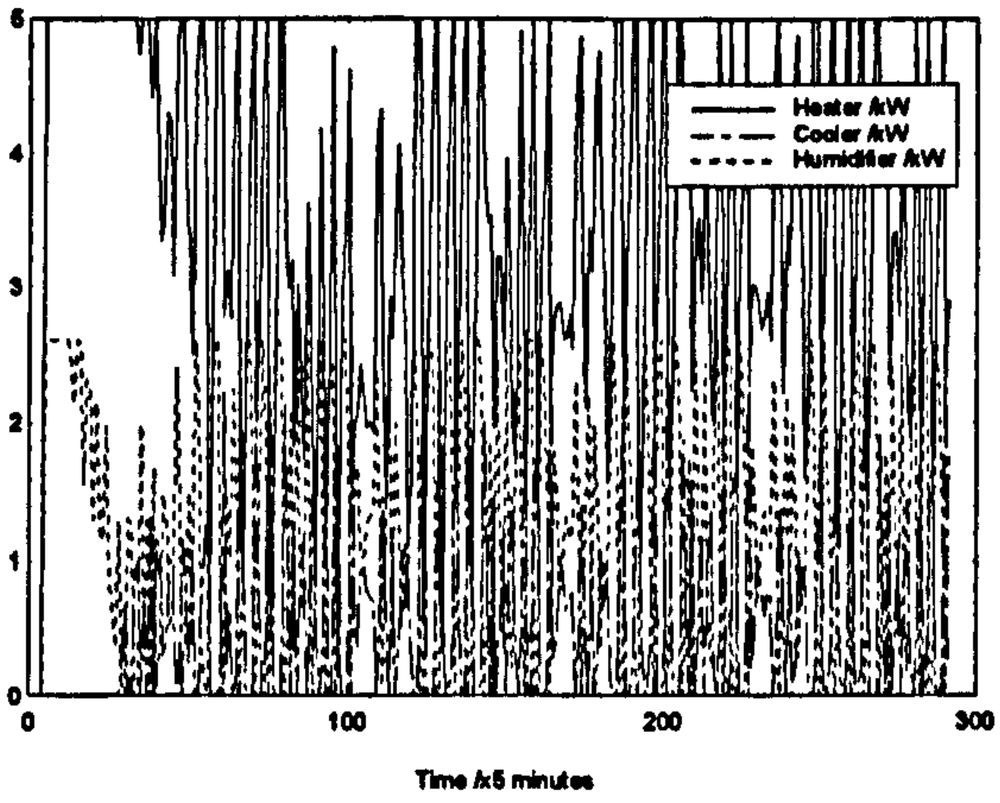

a) Control inputs

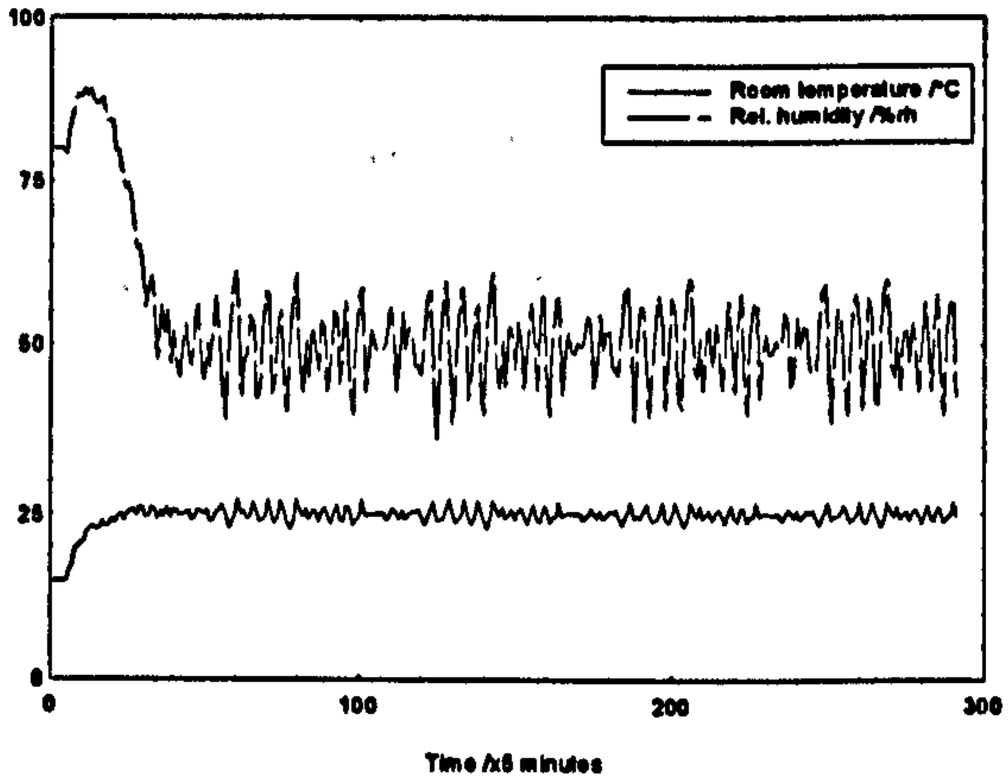

b) System outputs

Figure 3.8: Control performance with noise

3.4. Methodology to minimise the number of PI controllers

It is worthwhile to reduce the number of PI controllers used in the overall system so that excessive hardware is not used; to do this objectively requires the use of each PI controller to be justified by quantifying the benefits achieved by its inclusion.

We present a possible strategy by considering our results in Section 3.3. From Figures (3.6a) and (3.7a) and that the required control inputs are different for the two setpoints considered, namely $\{T_r, H_r\}$ are required to be at {25°C, 50%rh} and at {20°C, 40%rh}. In addition the contribution from each PI controller to the system during the control process is analysed and only those units which are active are selected for particular situations.

For example, let us consider the results for the setpoints {20°C, 40%rh}; from Figure 3.7 a), we can see that at the steady-state condition, the lowest energy is required from the humidifier, i.e. only 20% of it's maximum power. Therefore, we can ignore PI#5 and PI#6. Moreover, PI#1 and PI#4 form the majority of the control actions used in the system, and so the controllers PI#2 and PI#3 can be ignored. Therefore, as a possible solution for this setpoint we can use only 2 PI controllers, one for the heater and one for the cooler with the output ranges set to 0 - 5.0 kW and 0 - 2.6 kW for PI#1 and PI#4 respectively.

When this solution is tested we observe an excellent controlled response as shown in Figure 3.8; the performance over the last 100 sampling intervals are as follows:

- the heater and cooler consumed energies of 20.6 and 4.1 kWh respectively; and
- the total temperature and the humidity squared errors are $0.0°C^2$ and $0.001\%rh^2$ respectively,

which is in fact a better performance from that achieved using the six controllers!

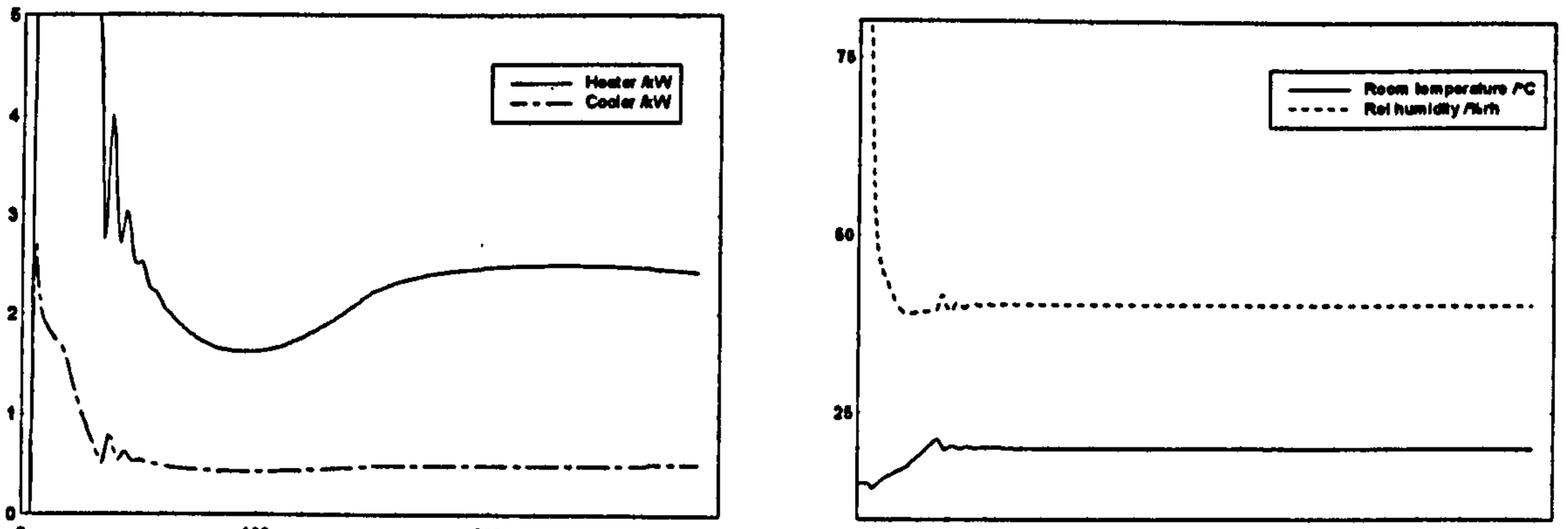

a) Control inputs b) System outputs

Figure 3.9: Control performance using 2 PI controllers (PI#1 and PI#4)

We also found that this controller is also capable of maintaining the system at the setpoints of 20°C < T_r < 25°C and 30%rh < H_r < 45%rh, for which the output squared errors are quite small.

Also consider the second situation from Section 3.3 where we have a setpoint of {25°C, 50%rh}. In this case it was found that the lowest energy is required from the cooler. Moreover, the presence of the cooler will require more energy from the heater in order to maintain the required setpoints. Therefore, we can ignore the cooler as well as the controllers PI#3 and PI#4. When this is done we found that the control performance is deteriorated and the performance over the last 100 sampling intervals are as follows:

- the heater and humidifier consumed energies of 23.0 and 5.6 kWh respectively; and
- the total temperature and the humidity squared errors are 11.9°C^2 and 241.0%rh^2 respectively

which are still within a comfort zone. In another word, It is also possible to use the heater and the humidifier only to regulate the temperature and the relative humidity at 25°C and 50%rh respectively.

3.5. Conclusions

In this chapter a simple yet effective tuning methodology of multi PI-loop controllers for our HVAC plant /office zone system is described. It has been shown that good control performances can be achieved by using the proportional and integration gains tuned by this method. Although the methodology is specific to this application it is hoped it can be generalised to cover a wider range of situations.

The methodology is also useful for minimising the number of PI controllers that are necessary for effective results. It is found that only two PI controllers are required for good temperature and relative humidity regulation; one is for the heater (driven by the temperature loop) and the other for the cooler (driven by the rh loop).

Chapter 4

State-Space Methods

In the previous chapters, the simulation and control of air conditioned systems using discrete transfer function has been discussed. Another recent development in control theory is to use state-space representations which allow more insight into the internal behaviour of the system under study (see for example Friedland, 1986). To undertake this type of study it is necessary to convert the transfer function form of model equations (2.1) and (2.2) into a state-space representation. We begin our discussions concerning the state-space analysis by first deriving a suitable state-space format for our HVAC system.

4.1. State-space representation

The normal approach employed to obtain a state-space description is to define the state variables as delayed versions of the system output (T_c and H_c in our case). Following this methodology we define the state variables as

$$\tilde{x}_1(t) = T_c(t\text{-}2\mathrm{T}), \qquad \tilde{x}_2(t) = T_c(t\text{-}\mathrm{T}), \qquad \tilde{x}_3(t) = T_c(t),$$

$$\tilde{x}_4(t) = H_c(t\text{-}2\mathrm{T}), \qquad \tilde{x}_5(t) = H_c(t\text{-}\mathrm{T}) \text{ and } \tilde{x}_6(t) = H_c(t) \tag{4.1}$$

where upon it is straightforward to deduce the individual state equations as:

$$\tilde{x}_1(t+\mathrm{T}) = \tilde{x}_2(t) \tag{4.2}$$

$$\tilde{x}_2(t+\mathrm{T}) = \tilde{x}_3(t) \tag{4.3}$$

$$\begin{aligned}\tilde{x}_3(t+\mathrm{T}) = {} & 0.02\tilde{x}_1(t) - 0.64\tilde{x}_2(t) + 1.61\tilde{x}_3(t) - 0.006\tilde{x}_5(t) + 0.004\tilde{x}_6(t) \\ & + 0.22W(t) + 0.07\,W(t-T) - 0.26W(t-2\mathrm{T}) - 0.62C(t) \\ & + 0.36\,C(t-\mathrm{T}) + 0.19C(t-2\mathrm{T}) + 0.04H(t) + 0.001T_o\,(t) \\ & + 0.015S(t) + V_1\,(t+\mathrm{T}) - 1.36V_1\,(t) + 0.48V_1\,(t-T) + \mathrm{k}_1 \end{aligned} \tag{4.4}$$

$$\tilde{x}_4(t+\mathrm{T}) = \tilde{x}_5(t) \tag{4.5}$$

$$\tilde{x}_5(t+\mathrm{T}) = \tilde{x}_6(t) \tag{4.6}$$

$$\begin{aligned}\tilde{x}_6(t+\mathrm{T}) = {} & 0.003\tilde{x}_2(t) - 0.04\tilde{x}_3(t) + 0.02\tilde{x}_4(t) - 0.58\tilde{x}_5(t) + 1.54\tilde{x}_6(t) \\ & - 0.71W(t) + 0.37W(t-\mathrm{T}) + 0.29W(t-2\mathrm{T}) - 4.02C(t) + 3.73C(t-\mathrm{T}) \\ & + 3.29H(t) - 2.42H(t-\mathrm{T}) - 0.49H(t-2\mathrm{T}) + 0.01\,T_i\,(t) + 0.01T_o\,(t) \\ & + 0.002\,H_o\,(t) - 0.09S(t) + V_2\,(t+\mathrm{T}) - 1.24\,V_2\,(t) \\ & + 0.32\,V_2\,(t-\mathrm{T}) + \mathrm{k}_2 \end{aligned} \tag{4.7}$$

or in matrix form as

$$\begin{aligned}\tilde{\boldsymbol{x}}\,(t+\mathrm{T}) = {} & \mathbf{A}\,\tilde{\boldsymbol{x}}\,(t) + \mathbf{B}_1\,u(t) + \mathbf{B}_2\,u(t-\mathrm{T}) + \mathbf{B}_3\,u(t-2\mathrm{T}) + \mathbf{D}\,w(t) \\ & + \mathbf{E}_0\,v(t+\mathrm{T}) + \mathbf{E}_1\,v(t) + \mathbf{E}_2\,v(t-\mathrm{T}) + \mathbf{K} \end{aligned} \tag{4.8}$$

where

$$\mathbf{A} = \begin{bmatrix} 0 & 1 & 0 & 0 & 0 & 0 \\ 0 & 0 & 1 & 0 & 0 & 0 \\ 0.02 & -0.64 & 1.61 & 0 & -0.006 & 0.004 \\ 0 & 0 & 0 & 0 & 1 & 0 \\ 0 & 0 & 0 & 0 & 0 & 1 \\ 0 & 0.003 & -0.04 & 0.02 & -0.58 & 1.54 \end{bmatrix}, \quad \mathbf{B}_1 = \begin{bmatrix} 0 & 0 & 0 \\ 0 & 0 & 0 \\ 0.22 & -0.62 & 0.04 \\ 0 & 0 & 0 \\ 0 & 0 & 0 \\ -0.71 & -4.02 & 3.29 \end{bmatrix},$$

$$\mathbf{B}_2 = \begin{bmatrix} 0 & 0 & 0 \\ 0 & 0 & 0 \\ 0.07 & 0.36 & 0 \\ 0 & 0 & 0 \\ 0 & 0 & 0 \\ 0.37 & 3.73 & -2.42 \end{bmatrix}, \mathbf{B}_3 = \begin{bmatrix} 0 & 0 & 0 \\ 0 & 0 & 0 \\ -0.26 & 0.19 & 0 \\ 0 & 0 & 0 \\ 0 & 0 & 0 \\ 0.29 & 0 & -0.49 \end{bmatrix}, \mathbf{E}_0 = \begin{bmatrix} 0 & 0 \\ 0 & 0 \\ 1 & 0 \\ 0 & 0 \\ 0 & 0 \\ 0 & 1 \end{bmatrix},$$

$$\mathbf{D} = \begin{bmatrix} 0 & 0 & 0 & 0 \\ 0 & 0 & 0 & 0 \\ 0 & 0.001 & 0 & 0.015 \\ 0 & 0 & 0 & 0 \\ 0 & 0 & 0 & 0 \\ 0.01 & 0.01 & 0.002 & -0.09 \end{bmatrix}, \mathbf{E}_1 = \begin{bmatrix} 0 & 0 \\ 0 & 0 \\ -1.36 & 0 \\ 0 & 0 \\ 0 & 0 \\ 0 & -1.24 \end{bmatrix}, \mathbf{E}_2 = \begin{bmatrix} 0 & 0 \\ 0 & 0 \\ 0.48 & 0 \\ 0 & 0 \\ 0 & 0 \\ 0 & 0.32 \end{bmatrix},$$

$$\mathbf{K} = \begin{bmatrix} 0 \\ 0 \\ k_1 \\ 0 \\ 0 \\ k_2 \end{bmatrix}, \tilde{\boldsymbol{x}} = \begin{bmatrix} \tilde{x}_1 \\ \tilde{x}_2 \\ \tilde{x}_3 \\ \tilde{x}_4 \\ \tilde{x}_5 \\ \tilde{x}_6 \end{bmatrix}, \boldsymbol{u} = \begin{bmatrix} W \\ C \\ H \end{bmatrix}, \boldsymbol{w} = \begin{bmatrix} T_i \\ T_o \\ H_o \\ S \end{bmatrix} \text{ and } \boldsymbol{v} = \begin{bmatrix} V_1 \\ V_2 \end{bmatrix}.$$

From equation (4.1), the output equation becomes

$$y(t) \equiv \begin{bmatrix} T_c(t) \\ H_c(t) \end{bmatrix} = \begin{bmatrix} \tilde{x}_3(t) \\ \tilde{x}_6(t) \end{bmatrix}$$

or in compact form as

$$y(t) = \mathbf{C}\,\tilde{\boldsymbol{x}}(t) \tag{4.9}$$

where

$$\mathbf{C} = \begin{bmatrix} 0 & 0 & 1 & 0 & 0 & 0 \\ 0 & 0 & 0 & 0 & 0 & 1 \end{bmatrix}.$$

Equation (4.8) is not in standard form in which the state-space equations are normally presented; the reason is that there are terms explicitly present which are dependent on delayed values of the inputs and noise. It is possible to transform this form

by absorbing the previous regressions of the input and noise terms so that equation (4.8) becomes a standard form of state-space equation, namely it is of the form:

$$x(t+\mathrm{T}) = \mathbf{M}\,x(t) + \mathbf{B}\,u(t) + \mathbf{N}\,w(t) + \mathbf{E}\,v(t+\mathrm{T}) + \mathbf{J} \qquad (4.10)$$

where **M, B, N, E** and **J** are 6x6, 6x3, 6x4, 6x2 and 6x1 matrices/vectors respectively.

The relationship between the transformed state x and the original state $\tilde{x}$ can be obtained by assuming that the transformed states have terms due to previous input and noise values included in their respective equations; the coefficients for these values need to be calculated so that the new state-space equation has the required standard form. We will assume these coefficients are unknown at present and that the new states are defined by:

$$x(t) = \tilde{x}(t) + \mathbf{P}_1\,u(t\text{-}\mathrm{T}) + \mathbf{P}_2\,u(t\text{-}2\mathrm{T}) + \mathbf{Q}_0\,v(t) + \mathbf{Q}_1\,v(t\text{-}\mathrm{T}) \qquad (4.11)$$

where $\mathbf{P}_1$ and $\mathbf{P}_2$ matrices are of dimension 6x3, $\mathbf{Q}_0$ and $\mathbf{Q}_1$ are 6x2 matrices, and $x = \begin{bmatrix} x_1 & x_2 & x_3 & x_4 & x_5 & x_6 \end{bmatrix}^T$ is the new state variables where $[.]^T$ denotes the transpose of a vector.

The **B, E, J, M** and **N** matrices in equation (4.10) can be obtained by using equation (4.11). This can be done by substituting the state variable $\tilde{x}$ with x by using equations (4.8) and (4.11) and ensuring that the coefficients of the previous terms $u(t\text{-}\mathrm{T})$, $u(t\text{-}2\mathrm{T})$ and $v(t\text{-}\mathrm{T})$ and also $v(t)$ of equation (4.10) reduce to zero. To illustrate the procedure let us manipulate equation (4.11) by shifting time t to $(t+\mathrm{T})$; the equation then becomes

$$x(t+\mathrm{T}) = \tilde{x}(t+\mathrm{T}) + \mathbf{P}_1\,u(t) + \mathbf{P}_2\,u(t\text{-}\mathrm{T}) + \mathbf{Q}_0\,v(t+\mathrm{T}) + \mathbf{Q}_1\,v(t)$$

Substituting for $\tilde{x}(t+\mathrm{T})$ using equation (4.8) gives:

$$x(t+\mathrm{T}) = \mathbf{A}\,\tilde{x}(t) + (\mathbf{B}_1 + \mathbf{P}_1)\,u(t) + (\mathbf{B}_2 + \mathbf{P}_2)\,u(t\text{-}\mathrm{T}) + \mathbf{B}_3\,u(t\text{-}2\mathrm{T})$$

$$+ \mathbf{D}\,w(t) + (\mathbf{E}_0 + \mathbf{Q}_0)\,v(t+\mathrm{T}) + (\mathbf{E}_1 + \mathbf{Q}_1)\,v(t) + \mathbf{E}_2\,v(t\text{-}\mathrm{T}) + \mathbf{K}.$$

Now using equation (4.11) we have

$$x(t+T) = A\{x(t) - P_1 u(t-T) - P_2 u(t-2T) - Q_0 v(t) - Q_1 v(t-T)\}$$

$$+ (B_1 + P_1) u(t) + (B_2 + P_2) u(t-T) + B_3 u(t-2T) + D w(t)$$

$$+ (E_0 + Q_0) v(t+T) + (E_1 + Q_1) v(t) + E_2 v(t-T) + K$$

which can be reduced to

$$x(t+T) = A x(t) + (B_1 + P_1) u(t) + (B_2 + P_2 - AP_1) u(t-T)$$

$$+ (B_3 - AP_2) u(t-2T) + D w(t) + (E_0 + Q_0) v(t+T)$$

$$+ (E_1 + Q_1 - AQ_0) v(t) + (E_2 - AQ_1) v(t-T) + K \qquad (4.12)$$

By equating the coefficients of each matrix term in equations (4.10) and (4.12), we obtain

$$M = A, N = D, J = K \qquad (4.13)$$

$$B = B_1 + P_1 \qquad (4.14)$$

$$E = E_0 + Q_0 \qquad (4.15)$$

$$B_2 + P_2 - AP_1 = 0 \equiv \text{ 6x3 zero matrix} \qquad (4.16)$$

$$B_3 - AP_2 = 0 \equiv \text{ 6x3 zero matrix} \qquad (4.17)$$

$$E_1 + Q_1 - AQ_0 = 0 \equiv \text{ 6x2 zero matrix} \qquad (4.18)$$

$$E_2 - AQ_1 = 0 \equiv \text{ 6x2 zero matrix} \qquad (4.19)$$

The matrix elements of P_2 can be obtained by solving equations (4.17) and the P_1 matrix can then be calculated by substituting for P_2 into equation (4.16). It is straightforward to deduce that

$$\mathbf{P}_1 = \begin{bmatrix} -408.15 & 322.00 & -7.35 \\ -13.00 & 9.50 & 0 \\ 0 & 0 & 0 \\ 440.95 & 185.08 & -831.50 \\ 14.5 & 0 & -24.5 \\ 0 & 0 & 0 \end{bmatrix} \text{ and } \mathbf{P}_2 = \begin{bmatrix} -13.0 & 9.5 & 0 \\ 0 & 0 & 0 \\ 0 & 0 & 0 \\ 14.5 & 0 & -24.5 \\ 0 & 0 & 0 \\ 0 & 0 & 0 \end{bmatrix}.$$

Similar calculations are performed to obtain the $\mathbf{Q}_0$ and $\mathbf{Q}_1$ matrices from equations (4.18) and (4.19). The values are found to be

$$\mathbf{Q}_0 = \begin{bmatrix} 700.0 & 4.8 \\ 24.0 & 0 \\ 0 & 0 \\ -3.6 & 402.0 \\ 0 & 16.0 \\ 0 & 0 \end{bmatrix} \text{ and } \mathbf{Q}_1 = \begin{bmatrix} 24 & 0 \\ 0 & 0 \\ 0 & 0 \\ 0 & 16 \\ 0 & 0 \\ 0 & 0 \end{bmatrix}.$$

From equations (4.14) and (4.15), the **B** and **E** matrices can be obtained and equal

$$\mathbf{B} = \begin{bmatrix} -408.15 & 322.00 & -7.35 \\ -13.00 & 9.50 & 0 \\ 0.22 & -0.62 & 0.04 \\ 440.95 & 185.08 & -831.50 \\ 14.50 & 0 & -24.50 \\ -0.71 & -4.02 & 3.29 \end{bmatrix} \text{ and } \mathbf{E} = \begin{bmatrix} 700.0 & 4.8 \\ 24.0 & 0 \\ 1.0 & 0 \\ -3.6 & 402.0 \\ 0 & 16.0 \\ 0 & 1.0 \end{bmatrix}.$$

For convenience we rewrite the relationship between x and $\tilde{x}$ from equation (4.11) in term of these coefficients.

$$x_1(t) = \tilde{x}_1(t) - 408.15\ W(t\text{-T}) - 13\ W(t\text{-2T}) + 322\ C(t\text{-T}) + 9.5\ C(t\text{-2T}) - 7.35\ H(t\text{-T}) + 700\ V_1(t) + 24\ V_1(t\text{-T}) + 4.8\ V_2(t) \quad (4.20)$$

$$x_2(t) = \tilde{x}_2(t) - 13\ W(t\text{-T}) + 9.5\ C(t\text{-T}) + 24\ V_1(t) \quad (4.21)$$

$$x_3(t) = \tilde{x}_3(t) \quad (4.22)$$

$$x_4(t) = \tilde{x}_4(t) + 440.95\ W(t\text{-T}) + 14.5\ W(t\text{-2T}) + 185.08\ C(t\text{-T}) - 831.5\ H(t\text{-T}) - 24.5\ H(t\text{-2T}) - 3.6\ V_1(t) + 402\ V_2(t) + 16\ V_2(t\text{-T}) \quad (4.23)$$

$$x_5(t) = \tilde{x}_5(t) + 14.5\ W(t\text{-T}) - 24.5\ H(t\text{-T}) + 16\ V_2(t) \tag{4.24}$$

$$x_6(t) = \tilde{x}_6(t) \tag{4.25}$$

From equations (4.10) and (4.13), the transformed state-space equation is given by

$$x(t+\text{T}) = \mathbf{A}\,x(t) + \mathbf{B}\,u(t) + \mathbf{D}\,w(t) + \mathbf{E}\,v(t+\text{T}) + \mathbf{K} \tag{4.26}$$

and the output equation is obtained from equations (4.9), (4.22) and (4.25) as

$$y(t) = \mathbf{C}\,x(t) \tag{4.27}$$

We can confirm that the original state-space representation (4.8) and (4.9), the transformed state-space (4.26) and (4.27) and the transfer function equations (2.1) and (2.2) are equivalent to each other. This can be done by calculating the output responses using all three formats to establish that the three simulations are identical. These are calculated for the case when the model has settled to the zero input case.

To calculate the simulations, the initial condition for air temperature and relative humidity are assumed to be 20°C and 50%rh respectively, and the contribution of the external disturbances such as the laboratory temperature T_l, the outside air temperature T_o, the outside relative humidity H_o and the total solar irradiance S are constant at 20°C, 10°C, 70%rh and 0 Wm^{-2} respectively, and the white noise processes V_1 and V_2, and the constants k_1 and k_2 are absent.

For the transfer function method (section 2.3.1), we found that the responses converge to the steady state values of 9.9°C for temperature and 69.5%rh for relative humidity.

In the original state-space formulations, we calculate the responses from equations (4.8) and (4.9) where the normalised value of $\tilde{x}(0)$ for the above initial condition is given by

$$\tilde{x}(0) = \begin{bmatrix} 2.05 & 2.05 & 2.05 & -3.26 & -3.26 & -3.26 \end{bmatrix}^T \tag{4.28}$$

The simulated results via this state-space equation can easily be shown to give the same response as the transfer function method. In a similar way the transformed state-space representation can also be shown to give the same response. It should be noted that before the state-space method can be applied, the initial values of the state vector in the function should be calculated using equation (4.20) - (4.25) by assuming that the controlling inputs have not been applied. Identical output responses to those shown in Figure 2.3 were obtained for all the three methods and hence we can conclude equivalence of the approaches.

Next, we design a control system whereby the output is required to track the desired setpoints; we will use the pole placement method and modal control techniques to obtain the desired dynamic behaviour of the system and the final value theorem to calculate the feedforward matrix needed to achieve zero steady state error. We select two structures for the closed-loop control system, one using state feedback and the other using output feedback in achieving these objectives.

4.2. State-feedback design

In this section, our aim is to design a control system using state feedback where the outputs converge to required values. We have chosen a state feedback system (see for example Chen, 1984) as shown in Figure 4.1 where the state $x(t)$ is fedback to the input $u(t)$ via the feedback matrix **F**. The variable $r(t)$ denotes the reference set-point and **H** is a feedforward conversion matrix. We will determine the appropriate values of **F** and **H** so that the output response is critically damped and tracks the desired reference values; **F** will be obtained by using the pole-placement method and **H** by using the final value theorem (see for example Leigh, 1985).

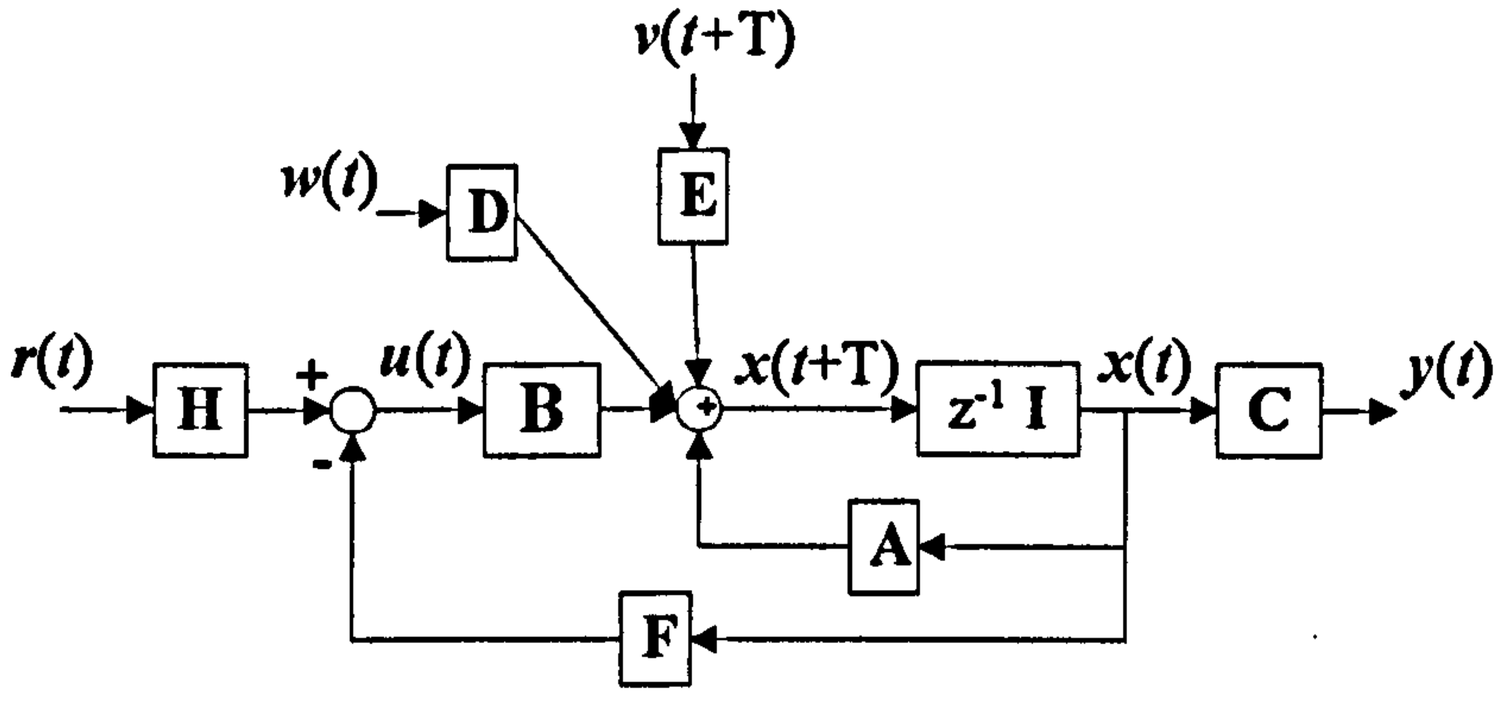

Figure 4.1: State feedback tracking system.

It is assumed that $r(t)$ is a step change from the steady state condition to a preset value and is given by

$$r(t) \equiv \begin{bmatrix} T_r(t) \\ H_r(t) \end{bmatrix}, \quad t \geq 0 \tag{4.29}$$

where T_r and H_r are the required values of the room temperature and relative humidity respectively.

From Figure 4.1, the controlling input is given by

$$\boldsymbol{u}(t) = -\mathbf{F}\,\boldsymbol{x}(t) + \mathbf{H}\,\boldsymbol{r}(t) \tag{4.30}$$

Since $\boldsymbol{u}$ is 3×1, $\boldsymbol{x}$ is 6×1 and $\boldsymbol{r}$ is 2×1, then we have that $\mathbf{F}$ is a 3×6 matrix if the feedback is applied to all three inputs and $\mathbf{H}$ is a 3×2 matrix if feedforward compensation is applied to both control loops. By substituting equations (4.30) into equation (4.26), we obtain the state equation of the closed-loop system as

$$\boldsymbol{x}(t+\mathrm{T}) = (\mathbf{A} - \mathbf{BF})\,\boldsymbol{x}(t) + \mathbf{BH}\,\boldsymbol{r}(t) + \mathbf{D}\,\boldsymbol{w}(t) + \mathbf{E}\,\boldsymbol{v}(t+\mathrm{T}) + \mathbf{K} \tag{4.31}$$

and the system output is given as in equation (4.27).

If we ignore the contributions of the external disturbances and the constants k_1 and k_2 are zero, then equation (4.31) reduces to a basic form of the state-space equations, namely,

$$\boldsymbol{x}(t+\mathrm{T}) = (\mathbf{A} - \mathbf{BF})\,\boldsymbol{x}(t) + \mathbf{BH}\,\boldsymbol{r}(t) \tag{4.32}$$

The simulation and analysis of this digital state-space representation can easily be performed via the *z*-transform method. By taking the *z* transforms of both sides of equation (4.32), substituting into equation (4.27) and assuming the initial conditions are zero, we obtain

$$\boldsymbol{Y}(z) = \mathbf{C}\,[z\mathbf{I} - (\mathbf{A} - \mathbf{BF})]^{-1}\mathbf{BH}\,\boldsymbol{R}(z)$$

$$= \boldsymbol{G}(z)\,\boldsymbol{R}(z) \tag{4.33}$$

where $\boldsymbol{G}(z) = \mathbf{C}\,[z\mathbf{I}_6 - (\mathbf{A} - \mathbf{BF})]^{-1}\mathbf{BH} \equiv \begin{bmatrix} G_{11}(z) & G_{12}(z) \\ G_{21}(z) & G_{22}(z) \end{bmatrix}$,

$$\boldsymbol{Y}(z) = \begin{bmatrix} T_c(z) \\ H_c(z) \end{bmatrix},\ \boldsymbol{R}(z) = \begin{bmatrix} T_r(z) \\ H_r(z) \end{bmatrix},$$

and $\mathbf{I}_6$ is a 6x6 identity matrix, G_{11}, G_{12}, G_{21} and G_{22} are the individual input/output polynomials. Equation (4.33) can easily be transformed into the time domain by the method of residues, and the solution is given by

$$y(k\mathrm{T}) = \sum_{i=1}^{6} \lim_{z \to p_i} (z - \rho_i)\ G(z)R(z)\ z^{k-1} \text{ for } k = 0, 1, 2, \ldots \qquad (4.34)$$

where ρ_i are the closed loop poles. Thus, the responses of the room temperature $T_c\ (k\mathrm{T})$ and the relative humidity $H_c\ (k\mathrm{T})$ are given by

$$\begin{aligned} T_c\ (k\mathrm{T}) = [\ & g_{111}\ \rho_1{}^k + g_{112}\ \rho_2{}^k + g_{113}\ \rho_3{}^k + g_{114}\ \rho_4{}^k + g_{115}\ \rho_5{}^k \\ & + g_{116}\ \rho_6{}^k\ ]T_r(k\mathrm{T}) + [\ g_{121}\ \rho_1{}^k + g_{122}\ \rho_2{}^k + g_{123}\ \rho_3{}^k \\ & + g_{124}\ \rho_4{}^k + g_{125}\ \rho_5{}^k + g_{126}\ \rho_6{}^k\ ]\ H_r(k\mathrm{T}) \qquad (4.35) \end{aligned}$$

$$\begin{aligned} H_c\ (k\mathrm{T}) = [\ & g_{211}\ \rho_1{}^k + g_{212}\ \rho_2{}^k + g_{213}\ \rho_3{}^k + g_{214}\ \rho_4{}^k + g_{215}\ \rho_5{}^k \\ & + g_{216}\ \rho_6{}^k\ ]\ T_r(k\mathrm{T}) + [\ g_{221}\ \rho_1{}^k + g_{222}\ \rho_2{}^k + g_{223}\ \rho_3{}^k \\ & + g_{224}\ \rho_4{}^k + g_{225}\ \rho_5{}^k + g_{226}\ \rho_6{}^k\ ]\ H_r(k\mathrm{T}) \qquad (4.36) \end{aligned}$$

for k = 1, 2, 3,... g_{111},..., g_{116}, g_{121},..., g_{126}, g_{211},..., g_{216} and g_{221},..., g_{226} are calculated from equation (4.34) by factorising the numerator and denominator of the individual input/output polynomials G_{11}, G_{12}, G_{21} and G_{22} respectively.

At steady state, we require the output to equal the reference input; hence by applying the final value theorem (see for example Leigh, 1985) to equation (4.33) and assuming that $r(t)$ is a unit step function at $t = 0$, we obtain

$$\lim_{z \to 1} \frac{z-1}{z} \{ G(z) \frac{z}{z-1} \} = \mathbf{I}_2$$

or

$$\mathbf{C}\ [\ \mathbf{I}_6\ - (\mathbf{A} - \mathbf{BF})\ ]^{-1}\mathbf{BH} = \mathbf{I}_2 \qquad (4.37)$$

where $\mathbf{I}_2$ is a 2x2 identity matrix.

From equation (4.37), the multiplier to the **H** matrix can be calculated; for convenience assume it is equal to

$$\mathbf{C}\,[\,\mathbf{I}_6 - (\mathbf{A} - \mathbf{BF})\,]^{-1}\mathbf{B} = \begin{bmatrix} s_{11} & s_{12} & s_{13} \\ s_{21} & s_{22} & s_{23} \end{bmatrix} \quad \text{and} \quad \mathbf{H} = \begin{bmatrix} h_{11} & h_{12} \\ h_{21} & h_{22} \\ h_{31} & h_{32} \end{bmatrix} \tag{4.38}$$

In equations (4.37) and (4.38), we can see that there are six unknown parameters from the **H** matrix which are required to be solved from 4 equations. These parameters can be calculated by assuming that two of them are known that is if h_{31} and h_{22} are known (arbitrary set), then h_{21}, h_{11}, h_{32} and h_{12} can be obtained equal to

$$h_{21} = (s_{21} - (s_{13}s_{21} - s_{11}s_{23})h_{31}) \Big/ (s_{12}s_{21} - s_{11}s_{22}) \tag{4.39}$$

$$h_{11} = (1 - s_{12}h_{21} - s_{13}h_{31}) \Big/ s_{11} \tag{4.40}$$

$$h_{32} = (s_{11} - (s_{11}s_{22} - s_{12}s_{21})h_{22}) \Big/ (s_{11}s_{23} - s_{13}s_{21}) \tag{4.41}$$

$$h_{12} = (1 - s_{22}h_{22} - s_{23}h_{32}) \Big/ s_{21} \tag{4.42}$$

From equation (4.32), the response of the closed-loop system is governed by the 6× 6 matrix **(A - BF)** whose eigenvalues depend on the feedback loops. There are 6 eigenvalues and these should satisfy $0 \le |\rho_i| \le 1$, $i = 1, 2,.., 6$, for stability (see for example Leigh, 1985).

4.2.1. Pole-placement design by state feedback

In this design method, the eigenvalues of **A - BF** of equation (4.32) can be arbitrarily assigned if and only if the pair **(A, B)** is completely controllable (see for example Kuo, 1992). For our system, since the rank of the 6x18 controllability matrix **S ≡ [B AB**

$\mathbf{A}^2\mathbf{B}$ . . $\mathbf{A}^5\mathbf{B}$] is 6, then the system is completely state controllable. The design problem is to find the feedback matrix **F** such that the control input u of equation (4.30) places the eigenvalues of **A - BF** at arbitrarily assigned positions in the z-plane.

Let us construct a single-input system from equation (4.26) by temporarily ignoring the contributions of the external disturbances w and v, and the constant **K**; it then becomes

$$x(t+T) = \mathbf{A}\,x(t) + \mathbf{B}^{\bullet}u(t) \tag{4.43}$$

where $\mathbf{B}^{\bullet}u = \mathbf{B}\,u$, and the 6x1 matrix $\mathbf{B}^{\bullet}$ is defined as

$$\mathbf{B}^{\bullet} = \mathbf{B}\,\mathbf{w} \tag{4.44}$$

where **w** is a vector of dimension (3x1) for our case. This vector must be chosen so that the pair (**A**, $\mathbf{B}^{\bullet}$) is controllable. Then, we can apply the feedback of the single-input, $\mathbf{F}^{\bullet}$, which is defined as

$$u(t) = -\mathbf{F}^{\bullet}\,x(t) \tag{4.45}$$

to place the eigenvalues of **A** - $\mathbf{B}^{\bullet}\,\mathbf{F}^{\bullet}$ at the same locations as those of **A - BF**. Then, the problem becomes that of designing the state feedback for the single-input system of equation (4.43). Once the feedback matrix $\mathbf{F}^{\bullet}$ is determined, **F** is given by

$$\mathbf{F} = \mathbf{w}\mathbf{F}^{\bullet} \tag{4.46}$$

since $\mathbf{B}\,\mathbf{F} = \mathbf{B}^{\bullet}\,\mathbf{F}^{\bullet}$.

It is apparent that in general **w** is not unique, and it only has to satisfy the condition that (**A, Bw**) is controllable. For our case, let us assume that $\mathbf{w} = [10 \quad 10 \quad 1]^T$, it is found that the determinant of controllability matrix $\mathbf{S} \equiv \left|\mathbf{B}^{\bullet} \quad \mathbf{A}\mathbf{B}^{\bullet} \quad .. \quad \mathbf{A}^5\mathbf{B}^{\bullet}\right| = -0.47 \neq 0$ and is therefore nonsingular. Thus, the pair (**A**, $\mathbf{B}^{\bullet}$) is controllable. The characteristic equation of the open-loop system is given by

$$|z\mathbf{I}_6 - \mathbf{A}| = z^6 - 3.15\,z^5 + 3.70\,z^4 - 1.96\,z^3 + 0.43\,z^2 - 0.02\,z + 0.0004$$

$$\equiv z^6 + a_6\,z^5 + a_5\,z^4 + a_4\,z^3 + a_3\,z^2 + a_2\,z + a_1 \qquad (4.47)$$

If the desired poles of the closed-loop system are distinct at say $\rho_i = 0.4, 0.5, 0.6, 0.7, 0.8$ and 0.9 for stability of the system, then the characteristic equation of $\mathbf{A} - \mathbf{B}^{*}\,\mathbf{F}^{*}$ becomes

$$|z\mathbf{I}_6 - \mathbf{A} + \mathbf{B}^{*}\,\mathbf{F}^{*}| = (z - 0.4)(z - 0.5)(z - 0.6)(z - 0.7)(z - 0.8)(z - 0.9)$$

$$\equiv z^6 + \alpha_6\,z^5 + \alpha_5\,z^4 + \alpha_4\,z^3 + \alpha_3\,z^2 + \alpha_2\,z + \alpha_1 \qquad (4.48)$$

which is equal to

$$|z\mathbf{I}_6 - \mathbf{A} + \mathbf{B}^{*}\,\mathbf{F}^{*}| = z^6 - 3.90\,z^5 + 6.25\,z^4 - 5.27\,z^3 - 2.46\,z^2$$

$$- 0.60\,z + 0.06 \qquad (4.49)$$

The elements of $\mathbf{F}^{*}$ can be calculated via the formula:

$$\mathbf{F}^{*} = [(\mathbf{M}\,\mathbf{S}^{T})^{-1}\,(\alpha - a)]^{T} \qquad (4.50)$$

which is of dimension 1x6. The detailed derivation of this formula can be found in Kuo (1992).

The parameters on the right-hand side of equation (4.50) when applied to our system with the prescribed poles become

$$\mathbf{M} = \begin{bmatrix} 1 & 0 & 0 & 0 & 0 & 0 \\ -3.15 & 1 & 0 & 0 & 0 & 0 \\ 3.70 & -3.15 & 1 & 0 & 0 & 0 \\ -1.96 & 3.70 & -3.15 & 1 & 0 & 0 \\ 0.43 & -1.96 & 3.70 & -3.15 & 1 & 0 \\ -0.02 & 0.43 & -1.96 & 3.70 & -3.15 & 1 \end{bmatrix},$$

$$\alpha = [\,-3.90 \;\; 6.25 \;\; -5.27 \;\; -2.46 \;\; -0.60 \;\; 0.06\,]^{T}$$

and

$$a = [\,-3.15 \;\; 3.70 \;\; -0.96 \;\; 0.43 \;\; -0.02 \;\; 0.0004\,]^{T}$$

Substituting these values into equation (4.50), we find that

$$\mathbf{F}^{*} = [\ 0.20\ \ -1.87\ \ 2.59\ \ 0.02\ \ 0.08\ \ -0.25\ ]$$

Applying equation (4.46), the feedback gain becomes

$$\mathbf{F} \equiv \mathbf{w}\mathbf{F}^{*} = \begin{bmatrix} 2.00 & -18.70 & 25.90 & 0.20 & 0.80 & -2.50 \\ 2.00 & -18.70 & 25.90 & 0.20 & 0.80 & -2.50 \\ 0.20 & -1.87 & 2.59 & 0.02 & 0.08 & -0.25 \end{bmatrix} \tag{4.51}$$

The validity of the obtained feedback matrix **F** in equation (4.51) can be performed by calculating the eigenvalues of matrix **A - BF**, and for this case, it is found that these eigenvalues are identical to the desired poles.

Another method in the pole-placement design for state feedback is to use a robust design (Kautsky et al., 1985) by using the 'place' function in MATLAB Control Toolbox (1994) to calculate the feedback matrix **F**. For identical values of the desired closed-loop poles, the feedback matrix via this approach is found to be

$$\mathbf{F} = \begin{bmatrix} -0.73 & 23.00 & -36.52 & 0.07 & -1.93 & 3.84 \\ -0.95 & 29.89 & -47.44 & 0.10 & -2.50 & 4.98 \\ -0.60 & 18.75 & -29.77 & 0.06 & -1.57 & 3.13 \end{bmatrix} \tag{4.52}$$

The performance of the closed-loop system using the pole-placement design is studied by assuming that the external disturbances $w(t)$ and the white noise processes $v(t)$ are not present in the system, and then calculating the state variable $x(t)$, output $y(t)$ and input $u(t)$ responses by using equation (4.32), (4.27) and (4.30) respectively. As an example, let us consider for the closed-loop system with poles at 0.60, 0.65, 0.70, 0.75, 0.80 and 0.95, the desired set-points T_r and H_r at 25°C and 50%rh respectively and the system is at steady state conditions initially, i.e. the controlling inputs were all 'off', i.e. $W(0) = C(0) = H(0) = 0$ kW and the room temperature T_c and relative humidity H_c

respectively, are at 9.9°C and 69.5%rh. In this way the initial state $x(0)$ is calculated by using equations (4.20) - (4.25); It is found that the normalised value of $x(0)$ has the value

$$x(0) = [757.16 \;\; 16.09 \;\; -7.95 \;\; -370.17 \;\; 6.13 \;\; 16.04]^T \tag{4.53}$$

The feedback matrix **F** is calculated by using the 'place' routine and the feedforward matrix, **H**, is calculated from the final value theorem. If we choose $h_{31} = 0.5$ and $h_{22} = 2.5$ then the remaining four elements of **H** can be calculated from equations (4.38) - (4.42) and hence,

$$\mathbf{H} = \begin{bmatrix} 0.65 & 2.05 \\ 0.34 & 2.50 \\ 0.50 & 1.69 \end{bmatrix}$$

The zeros of the individual transfer functions $G_{11}(z)$, $G_{12}(z)$, $G_{21}(z)$ and $G_{22}(z)$ for the **F** in equation (4.52) can be calculated from equation (4.33) and they are found to be as follows:

$G_{11}(z)$: 1.55, 0.91±0.17i, 0.69±0.09i.

$G_{12}(z)$: 1.00, 0.94, 0.76, 0.69, 0.51.

$G_{21}(z)$: 1.00, 0.75±0.11i, 0.59, -0.32.

$G_{22}(z)$: 1.01, 0.94, 0.76, 0.69, 0.59.

where i = $\sqrt{-1}$. We can see that the transfer function $G(z)$ of this system has nonminimum-phase problem where some of the zeros are greater than 1.

The simulated results are shown in Figure 4.2 where we can see that although the system outputs are regulated at the desired set-points at the steady state situation, but a peculiar performance is obtained where all the three control inputs are negatively used to produce a large overshoot of the relative humidity. This is due to the effects of the

nonminimum-phase of the transfer function which is not very easy to control (Clarke, 1984). This situation is clearly not allowed due to the constraints on the inputs.

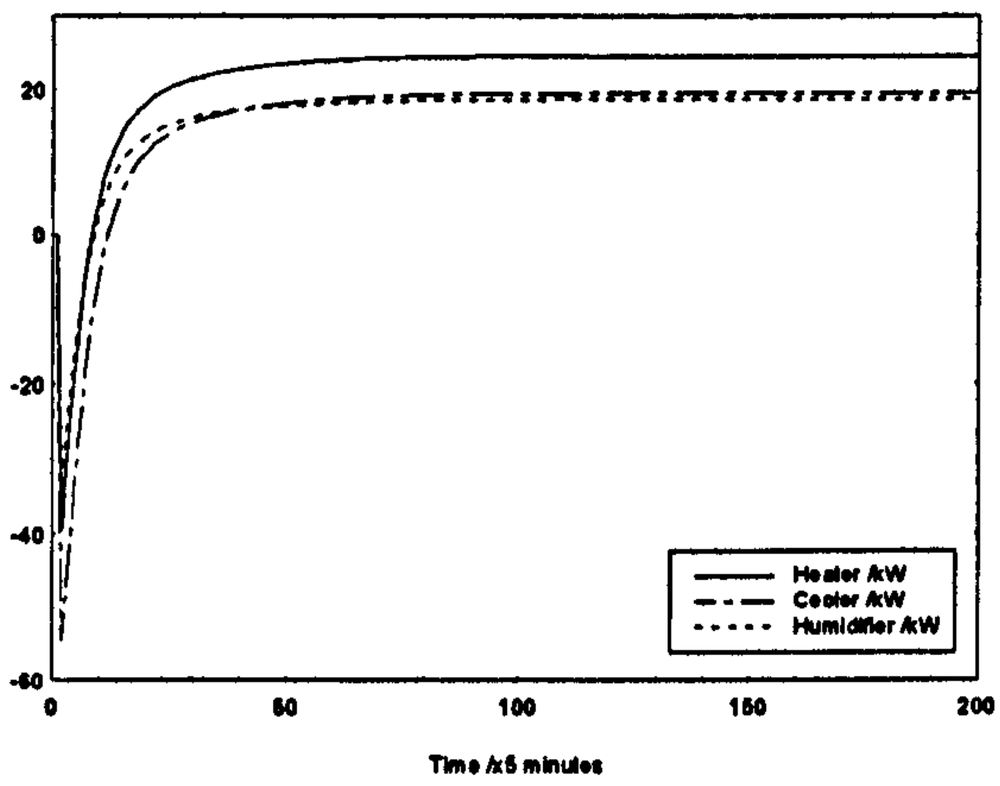

a) Control inputs

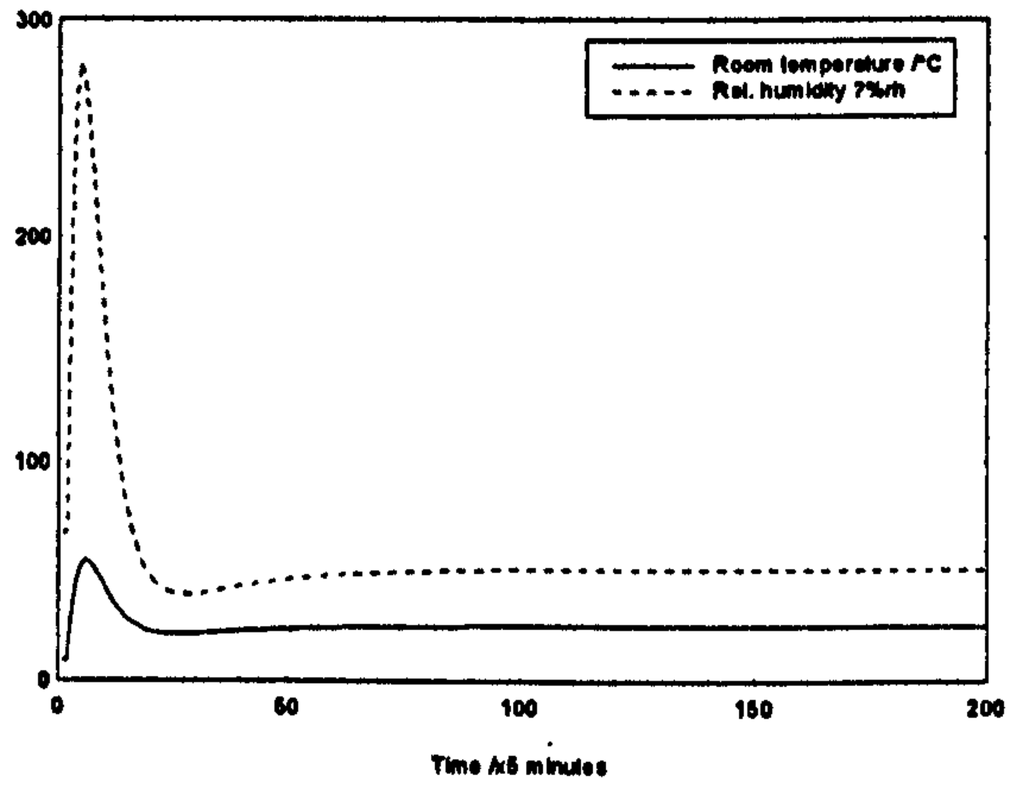

b) System outputs

Figure 4.2: Control performance of the state feedback using pole-placement robust design to calculate **F**

If we were to include the climatic disturbances $w(t)$ and other influences $v(t)$ into the system, equations (4.27), (4.30) and (4.31) can be used to recalculate the system performance; when this is done it is found that these terms only deteriorate the system performance and there is now steady state error as shown in Figure 4.3. A set of actual climatic data (Loveday and Virk, 1992b) as shown in Figure 4.4 is used for $w(t)$, and a pseudo random binary sequences (PRBS) generated using six shift registers (see for example Godfrey, 1980) switching between ± 0.1 is used for $v(t)$.

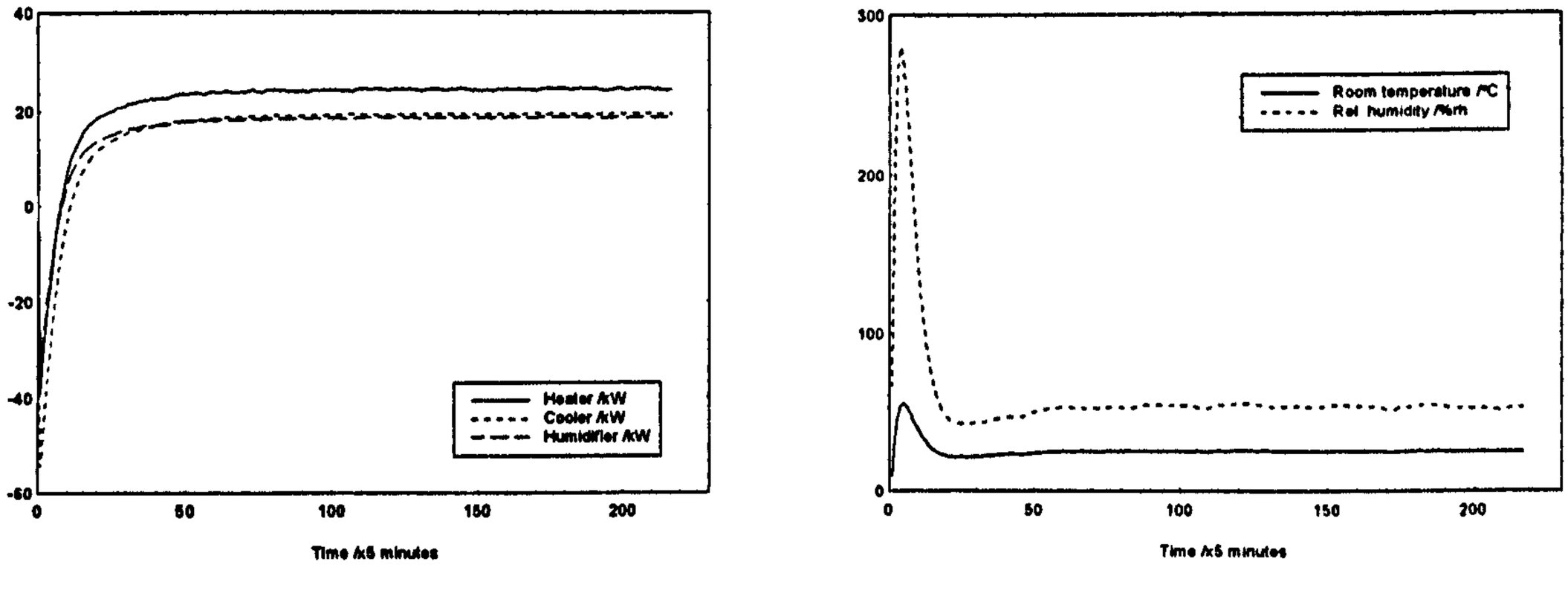

a) Control inputs b) System outputs

Figure 4.3: Control performance of the state feedback with disturbance and noise present

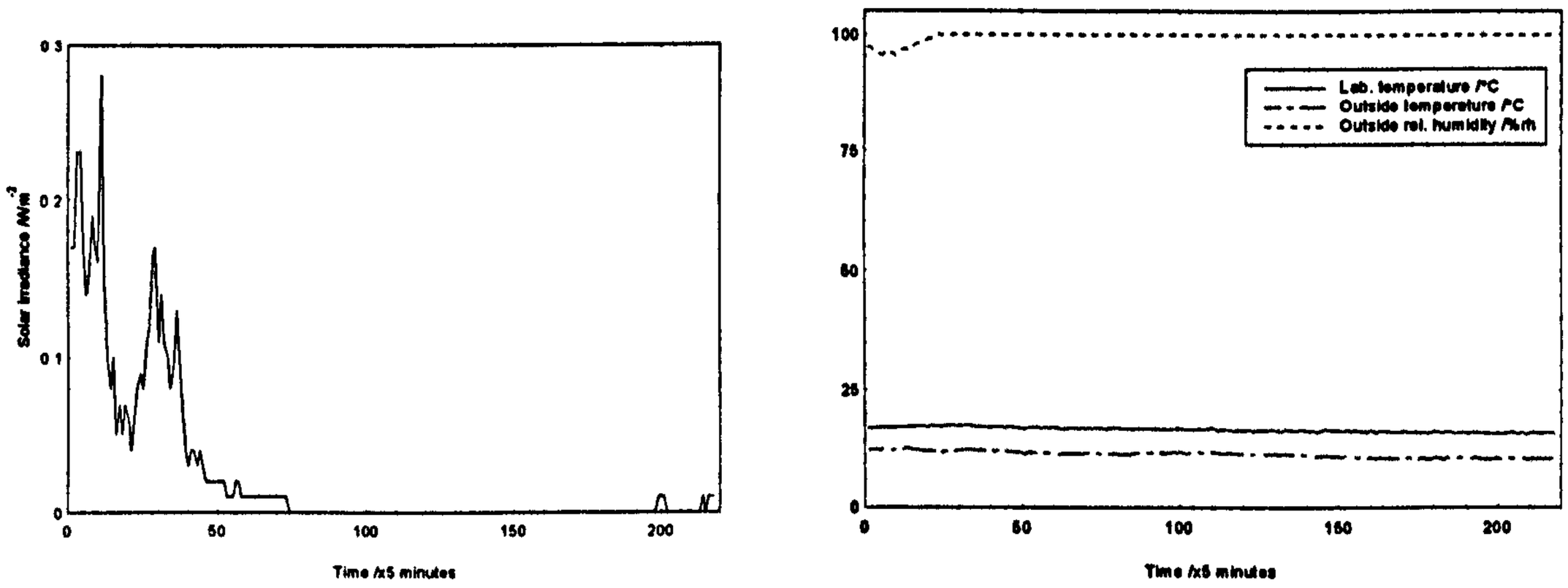

a) Solar irradiance b) other climatic disturbances

Figure 4.4: Actual climatic data used in the simulation studies

The results do not make any sense in practice, since all the three control inputs are beyond the permitted ranges and they are 'fighting one another", that is excessive heating is used because the cooling is excessive and vice versa, etc. This type of result is also obtained when **F** is calculated using equations (4.46) and (4.50). Furthermore, we also found that the magnitude of the control inputs are determined by the desired pole

locations; the near the locations are to the origin in *z*-plane, the larger the required control inputs and the larger the 'overshoot', and vice versa. In another words, if we require a fast output response then a large control signal is needed but the priority criteria as to which control signals should be used is not clearly shown by this methodology and hence the above conflicts; this fact is important to highlight in actual situations in order that the total energy consumption is minimised.

We notice that the two techniques of pole-placement design presented here although commonly used, do not consider the constraints on the control inputs; the methods are however extremely powerful for designing control systems with the desired closed-loop poles. In order for arbitrary pole placement to be possible, the system must be completely state controllable and the magnitude of the control input must be unbounded (Ogata, 1987). Our control inputs, namely, the heater W, cooler C and humidifier H have limits of 0 - 5.0, 0 - 2.7 and 0 - 2.6 kilowatts respectively, and hence the normal pole-placement design for calculating the feedback matrix **F** is not applicable in our situation. In another word, the closed-loop poles ρ_i can not be simply chosen to lie at any arbitrary locations in *z*-plane. This is obvious since we can not expect infinitely fast behaviour when we have finite limits on the control signals.

Furthermore when we are dealing with mutli-input applications it is not obvious which input should be used to modify which eigenvalue. In theory if the system is controllable using only one input then feedback is required only on this loop but in practice there are constraints present on most control systems and these restrict the general results which are possible. For example using the 'place' function leads to very peculiar results which look good at a quick glance but when they were studied more closely it transpires that the control inputs were being used incorrectly - the negative of

the heating input is used for the cooling and the negative of the cooling input is used for the heating. Large signals for the heating and the cooling were again being displayed to give rapid response and as already mentioned there was considerable wastage in energy cancellation of the heating with cooling inputs. The 'place' routine merely attempts to achieve the desired pole locations and no sense is made of the final result. Clearly, in practice we do not have negative heating or negative cooling signals and the strategy can not be implemented.

In order that sensible state-feedback designs can be carried out in multivariable application it is necessary to use an iterative design procedure where each individual control loop is closed in sequence and the most appropriate eigenvalues set at each stage. Modal control offers a suitable methodology in this respect and we discuss it next.

4.2.2. Multistage design procedure for state feedback

In view of the above problems with the standard state feedback method we discuss the multi-stage procedure presented in Porter and Crossley (1972). This approach utilises the mode controllability matrix Φ at each stage to determine the number of modes to be controlled by each control loop. The details of the method are now presented.

First of all, the input matrix **B** is partitioned into its elemental column vectors; for our case this is as follows

$$\mathbf{B} = [\, \mathbf{b}_1 \;\; \mathbf{b}_2 \;\; \mathbf{b}_3 \,] \tag{4.54}$$

as there are three inputs. The state equation (4.26) with the input terms partitioned in this way become

$$x(t+\mathrm{T}) = \mathbf{A}\,x(t) + \mathbf{b}_1 W(t) + \mathbf{b}_2 C(t) + \mathbf{b}_3 H(t) + \mathbf{D}\,w(t) + \mathbf{E}\,v(t+\mathrm{T}) + \mathbf{K}$$

or

$$x(t+\mathrm{T}) = \mathbf{A}\,x(t) + \sum_{i=1}^{3} \mathbf{b}_i \;\; u_i(t) + \mathbf{D}\,w(t) + \mathbf{E}\,v(t+\mathrm{T}) + \mathbf{K} \qquad (4.55)$$

where $u_1 = W$, $u_2 = C$ and $u_3 = H$.

In this section, our aim is to design a control law for which we can alter one or more eigenvalues of the plant matrix namely **A**, to the desired eigenvalues of the closed-loop system, provided that the appropriate modes are controllable. The design method involved in this control law, known as multi-stage modal control, will be applied to our system with the structure as shown in Figure 4.1, to calculate the feedback matrix **F**.

Let us define the control signal as

$$u_i(t) = \sum_{j=1}^{n} K_j \mathbf{v}_j^{(i)T}\, x(t), \;\; i = 1, 2, \ldots, r. \qquad (4.56)$$

where r is the number of control inputs (equal to three in our case), $\mathbf{v}_j^{(i)}$ is the j-th eigenvector of the transposed plant matrix ($= \psi_i^T$), associated with the control input u_i, K_j is the j-th proportional controller gain and n is the number of modes of an appropriate selection for the i-th control input u_i.

By substituting the expression for u_i given in equation (4.56) into equation (4.55) we then have the effect of the control input u_i to change the plant matrix ψ_i to the new plant matrix ψ_{i+1}, which is given by

$$\psi_{i+1} = \psi_i + \mathbf{b}_i \sum_{j=1}^{n} K_j \mathbf{v}_j^{(i)T} \quad (i = 1, 2, \ldots, r\text{-}1) \qquad (4.57)$$

where

$$\psi_1 = \mathbf{A} \qquad (4.58)$$

Therefore, the effect of using n eigenvectors $\mathbf{v}_j^{(i)}$ (j = 1, 2, ..., n) is to change the eigenvalues λ_j of ψ_i to some new values ρ_j of ψ_{i+1}, and the eigenvectors $\mathbf{u}_j$ of ψ_i to some corresponding new eigenvectors $\mathbf{w}_j$ of ψ_{i+1}, leaving the remaining (m - n) pairs of eigenvalues and eigenvectors of the plant matrix of the uncontrolled system unchanged. For our case, m = 6, which is the number of eigenvalues of the plant matrix ψ_i .

Let us we define $u_i(t) \equiv \mathbf{g}_i^T x(t)$ then from equation (4.56), we have

$$\mathbf{g}_i^T = \sum_{j=1}^{n} K_j \mathbf{v}_j^{(i)T} \tag{4.59}$$

where $\mathbf{g}_i^T$ is the i-th feedback vector associated with u_i.

The proportional controller gain K_j can be derived in term of the eigenvalues of ψ_i and the required eigenvalues of ψ_{i+1} of i-th input, then equation (4.59) becomes

$$\mathbf{g}_i^T = \sum_{j=1}^{n} \frac{\prod_{k=1}^{n} (\rho_k - \lambda_j) \mathbf{v}_j^{(i)T}}{\Phi_k^{(i)} \prod_{k=1, k\neq j}^{n} (\lambda_k - \lambda_j)} \tag{4.60}$$

where ρ_k (k =1, 2,..., n) are the desired closed-loop poles of the new plant matrix ψ_{i+1}, λ_i (i = 1, 2,..,6) are the eigenvalues of plant matrix **A**, $\Phi_k^{(i)}$ is the k-th element of the appropriate mode-controllability matrix, $\mathbf{\Phi}_i$, and n is obtained on the basis of the magnitudes of the elements of $\mathbf{\Phi}_i$, in view of the form of equation (4.60).

The vector $\mathbf{g}_i^T$ is related to the feedback matrix **F** via equations (4.30) and (4.56) and is given by

$$\mathbf{F} = -\left[\mathbf{g}_1^T \quad \mathbf{g}_2^T \quad \mathbf{g}_3^T\right]^T \tag{4.61}$$

The $\mathbf{v}_j^{(i)}$ vectors are the columns of the modal matrix, $\mathbf{V}_i$ of equation (4.60), which is defined as the eigenvector of the transposed plant matrix (= ψ_i^T), associated with the

i-th stage of the design procedure. By substituting $\mathbf{g}_i^T$ from equation (4.59) into equation (4.57), we have

$$\psi_{i+1} = \psi_i + \mathbf{b}_i \quad \mathbf{g}_i^T \quad (i = 1, 2, \ldots, r\text{-}1) \tag{4.62}$$

The mode-controllability matrix, Φ_i, associated with the i-th stage of the design procedure is given by the equation

$$\Phi_i = \mathbf{V}_i^T \ \mathbf{B}_i \quad (i = 1, 2, \ldots, r) \tag{4.63}$$

It is well known (see for example Porter and Crossley, 1972) that if we premultiply the eigenvector of ψ_i (= $\mathbf{U}_i$) by the transposed eigenvector of ψ_i (= $\mathbf{V}^T$) we will obtain an identity matrix of order equal to rank of ψ_i; in mathematical form this can be written as

$$\mathbf{V}_i^T \ \mathbf{U}_i = \mathbf{I}_6 \tag{4.64}$$

where

$$\mathbf{V}_i = \left[\mathbf{v}_1^{(i)} \quad \mathbf{v}_2^{(i)} \quad \mathbf{v}_3^{(i)} \quad \mathbf{v}_4^{(i)} \quad \mathbf{v}_5^{(i)} \quad \mathbf{v}_6^{(i)}\right] \text{ for } i = 1, 2, 3$$

and

$$\mathbf{U}_i = \left[\mathbf{u}_1^{(i)} \quad \mathbf{u}_2^{(i)} \quad \mathbf{u}_3^{(i)} \quad \mathbf{u}_4^{(i)} \quad \mathbf{u}_5^{(i)} \quad \mathbf{u}_6^{(i)}\right] \text{ for } i = 1, 2, 3$$

The relationship in equation (4.64) is important to confirm first before proceeding to the next stage of the design procedure. If this relation does not comply (due to incorrect normalisation of the eigenvectors) then further rescaling of the **V** matrix with respect to the **U** matrix needs to be carried out.

The eigenvalues λ_i of **A** are calculated and are equal to 0.99, 0.94, 0.61, 0.54, 0.03 and 0.04. It is desired to move these eigenvalues to the required locations as well as ensuring that the output will track the reference inputs.

As an example, let us consider the desired locations, ρ_i, are at 0.5, 0.6, 0.7, 0.8, 0.85 and 0.9 and the modal control design stage input sequence is $\{W, C, H\}$, that is the heater input feedback design is carried out first followed by the cooler and then the humidifier feedback design is carried out last. In this case the mode-controllability matrix Φ_1 is obtained from equation (4.63) and is equal to

$$\Phi_1 = \begin{bmatrix} 0.25 & -0.22 & -0.07 \\ -0.038 & 0.32 & -0.92 \\ 1.89 & -6.38 & 2.28 \\ -6.74 & -11.64 & 14.23 \\ 365.99 & -345.85 & 93.71 \\ -437.83 & -209.75 & 853.15 \end{bmatrix}.$$

We can determine the modes to be controlled by the heater by examining the rows of the Φ_1 matrix. It is clearly indicated that the first and fifth modes would be chosen since the first and the fifth elements in the first column are dominant, i.e.

$$|0.25| > |-0.22|,\ |0.25| > |-0.07|$$

and

$$|365.99| > |-345.85|,\ |365.99| > |93.71|.$$

Therefore, the W input should be used to move the first and fifth eigenvalues $\lambda_1 = 0.99$ and $\lambda_5 = 0.03$ to the required values $\rho_1 = 0.5$ and $\rho_5 = 0.85$ respectively. Thus, by using equation (4.60), we can calculate the feedback vector, $\mathbf{g}_1$, which is given by

$$\mathbf{g}_1^T = \frac{(\rho_1 - \lambda_1)(\rho_5 - \lambda_1)\mathbf{v}_1^{(1)T}}{0.25(\lambda_5 - \lambda_1)} + \frac{(\rho_1 - \lambda_5)(\rho_5 - \lambda_5)\mathbf{v}_5^{(1)T}}{365.99(\lambda_1 - \lambda_5)}$$

$$= [-0.05 \quad 1.48 \quad -2.36 \quad 0.01 \quad -0.18 \quad 0.34] \qquad (4.65)$$

After completing the first stage of the design, equation (4.62) can be used to calculate the modified plant matrix, ψ_2 by using

$$\psi_2 = \mathbf{A} + \mathbf{b}_1 \mathbf{g}_1^T \qquad (4.66)$$

and it's eigenvalues should be equal to $[\rho_1 \quad \lambda_2 \quad \lambda_3 \quad \lambda_4 \quad \rho_5 \quad \lambda_6]$.

A similar procedure as above, is repeated for the second stage of the design to calculate $\mathbf{g}_2^T$. The mode controllability matrix Φ_2 is found to equal:

$$\Phi_2 = \begin{bmatrix} -868.84 & 166.56 \\ 0.25 & -0.93 \\ -18.86 & 4.19 \\ -96.30 & 5.11 \\ 213.14 & 3.79 \\ -627.79 & 966.24 \end{bmatrix}.$$

Since input u_1, i.e. the heater, has already been used to control the first and the fifth modes of the system, then only the second, third, fourth and sixth rows of Φ_2 are relevant; examining these rows indicates that the third and fourth modes should be chosen to be controlled by input u_2 i.e. the cooler, by moving the λ_3 and λ_4 eigenvalues of **A** matrix, to the required locations $\rho_3 = 0.7$ and $\rho_4 = 0.8$ respectively. Following the procedure as for the first iteration the gain vector $\mathbf{g}_2^T$ is calculated as

$$\mathbf{g}_2^T = \frac{(\rho_3 - \lambda_3)(\rho_4 - \lambda_3)\mathbf{v}_3^{(2)T}}{-18.86(\lambda_4 - \lambda_3)} + \frac{(\rho_3 - \lambda_4)(\rho_4 - \lambda_4)\mathbf{v}_4^{(2)T}}{-96.3(\lambda_3 - \lambda_4)}$$

$$= [-0.06 \quad 1.75 \quad -2.75 \quad 0.01 \quad -0.16 \quad 0.34]. \tag{4.67}$$

and the modified plant matrix becomes

$$\Psi_3 = \Psi_2 + \mathbf{b}_2 \mathbf{g}_2^T \tag{4.68}$$

and it's eigenvalues are $[\rho_1 \quad \lambda_2 \quad \rho_3 \quad \rho_4 \quad \rho_5 \quad \lambda_6]$.

Repeating the design procedure for the third control input, u_3, we find

$$\Phi_3 = \begin{bmatrix} -146.26 \\ 0.85 \\ 246.32 \\ -458.56 \\ -240.62 \\ -975.89 \end{bmatrix}$$

and change the remaining modes, namely the second and sixth modes. Here $\lambda_2 = 0.94$ and $\lambda_6 = 0.04$ need to be moved to the required locations $\rho_2 = 0.6$ and $\rho_6 = 0.9$ respectively by the humidifier, u_3, and $\mathbf{g}_3^T$ is given by

$$\mathbf{g}_3^T = \frac{(\rho_2 - \lambda_2)(\rho_6 - \lambda_2)\mathbf{v}_2^{(3)T}}{0.85(\lambda_6 - \lambda_2)} + \frac{(\rho_2 - \lambda_6)(\rho_6 - \lambda_6)\mathbf{v}_6^{(3)T}}{-975.89(\lambda_2 - \lambda_6)}$$

$$= \begin{bmatrix} -0.03 & 0.87 & -1.36 & 0 & -0.03 & 0.09 \end{bmatrix}. \qquad (4.69)$$

By comparing the closed-loop state equation (4.31) and the modified plant matrix of the final stage design ψ, we can confirm that this plant matrix should be equal to the characteristic matrix of the closed-loop system, $\mathbf{A} - \mathbf{BF}_{WCH}$, that is

$$\psi \equiv \psi_3 + \mathbf{b}_3\, \mathbf{g}_3^T = \mathbf{A}\text{-}\mathbf{BF}_{WCH} \qquad (4.70)$$

where $\mathbf{F}_{WCH}$ is the feedback matrix, which is obtained by using the relationship in equation (4.61) and the values in equations (4.65), (4.67) and (4.69).

$$\mathbf{F}_{WCH} = \begin{bmatrix} 0.05 & -1.48 & 2.36 & -0.01 & 0.18 & -0.34 \\ 0.06 & -1.75 & 2.75 & -0.01 & 0.16 & -0.34 \\ 0.03 & -0.87 & 1.366 & 0 & 0.03 & -0.09 \end{bmatrix}. \qquad (4.71)$$

To ensure the matrix $\mathbf{F}_{WCH}$ is valid, the eigenvalues of ψ are calculated from equation (4.70) and they are found to be identical to the desired locations, i.e. equal to 0.5, 0.6, 0.7, 0.8, 0.85 and 0.9.

Alternatively, there are 5 other permutations of the three control input which can be used to obtain **F**, namely the sequences $\{W, H, C\}$, $\{C, W, H\}$, $\{C, H, W\}$, $\{H, W, C\}$

and $\{H, C, W\}$. In other words the order in which the control input designs are carried out alter the solution obtained. To illustrate this we discuss the design procedure for the $\{C, W, H\}$ sequence. We can apply the same strategy as above, for which the closed-loop poles, ρ_3 and ρ_4 are used to calculate $\mathbf{g}_2^T$ using the cooler, ρ_1 and ρ_5 are for $\mathbf{g}_1^T$ using the heater and ρ_2 and ρ_6 are for $\mathbf{g}_3^T$ using the humidifier. For this sequence, the eigenvector of the first stage, $\mathbf{V}_1$ is identical to the previous example, i.e. equal to the eigenvectors of $\mathbf{A}^T$ and the mode controllability vector θ_1 is given by

$$\theta_1 = \mathbf{V}_1^T \mathbf{b}_2 = [\,-0.22 \;\; 0.32 \;\; -6.38 \;\; -11.64 \;\; -345.85 \;\; -209.75\,]^T$$

and the feedback vector for the cooler $\mathbf{g}_2^T$ and the modified plant matrix ψ_2 respectively, are given by

$$\mathbf{g}_2^T = \frac{(\rho_3 - \lambda_3)(\rho_4 - \lambda_3)\mathbf{v}_3^{(1)T}}{-6.38(\lambda_4 - \lambda_3)} + \frac{(\rho_3 - \lambda_4)(\rho_4 - \lambda_4)\mathbf{v}_4^{(1)T}}{-11.64(\lambda_3 - \lambda_4)}$$

$$= [0.03 \quad -1.01 \quad 1.60 \quad 0 \quad 0.11 \quad -0.22]$$

and

$$\psi_2 = \mathbf{A} + \mathbf{b}_2 \mathbf{g}_2^T$$

For the second stage of the design, these parameters are given by

$$\theta_2 = \mathbf{V}_2^T \mathbf{b}_1 = [\,0.38 \;\; -1.30 \;\; -198.2 \;\; -365.4 \;\; 519.3 \;\; -344.5\,]^T$$

$$\mathbf{g}_1^T = \frac{(\rho_1 - \lambda_1)(\rho_5 - \lambda_1)\mathbf{v}_1^{(2)T}}{0.38(\lambda_5 - \lambda_1)} + \frac{(\rho_1 - \lambda_5)(\rho_5 - \lambda_5)\mathbf{v}_5^{(2)T}}{519.3(\lambda_1 - \lambda_5)}$$

$$= [-0.02 \quad 0.47 \quad -0.45 \quad 0.01 \quad -0.20 \quad 0.20]$$

$$\psi_3 = \psi_2 + \mathbf{b}_1 \mathbf{g}_1^T$$

and for the final stage of the design, we have

$$\theta_3 = \mathbf{V}_3^T \mathbf{b}_3 = [\,571.0 \;\; -2.3 \;\; -1172.6 \;\; -4042.4 \;\; -2371.2 \;\; 598.4\,]^T$$

$$\mathbf{g}_3^T = \frac{(\rho_2 - \lambda_2)(\rho_6 - \lambda_2)\mathbf{v}_2^{(3)T}}{-2.3(\lambda_6 - \lambda_2)} + \frac{(\rho_2 - \lambda_6)(\rho_6 - \lambda_6)\mathbf{v}_6^{(3)T}}{598.4(\lambda_2 - \lambda_6)}$$

$$= \begin{bmatrix} -0.02 & 0.37 & -0.45 & 0 & -0.13 & 0.16 \end{bmatrix}$$

$$\psi \equiv \psi_3 + \mathbf{b}_3\, \mathbf{g}_3^T = \mathbf{A}\text{-}\mathbf{B}\mathbf{F}_{CWH}$$

where $\mathbf{F}_{CWH}$ is the feedback matrix for the input sequence $\{C, W, H\}$ is equal to

$$\mathbf{F}_{CWH} = \begin{bmatrix} -0.03 & 1.01 & -1.60 & 0 & -0.11 & 0.22 \\ 0.02 & -0.47 & 0.45 & -0.01 & 0.20 & -0.20 \\ 0.02 & -0.37 & 0.45 & 0 & 0.13 & -0.16 \end{bmatrix}. \qquad (4.72)$$

Once again, it was found that the required poles of the closed-loop system, $\mathbf{A} - \mathbf{B}\mathbf{F}_{CWH}$, are equal to the desired locations.

Similarly, if we choose the input sequence as $\{H, C, W\}$ then the modified plant matrices become

$$\psi_2 = \mathbf{A} + \mathbf{b}_3\, \mathbf{g}_3^T \quad , \psi_3 = \psi_2 + \mathbf{b}_2 \mathbf{g}_2^T \text{ and } \psi \equiv \psi_3 + \mathbf{b}_1 \mathbf{g}_1^T = \mathbf{A}\text{-}\mathbf{B}\mathbf{F}_{HCW} \qquad (4.73)$$

and the feedback matrix, $\mathbf{F}_{HCW}$ in equation (4.67) is different from $\mathbf{F}_{WCH}$ and $\mathbf{F}_{CWH}$, although the poles of the closed-loop system are identical to the desired locations.

By using the feedback matrix **F** from one of these input sequences and assuming that the initial conditions and the desired setpoints are identical to the example in the pole-placement design (section 4.2.1), we can calculate the output response $y(t)$ from the state equations (4.31) for the system with disturbances, and equation (4.32) for the system without disturbances, and the output equation (4.27). The control input $u(t)$ is calculated from equation (4.30) where the feedforward matrix **H** is obtained from the final value theorem (equations (4.38) - (4.42)). It is straightforward to deduce that a suitable value of **H** for the feedback matrix $\mathbf{F}_{WCH}$ is

$$\mathbf{H} = \begin{bmatrix} 0.98 & 0.05 \\ 1.10 & 0.10 \\ 0.60 & 0.16 \end{bmatrix} \tag{4.74}$$

The zeros of the individual transfer functions $G_{11}(z)$, $G_{12}(z)$, $G_{21}(z)$ and $G_{22}(z)$ for $\mathbf{F}_{WCH}$ and the above $\mathbf{H}$ can be calculated from equation (4.33) and they are found to be equal to:

$G_{11}(z)$: 1.18, 0.91, 0.90, 0.48±0.06i.

$G_{12}(z)$: 0.80±0.22i, 1.00, 0.89, 0.07.

$G_{21}(z)$: 1.00, 0.89, 0.79, 0.66, 0.48.

$G_{22}(z)$: -2.10, 0.91±0.05i, 0.79, 0.67.

where i = √-1, and their poles equal to 0.50, 0.60, 0.70, 0.80, 0.85 and 0.9. We can see that the transfer function $G(z)$ of this system has nonminimum-phase problem which is not easy to control.

The simulated results for the input sequence $\{W, C, H\}$ are shown in Figure 4.5 where we can see that the responses are reasonable for steady state conditions, but the control signal values exceed the limits near startup. It is also seen that a peculiar behaviour of closed-loop system takes place during initial transient phase whereby a lot of energy is wasted to produce a large negative relative humidity reading followed by tracking to the setpoints. Furthermore, this type of problem cannot be overcome by simply selecting the desired poles ρ_i to fall within [0, 1] in the z-plane; this is due to the way the multi-stage design is calculating the feedback matrix $\mathbf{F}$ without considering the constraints on the controlling inputs and the strategy to optimise the energy. It was also found that the required levels of the input signals to maintain a zero steady state errors for the room air temperature and relative humidity setpoints were 3.70, 0.87 and 1.72

kW for the heater, cooler and humidifier respectively. This is acceptable since the temperature setpoint is higher than the ambient temperature. For the other control input permutation designs, the required powers for zero steady state errors are given in Table 4.1. In the calculation of the feedback matrix **F** for these sequences, we can observe that the heater, cooler and humidifier were always used to move the plant matrix eigenvalues λ_1 and λ_5, λ_3 and λ_4, and λ_2 and λ_6 to the desired closed loop poles ρ_1 and ρ_5, ρ_3 and ρ_4, and ρ_2 and ρ_6 respectively but the calculation of the feedback vectors $\mathbf{g}_1^T$ via the heater, $\mathbf{g}_2^T$ via the cooler and $\mathbf{g}_3^T$ via the humidifier were carried out by following the input design sequences where the mode controllability vectors θ_1, θ_2 and θ_3 are different for one sequence to the others; and hence gives different values in the feedback matrix **F**. We then would expect to obtain different combinations of the required control signals W, C and H at steady state conditions and these are shown in Table 4.1. We can see that excessive powers are required for the input design sequence numbers 3, 4, 5, and 6 where the control inputs are fighting one another to maintain the desired setpoints; excessive heating requires more cooling and humidifying and vice versa. This situation is not recommended in practice since minimal cost of operation is the main target of the operators.

By studying the results of these different design we can obtain the optimal solution in the sense of minimal energy consumption; it is clear that the $\{W, C, H\}$ sequence is the best one for this design because the energy is minimal and all the three inputs fall within the permitted limits. This sequence is not optimal for all situations; when the closed loop poles are allocated to the positions 0.3, 0.4, 0.5, 0.6, 0.7 and 0.8 the modal control design procedure gives the best sequence as $\{H, C, W\}$ although the inputs still control the same modes, namely the heater (modes 1 and 5), cooler (modes 3 and 4) and the

humidifier (modes 2 and 6). Therefore, to establish the most appropriate sequence for a particular design, it is necessary to simulate all permutations so that the best one can be identified.

If we were to include the climatic disturbances $w(t)$ and other influences $v(t)$ into the system, equations (4.27) (4.30) and (4.31) can be used to recalculate the system performance; however as before it is found that the system performance deteriorates as shown in Figure 4.6. A set of actual climatic data as shown in Figure 4.4 is used for $w(t)$, and a pseudo random binary sequences (PRBS) generated using six shift registers and switching between ± 0.1 is used for $v(t)$.

Table 4.1: Input power required for zero steady state error

No.	Input Design Sequence	Heater, kW	Cooler, kW	Humidifier, kW
1	$\{W, C, H\}$	3.70	0.87	1.72
2	$\{W, H, C\}$	6.89	3.72	4.32
3	$\{C, W, H\}$	11.48	7.82	8.05
4	$\{C, H, W\}$	8.42	5.09	5.56
5	$\{H, W, C\}$	6.96	3.78	4.37
6	$\{H, C, W\}$	7.58	4.34	4.88

When the control inputs to this closed loop system (Figure 4.5) are truncated to their limits, we found that the system is unable to regulate the outputs as all the three control signals always require the control inputs beyond their upper limits since the initial start-up require excessive control signals. Similarly, when the system in Figure 4.2 has

enforced the control limits, we found that the system is out of control as all the three control signals always require the negative control signals since the initial start-up requires excessive negative powers. From these two situations, we can conclude that the closed loop systems with constrained control inputs are unable to regulate the output if the feedback matrix **F** is calculated via the pole placement methods.

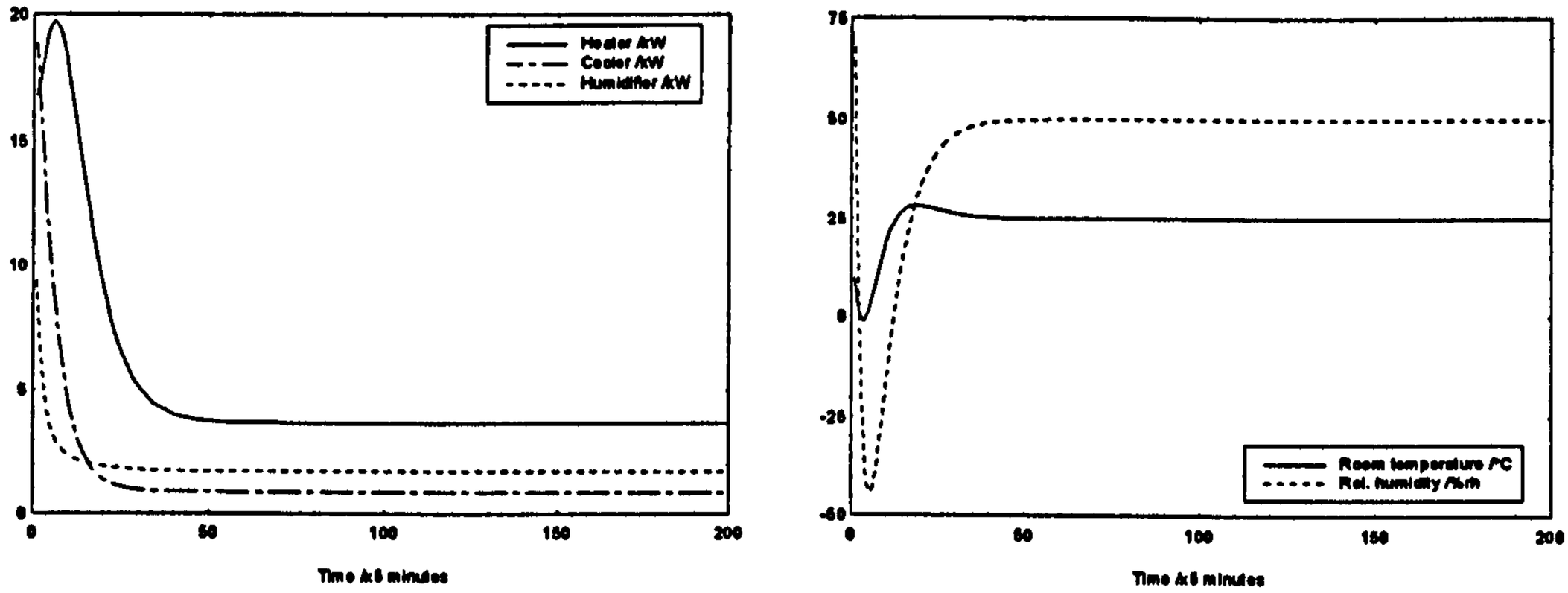

a) Control inputs b) System outputs

Figure 4.5: Control performance of the multi-stage design - $\{W, C, H\}$ sequence

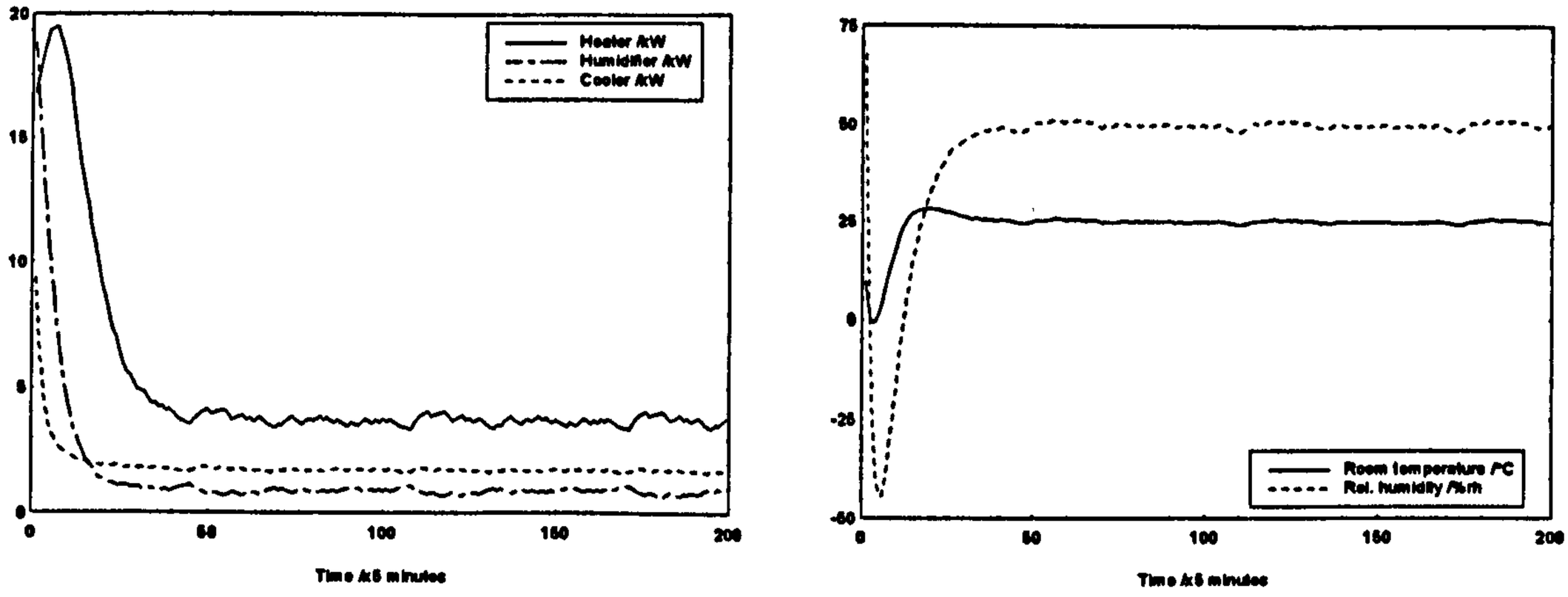

a) Control inputs b) System outputs

Figure 4.6: Multi-stage design - $\{W, C, H\}$ sequence (with noise)

4.3. Output feedback design

In traditional control system design, output-feedback is utilized to achieve the closed-loop structure; having discussed state-feedback systems it is useful to study how the state-space formulation compares to this standard input-output based methodology. The structure of the output-feedback system within the modern control setting is shown in Figure 4.7. Here the input to the system is given by

$$u(t) = - \mathbf{L}\, y(t) + \mathbf{H}\, r(t) \tag{4.75}$$

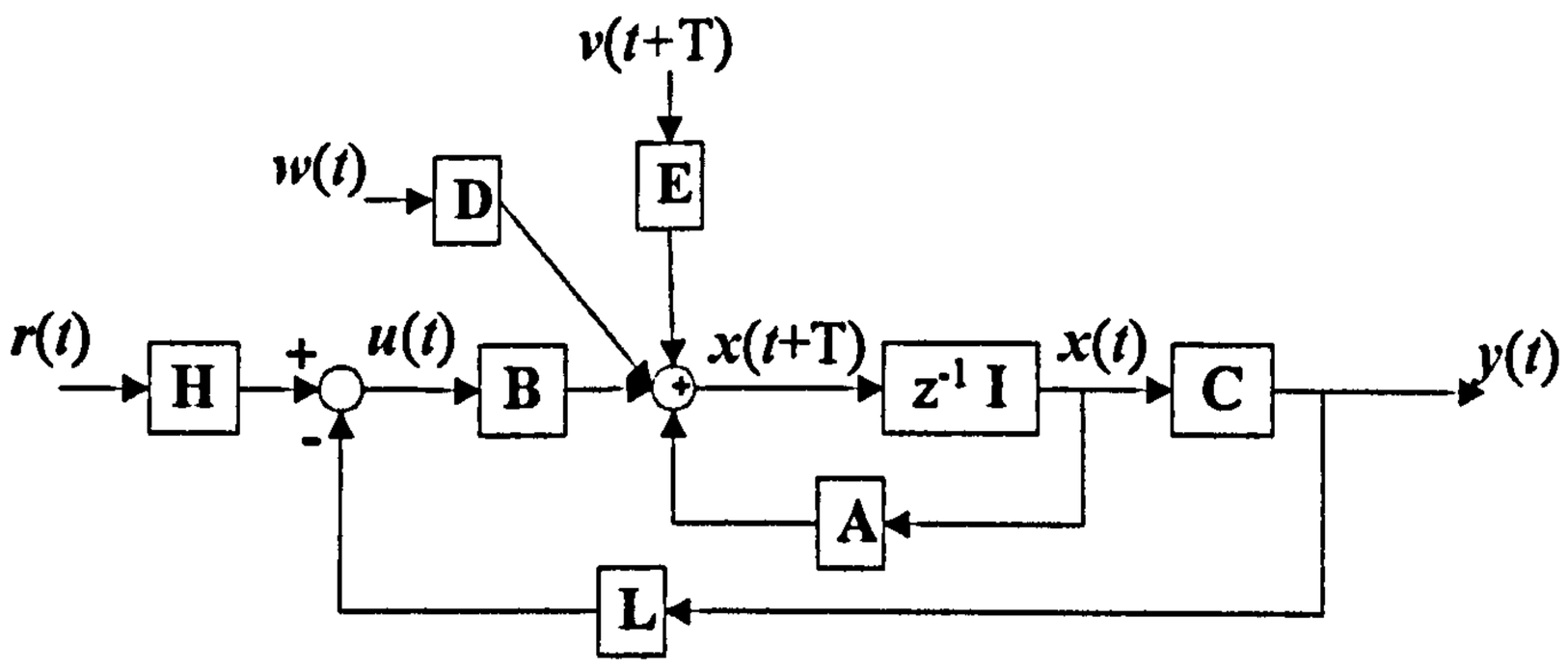

Figure 4.7: Output feedback controlled system

and the state equation for the closed-loop system equals

$$x(t+\mathrm{T}) = (\mathbf{A} - \mathbf{BLC})\, x(t) + \mathbf{BH}\, r(t) + \mathbf{D}\, w(t) + \mathbf{E}\, v(t+\mathrm{T}) + \mathbf{K} \tag{4.76}$$

A similar approach as for the state-feedback method can be applied for this situation to obtain the suitable values for the **L** and **H** matrices (both are of dimension 3×2). If we ignore the external disturbances and the noise processes to the system, then equation (4.76) reduces to the basic state-space equations, namely,

$$x(t+\mathrm{T}) = (\mathbf{A} - \mathbf{BLC})\, x(t) + \mathbf{BH}\, r(t) \tag{4.77}$$

As in section 4.2, the **H** matrix in equation (4.77) can be calculated using the final value theorem to achieve zero steady-state error. From equations (4.27) and (4.77), the z transform of the output becomes

$$\boldsymbol{Y(z) = C\,[\,zI - (A - BLC)\,]^{-1}\,BH\,R(z)} \tag{4.78}$$

and applying the final value theorem we obtain

$$\mathbf{C\,[I - (A - BLC)\,]^{-1}\,BH = I_2} \tag{4.79}$$

so that the system output equals the desired set point. Equation (4.79) can be used to calculate the **H** matrix by defining

$$\mathbf{C\,[I - (A - BLC)\,]^{-1}\,B} \equiv \begin{bmatrix} t_{11} & t_{12} & t_{13} \\ t_{21} & t_{22} & t_{23} \end{bmatrix} \tag{4.80}$$

and assuming that two of the matrix elements of **H** are known. As in section 4.2, if h_{31} and h_{22} are known, then h_{21}, h_{11}, h_{32} and h_{12} can be calculated using equations (4.39) - (4.42) by replacing s with t.

4.3.1. Pole-placement design by output feedback

The design of the output feedback controller can be carried out in a manner similar to that of the state-feedback control. Since equation (4.76) is equivalent to the state equation of a closed-loop system with state-feedback gain **LC** and the pair (**A**, **B**) is completely controllable, then this gain can be solved directly from equation (4.50). Thus, we have

$$\mathbf{L^{\bullet}C} = [(\mathbf{M\,S}^T)^{-1}\,(\alpha - a)]^T \tag{4.80}$$

and the output feedback gain

$$\mathbf{L = wL^{\bullet}} \tag{4.81}$$

Since the right-hand side of equation (4.80) is of dimension 1x6 and from equation (4.9), $\mathbf{C}$ is defined by $\mathbf{C} = \begin{bmatrix} 1 & 0 & 0 & 0 & 0 & 0 \\ 0 & 0 & 0 & 1 & 0 & 0 \end{bmatrix}$, then the vector $\mathbf{L}^*$ should be of dimension 1x2 and let us define $\mathbf{L}^* \equiv [\, l_1^* \quad l_2^* \,]$ and hence, $\mathbf{L}^*\mathbf{C} = [\, l_1^* \;\; 0 \;\; 0 \;\; l_2^* \;\; 0 \;\; 0 \,]$. The $\boldsymbol{\alpha}$ vector can be calculated from equation (4.80) where the right-hand side becomes

$$[(\mathbf{M}\,\mathbf{S}^T)^{-1}(\boldsymbol{\alpha} - \boldsymbol{a})]^T = [\, l_1^* \;\; 0 \;\; 0 \;\; l_2^* \;\; 0 \;\; 0 \,].$$

The term $(\mathbf{M}\,\mathbf{S}^T)^{-1}$ can be calculated and for convenience, let it equal

$$(\mathbf{M}\,\mathbf{S}^T)^{-1} = \begin{bmatrix} z_{11} & z_{12} & z_{13} & z_{14} & z_{15} & z_{16} \\ z_{21} & z_{22} & z_{23} & z_{24} & z_{25} & z_{26} \\ z_{31} & z_{32} & z_{33} & z_{34} & z_{35} & z_{36} \\ z_{41} & z_{42} & z_{43} & z_{44} & z_{45} & z_{46} \\ z_{51} & z_{52} & z_{53} & z_{54} & z_{55} & z_{56} \\ z_{61} & z_{62} & z_{63} & z_{64} & z_{65} & z_{66} \end{bmatrix}, \text{ we then have}$$

$$\begin{bmatrix} z_{11} & z_{12} & z_{13} & z_{14} & z_{15} & z_{16} \\ z_{21} & z_{22} & z_{23} & z_{24} & z_{25} & z_{26} \\ z_{31} & z_{32} & z_{33} & z_{34} & z_{35} & z_{36} \\ z_{41} & z_{42} & z_{43} & z_{44} & z_{45} & z_{46} \\ z_{51} & z_{52} & z_{53} & z_{54} & z_{55} & z_{56} \\ z_{61} & z_{62} & z_{63} & z_{64} & z_{65} & z_{66} \end{bmatrix} \begin{bmatrix} \alpha_6 - a_6 \\ \alpha_5 - a_5 \\ \alpha_4 - a_4 \\ \alpha_3 - a_3 \\ \alpha_2 - a_2 \\ \alpha_1 - a_1 \end{bmatrix} = \begin{bmatrix} l_1^* \\ 0 \\ 0 \\ l_2^* \\ 0 \\ 0 \end{bmatrix} \tag{4.82}$$

By substituting $\mathbf{w} \equiv [\, w_1 \quad w_2 \quad w_3 \,]^T$ into equation (4.81), we have

$$\mathbf{L} = \mathbf{w}\mathbf{L}^* = \begin{bmatrix} w_1 l_1^* & w_1 l_2^* \\ w_2 l_1^* & w_2 l_2^* \\ w_3 l_1^* & w_3 l_2^* \end{bmatrix} \tag{4.83}$$

and the characteristic equation of the closed-loop system is

$$|z\mathbf{I}_6 - \mathbf{A} + \mathbf{BLC}| = |\, z\mathbf{I}_6 - \mathbf{A} + \mathbf{B}^*\mathbf{L}^*\mathbf{C} \,| = 0 \tag{4.84}$$

Since the rank of $\mathbf{B}$ (= 3) is greater than that of $\mathbf{C}$ (= 1), we cannot arbitrarily assign all the elements of $\mathbf{w}$ if we wish to arbitrarily assign a maximum number of eigenvalues of the closed-loop system. But if all the three elements of $\mathbf{w}$ were arbitrarily assigned so that

the pair ($\mathbf{A}$, $\mathbf{B}^*$) is controllable then applying equation (4.82), we then have only 2 out of 6 elements of α to be chosen so that the closed-loop system is stable. The remaining elements can be obtained from the rows of which the right-hand side of equation (4.82) are zero, i.e. the second, third, fifth and sixth equations. These α elements will determine the eigenvalues of the system, namely ρ_1, ρ_2, ρ_3, ρ_4, ρ_5 and ρ_6, through the closed-loop characteristic equation (4.77) of which it can be factorized as:

$$|z\mathbf{I}_6 - \mathbf{A} + \mathbf{BLC}| \equiv (z - \rho_1)(z - \rho_2)(z - \rho_3)(z - \rho_4)(z - \rho_5)(z - \rho_6) = 0$$

or equivalently,

$$|z\mathbf{I}_6 - \mathbf{A} + \mathbf{BLC}| \equiv z^6 + \alpha_6 z^5 + \alpha_5 z^4 + \alpha_4 z^3 + \alpha_3 z^2 + \alpha_2 z + \alpha_1 = 0$$

where $\alpha_1 = \rho_1 \rho_2 \rho_3 \rho_4 \rho_5 \rho_6$, etc.

The elements of $\mathbf{L}^*$, i.e. l_1^* and l_2^* can be calculated from the first and the fourth elements of the left-hand side of equation (4.82).

As mentioned earlier, the conditions for stability of the desired closed-loop system is that the absolute eigenvalues should be $0 < |\rho_i| < 1$, $i = 1, 2, ..., 6$. We can see that α_i in terms of ρ_i are not linearly related. Therefore, we must find the 2 starting elements of α so that the system's stability as well as equation (4.82) are satisfied, before being used to obtain $\mathbf{L}^*$ and hence the output feedback gain $\mathbf{L}$.

As an example, we can again use $\mathbf{w} = [10 \quad 10 \quad 1]^T$ because it makes the pair ($\mathbf{A}$, $\mathbf{B}^*$) controllable. Let us assume that the values of α_3 and α_4 are known, then from equation (4.82), we can calculate the remaining α's by solving 4 unknown parameters such as α_1, α_2, α_5 and α_6 from 4 linear equations. It is found that a solution for stability of the closed-loop system is as follows: α_3 and α_4, respectively, equal to -0.040 and -0.783, which gives α_1, α_2, α_5 and α_6, respectively, equal to -0.001, 0.251,

2.425 and -2.853, and the closed-loop eigenvalues ρ_1, ρ_2, ρ_3, ρ_4, ρ_5 and ρ_6 as 0.035, 0.035, 0.542, 0.833, 0.985 and 0.963 respectively; Finally, **L** is obtained from equations (4.82) and (4.83) and is equal to:

$$\mathbf{L} = \begin{bmatrix} 0.219 & 0.036 \\ 0.219 & 0.036 \\ 0.022 & 0.004 \end{bmatrix} \tag{4.85}$$

The **H** matrix is calculated by using the final value theorem of equation (4.79) and is equal to

$$\mathbf{H} = \begin{bmatrix} 1.45 & 1.67 \\ 1.16 & 1.50 \\ 1.00 & 1.39 \end{bmatrix} \tag{4.86}$$

The zeros of the individual transfer functions $G_{11}(z)$, $G_{12}(z)$, $G_{21}(z)$ and $G_{22}(z)$ for the above **L** and **H** can be calculated from equation (4.78) and they are found to be as follows:

$G_{11}(z)$: 1.02, 0.98, 0.50±0.18i, 0.02.

$G_{12}(z)$: 1.00, 0.99, 0.55, 0.35, 0.01.

$G_{21}(z)$: 1.00, 0.98, 0.60, ±0.09i.

$G_{22}(z)$: 1.00, 0.99, 0.54, 0.03±0.10i.

where i = $\sqrt{-1}$, and their poles equal 0.035, 0.035, 0.542, 0.833, 0.985 and 0.963. We can see that the transfer function $G(z)$ of this system has also a nonminimum-phase characteristic.

A similar condition as in section 4.2 can be used, and the control performance for the closed-loop system without any disturbances or noise effects is investigated. The simulated result is shown in Figure 4.8 where we can see that all the three input signals exceed the permitted ranges. Although, the system outputs reach the desired set-points at

a slow rate ($t \approx 900$ minutes) due to the dominance of the coefficients of the ρ_5 and ρ_6 eigenvalues in equations (4.35) and (4.36). The same peculiar response is obtained during the early transient period where the outputs overshoot due to excessive control action. This result shows that a good control performance using output feedback is difficult to achieve if the pole-placement design is utilized to calculate the feedback matrix **F**. The disadvantages of using the pole-placement technique for multi-input/ multi-output (MIMO) system with constrained inputs as discussed in section 4.2, can also be applied to the output feedback system.

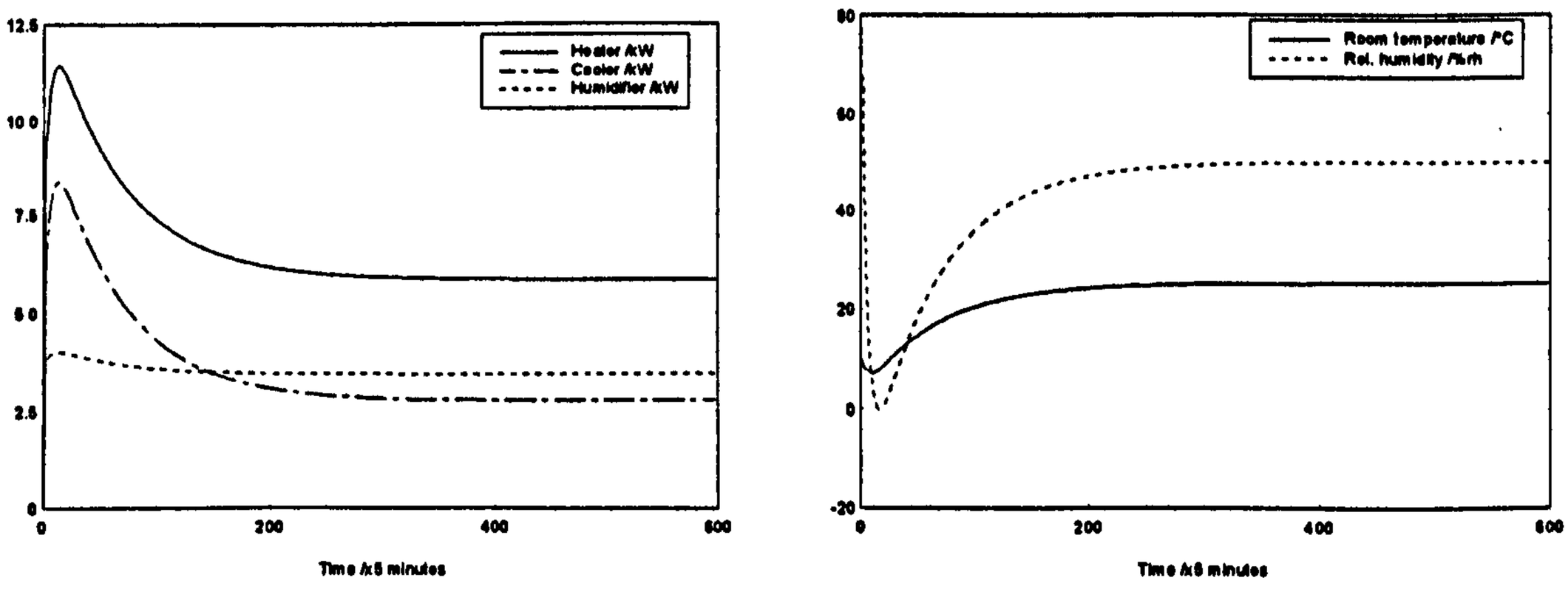

a) Control inputs

b) System outputs

Figure 4.8: Control performance of the output feedback

Again, if we were to include the climatic disturbances $w(t)$ and other influences $v(t)$ into the system, it is found that the system performance is deteriorated as shown in Figure 4.9. A set of actual climatic data shown in Figure 4.4 is used for $w(t)$, and a pseudo random binary sequences (PRBS) generated using six shift registers as before and switching for ± 0.1 is used for $v(t)$.

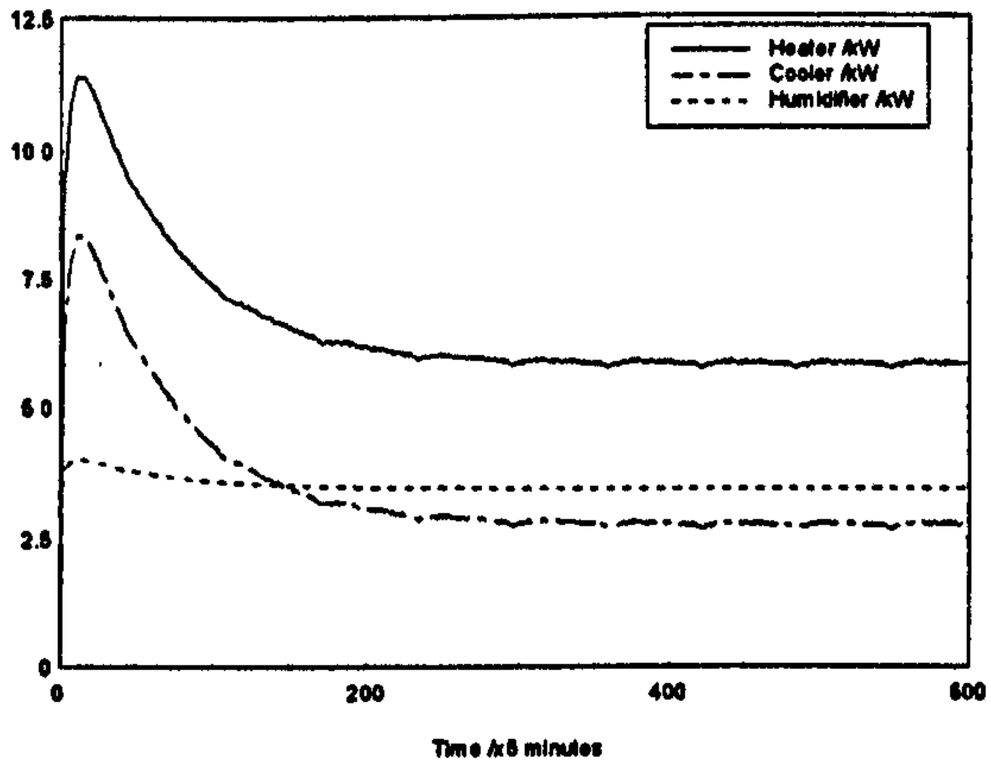

a) Control inputs

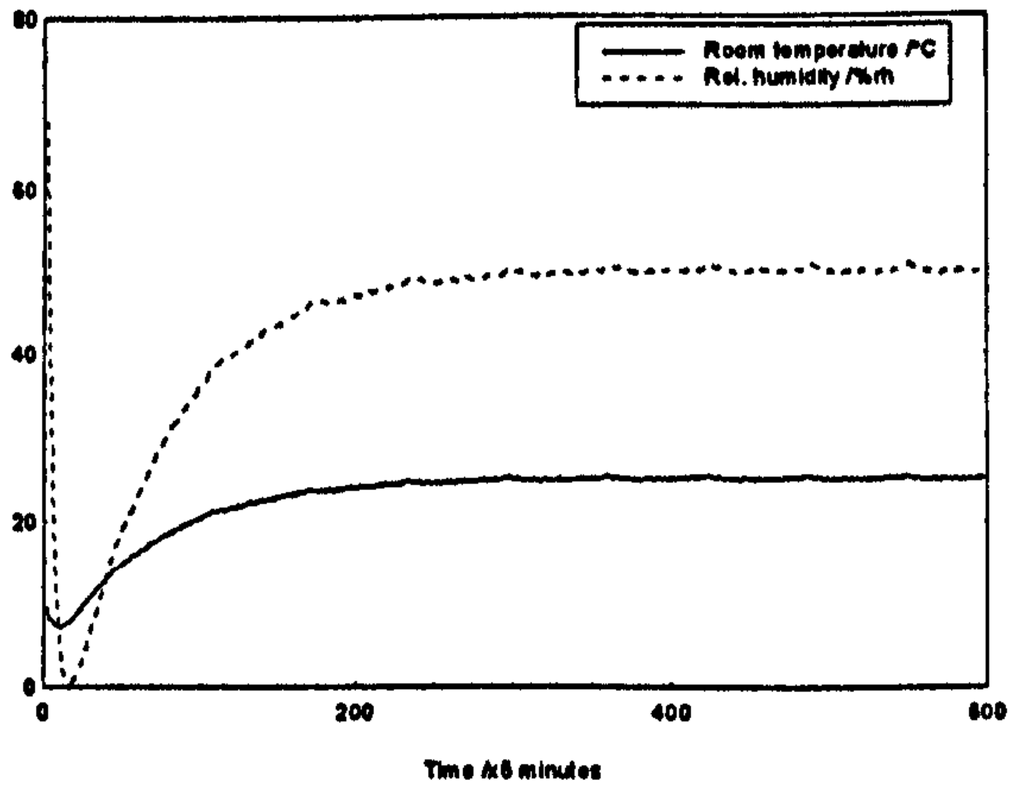

b) System outputs

Figure 4.9: Control performance of the output feedback (with noise)

4.4. Practical aspects of the state-space method

In this chapter, we have discussed the methods to obtain the feedback and feedforward matrices of the closed-loop system so that the system outputs track the desired set-point without considering the control input constraints. However, in a practical control system, this situation is not true, especially in our case where the heater, cooler and humidifier have limits on their power ratings as described earlier. Nevertheless, the control signals at steady state conditions can be used to set these three control inputs so that both the air temperature and the relative humidity in the room will settle at their respective set-points after some time. This fact is shown in Figure 4.10 where the converged values of the control inputs of $\{W, C, H\}$ sequence required are applied to the state-space equations (4.26) and (4.27). This solution requires the power levels of the heater, cooler and humidifier to be set to 3.70, 0.87 and 1.72 kilowatts respectively in order that the room temperature and the relative humidity converge to the required set-points, i.e. 25°C and

50%rh respectively. Identical responses as in Figure 4.10 are also obtained when the simulation trial is carried out via the original model equations (2.1) and (2.2).

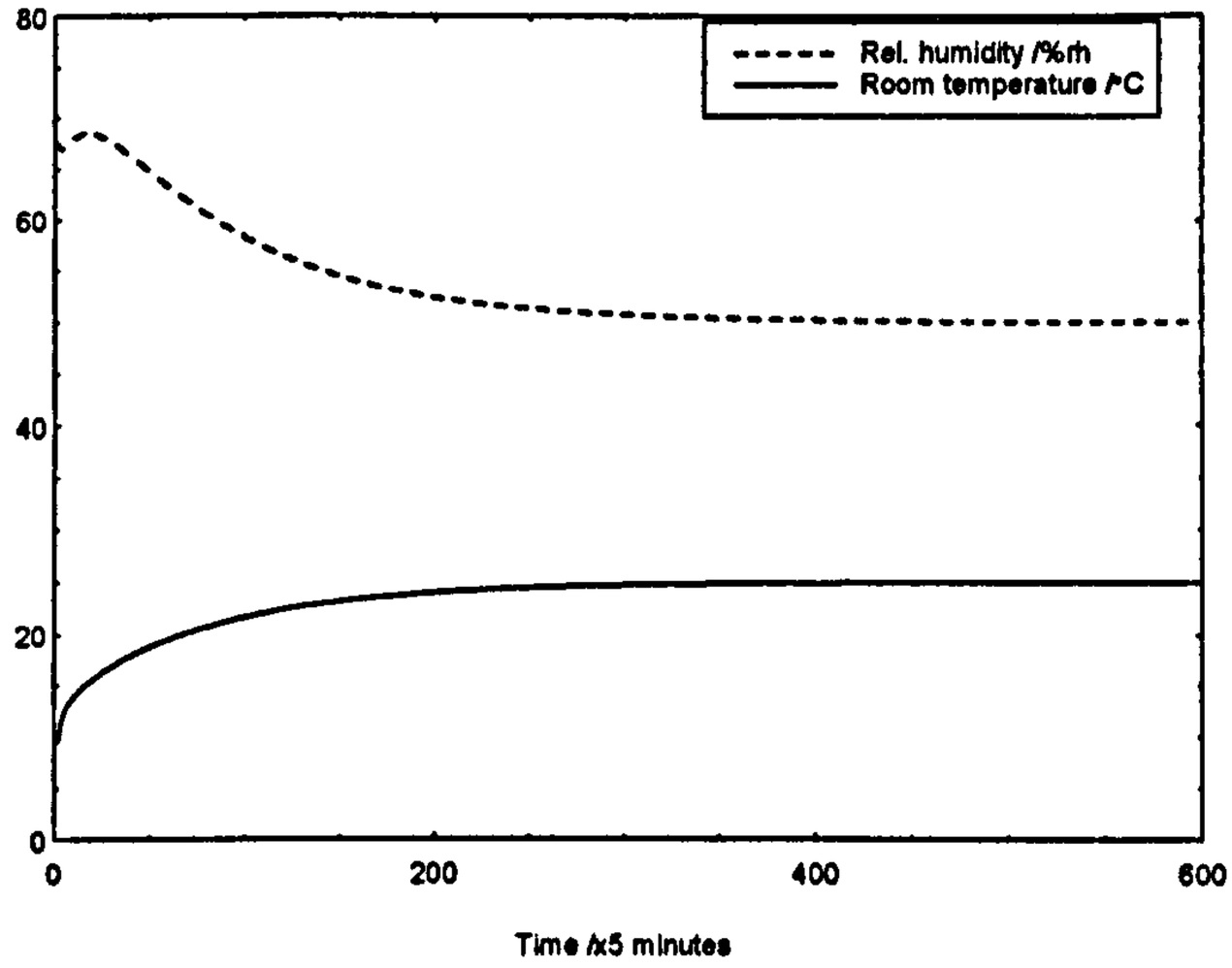

Figure 4.10: System response for steady state values for the control inputs

In the calculation of the control inputs W, C and H from the modal controller, the climatic disturbances $w(t)$ and the stochastic noises $v(t)$ were not included into the system. When these terms are present, such as the laboratory temperature, the outside temperature, the outside humidity and the solar irradiance are constant at 20°C, 10°C, 70%rh and 0Wm^{-2} respectively and the other stochastic effects are ignored, we found that the temperature and the humidity converged to 25.4°C and 51.8%rh respectively due to the calculated feedback, **F**, and feedforward, **H**, matrices were based on the plant, **A**, and input, **B**, matrices only. This shows that the method to calculate **F** by temporarily ignoring these external disturbances is acceptable for this example since the steady state values are slightly different from the required setpoints.

4.5. Conclusions

This chapter has discussed the state-space methodology for solving the control problems in the building energy management application area. The techniques such as the pole-placement design and the modal control do not consider the constrained input situations as well as the strategies for control input optimization. Therefore, both methods are at first sight unable to achieve a good control performance in realistic applications. However, the results can be used to get an idea of the control signal ratios for the required set-points and the desired poles.

More advanced methods such as using MIMO adaptive control with constrained inputs or more intelligently, the fuzzy logic and genetic algorithm techniques can be utilized to solve this type of control problems; these are discussed in the remaining chapters.

Chapter 5

MIMO Adaptive Control with Constrained Inputs

In most control systems, the main problem is to design a control strategy which has the ability to adjust itself according to the changing properties of the controlled processes and the restrictions on the signals. A relatively new approach, namely, adaptive control, can provide the ability to carry out such designs. These control systems can be divided into two main groups, namely, feedforward and feedback adaptive controllers (Isermann et al., 1992). Feedforward adaptive control systems are based on the fact that the changing properties of the plant can be monitored by measurement of the signals acting on the process. If the process behaviour changes cannot be determined directly by measurement of external process signals, the feedback type of adaptive controllers should be used. Amongst many types of feedback adaptive controller, the model identification adaptive controllers (MIACs), sometimes also called self-optimising controllers or self-tuning controllers are well known to control practitioners.

Numerous papers discuss the MIMO adaptive controllers, but many of them deal with only square systems, i.e. the number of inputs equals the number of outputs (see for

examples Borrisson, 1979; Elliott et al., 1984; Mohtadi et al., 1986). Mikles (1990) has developed a multivariable self-tuning controller based on the pole-placement design which is suitable for nonsquare systems but it does not consider any constraints on the control inputs. A number of papers deal with constrained inputs for designing MIMO adaptive controllers. Most of these are based on the dynamic matrix control approach (DMC) developed by Cutler and Ramaker (1980) which use the predicted output errors in the presence of physical constraints. Some of them use saturated inputs instead of the actual computed inputs (see for examples Ohkawa and Yonezawa, 1982; Payne, 1986). Another approach is to re-compute the reference model whenever the computed control input is out of the permitted input range (see Ortega et al., 1984).

In this chapter, we present a MIAC with input and output constraints, which are usually found in real systems. The theory of designing the control law for the adaptation mechanism presented here is based on the methods developed by Dion et al. (1991), and for the process model identification, a multivariable recursive least square method is used (see for examples Mikles, 1990; Peterka, 1975). In applying this control law, the control input is computed on a receding horizon principle, based on the generalized predictive control methodology (Clarke et al., 1987). The constraints on the inputs are not only applied to the present control input but also to future computed control inputs. All these control inputs are not actually applied since, at each sampling time, only the current computed constrained input is applied. However, it may be noticed in the proposed algorithm, that the current control input has been computed under the hypothesis that the future control inputs and/or their derivatives also satisfy the constraints. The adaptive constrained control problem is then solved iteratively, using classical "quadratic programming with constraints" methods (see for example Fletcher, 1981).

The proposed algorithm can deal with nonsquare systems which is suitable for our system with 3 control inputs and 2 outputs (Figure 2.1). These inputs have physical limitations on their maximum power ratings, as well as the power changes between the sampling periods that they can provide to the system. Furthermore, it may also be required to set the output ranges as required in the algorithm.

This chapter is organised as follows: we present the theory of the control law developed by Dion et al and then follow this by it's application in our BEMS. The theory begins with a statement of the problem and then it's solution for this application.

5.1. Statement of the problem

Let us consider the following multivariable process model:

$$A(z^{-1})y(t) = B(z^{-1})u(t) \tag{5.1}$$

where

$$A(z^{-1}) = \mathbf{I} + A_1 z^{-1} + \ldots + A_n z^{-n}$$

$$B(z^{-1}) = B_1 z^{-1} + \ldots + B_n z^{-n}$$

are (p x p) and (p x m) polynomial matrices respectively, n is an upper bound on the observability index of the process model, **I** is (p x p) identity matrix, $u(t)$ and $y(t)$ are, respectively, the input and output vectors, and for convenience, the term z is defined slightly different from other type of controllers in this thesis, that is z^{-1} f(t) = f(t-1) where the sampling interval T is assumed to be unity.

The control objectives are the following:

Let us consider the following finite horizon quadratic criterion:

$$J(t) = \sum_{j=1}^{N} (y(t+j) - y_M(t+j))^T \; R \;\; (y(t+j) - y_M(t+j))$$

$$+ \sum_{j=1}^{N} \Delta u^T(t+j-1) \;\; Q_1 \;\; \Delta u(t+j-1) + \sum_{j=1}^{N} u^T(t+j-1) \;\; Q_2 \;\; u(t+j-1) \quad (5.2)$$

where N is the prediction horizon, $\{y_M(t)\}$ is the output reference vector sequence, Δ is the difference operator $(1 - z^{-1})\mathbf{I}$, and R, Q_1 and Q_2 are the weighting factors on the predicted output error, rate of predicted input and the predicted input respectively and they are positive definite matrices. We can see from the Lfunction(5.2) that the first, second and third terms on the right hand side of the equation deal with the predicted cost of regulation errors, the rate of energy consumed and the actual energy consumed respectively; these are all variables which we intend to minimise. The weight Q_1 on the input increments Δu incorporates some integral action of the predicted input and the weight Q_2 on the input u allows one to save control energy when we have degrees of freedom on the inputs.

We require that, at each time t, the control inputs that minimise the quadratic criterion $J(t)$ and satisfy constraints on the inputs and outputs of the following type:

$$C \Delta u_t \geq \psi_u (\theta, \phi(t), t)$$

$$D(\theta) y_t \geq \psi_y (\theta, \phi(t), t) \quad (5.3)$$

where

$\Delta u_t = [\Delta u^T(t), \ldots, \Delta u^T(t+N-1)]$ $(1 \times Nm)$ is the predictions in the rate of change of the control sequence from the current time (t) to the future time $(t+N-1)$.

$y_t^T = [y^T(t+1), \ldots, y^T(t+N)]$ $(1 \times Np)$ is the predictions of the output y from time $(t+1)$ to time $(t+N)$.

$\theta = [A_1, \ldots, A_n, B_1, \ldots, B_n]^T$ $(n(p+m) \times p)$ is the matrix of coefficients in the process model.

$$\phi^T(t) = [-y^T(t), \ldots, -y^T(t-n+1), u^T(t), \ldots, u^T(t-n+1)] \qquad (5.4)$$

C, $D(\theta)$, $\psi_u(.)$ and $\psi_y(.)$ depend on the constraints and will be specified later.

The inequalities given by equation (5.3) can express different types and combinations of constraints on $u(.)$ and $y(.)$; for instance constraints on the magnitude of u and y, the magnitude of the derivatives of u and y or on some linear combination of u and y.

5.2. Multivariable adaptive control law

When the A_i and B_i parameter matrices are known, we can transform the above problem, i.e. minimisation of the objective (5.2) while satisfying the process dynamics (5.3) into a classical one, namely, quadratic minimisation with constraints. The control law is then computed, using quadratic programming methods with constraints.

Let us first build general j-step ahead predictors with the following Bezout identities:

$$\mathbf{I} = E_j(z^{-1})\, A(z^{-1})\, \Delta + F_j(z^{-1})\, z^{-j}, \text{ for } j = 1, \ldots, N \qquad (5.5)$$

where $E_j(z^{-1})$ and $F_j(z^{-1})$ are polynomial matrices defined by

$$E_j(z^{-1}) = \mathbf{I} + E_1^j\, z^{-1} + \ldots + E_{j-1}^j\, z^{-j+1}$$

$$F_j(z^{-1}) = F_0^j + F_1^j\, z^{-1} + \ldots + F_n^j\, z^{-n}. \qquad (5.6)$$

These polynomial matrices are uniquely defined by $A(z^{-1})$, Δ, and the prediction horizon j. By postmultiplying $y(t+j)$ into equation (5.5) we get

$$y(t+j) = E_j(z^{-1})\,A(z^{-1})\,\Delta\,y(t+j) + F_j(z^{-1})\,z^{-j}y(t+j)$$

Using equation (5.1) on the first term on the right hand side gives

$$y(t+j) = E_j(z^{-1})\,B(z^{-1})\,\Delta u(t+j) + F_j(z^{-1})\,y(t) \text{ for } j = 1, \ldots, N \tag{5.7}$$

Defining $G^j(z^{-1})$ as $E_j(z^{-1})\,B(z^{-1})$ and letting

$$G^j(z^{-1}) = G_0^j\,z^{-1} + G_1^j\,z^{-2} + \ldots + G_{n+j-1}^j\,z^{-j-n} \tag{5.8}$$

we have the following set of predictors

$$y(t+1) = G_0^1\,\Delta u(t) + (z\,G^1(z^{-1}) - G_0^1)\,\Delta u(t) + F_1(z^{-1})\,y(t)$$

$$y(t+2) = (G_0^2 + G_1^2 z^{-1})\,\Delta u(t+1) + (z\,G^2(z^{-1}) - G_0^2 - G_1^2 z^{-1})\,\Delta u(t+1)$$

$$+ F_2(z^{-1})\,y(t)$$

.

.

.

$$y(t+N) = \left(\sum_{i=0}^{N-1} G_i^N\,z^{-i}\right)\Delta u(t+N-1) + (z\,G^N(z^{-1}) - \sum_{i=0}^{N-1} G_i^N\,z^{-i})\,\Delta u(t+N-1)$$

$$+ F_N(z^{-1})\,y(t). \tag{5.9}$$

It is easily shown (Clarke et al., 1987) that

$$G_0 = G_0^1 = G_0^2 = \ldots = G_0^{N-1} = G_0^N$$

$$G_1 = G_1^2 = G_1^3 = \ldots = G_1^N$$

.

.

.

$$G_{N-1} = G_{N-1}^N. \tag{5.10}$$

The set of equations (5.9) can then be rewritten in a condensed form:

$$y_t = \overline{G}_N \, \Delta u_t + f_t \tag{5.11}$$

where

$$y_t = [y^T(t+1), \ldots, y^T(t+N)]$$

$$\Delta u_t^T = [\Delta u^T(t), \ldots, \Delta u^T(t+N-1)] \tag{5.12}$$

$$f_t = [f_1^T(t), \ldots, f_N^T(t)]$$

$$f_j(t) = \left(z\, G^j(z^{-1}) - \sum_{i=0}^{j-1} G_i^j\, z^{-i}\right) \Delta u(t+j-1) + F_j(z^{-1})\, y(t) \tag{5.13}$$

$$\overline{G}_N = \begin{bmatrix} G_0 & & & & & \\ G_1 & G_0 & & & 0 & \\ & G_1 & . & & & \\ . & & . & . & & \\ . & & & . & . & \\ . & & & & G_1 & G_0 \\ G_{N-1} & G_{N-2} & . & . & G_1 & G_0 \end{bmatrix} \quad (Np \times Nm). \tag{5.14}$$

The term $\overline{G}_N \, \Delta u_t$ contains present and future inputs, and the term f_t contains present and past outputs (up to time t), and past inputs (up to time t - 1).

The quadratic criterion (5.2) can then be rewritten as

$$J(t) = (y_t - y_{Mt})^T \, \overline{R} (y_t - y_{Mt}) \; + \; \Delta u_t^T Q_1 \, \Delta u_t \; + \; u_t^T \overline{Q}_2 u_t \tag{5.15}$$

where

$$\overline{R} = \text{diag}\,(R, \ldots, R) \qquad (Np \times Np)$$

$$\overline{Q}_1 = \text{diag}\,(Q_1, \ldots, Q_1) \qquad (Nm \times Nm)$$

$$\overline{Q}_2 = \text{diag}\,(Q_2, \ldots, Q_2) \qquad (Nm \times Nm)$$

$$y_{Mt}^T = [y_M^T(t+1), \ldots, y_M^T(t+N)] \qquad (1 \times Np)$$

$$u_t^T = [u^T(t), \ldots, u^T(t+N-1)] \qquad (1 \times Nm). \tag{5.16}$$

Defining $\overline{u}_{t-1}^T$ as $[u^T(t-1), u^T(t-1), \ldots, u^T(t-1)]$ $(1 \times Nm)$, u_t may be rewritten as:

$$u_t = \overline{H}_N \ \Delta u_t + \overline{u}_{t-1} \tag{5.17}$$

where

$$\overline{H}_N = \begin{bmatrix} \mathbf{I} & & & \\ \mathbf{I} & . & & \mathbf{0} \\ . & . & . & \\ . & & . & . \\ \mathbf{I} & . & . & \mathbf{I} \quad \mathbf{I} \end{bmatrix} \qquad (Nm \times Nm)$$

Using equation (5.11), the criterion (5.15) becomes

$$J(t) = (\overline{G}_N \Delta u_t + f_t - y_{Mt})^T \overline{R}(\overline{G}_N \Delta u_t + f_t - y_{Mt})$$

$$+ \Delta u_t^T \overline{Q}_1 \Delta u_t + u_t^T \overline{Q}_2 u_t$$

Now, using equation (5.17) we have

$$J(t) = (\overline{G}_N \Delta u_t + f_t - y_{Mt})^T \overline{R}(\overline{G}_N \Delta u_t + f_t - y_{Mt}) + \Delta u_t^T \overline{Q}_1 \Delta u_t$$

$$+ \Delta u_t^T \overline{H}_N^T \overline{Q}_2 \overline{H}_N \Delta u_t + 2\Delta u_t^T \overline{H}_N^T \overline{Q}_2 \overline{u}_{t-1} + \overline{u}_{t-1}^T \overline{Q}_2 \overline{u}_{t-1} \tag{5.18}$$

The control law input implemented at time t is the control at time (t-1) plus the change needed to maintain the required objective, that is:

$$u(t) = u(t - 1) + \Delta u(t) \tag{5.19}$$

where the change in the control signals, $\Delta u(t)$ is obtained by minimisation of the objective (5.2) while satisfying equation (5.3), and can be expressed as:

$$\min_{\Delta u_t} \{\Delta u_t^T \ \Psi \Delta u_t - 2\Omega^T \Delta u_t\} \tag{5.20}$$

subject to the constraints (5.3).

where

$$\Psi = \overline{G}_N^T \ \overline{R}\,\overline{G}_N + \overline{Q}_1 + \ \overline{H}_N^T \overline{Q}_2 \overline{H}_N \qquad (Nm \times Np) \tag{5.21}$$

$$\Omega^T = \left(y_{Mt} - f_t\right)^T \overline{R}\,\overline{G}_N - \overline{u}_{t-1}^T \overline{Q}_2 \overline{H}_N . \qquad (1 \times Nm) \tag{5.22}$$

Equations (5.20), (5.21) and (5.22) are obtained by expanding the objective function (5.18) using the relations $(a + b)^T = a^T + b^T$ and $(ab)^T = b^T a^T$ where a and b are arbitrary matrices, and rearranging the terms containing Δu_t and without it; then the minimisation of this objective applies only to the terms with Δu_t because the other terms are constant.

The constraints on the process dynamics defined by equation (5.3) can also be rewritten as

$$C_{uy}(\theta)\,\Delta u_t \geq \psi_{uy}(\theta, \phi(t), t) \qquad (5.23)$$

where $C_{uy}(\theta)$ is a matrix and $\psi_{uy}(.)$ is some vector function defined by the constraints on the inputs and outputs.

Thus, at each sampling instant, the problem is solved by iteratively computing the change in the control input vector Δu_t, using standard quadratic programming algorithms with constraints (see for example Fletcher, 1981) and then applying the new control $u(t)$ as defined by equation (5.19) to the system.

We will now define the input-output constraints:

$$u_{low} \leq u(t) \leq u_{high}$$

$$-D_u \leq \Delta u(t) \leq D_u$$

$$y_{low} \leq y(t) \leq y_{high}$$

$$-D_y \leq \Delta y(t) \leq D_y. \qquad (5.24)$$

The inequalities should be read as: each component of the different vectors is bounded by the corresponding component of the constraint vectors; u_{low}, u_{high}, D_u, y_{low}, y_{high} and D_y are the lower threshold, upper threshold and the derivative threshold vectors of the control inputs and outputs respectively.

It is shown by Dion, et al. (1991) that

$$C_{uy}(\theta) = \left[C_1^T,\ -C_1^T,\ C_2^T,\ -C_2^T,\ C_3^T,\ -C_3^T,\ C_4^T,\ -C_4^T\right] \quad (4N(m+p) \times Nm)$$

$$\psi_{uy}(\theta, \phi(t), t) = [-\psi_1^T, -\psi_1^T, \psi_2^T(t-1), -\psi_3^T(t-1), \psi_4^T(t), -\psi_5^T(t), \psi_6^T(t), -\psi_7^T(t)]^T$$

$$(4N(m+p) \times 1) \qquad (5.25)$$

where

$$C_1 = \mathbf{I}, \qquad (Nm \times Nm)$$

$$C_2 = \begin{bmatrix} \mathbf{I} & & & \\ \mathbf{I} & . & \mathbf{0} & \\ . & . & . & \\ . & & . & . \\ \mathbf{I} & . & . & \mathbf{I} \quad \mathbf{I} \end{bmatrix}, \qquad (Nm \times Nm)$$

$$C_3 = \overline{G}_N \qquad (Nm \times Nm)$$

$$C_4 = \overline{G}_N - \begin{bmatrix} \mathbf{0} & & & \\ G_0 & . & & \mathbf{0} \\ & . & . & \\ . & & . & \\ . & & . & . \\ G_{N-2} & . & . & G_0 \quad \mathbf{0} \end{bmatrix} = \overline{G}_N - \overline{G}'_N \qquad (Nm \times Nm) \qquad (5.26)$$

and

$$\psi_1^T = [D_u^T, \ldots, D_u^T] \qquad (1 \times Nm)$$

$$\psi_2^T(t-1) = [(u_{low} - u(t-1))^T, \ldots, (u_{low} - u(t-1))^T] \qquad (1 \times Nm)$$

$$\psi_3^T(t-1) = [(u_{high} - u(t-1))^T, \ldots, (u_{high} - u(t-1))^T] \qquad (1 \times Nm)$$

$$\psi_4^T(t) = [(y_{low} - f_1(t))^T, \ldots, (y_{low} - f_N(t))^T] \qquad (1 \times Np)$$

$$\psi_5^T(t) = [(y_{high} - f_1(t))^T, \ldots, (y_{high} - f_N(t))^T] \qquad (1 \times Np)$$

$$\psi_6^T(t) = [(-D_y - f_1(t) + y(t))^T, (-D_y - \Delta f_2(t))^T, \ldots, (-D_y - \Delta f_N(t))^T] \quad (1 \times Np)$$

$$\psi_7^T(t) = [(D_y - f_1(t) + y(t))^T, (D_y - \Delta f_2(t))^T, \ldots, (D_y - \Delta f_N(t))^T] \quad (1 \times Np)$$

(5.27)

$f_j(t)$ have been previously defined in equation (5.13) and $\Delta f_j(t) = f_j(t) - f_j(t-1)$ for $j = 1, 2, \ldots, N$.

5.3. Multivariable parameter estimation

In order to derive an adaptive version of the control laws described in section 5.2, it is necessary to add a parameter estimation procedure. Hence, at each sampling time, the process model parameters (the A_i and B_i matrices appearing in Θ) can be estimated using standard recursive identification algorithms. The design of the control law is then made analogously to the known parameters case, but that the estimated values are used instead of the true ones.

For the parameter estimation, the process model equation (5.1) is rewritten with the estimated model parameters as the observation equation:

$$y(t) = \Theta^T(t-1)\, \Phi(t) + \bar{e}(t) \tag{5.28}$$

where

$\Phi(t) = [-y^T(t-1), \ldots, -y^T(t-n), u^T(t-1), \ldots, u^T(t-n)]$ $\quad (n(p+m) \times 1)$

$\Theta(t-1) = [A_1, \ldots, A_n, B_1, \ldots, B_n]^T$ $\quad (n(p+m) \times p)$ is the matrix of coefficients in the process model at time $t-1$,

and $\bar{e}$ is a p-vector of the prediction errors.

A set of N j-step ahead adaptive predictors is built similarly to equations (5.5) - (5.10), where the predicted output parameters y_t and f_t as well as the cost function J are the estimated ones, Ψ and Ω vary with time t as they depend on $\overline{G}_N(t)$ and $f_t(t)$, and the matrix of coefficients to the process model θ becomes $\Theta(t)$.

For the identification of the process model, $\Theta(t)$ at time t, the recursive least square method can be used (Mikles, 1990); the essence of this method is as follows: at the tth time step, the following parameters are calculated:

$$p(t) = N(t-1)\,\Phi(t) \qquad (n(p+m) \times 1)$$

$$\xi(t) = \Phi^T(t)\,p(t) \qquad \text{a scalar}$$

$$\overline{e}(t) = y(t) - \Theta^T(t-1)\,\Phi(t) \qquad (p \times 1)$$

$$\delta^2(t) = \varphi^2 + \xi(t) \qquad \text{a scalar}$$

$$\Theta(t) = \Theta(t-1) + \frac{1}{\delta^2(t)}\,p(t)\,\overline{e}^T(t) \qquad (n(p+m) \times p)$$

$$N(t) = N(t-1) - \frac{1}{\delta^2(t)}\,p(t)\,p^T(t) \qquad (n(p+m) \times n(p+m)) \qquad (5.29)$$

where N is the covariance matrix to measure the variability and covariability of the parameter estimates, φ is the forgetting factor to progressively reduce the emphasis placed on the past information; for example the past errors (see for example Wellstead and Zarrop, 1991), and ξ and δ are scalars.

We can see that the covariance matrix $N(t)$ in algorithm (5.29) needs to be updated as the samplings are in progress. From a numerical point of view it is more accurate to update $N(t)$ in the factored form:

$$N(t) \equiv \Gamma(t)\,\Gamma^T(t) \qquad (5.30)$$

where $\Gamma(t)$ is a lower triangular matrix. By this factorisation, $N(t)$ can never become indefinite if its square root $\Gamma(t)$ is propagated instead of $N(t)$. This is the fundamental idea of square root filtering. Therefore, a well known method to update $\Gamma(t)$ is to use the square root filter (Paterka, 1975) and then substituting it into $N(t)$ by the definition (5.30). In this method, we first update the diagonal elements of $\Gamma(t)$, namely, Γ_{jj} for j = 1, 2, ... , $n(p+m)$, and then followed by its lower elements Γ_{ij} for i = 1, 2, ... , j-1. We summarise the steps as follows:

Step 1: Set $t = 1$, $\sigma_0 = \varphi$

Step 2: $h = \Gamma(t-1)\,\Phi(t) \equiv h_1, h_2, \ldots, h_{n(p+m)}$ $\qquad (n(p+m) \times 1)$

Step 3: For $j = 1, 2, \ldots, n(p+m)$

Calculate the following parameters:

$$a = \sigma_{j-1} / \varphi$$

$$b = h_j / \varphi^2$$

$$\sigma_j^2 = \sigma_{j-1}^2 + h_j^2$$

$$\sigma_j = \sqrt{\sigma_j^2}$$

$$c = a / \sigma_j$$

$$g_j = \Gamma_{ij}(t-1) h_j$$

$$\Gamma_{ij}(t) = c\,\Gamma_{ij}(t-1)$$

For $i = 1, 2, \ldots, j$-1

Calculate the following parameters:

$$q = \Gamma_{ij}(t-1)$$

$$\Gamma_{ij}(t) = c(q - bg_i)$$

$$g_i = qh_j + g_i$$

end

end

Step 4: $t = t+1$, goto 2 (5.31)

Note that the forgetting factor φ is usually set near to 1. For our application, we used $\varphi = 0.99$. The magnitude of the initial covariance matrix $N(0)$ depends on our prior knowledge of the process model parameters $\Theta(0)$. If the initial parameters are known to be close to the true values, then a small covariance matrix could be used, Otherwise, a large initial covariance matrix would reflect this. A standard choice for $N(0)$ is the unit matrix scaled by a positive scalar r, i.e. $N(0) = r\mathbf{I}$. Typically, r is set in the region of 100 to 10^6 and 1 to 10 for a large and a small initial covariance matrix respectively. A detailed discussion on $N(0)$ can be found in Wellstead and Zarrop (1991). For our system, the initial parameter $\Theta(0)$ is not known; therefore, we used $r = 10^6$ and the unit matrix I is the order of $n(p+m)$. In order to initialise the recursive least square algorithm (5.29), $\Theta(0)$ needs to be specified. For our case, we can arbitrary set the matrix coefficients to the outputs, y, and inputs, u, of the mathematical models (2.1) and (2.2) as $A_i(0)$ and $B_i(0)$, $i = 1, 2, ..., n$, respectively and these parameters will be self adjusted via algorithm (5.29) as the iteration advances. For the process model $n = 1$, we used:

$$A_1(0) = \begin{bmatrix} -1.61 & -0.004 \\ 0.04 & -1.54 \end{bmatrix}, B_1(0) = \begin{bmatrix} 0.22 & -0.62 & 0.04 \\ -0.71 & -4.02 & 3.29 \end{bmatrix}$$

and for $n = 2$, we used:

$$A_1(0) = \begin{bmatrix} -1.61 & -0.004 \\ 0.04 & -1.54 \end{bmatrix}, A_2(0) = \begin{bmatrix} 0.64 & 0.006 \\ -0.003 & 0.58 \end{bmatrix},$$

$$B_1(0) = \begin{bmatrix} 0.22 & -0.62 & 0.04 \\ -0.71 & -4.02 & 3.29 \end{bmatrix}, \quad B_2(0) = \begin{bmatrix} 0.07 & 0.36 & 0 \\ 0.37 & 3.73 & -2.42 \end{bmatrix}, \text{ etc.}$$

5.4. MIMO adaptive controller for the office zone system

The MIMO adaptive controller developed in sections 5.2 and 5.3 can be applied for the office zone system, consisting of three inputs ($m = 3$) and two outputs ($p = 2$). The block diagram of the system is depicted in Figure 2.1 where the climatic disturbances and other stochastic influences present in the system are clearly shown.

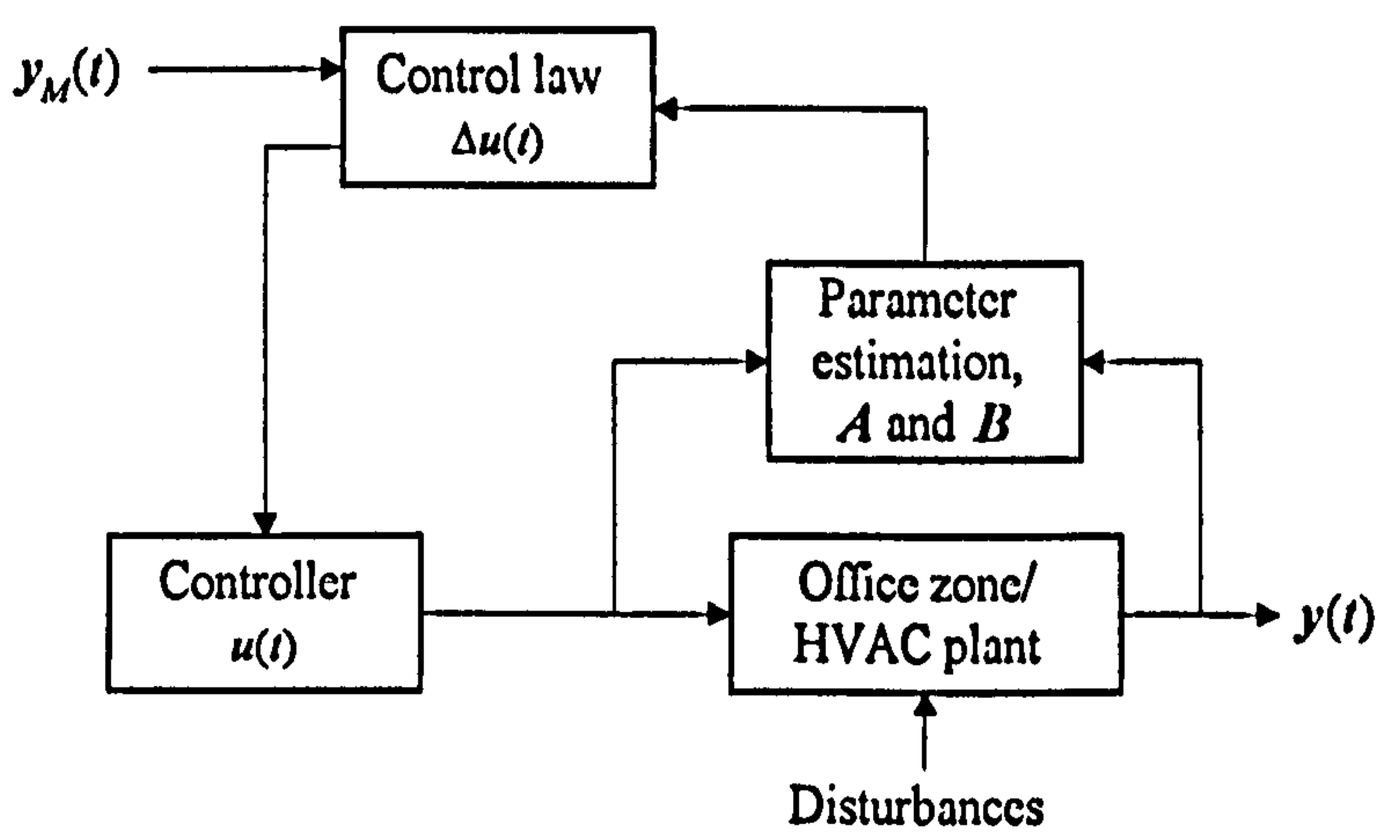

Figure 5.1: MIMO adaptive control scheme for the office zone system

The block diagram of MIMO adaptive controller is shown in Figure 5.1 where the parameter estimation of the polynomial matrices, A and B are first calculated before being used in the control law. The main objective of this controller system is to calculate

$u(t) \equiv [W(t) \quad C(t) \quad H(t)]^T$ so that the next system output, $y(t+1) \equiv [T_c(t+1) \quad H_c(t+1)]^T$ tracks the reference, $y_M(t+1) \equiv [T_r(t+1) \quad H_r(t+1)]^T$.

5.4.1. The objective function

In order to reduce computational complexity, it is advisable to take into account the knowledge about the plant; for example using the possible known delays in the process. For our system, we would consider two types of delay in the process model (5.1), one with a delay of one sampling interval giving a term with argument, t-1 (n = 1) and the other with argument t-2 (n = 2) and then derive all the necessary parameters for their objectives of the adaptation control law in equations (5.20), (5.21) and (5.22). We first derive the objective parameters for the process model with n = 1 where the polynomial matrices A and B are given by:

$$A(z^{-1}) = \mathbf{I}_2 + A_1 z^{-1} \tag{5.32}$$

$$B(z^{-1}) = B_1 z^{-1} \tag{5.33}$$

where $\mathbf{I}_2$ is an identity matrix of order 2. A_1 and B_1 are (2 x 2) and (2 x 3) matrices which can be obtained from the multivariable recursive least squares algorithm (5.29). The process model of this form means that the room temperature and the relative humidity at time t depends only on the previous values of the three control inputs up to time t-1.

The Bezout identities (5.5) for the above process model can be written as

$$\mathbf{I}_2 = E_j(z^{-1})(\mathbf{I}_2 + A_1 z^{-1})(\mathbf{I}_2 - \mathbf{I}_2 z^{-1}) + F_j(z^{-1})z^{-1} \tag{5.34}$$

Equation (5.34) is a linear diophantine equation (see for example Kucera, 1979) and it can be solved by using elementary row operations. It is straightforward to deduce that a minimum degree solution for the polynomial matrices $E_j(z^{-1})$ and $F_j(z^{-1})$ can be obtained if we make (see Mikles and Meszoros, 1991),

$$E_j(z^{-1}) = \mathbf{I}_2 \text{ and } \quad F_j(z^{-1}) = F_0^j + F_1^j z^{-1} \tag{5.35}$$

Then equation (5.34) becomes

$$\mathbf{I}_2 = \mathbf{I}_2 + (A_1 - \mathbf{I}_2 + F_0^j)z^{-1} + (-A_1 + F_1^j)z^{-2} \tag{5.36}$$

Equation (5.36) is true if the coefficients of z^{-1} and z^{-2} on the right hand side of the equation are 2x2 zero matrices, we then have

$$F_0^j = \mathbf{I}_2 - A_1, \; F_1^j = A_1$$

$$\text{and } F_j(z^{-1}) = (\mathbf{I}_2 - A_1) + A_1 z^{-1} \text{ for } j = 1, 2, ..., N \tag{5.37}$$

Now, we calculate the polynomial $G^j(z^{-1})$ from equation (5.8) which is given by

$$G^j(z^{-1}) = E_j(z^{-1})\, B(z^{-1}) = B_1 z^{-1} \tag{5.38}$$

and for the prediction horizon $N = 5$, we obtain

$$\overline{G}_N(t) = \begin{bmatrix} B_1 & 0 & 0 & 0 & 0 \\ 0 & B_1 & 0 & 0 & 0 \\ 0 & 0 & B_1 & 0 & 0 \\ 0 & 0 & 0 & B_1 & 0 \\ 0 & 0 & 0 & 0 & B_1 \end{bmatrix} \qquad (10 \text{ x } 15)$$

and

$$f_j(t) = (\mathbf{I}_2 - A_1)\, y(t) + A_1\, y(t-1), \quad j = 1, 2, 3, 4, 5 \qquad (2 \text{ x } 1) \tag{5.39}$$

From the definition of R, Q_1 and Q_2 in equation (5.16), Ψ in equation (5.21) and Ω^T in equation (5.22) can be obtained as follows:

$$\Psi(t) = \begin{bmatrix} B_1^T RB_1 + Q_1 + 5Q_2 & 4Q_2 & 3Q_2 & 2Q_2 & Q_2 \\ 4Q_2 & B_1^T RB_1 + Q_1 + 4Q_2 & 3Q_2 & 2Q_2 & Q_2 \\ 3Q_2 & 3Q_2 & B_1^T RB_1 + Q_1 + 3Q_2 & 2Q_2 & Q_2 \\ 2Q_2 & 2Q_2 & 2Q_2 & B_1^T RB_1 + Q_1 + 2Q_2 & Q_2 \\ Q_2 & Q_2 & Q_2 & Q_2 & B_1^T RB_1 + Q_1 + Q_2 \end{bmatrix} \quad (15 \times 15)$$

$$\Omega^T(t) = \begin{bmatrix} (y_M(t+1) - f_1(t))^T RB_1 - 5u^T(t-1)Q_2 \\ (y_M(t+2) - f_2(t))^T RB_1 - 4u^T(t-1)Q_2 \\ (y_M(t+3) - f_3(t))^T RB_1 - 3u^T(t-1)Q_2 \\ (y_M(t+4) - f_4(t))^T RB_1 - 2u^T(t-1)Q_2 \\ (y_M(t+5) - f_5(t))^T RB_1 - u^T(t-1)Q_2 \end{bmatrix} \quad (1 \times 15) \qquad (5.40)$$

For $n = 1$ and $N = 2$, these parameters are calculated to equal:

$$f_j(t) = (\mathbf{I}_2 - A_1)\, y(t) + A_1\, y(t-1), \quad j = 1, 2 \qquad (2 \times 1)$$

$$\Psi(t) = \begin{bmatrix} B_1^T RB_1 + Q_1 + 2Q_2 & Q_2 \\ Q_2 & B_1^T RB_1 + Q_1 + Q_2 \end{bmatrix} \qquad (6 \times 6)$$

$$\Omega^T(t) = \begin{bmatrix} (y_M(t+1) - f_1(t))^T RB_1 - 2u^T(t-1)Q_2 \\ (y_M(t+2) - f_2(t))^T RB_1 - u^T(t-1)Q_2 \end{bmatrix} \quad (1 \times 6) \qquad (5.41)$$

Similar calculations can also be performed to obtain the objective parameters for the process model with $n = 2$ and the prediction horizon $N = 5$. We then found:

$$F_j(z^{-1}) = (\mathbf{I}_2 - A_1) + (A_1 - A_2)\, z^{-1} + A_2 z^{-2} \quad \text{for } j = 1, 2, \ldots, 5$$

$$\overline{G}_N(t) = \begin{bmatrix} B_1 & 0 & 0 & 0 & 0 \\ B_2 & B_1 & 0 & 0 & 0 \\ 0 & B_2 & B_1 & 0 & 0 \\ 0 & 0 & B_2 & B_1 & 0 \\ 0 & 0 & 0 & B_2 & B_1 \end{bmatrix} \qquad (10 \times 15)$$

$$f_1(t) = B_2\,\Delta u(t\text{-}1) + (\mathrm{I}_2 - A_1)\,y(t) + (A_1\text{-}A_2)\,y(t-1) + A_2\,y(t-2)$$

$$f_j(t) = (\mathrm{I}_2 - A_1)\,y(t) + (A_1\text{-}A_2)\,y(t-1) + A_2\,y(t-2) \quad \text{for } j = 2, 3, 4, 5$$

$$\Psi(t) = \begin{bmatrix} B_1^T RB_1 + B_2^T RB_2 + Q_1 + 5Q_2 & B_2^T RB_1 + 4Q_2 \\ B_1^T RB_2 + 4Q_2 & B_1^T RB_1 + B_2^T RB_2 + Q_1 + 4Q_2 \\ 3Q_2 & B_1^T RB_2 + 3Q_2 \\ 2Q_2 & 2Q_2 \\ Q_2 & Q_2 \end{bmatrix}$$

$$\begin{matrix} 3Q_2 & 2Q_2 & Q_2 \\ B_2^T RB_1 + 3Q_2 & 2Q_2 & Q_2 \\ B_1^T RB_1 + B_2^T RB_2 + Q_1 + 3Q_2 & B_2^T RB_1 + 2Q_2 & Q_2 \\ B_1^T RB_2 + 2Q_2 & B_1^T RB_1 + B_2^T RB_2 + Q_1 + 2Q_2 & B_2^T RB_1 + Q_2 \\ Q_2 & B_1^T RB_2 + Q_2 & B_1^T RB_1 + Q_1 + Q_2 \end{matrix} \Bigg]$$

$$(15 \times 15)$$

$$\Omega^T(t) = \begin{bmatrix} (y_M(t+1) - f_1(t))^T RB_1 + ((y_M(t+2) - f_2(t))^T RB_2 - 5u^T(t-1)Q_2 \\ (y_M(t+2) - f_2(t))^T RB_1 + ((y_M(t+3) - f_3(t))^T RB_2 - 4u^T(t-1)Q_2 \\ (y_M(t+3) - f_3(t))^T RB_1 + ((y_M(t+4) - f_4(t))^T RB_2 - 3u^T(t-1)Q_2 \\ (y_M(t+4) - f_4(t))^T RB_1 + ((y_M(t+5) - f_5(t))^T RB_2 - 2u^T(t-1)Q_2 \\ (y_M(t+5) - f_5(t))^T RB_1 - u^T(t-1)Q_2 \end{bmatrix}$$

$$(1 \times 15) \qquad (5.42)$$

For $n = 2$ and $N = 2$, the required parameters are given as follows:

$$f_1(t) = B_2\,\Delta u(t\text{-}1) + (\mathrm{I}_2 - A_1)\,y(t) + (A_1\text{-}A_2)\,y(t-1) + A_2\,y(t-2)$$

$$f_2(t) = (\mathrm{I}_2 - A_1)\,y(t) + (A_1\text{-}A_2)\,y(t-1) + A_2\,y(t-2)$$

$$\Psi(t) = \begin{bmatrix} B_1^T RB_1 + B_2^T R B_2 + Q_1 + 2Q_2 & B_2^T RB_1 + Q_2 \\ B_1^T RB_2 + Q_2 & B_1^T RB_1 + Q_1 + Q_2 \end{bmatrix} \qquad (6 \times 6)$$

$$\Omega^T(t) = \begin{bmatrix} (y_M(t+1) - f_1(t))^T RB_1 + (y_M(t+2) - f_2(t))^T RB_2 - 2u^T(t-1)Q_2 \\ (y_M(t+2) - f_2(t))^T RB_1 - u^T(t-1)Q_2 \end{bmatrix}$$

$$(1 \times 6) \qquad (5.43)$$

Notice that the matrix coefficients R, Q_1 and Q_2 have to be chosen before $\Psi(t)$ and $\Omega(t)$ can be calculated. These matrices are selected so that we can achieve the required control performance by minimising the quadratic criterion J. In another words, the implemented control law would reduce the output errors, the rate of energy consumed between one sampling interval and the total energy consumption. In general, J requires the actual cost of regulation error so that its matrix coefficient R would be set to an identity matrix. Moreover, this control strategy will reduce the energy consumed if a larger magnitude of Q_2 is used and it will reduce the control switching between one sampling interval by increasing Q_1, but as a consequence, it will increase the settling time or the controller would be out of control. In order to choose the appropriate diagonal matrix values of R, Q_1 and Q_2 for our applications, we used the results shown in Dion et al (1991) as a reference with slight modification and they are given as follows:

Weight on the output R = diag(1, 1)

Weight on the input increment Q_1 = diag(0.005, 0.04, 0.04)

Weight on the input Q_2 = diag(0.0006, 0.001, 0.0006).

5.4.2. Input and output constraints

Let us define the control input changes, $\Delta u(t) \equiv \left[\Delta W(t) \quad \Delta C(t) \quad \Delta H(t)\right]^T$ and the output changes, $\Delta y(t) \equiv \left[\Delta T_c(t) \quad \Delta H_c(t)\right]^T$. For the input constraints, the heater W, cooler C and humidifier H have limits of 5.0, 2.7 and 2.6 kilowatts respectively. Therefore, from the definitions in equation (5.28), we have $u_{high} = \left[5.0 \quad 2.7 \quad 2.6\right]^T$ and $u_{low} = \left[0 \quad 0 \quad 0\right]^T$. We also need to set the maximum permissible change in the control input between sampling intervals, D_u; let this equal $\left[2 \quad 1 \quad 1\right]^T$.

For the output constraints, these limits are selected using common sense reasoning as follows: $y_{high} = \left[40 \quad 100\right]^T$, $y_{low} = \left[0 \quad 0\right]^T$, and $D_y = \left[10 \quad 10\right]^T$, i.e. the ranges of the room temperature and the relative humidity are 0 - 40°C and 0 - 100%rh; and their maximum permissible changes in one sampling interval are 10°C and 10%rh respectively.

The matrix $C_{uy}(\theta)$ and vector $\psi_{uy}(\theta, \phi(t), t)$ for the prediction horizon $N = 2$ are calculated from equations (5.25), (5.26) and (5.27) where it is straightforward to show that the matrices C_1, C_2, C_3 and C_4 are of dimensions (6 x 6), (6 x 6), (6 x 6) and (4 x 6) respectively, and the vectors ψ_1, ψ_2, ψ_3, ψ_4, ψ_5, ψ_6 and ψ_7 are of dimensions (6 x 1), (6 x 1), (6 x 1), (4 x 1), (4 x 1), (4 x 1) and (4 x 1) respectively, thus giving the matrix $C_{uy}(\theta)$ is of dimension (40 x 6) and the vector $\psi_{uy}(\theta, \phi(t), t)$ is of dimension (40 x 1). The required (6 x 1) predicted incremental inputs Δu_t is given by

$$\Delta u_t = \left[\Delta W(t) \quad \Delta C(t) \quad \Delta H(t) \quad \Delta W(t+1) \quad \Delta C(t+1) \quad \Delta H(t+1)\right]^T$$

Therefore, in this case we require to obtain 6 unknown parameters, i.e. $\Delta W(t)$, $\Delta C(t)$, ..., $\Delta H(t+1)$, with conditions (5.20) subjects to 40 constraints, at each sampling time.

Similarly, for the prediction horizon $N = 5$, the size of $C_{uy}(\theta)$ and $\psi_{uy}(\theta, \phi(t), t)$ are of dimensions (100 x 15) and (100 x 1) respectively and the required Δu_t is of dimension (15 x 1) and is given by

$$\Delta u_t = \left[\Delta W(t) \quad \Delta C(t) \quad \Delta H(t) \quad \ldots \right.$$

$$\left. \Delta H(t+3) \quad \Delta W(t+4) \quad \Delta C(t+4) \quad \Delta H(t+4)\right]^T$$

In this case we require to obtain 15 unknown parameters, i.e. $\Delta W(t)$, $\Delta C(t)$, ..., $\Delta H(t+4)$ with conditions (5.20) subjects to 100 constraints, at each sampling time.

5.4.3. Quadratic programming

If equations (5.20) - (5.22) are fulfilled the optimality conditions given by the Kuhn-Tucker conditions (see for example Koo, 1977), and it is possible to calculate Δu_t by using a quadratic programming method. The standard notation of quadratic programming is to find a solution for x^* from

$$\underset{x}{\text{minimize}}\ q(x) \equiv \tfrac{1}{2} x^T \mathbf{G} x + g^T x$$

$$\text{subject to } \mathbf{A}x \leq \mathbf{b}. \tag{5.44}$$

where $\mathbf{A}$ and $\mathbf{G}$ are (r x s) and (s x s) matrices respectively.

Under this notation, equation (5.23) can be written as

$$-C_{uy}(\theta)\, \Delta u_t \leq -\psi_{uy}(\theta, \phi(t), t) \tag{5.45}$$

and for the case in section 5.3, matrices $\mathbf{G}$ and $\mathbf{A}$, and vectors x and $\mathbf{b}$ from equation (5.44) can be given as follows:

$$\mathbf{G} = 2\Psi \tag{5.46}$$

$$g^T = -2\Omega^T \tag{5.47}$$

$$\mathbf{A} = -C_{uy}(\theta) \tag{5.48}$$

$$\mathbf{b} = -\psi_{uy}(\theta, \phi(t), t) \tag{5.49}$$

$$x = [x_1, x_2, \ldots, x_6]^T, \quad \text{for } N = 2 \tag{5.50}$$

where

$$x_1 = \Delta W(t),\ x_2 = \Delta C(t),\ \ldots,\ x_6 = \Delta H(t+1)$$

and $x = [x_1, x_2, \ldots, x_{15}]^T$, for $N = 5$ (5.51)

where

$$x_1 = \Delta W(t),\ x_2 = \Delta C(t),\ \ldots,\ x_{15} = \Delta H(t+4).$$

In the MATLAB language, a function called 'qp' can be used to calculate the solution x.

Finally, we are only interested in obtaining the values of x_1, x_2 and x_3, since these values are required to update $u(t)$ from the relationship

$$u(t) = u(t-1) + \Delta u(t) \tag{5.19}$$

where

$$\Delta u(t) = \begin{bmatrix} x_1 & x_2 & x_3 \end{bmatrix}^T \tag{5.52}$$

5.5. Simulation results

The developed MIMO adaptive control theory described in sections 5.2 – 5.4 is used to control the room temperature and the relative humidity by simultaneously calculating the three input signals to regulate the HVAC plant. It is assumed that the plant dynamics follow the model equations (2.1) and (2.2), and the adaptive process model is of the form of equations (5.32) and (5.33).

Let us consider the system with set-points T_r and H_r, and calculate the control performances of the simulation trials. It is assumed that the initial conditions for the room temperature $T_c(0)$ and the relative humidity $H_c(0)$ are known and all the three initial controlling inputs to the plant have not been implemented.

Figure 5.2 shows the performance of the MIMO adaptive controller with the prediction horizon, $N = 5$. For this trial, the external disturbances such as the laboratory temperature, outside temperature, outside relative humidity and the solar irradiance are assumed to be constant. Furthermore, the unmodelled stochastic influences (i.e. the white noises) are not included. The system simulation begins at iteration $t = 4$ to allow for the inclusion of delayed control inputs and disturbances, where we can see that an adaptation transient exists in the relative humidity loop, but this does not occur for the room temperature. At steady state conditions ($50 < t < 100$, $130 < t < 200$, $230 < t < 300$, $330 < t < 400$ and $420 < t < 500$), the controller is seen to produce small output errors. We can see that the non-minimum type of transient occurs when the reference outputs are changed; at $t = 100$ where both outputs are reduced, the transient occurs for the relative humidity loop only; at $t = 200$ where the temperature is reduced and the relative humidity is increased, the transient occurs for both loops, at $t = 300$ where only the temperature is increased, the transient occurs for temperature loop only; at $t = 400$ where only the humidity is reduced, the transient occurs for both loops. Note that in this simulation result, the output errors can be further reduced by suitable choices of the weighting factors R, Q_1 and Q_2 in the quadratic criterion (5.2) and these will be discussed later in this section.

Since the adaptive controller is performed with input and output constraints, the control input variations are within their ranges and thus, they are not truncated inputs.

For the output constraint, as we can see in Figure 5.2 c) that during the initial transient, the relative humidity grows beyond the limit, i.e. above 100%rh; this is due to the problem given by equation (5.20) and only that the constraints concerning $u(t)$ are satisfied. There are no guarantee that the constraints concerning $y(t)$ which is calculated from the mathematical model of air dynamics in the room, i.e. equations (2.1) and (2.2), are satisfied since these constraints deal with only the process model parameters, i.e. A_i and B_i matrices.

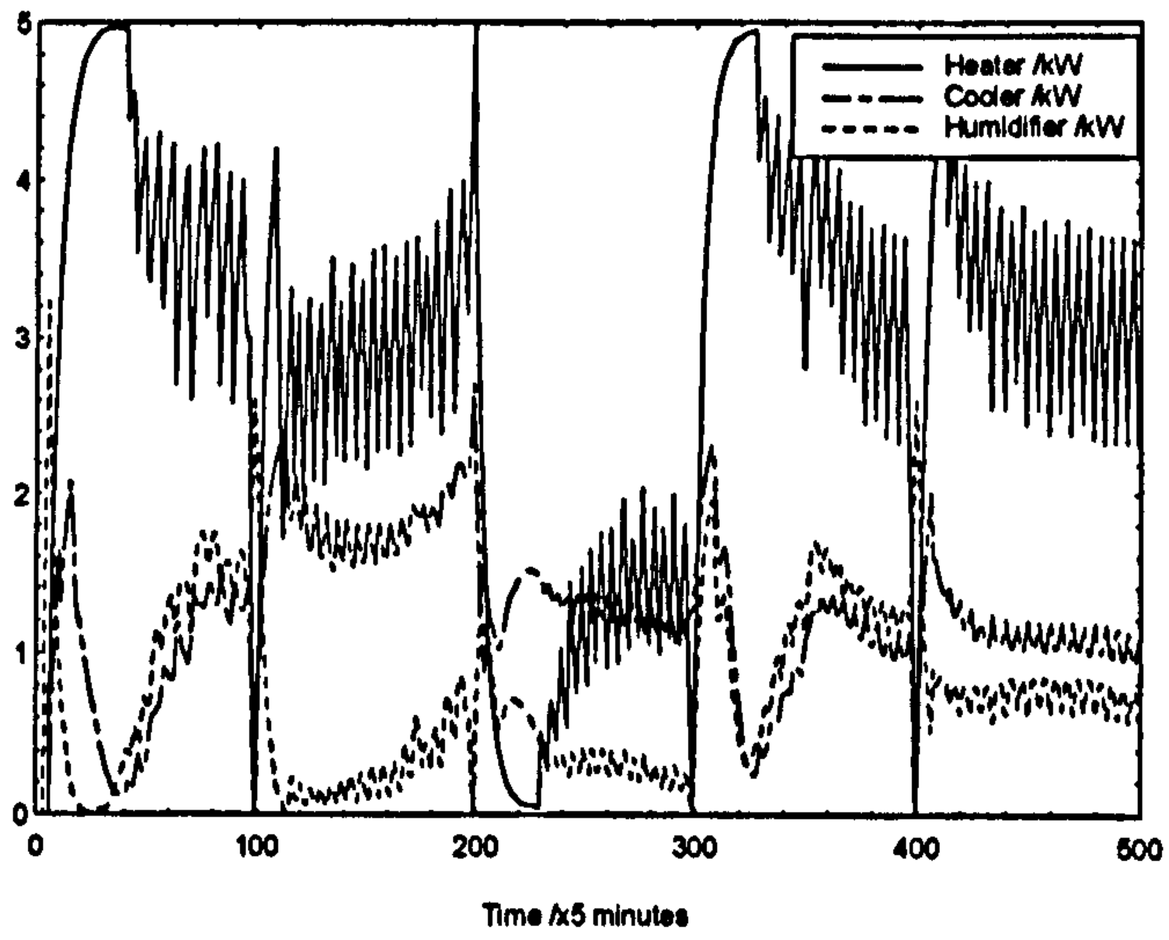

a). Control inputs

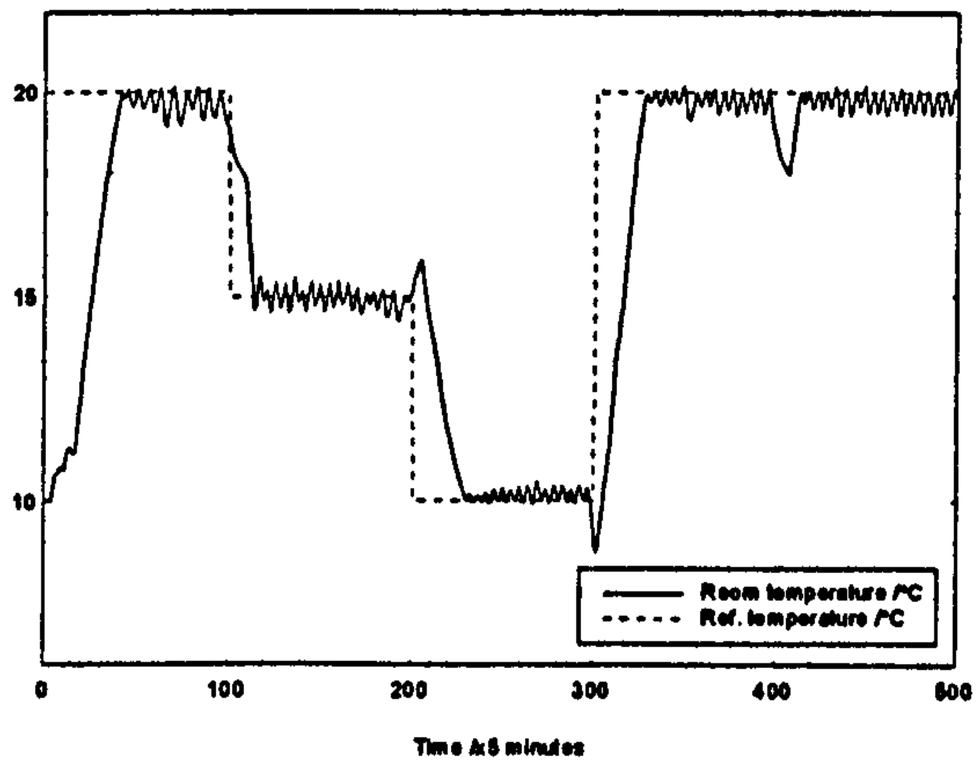

b). Room temperature

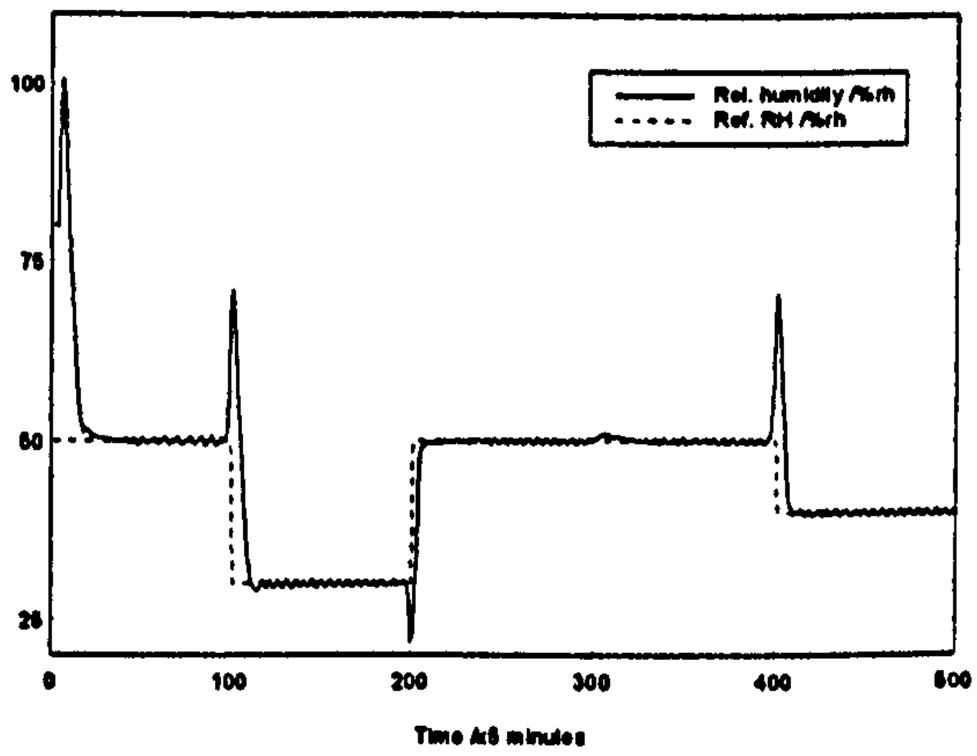

c). Relative humidity

Figure 5.2: Performance of the adaptive controller ($n = 1$; $N = 5$)

Figure 5.3 shows the performance of the controller with the process model of observability index, $n = 1$ and the prediction horizon, $N = 2$. We can see that the transients are better now but the controller action is still excessive. Also the output errors are a little larger but still within reasonable tolerances. This result shows that the non-minimum type of transient can be reduced by using smaller number of prediction horizon.

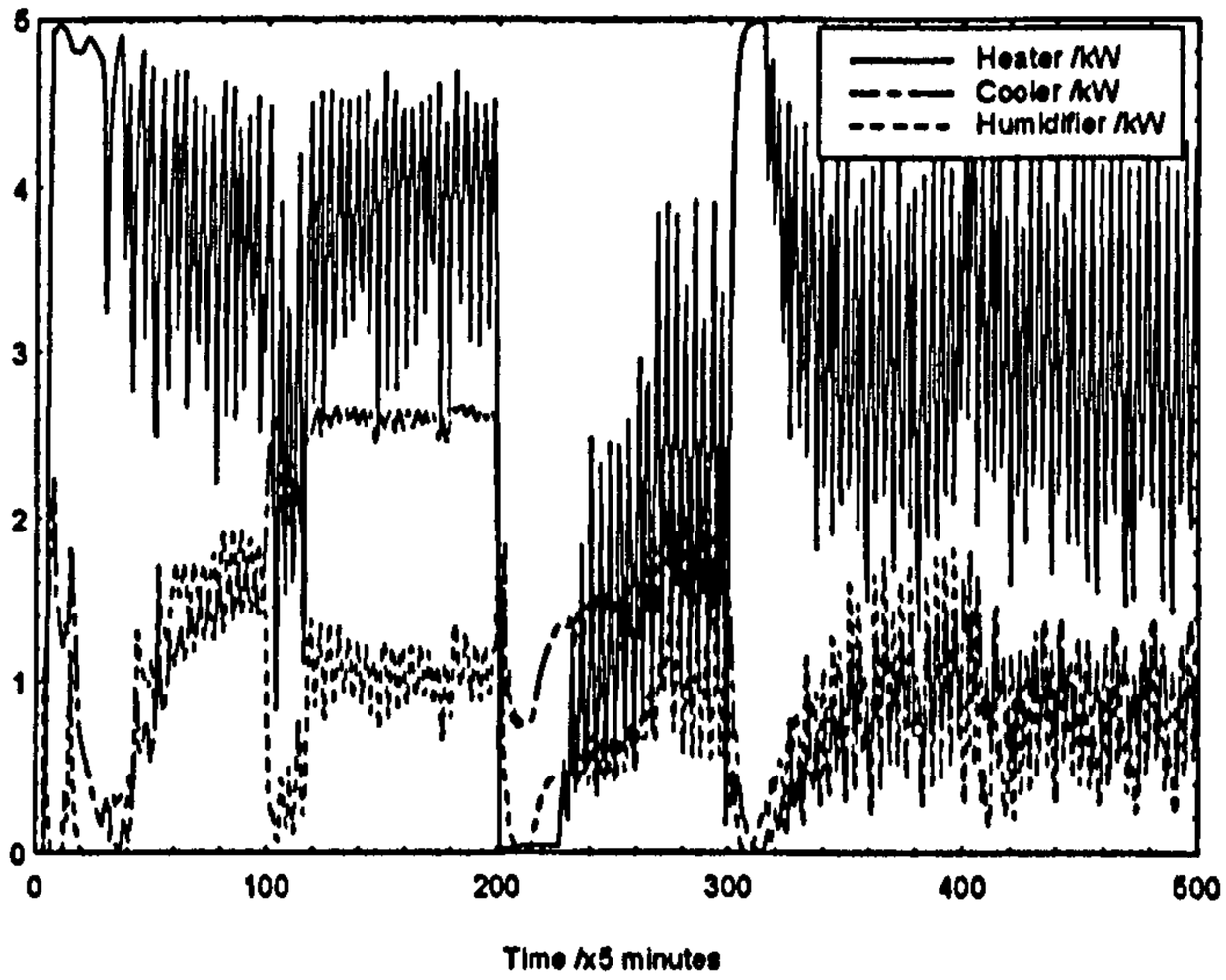

a). Control inputs

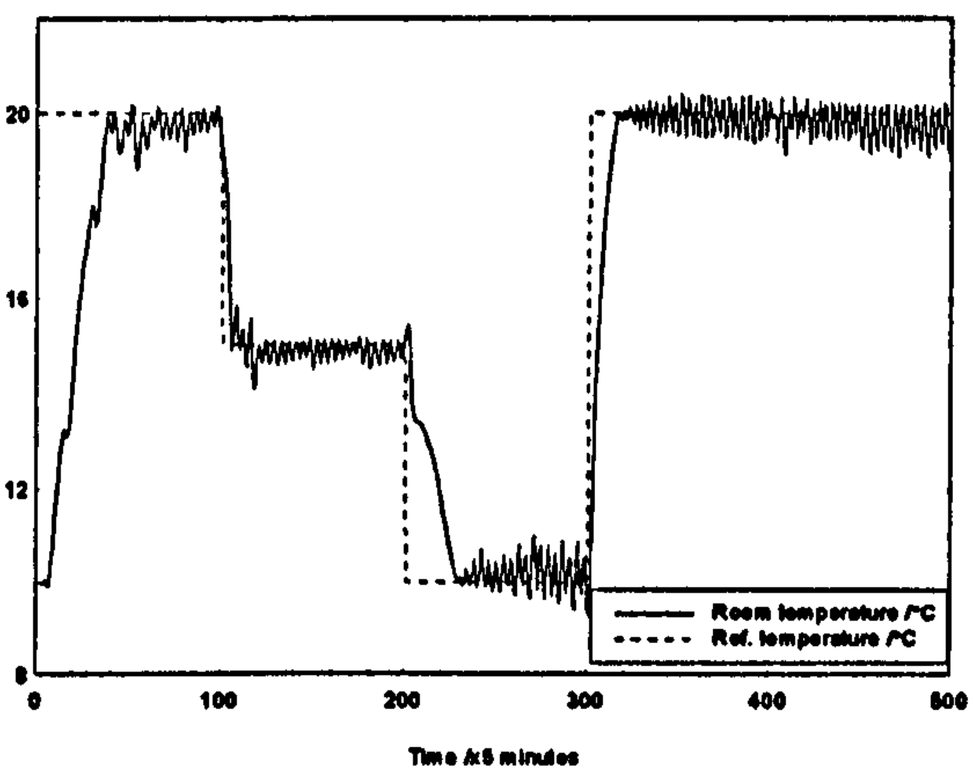

b). Room temperature

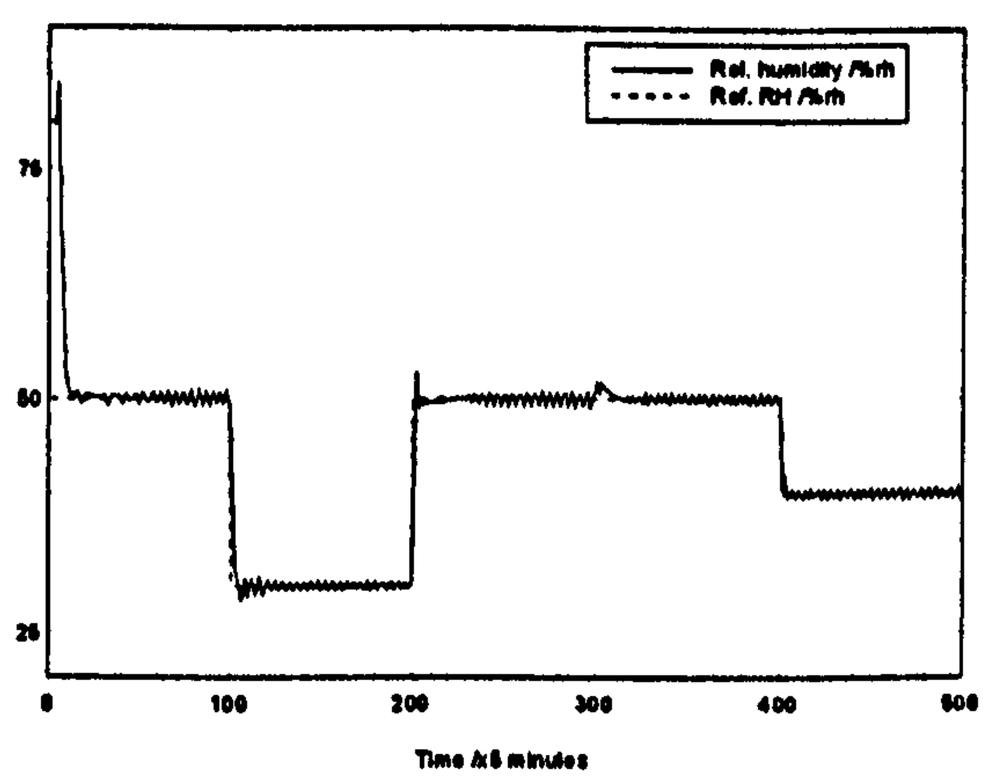

c). Relative humidity

Figure 5.3: Performance of the adaptive controller ($n = 1$; $N = 2$)

The simulation trials are also carried out for the process model of observability index, $n = 2$ with identical parameter values as used for Figures (5.2). The result is shown in the Figure 5.4 where we can see the non-minimum type of transients still exists during the step change of the setpoints but the output regulation as well as the control input switching were very much improved as compared to the result for $n = 1$. Similarly, we found that these transients are reduced when the prediction horizon, N, equals 2, and this is shown in Figure 5.5. The steady state performance over 100 data points, for example, from 101st to 200th iterations are calculated and found to be as follows:

- the required control input energies are 27.7, 7.2 and 11.5 kWh for the heater, cooler and humidifier respectively;
- the output squared errors are $0.3°C^2$ and $1.3\%rh^2$ for the temperature and relative humidity respectively; and
- the required times to reach the temperature and relative humidity setpoints are 1.7 and 0.8 hours respectively.

The values of the estimated parameters for the on-line process model with $n = 2$ and $N = 2$, namely A_1, A_2, B_1 and B_2, were calculated; the results are presented in Figure 5.6 where we can see that how the adaptive system responds to stepwise reference signals and to changes in the incremental control inputs via the presented control law. Here, the estimated parameters are defined as follows:

$$A_1 = \begin{bmatrix} a_{111} & a_{112} \\ a_{121} & a_{122} \end{bmatrix}, \quad A_2 = \begin{bmatrix} a_{211} & a_{212} \\ a_{221} & a_{222} \end{bmatrix}, \quad B_1 = \begin{bmatrix} b_{111} & b_{112} & b_{113} \\ b_{121} & b_{122} & b_{123} \end{bmatrix} \text{ and}$$

$$B_2 = \begin{bmatrix} b_{211} & b_{212} & b_{213} \\ b_{221} & b_{222} & b_{223} \end{bmatrix}$$

where the on-line process model is given by

$$y(t) + A_1 y(t\text{-}1) + A_2 y(t\text{-}2) = B_1 u(t\text{-}1) + B_2 u(t\text{-}2).$$

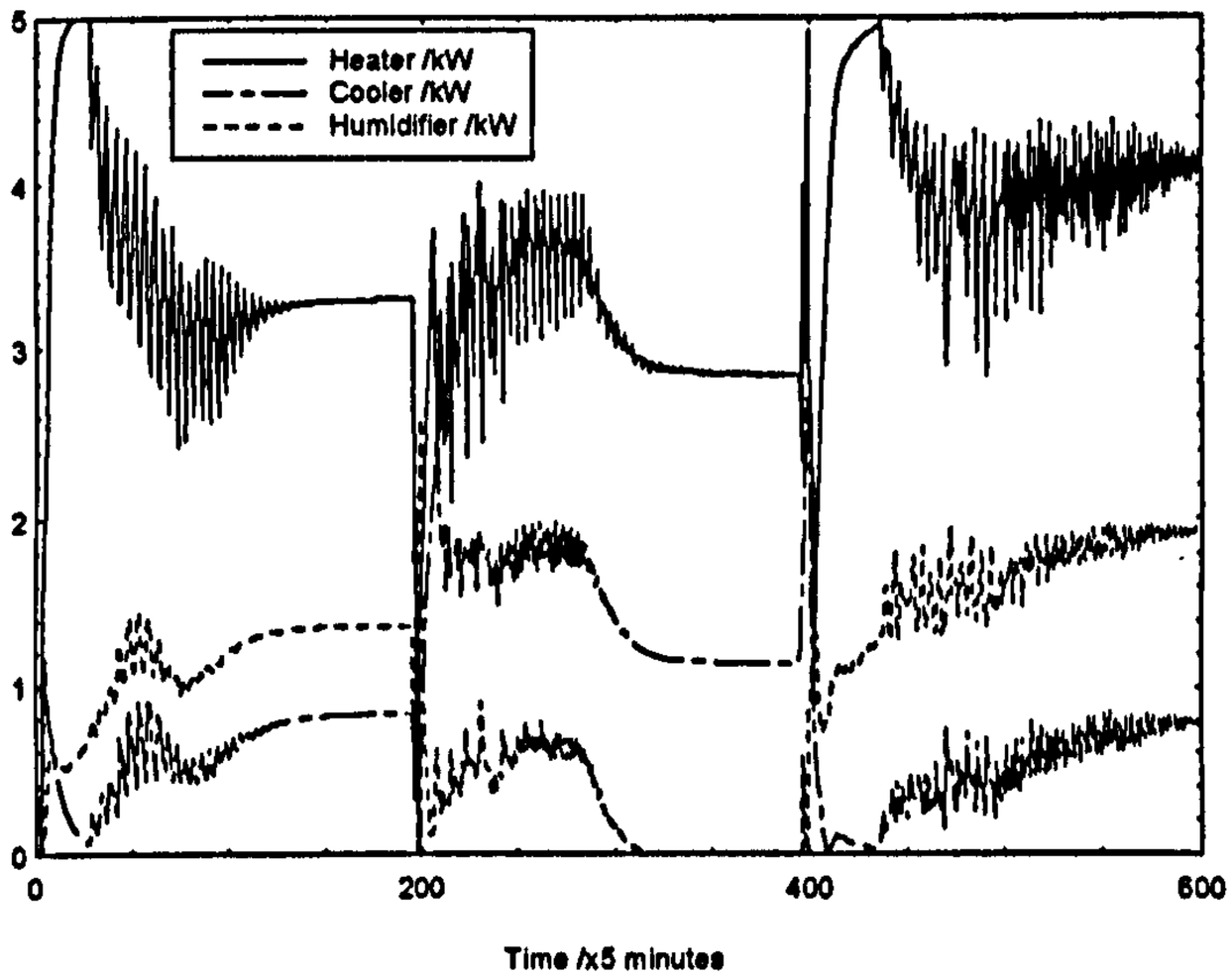

a). Control inputs

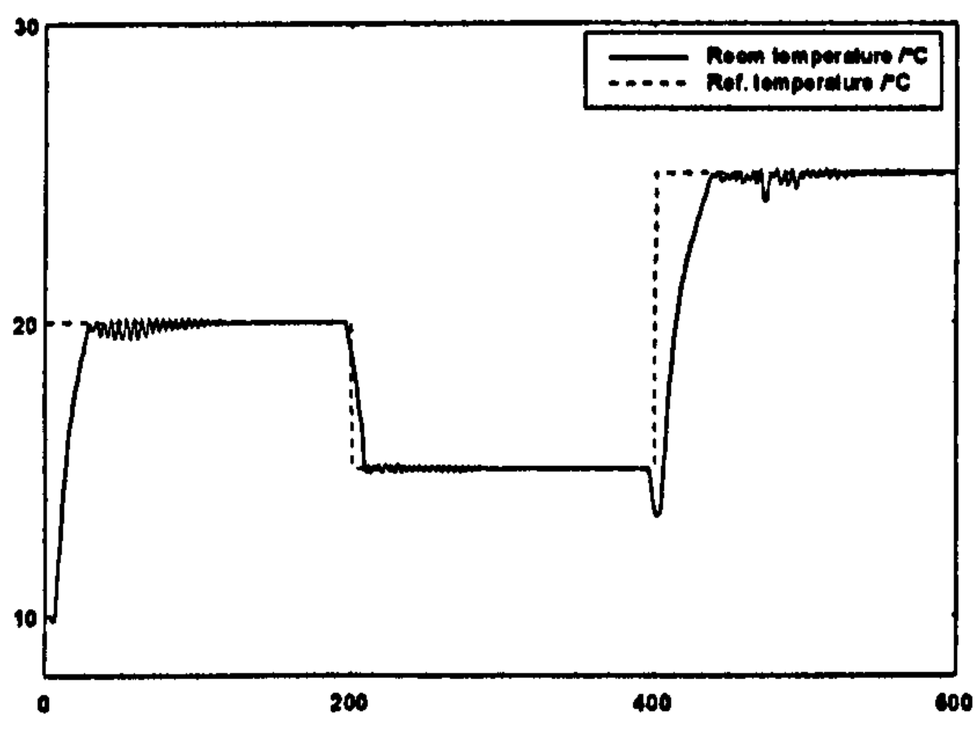

b). Room temperature

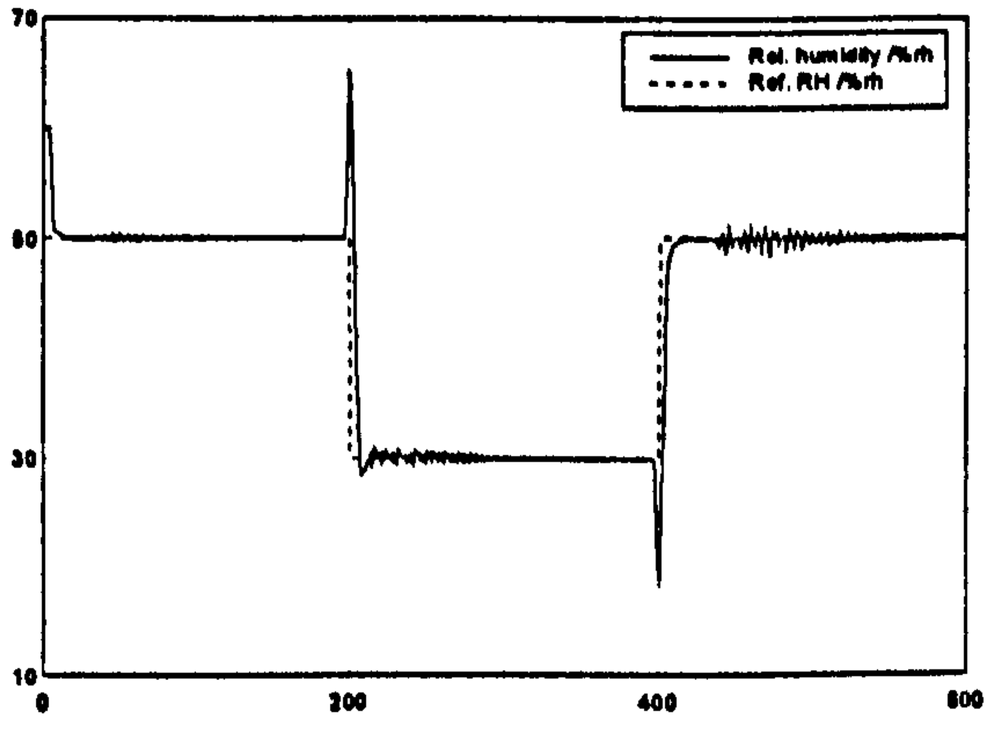

c). Relative humidity

Figure 5.4: Performance of the adaptive controller ($n = 2$; $N = 5$)

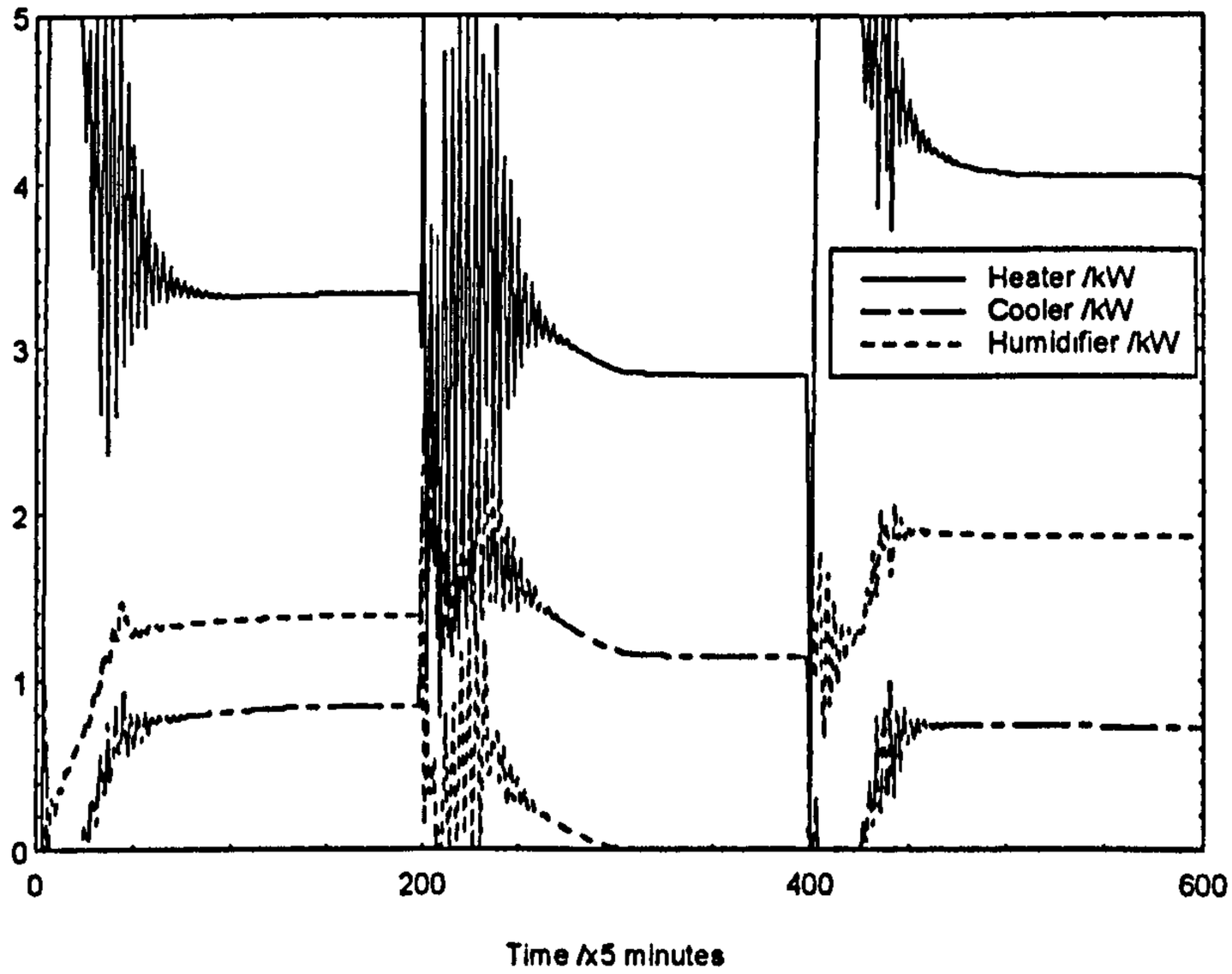

a). Control inputs

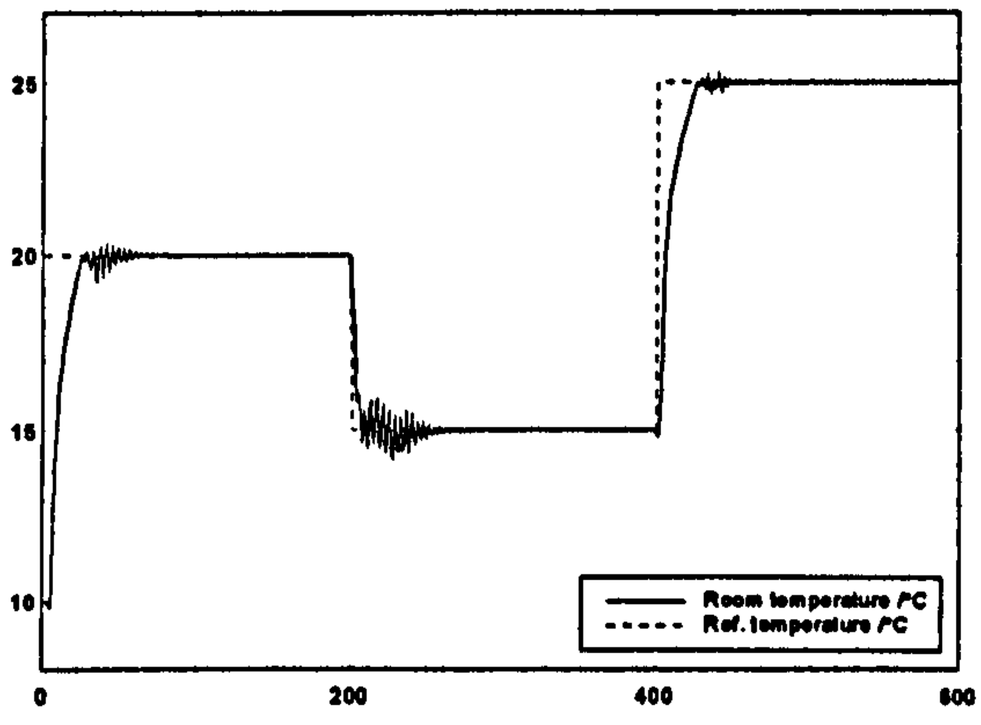

b). Room temperature

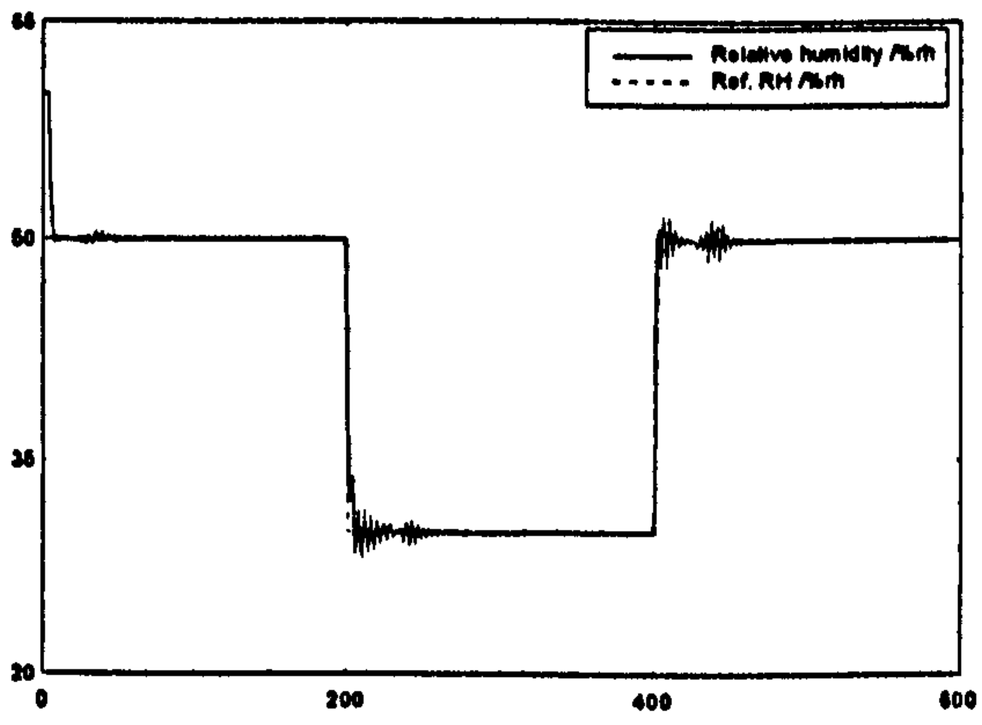

c). Relative humidity

Figure 5.5: Performance of the adaptive controller ($n = 2$; $N = 2$)

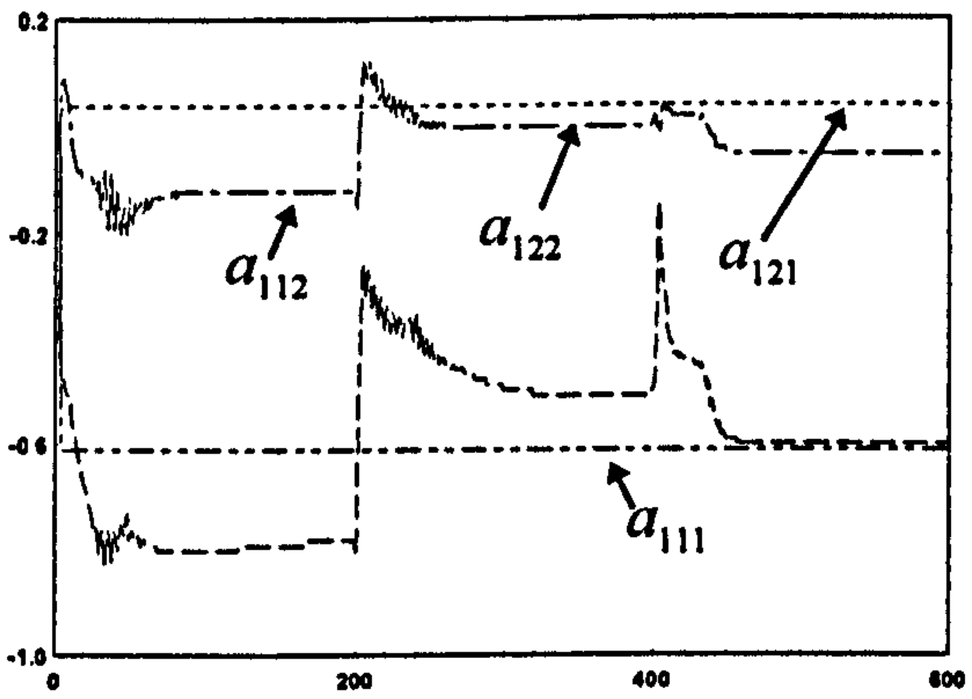

a) A_1

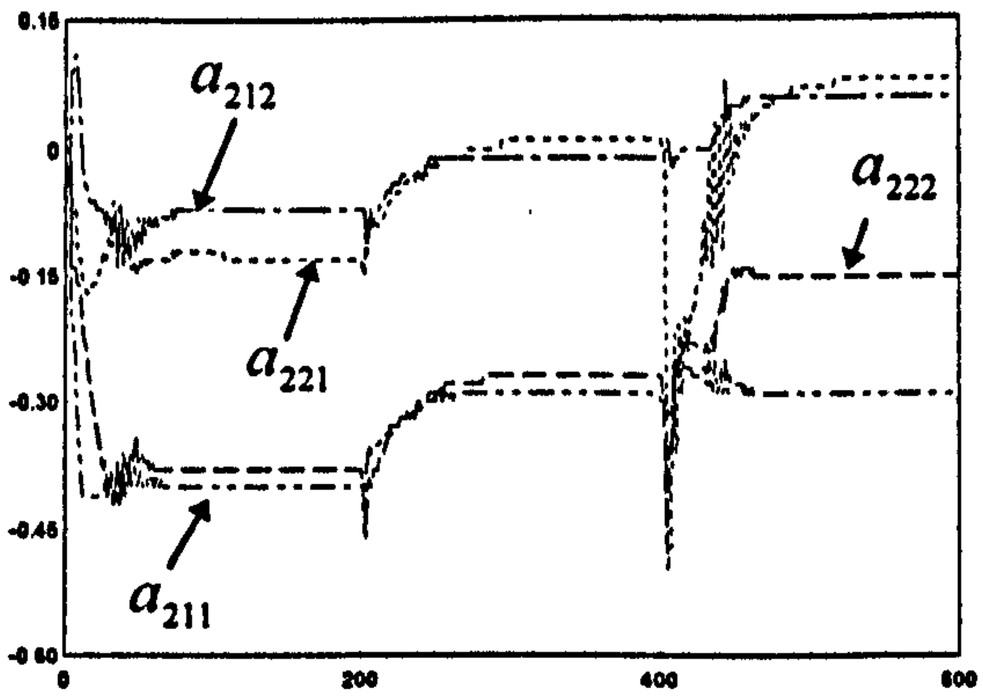

b) A_2

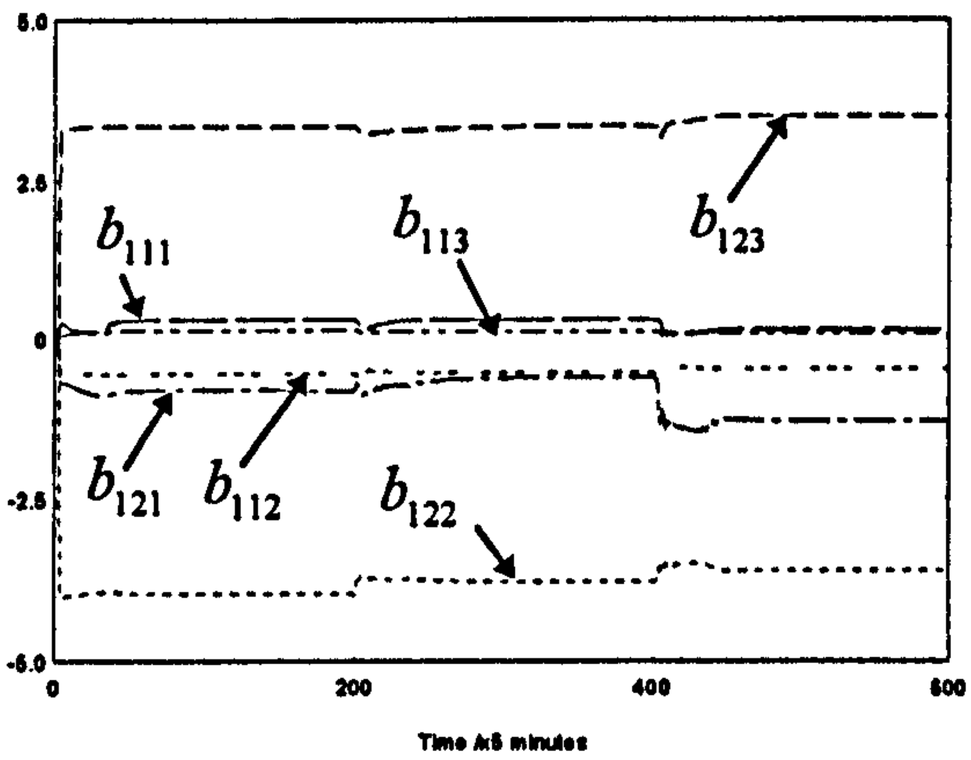

c) B_1

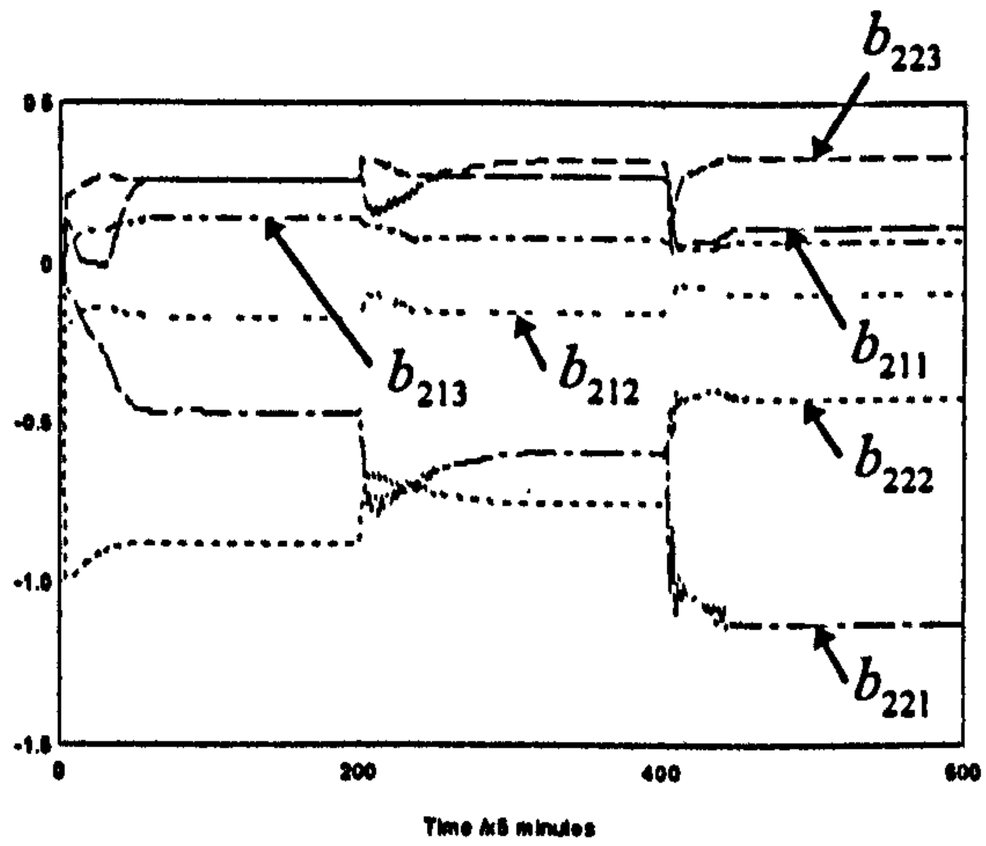

d) B_2

Figure 5.6: Parameter estimation values for the process model ($n = 2$; $N = 2$)

Now, we present the effect to the control performances as the weighting factors R, Q_1 and Q_2 are changed. We can use the controller parameters as used to obtain Figure 5.3 for comparison purposes. The simulation results are shown in Figures 5.6, 5.7 and 5.8 when only R is reduced to diag(0.8, 0.8), when only Q_1 is increased to diag(0.05, 0.4, 0.4), i.e. 10 times larger than the previous value, and when only Q_2 is increased to diag(0.006, 0.01, 0.006), i.e. 10 times larger than the previous value, respectively. We can see that the difference in the control performances as compared to that shown in

Figure 5.3 are not clearly distinguished, but all have excessive control signals in order to regulate the system outputs. These situations are due to the nature of multivariable adaptive systems where a perfect combination of the diagonal elements in the factors R, Q_1 and Q_2 matrices is required in order to obtain good control performance, which is not easy to identify.

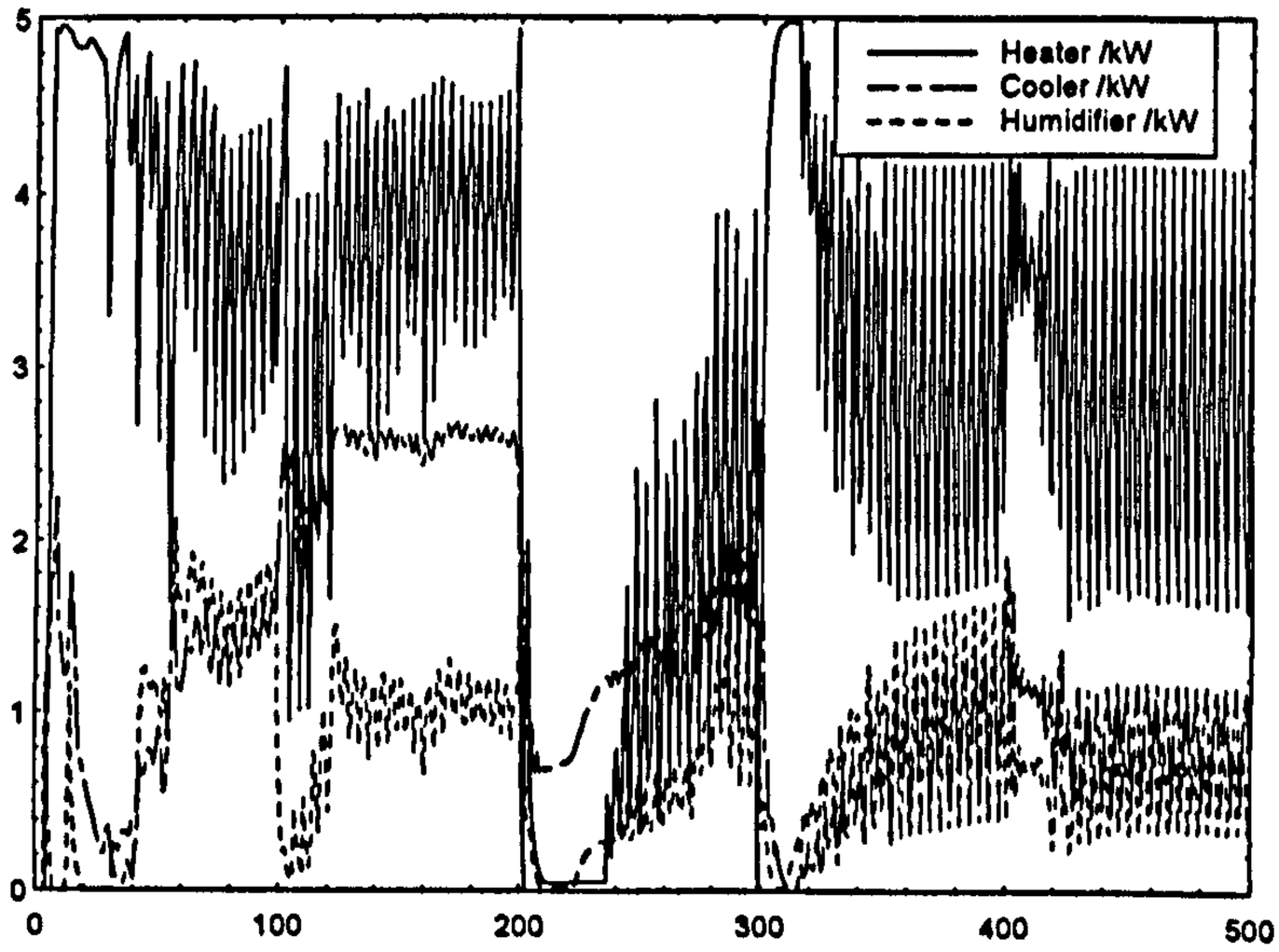

a). Control inputs

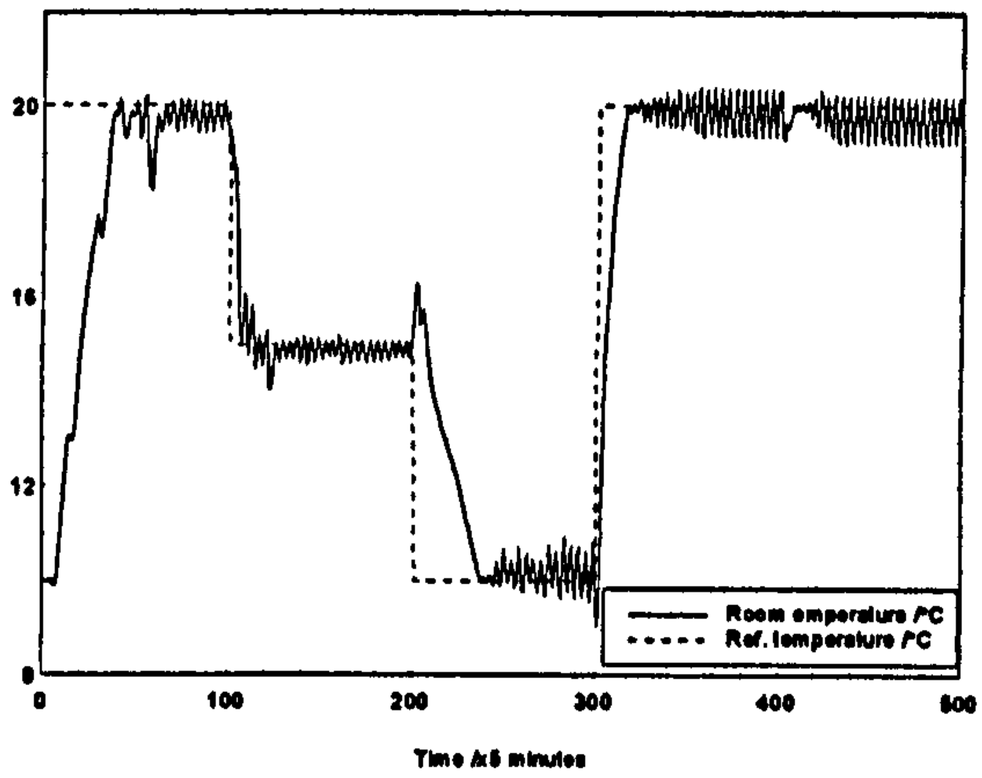

b). Room temperature

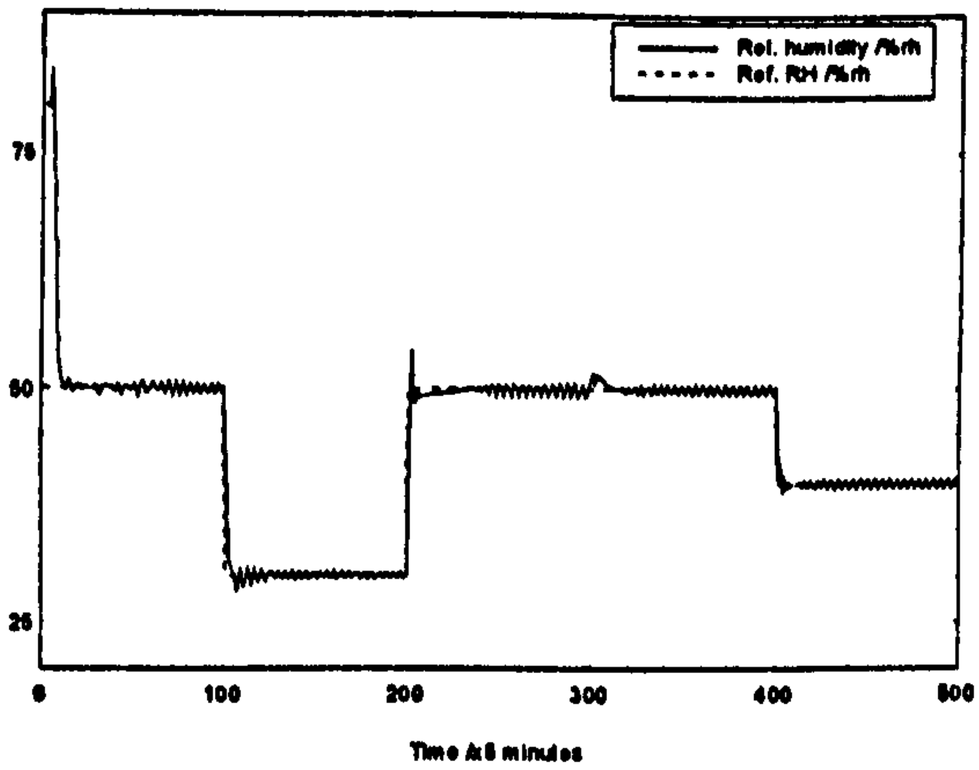

c). Relative humidity

Figure 5.6: Control performance for $n = 1$ and $N = 2$ with decreased R

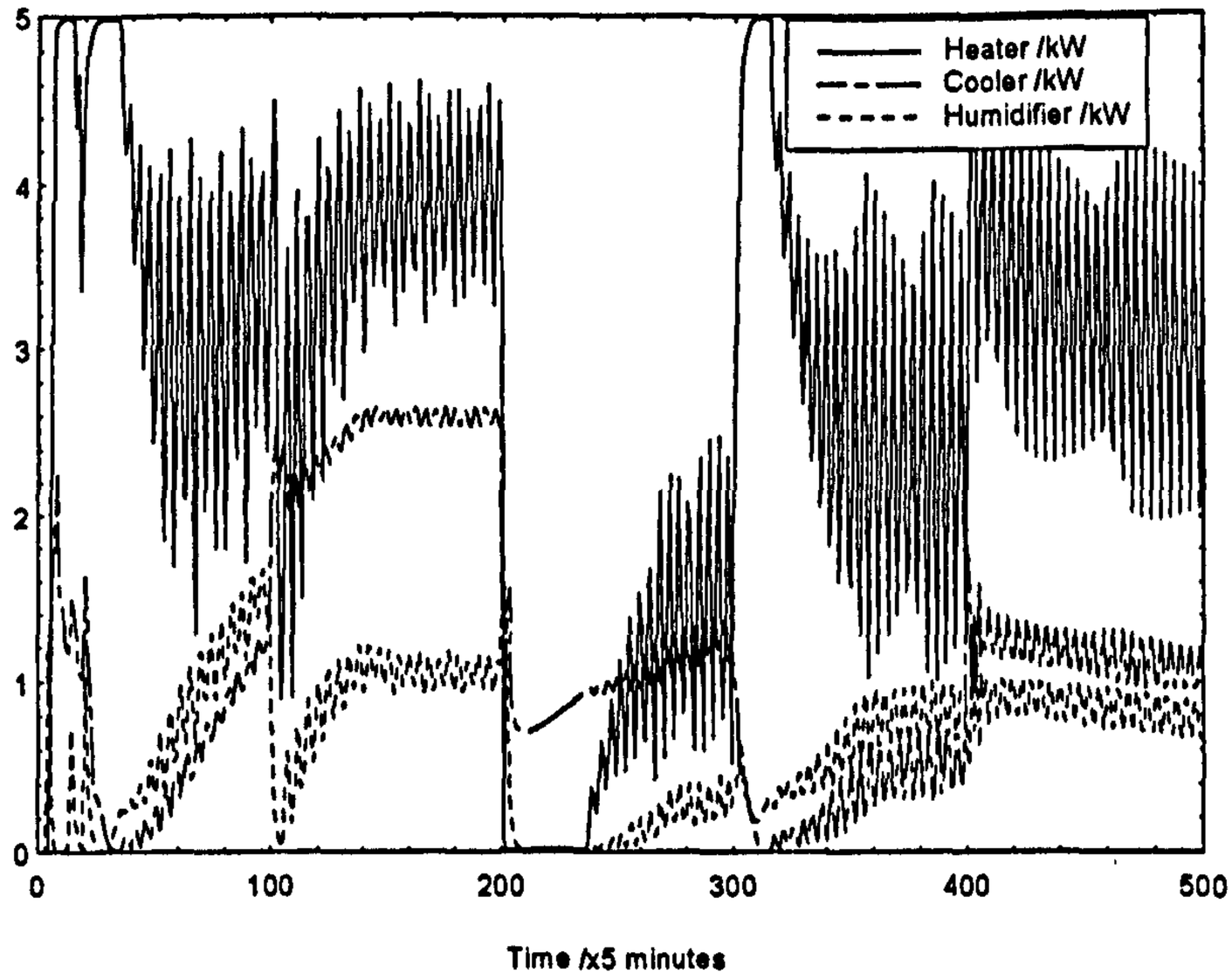

a). Control inputs

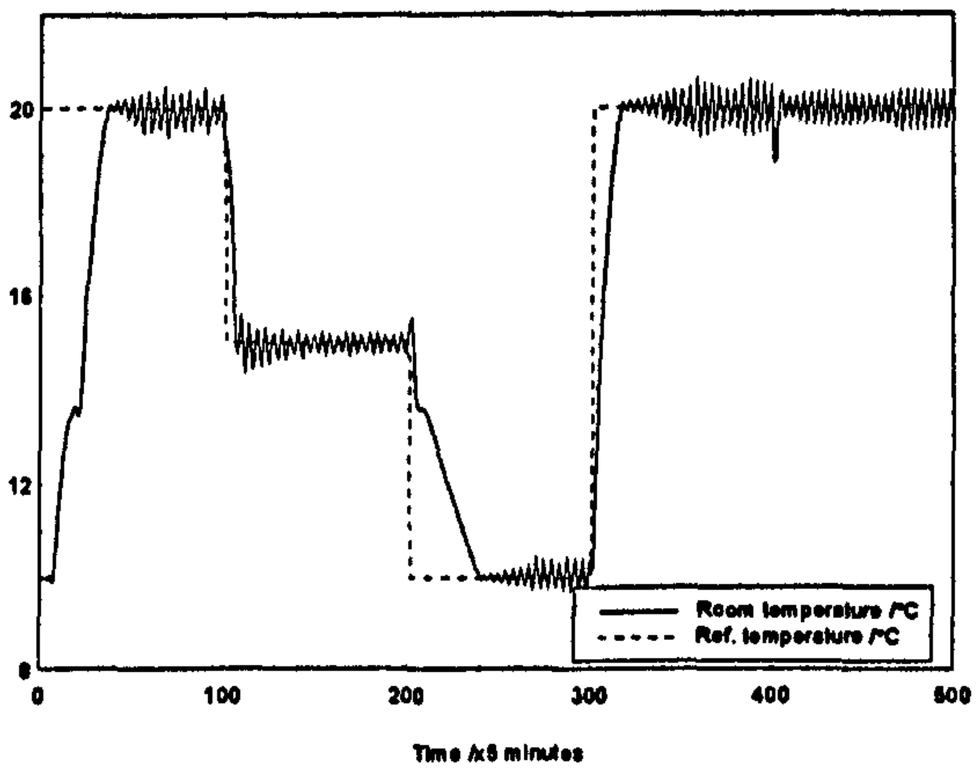

b). Room temperature

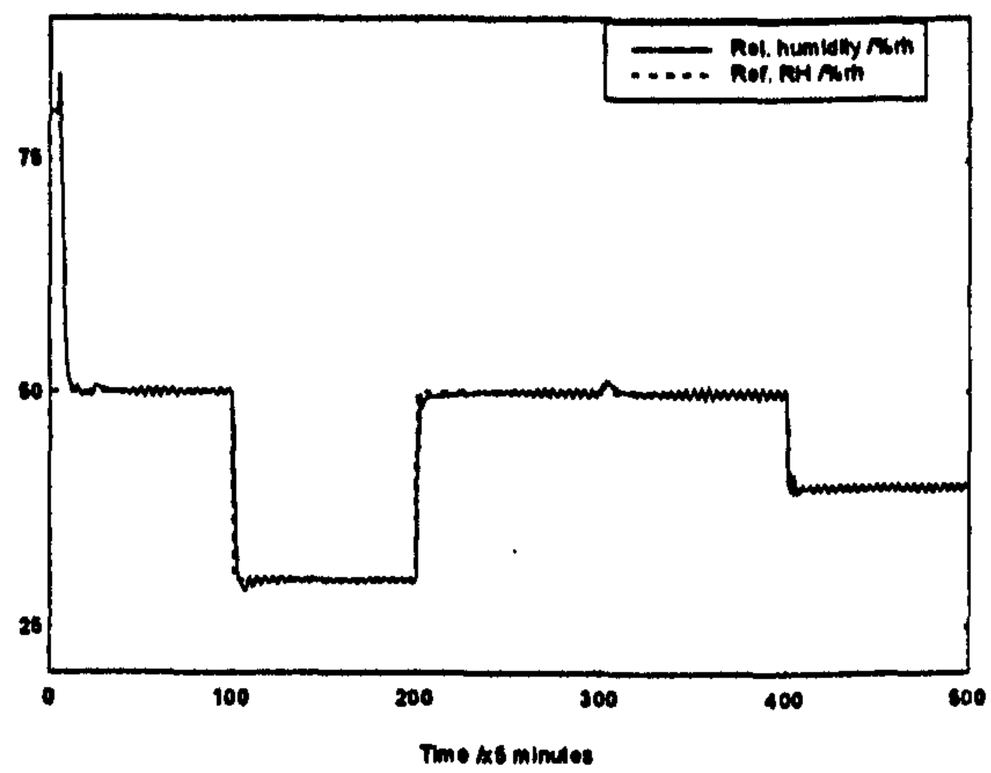

c). Relative humidity

Figure 5.7: Control performance for $n = 1$ and $N = 2$ with increased Q_1

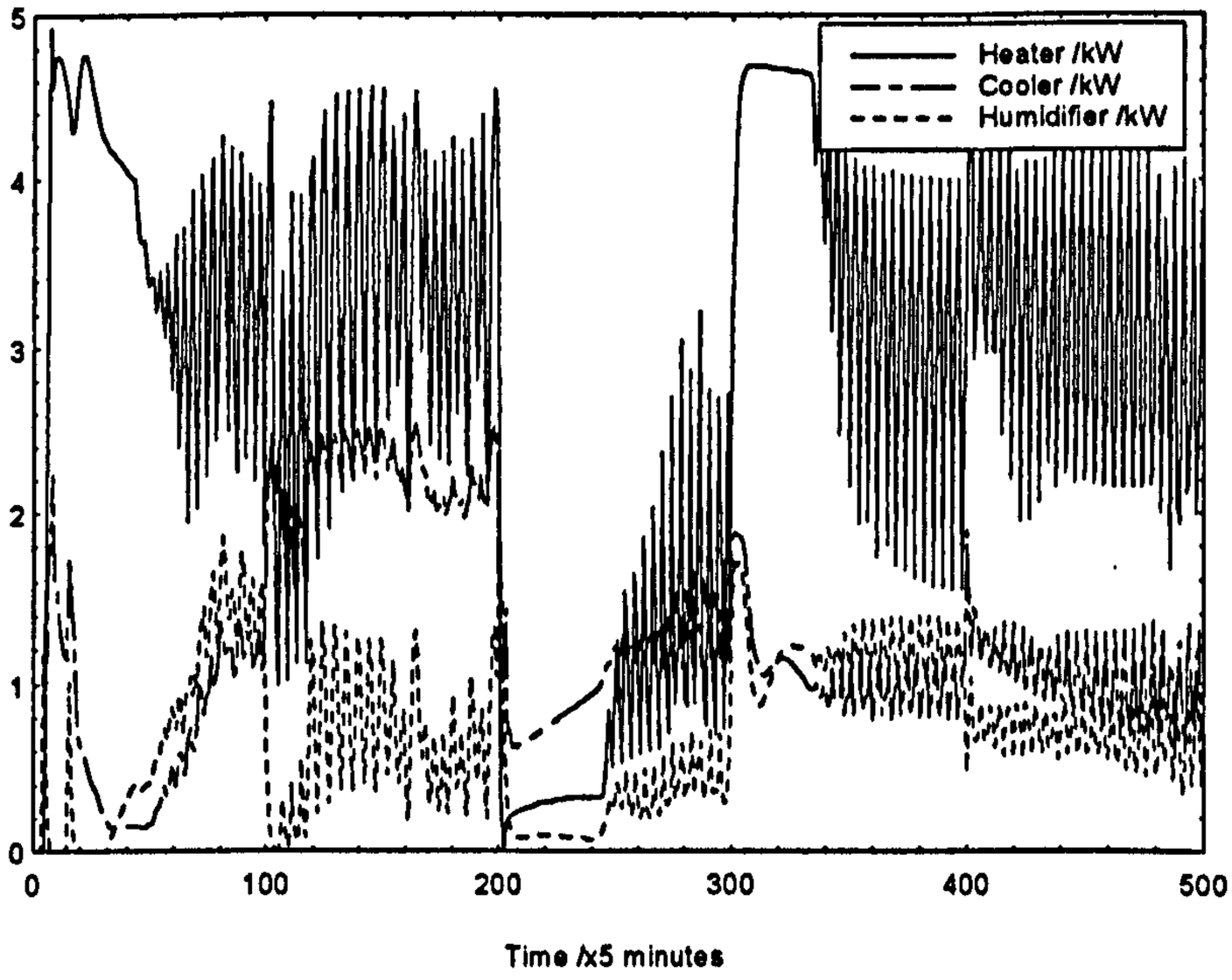

a). Control inputs

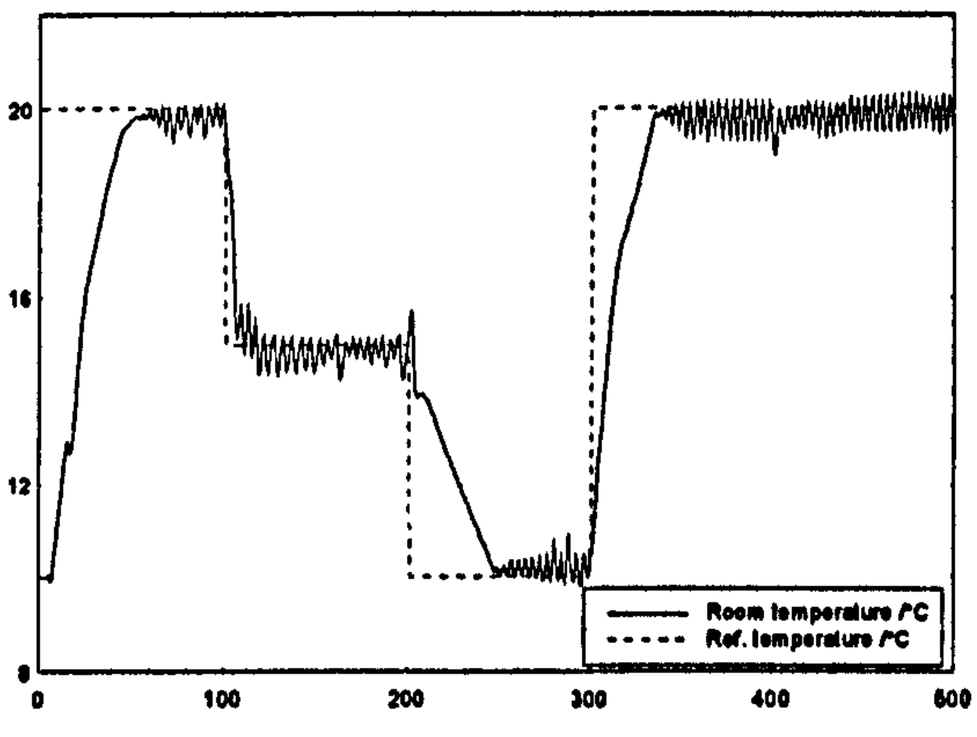

b). Room temperature

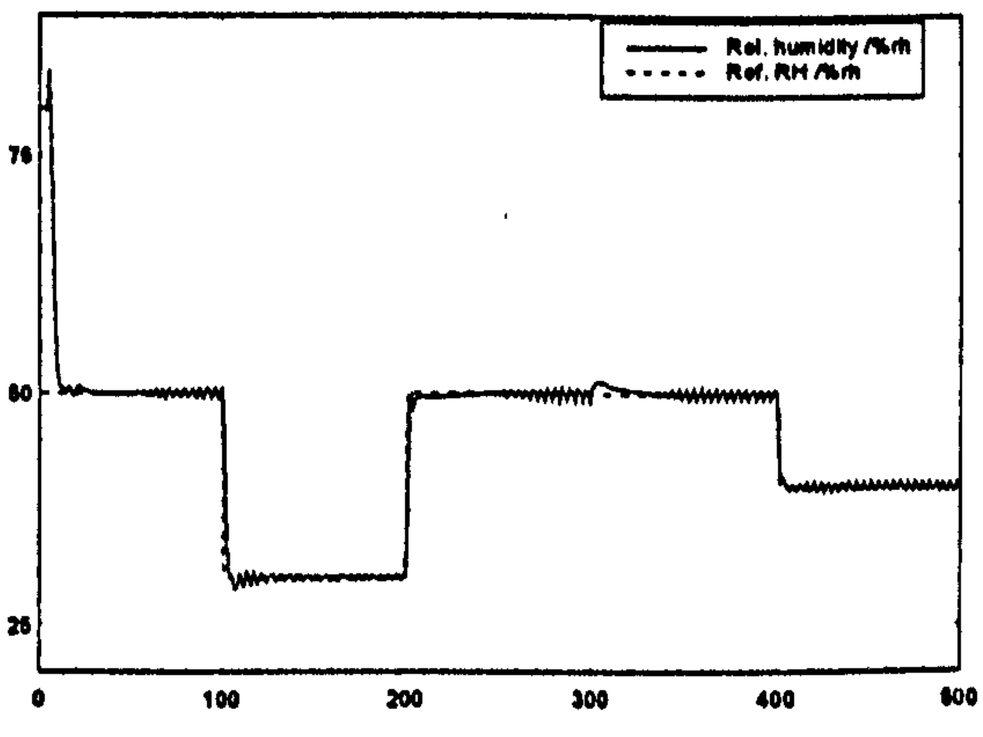

c). Relative humidity

Figure 5.8: Control performance for $n = 1$ and $N = 2$ with increased Q_2

Another possible approach to reduce the controller switching actions is to reduce the maximum permissible control changes D_u. To demonstrate this, a simulation trial is carried out as for the conditions in Figure 5.3, except that the room temperature and the relative humidity reference setpoints are arbitrary set at 20°C and 40%rh respectively, and the maximum permissible control changes D_u are smaller as compared to the one used to obtain Figure 5.3, say, equals $[0.5 \quad 0.3 \quad 0.3]^T$. The results are shown in Figure 5.9 where we can see that the output errors as well as the controllers switching at steady state conditions are reduced as compared to Figure 5.3 due to the smaller changes allowed in the control inputs. The steady state performance over the last 100 sampling intervals are as follows:

- the required control input energies are 33.7, 15.7 and 12.8 kWh for the heater, cooler and humidifier respectively;
- the output squared errors are 1.4°C^2 and 1.8%rh^2 for the temperature and relative humidity respectively; and
- the required times to reach the temperature and relative humidity setpoints are 5.0 and 1.6 hours respectively.

From this result, we notice that a disadvantage of this approach is that the temperature settling time is longer as compared to Figure 5.3 which is due to smaller amount of increment of the heater between one sampling interval.

Nevertheless, D_u may also have the lower limit at which the value lower than this causes the controller's out of control. One of the lower limit was found to be $D_u = [0.2 \quad 0.1 \quad 0.1]^T$.

Figure 5.10 shows the performance of the MIMO adaptive controller (n = 1 and N = 2) for the system with the actual climatic disturbances as shown in Figure 4.4, and for convenience, pseudo random binary sequences (PRBS) generated using 6 shift registers (Godfrey, 1980) and switching between ±0.5 were used as the stochastic noises included. We can see that the system performance is significantly degraded as compared to the system with constant disturbances and no noise case and this is to be expected. The steady state performance over the last 100 sampling intervals are as follows:

- the required control input energies are 35.3, 5.6 and 15.3 kWh for the heater, cooler and humidifier respectively;
- the output squared errors are 53.1°C^2 and 71.1%rh^2 for the temperature and relative humidity respectively; and
- the required times to reach the temperature and relative humidity setpoints are 6.7 and 1.6 hours respectively.

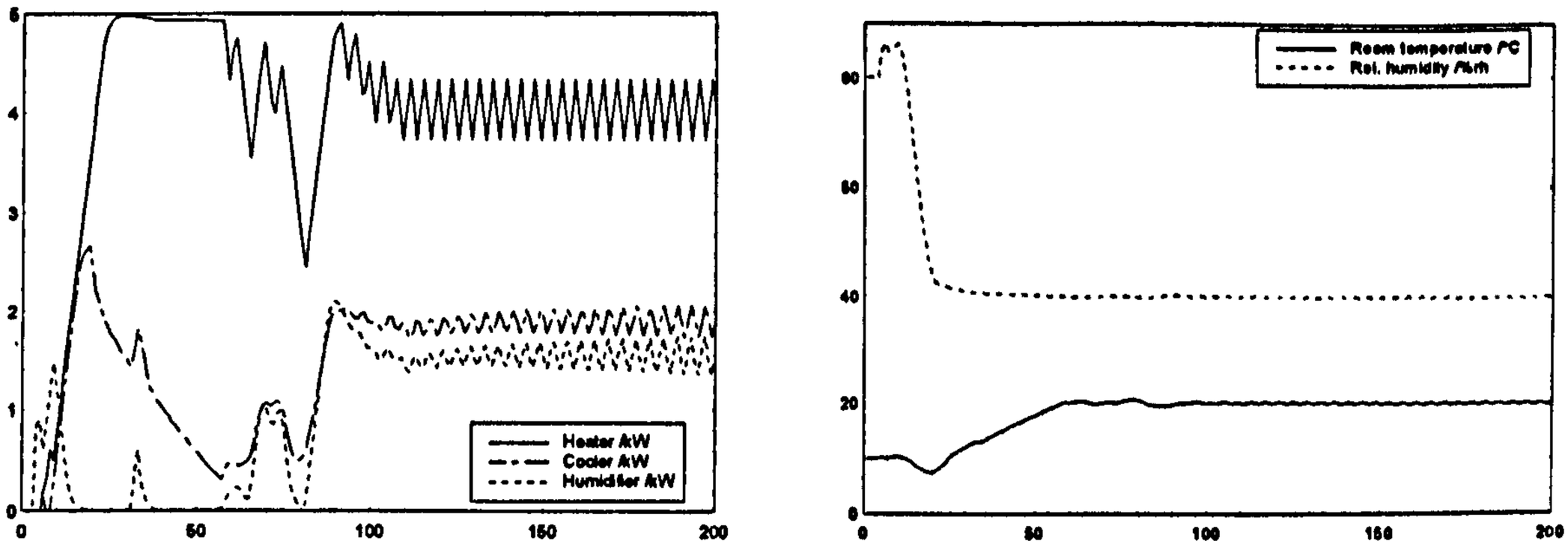

a). Control inputs b). System outputs

Figure 5.9: Control performance for n = 1, N = 2 and with reduced D_u

This result shows that the output regulation and the controller switching at steady state condition were improved as compared to Figure 5.3, although the total controlling input energy is about 1.2 times greater as compared to the multi PI-loop controller using 6 PI units (see section 3.3.1). As before, this performance can be improved further by suitable additional tuning of the weighting factors R, Q_1 and Q_2 in the quadratic criterion, $J(t)$.

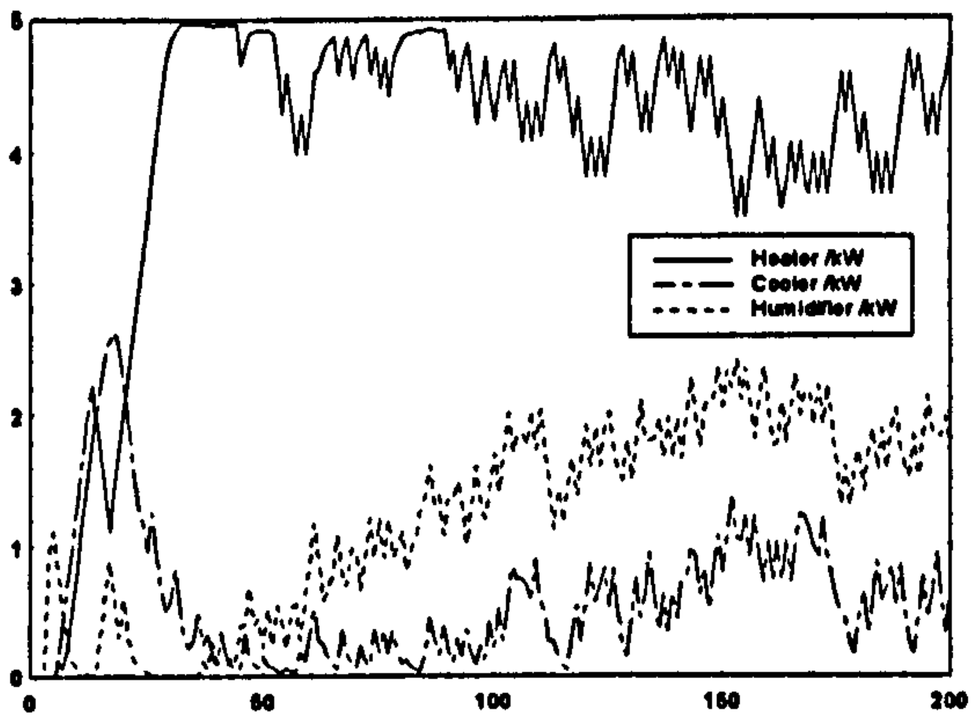

a). Control inputs

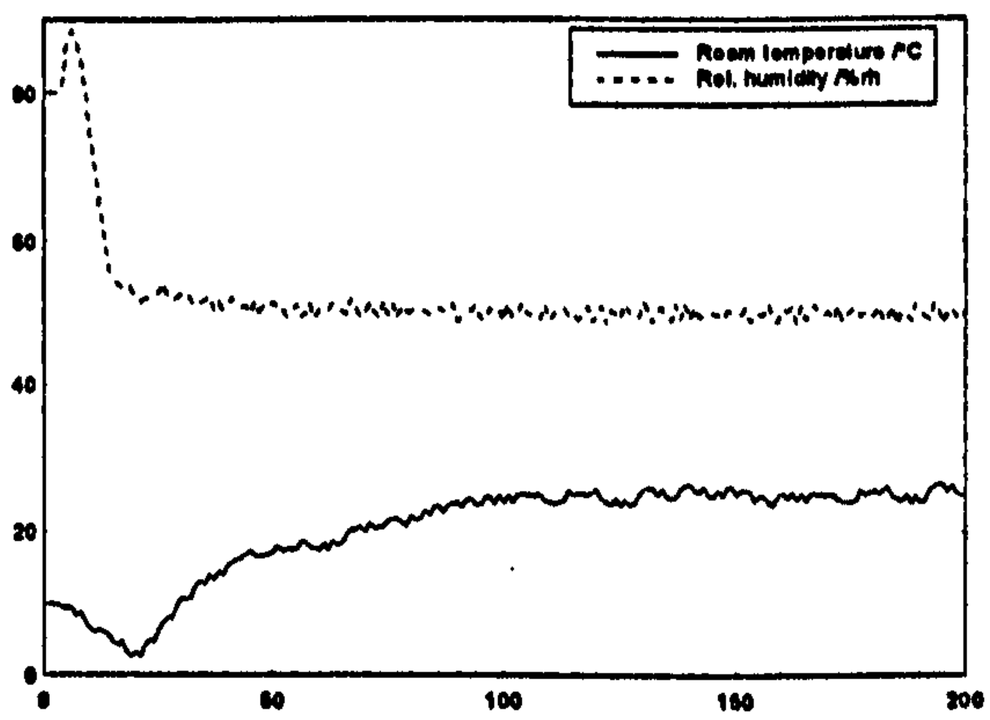

b). System outputs

Figure 5.10: Control performance for $n = 1$, $N = 2$ (with noise)

5.6. Conclusions

This chapter has discussed a multivariable adaptive control algorithm based on the generalized predictive control methodology which explicitly takes into account natural constraints on the input and output signals. The process model with observatory indexes of $n = 1$ and $n = 2$ were used to describe the dynamic processes of a heating, ventilating and air-conditioning plant consisting three control inputs and two outputs. From the results presented in Section 5.5, we can conclude that the selected process models together with the designed control law and the selected constraints are well suited to

controlling the overall system. The controller performance can be improved by suitable choice of the weighting factors R, Q_1 and Q_2 in the quadratic criterion as well as the prediction horizon, N, and the maximum permissible changes in the control input, D_u. Moreover, it may be possible to improve the system performance by selecting different prediction horizons for the predicted output y, rate of predicted input Δu and predicted input u terms in the quadratic criterion J. For example, a smaller prediction horizon for Δu and u will reduce the non-minimum phase overshoot effects in the output responses as well as stabilising the controller signals. This require reformulating the problem so that a suitable control law can be calculated; this will obviously be different from the law presented here.

Chapter 6

Fuzzy Logic Controllers

In recent years there has been growing interest in using fuzzy logic for the design of control systems. The advantage of using these techniques is that it is easy to apply heuristic knowledge and "rule-of-thumb" experiences without involving tedious mathematical analysis. Fuzzy controllers are usually based on expert knowledge that is given by linguistic rules (Zadeh, 1975), and many successful applications have been reported. One such application is in an air-conditioning plant (Ling and Dexter, 1994) where a rule-based supervisor is used to select a setpoint for the zone temperature which satisfies the majority of the occupants in the building as well as minimising the cost of operating the air-handling-unit (AHU); the results show that a significant cost savings without unacceptable increases in discomfort levels can be achieved. Furthermore, the solution was also able to compensate for day-to-day variations in conditions to maintain the control performance.

In view these encouraging results it is worthwhile to investigate the potential of fuzzy logic for HVAC applications; this was carried out and discussed here. We will design a fuzzy logic controller (FLC) which is based on the output errors to control an office zone system. The overall control objective is assumed to be to maintain acceptable

levels for the room temperature and the relative humidity variations as well as minimizing the energy costs of operating the HVAC plant.

6.1. Design of the FLC

Most FLCs developed so far employ error and error rates about a setpoint as their driving inputs (Ying et al., 1990). For our case, since the system has two setpoints, namely, the air temperature and the relative humidity in the test room, then using a similar reasoning we require four inputs; two from the output errors and two from the error rates, in order to calculate the three control signals to drive the HVAC plant using the fuzzy method.

Another FLC design is to employ fuzzy versions of the three terms in the PID controller (He et al., 1993). For our system, the PID-based fuzzy controller requires six inputs where two inputs are required for each term. Thus, the size of the fuzzy rules which depend on the number of crisp inputs, become quite large and the time required for calculating the control decision will be longer.

In this chapter, we present two types of FLC design; the first design is based on the proportional (P) controller and the second type is based on the Proportional and Integral (PI) controller. Both designs employ incremental control rather than the actual input so that integral action to eliminate steady state errors can be easily deployed. The three control input increments, namely, the heater increment dW, the cooler increment dC and the humidifier increment dH, are defined by:

$$dW(t) = W(t) - W(t\text{-T}) \tag{6.1}$$

$$dC(t) = C(t) - C(t\text{-T}) \tag{6.2}$$

$$dH(t) = H(t) - H(t\text{-T}) \tag{6.3}$$

respectively.

6.1.1. FLC based on proportional action

In this design, the system structure is shown in Figure 6.1 where the FLC employs only the proportional term with gain K_P is assumed to be unity to simplify the design. The required parameters are the output errors, namely the error signals in the air temperature $e_T(t)$ and the relative humidity $e_H(t)$ for which the FLC calculates the three control increments. The design follows the three main steps in fuzzy controller design, that is, fuzzification, control rule evaluation and defuzzification.

For the fuzzification process, singleton error signals are "fuzzified" into membership functions as shown in Figure 6.2. Both the error signals e_T and e_H are assumed to have five membership values: Negative Large (NL), Negative Small (NS), Zero (Z), Positive Small (PS) and Positive Large (PL) and the controller output increments have three membership functions: Negative (N), Zero (Z) and Positive (P). The constants l_1, l_2, l_3, s_1, s_2, s_3, z_1, z_2, x_l, n_m, n_r, z_l, z_m, z_r, p_l, p_m and x_u used in the definition of the membership functions shown in Figure 6.2 are chosen in accordance to the possible ranges in the error signals and the maximum possible controller changes, which will be fixed after being determined. Note that the constants l_1, l_2, .., x_u used in the two sets of the error signals can be different in general (according to the dynamics of the office zone), but we assume them to be the same here in order to simplify the design and notation in the following discussions.

Based on these membership functions, and our heuristic knowledge from the step responses of each control output (see section 2.3.1), the fuzzy control rules that we used are summarized in Table 6.1. Then, the FLC outputs, or equivalently, the control input increments $dW(t)$, $dC(t)$ and $dH(t)$ are respectively added to the previous control inputs, $W(t\text{-T})$, $C(t\text{-T})$ and $H(t\text{-T})$ in order to obtain the present control inputs, $W(t)$, $C(t)$ and $H(t)$ as indicated in equations (6.1), (6.2) and (6.3), before being fed to the HVAC plant at time t.

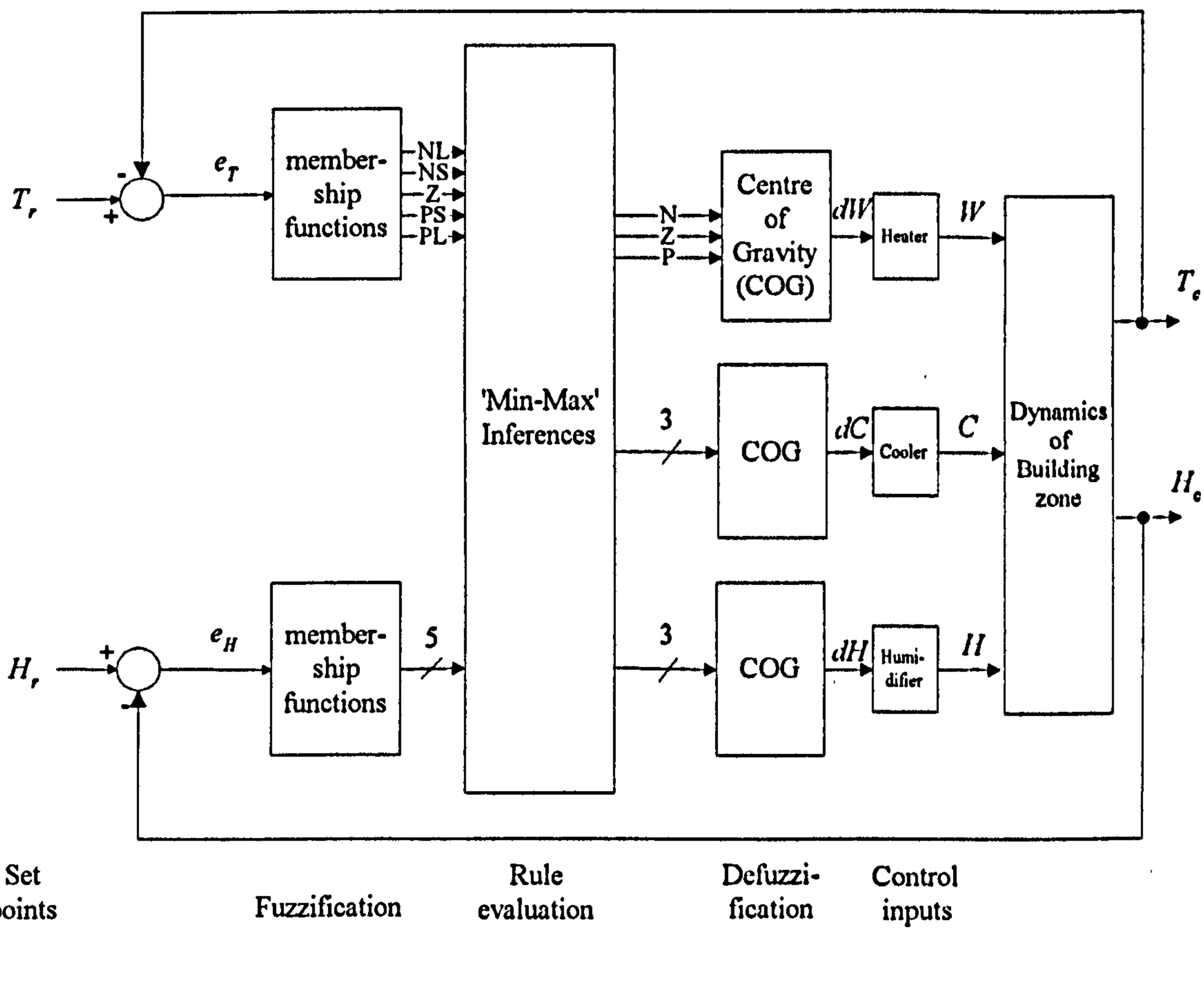

Figure 6.1: Block diagram of a FLC based on proportional controller

The reason for establishing these rules can be understood as follows: we assume that the air temperature and relative humidity setpoints are regulated in the ranges between

15°C - 25°C and 30%rh - 50%rh respectively. From Table 6.1, we can see that there are twenty five permutations for the fuzzy input for each FLC output; this require Zadeh's logical "AND" and 'OR" operations (Zadeh, 1965) in order to calculate the required incremental control values to maintain the required conditions in the test room. Since we have three membership functions of fuzzy output for each control signal, then the required fuzzy rules need to be as follows:

- Rules R1, R2 and R3 are for determining the increment for the heater *dW*, that is, it should be Negative (N), Zero (Z) or Positive (P) respectively.
- Rules R4, R5 and R6 are for the cooler increment *dC* N, Z and P respectively, and
- Rules R7, R8 and R9 are for the humidifier increment *dH* N, Z and P respectively.

These rules can be presented as logical statements and can be written as

Rule R1: *The heater increment, dW, is Negative if*

the temperature error is NS AND the relative humidity error is PL, OR

the temperature error is NL AND the relative humidity error is PL, OR

the temperature error is NS AND the relative humidity error is PS, OR

the temperature error is NL AND the relative humidity error is PS, OR

the temperature error is NS AND the relative humidity error is Z, OR

the temperature error is NL AND the relative humidity error is Z, OR

the temperature error is NS AND the relative humidity error is NS, OR

the temperature error is NL AND the relative humidity error is NS, OR

the temperature error is NS AND the relative humidity error is NL, OR

the temperature error is NL AND the relative humidity error is NL.

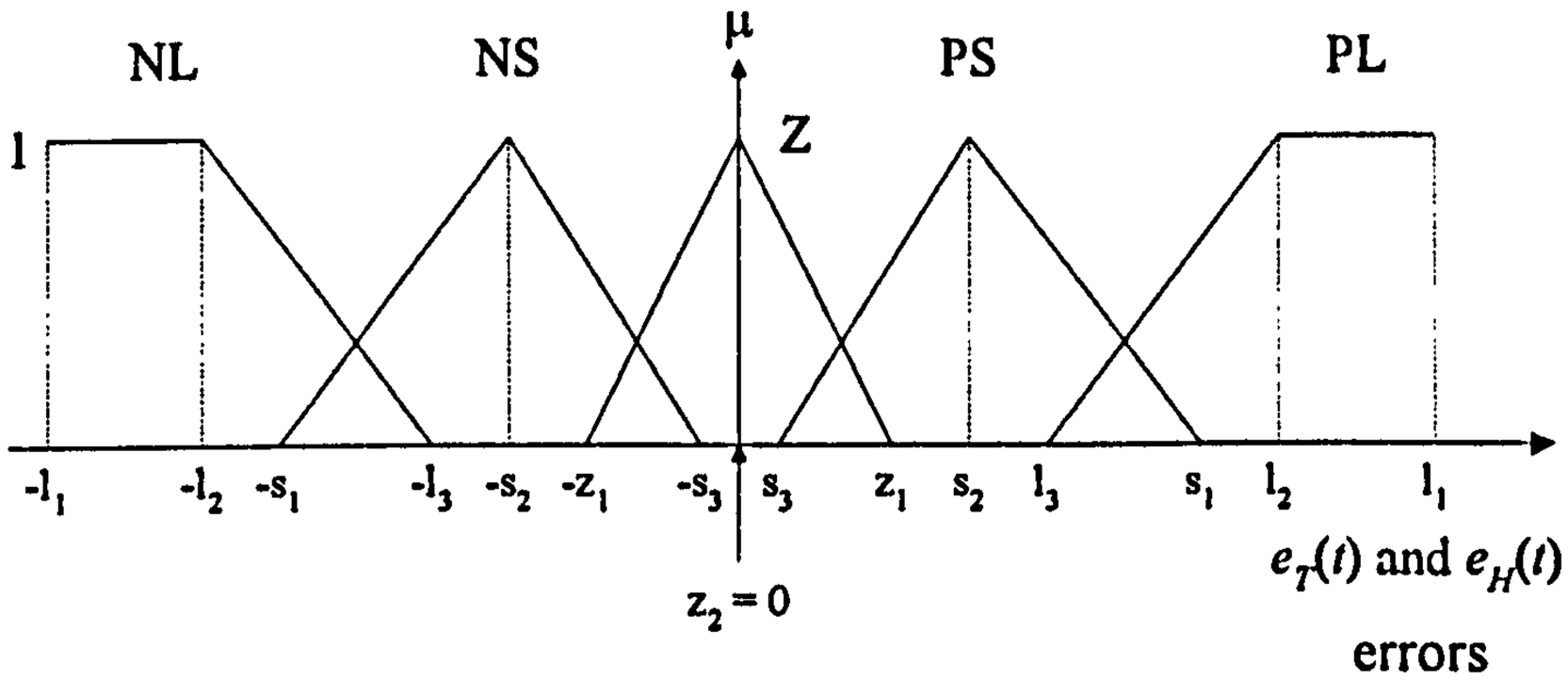

a) Fuzzy input sets

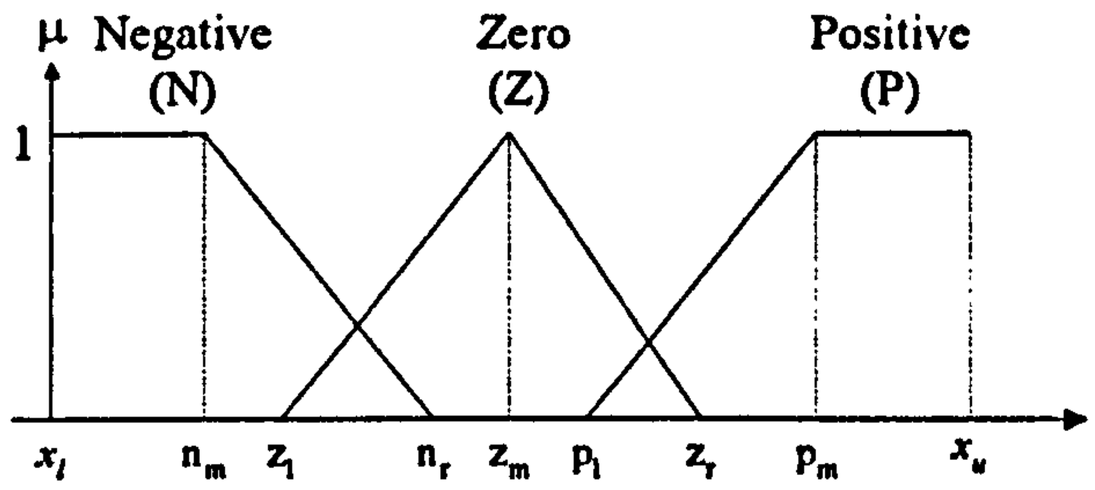

b) Fuzzy output sets

Figure 6.2: Fuzzy membership functions

Rule R2: *The heater increment, dW, is Zero if*

the temperature error is PS AND the relative humidity error is PL, OR

the temperature error is Z AND the relative humidity error is PL, OR

the temperature error is Z AND the relative humidity error is PS, OR

the temperature error is Z AND the relative humidity error is Z, OR

the temperature error is Z AND the relative humidity error is NS, OR

the temperature error is Z AND the relative humidity error is NL.

Table 6.1: Fuzzy control rules based on output errors

e_H \ e_T	PL	PS	Z	NS	NL
PL	dW = P	Z	Z	N	N
	dC = N	N	N	N	Z
	dH = P	P	P	P	P
PS	P	P	Z	N	N
	N	N	N	N	Z
	N	Z	Z	Z	Z
Z	P	P	Z	N	N
	N	N	Z	N	Z
	N	N	Z	N	N
NS	P	P	Z	N	N
	N	N	N	Z	P
	N	N	N	N	N
NL	P	P	Z	N	N
	N	N	Z	P	P
	N	N	N	N	N

P = Positive, Z = Zero, N = Negative

Rule R3: *The heater increment, dW, is Positive if*

the temperature error is PL AND the relative humidity error is PL, OR

the temperature error is PL AND the relative humidity error is PS, OR

the temperature error is PS AND the relative humidity error is PS, OR

the temperature error is PL AND the relative humidity error is Z, OR

the temperature error is PS AND the relative humidity error is Z, OR

the temperature error is PL AND the relative humidity error is NS, OR

the temperature error is PS AND the relative humidity error is NS, OR

the temperature error is PL AND the relative humidity error is NL, OR

the temperature error is PS AND the relative humidity error is NL.

Rule R4: *The cooler increment, dC, is Negative if*

the temperature error is PL AND the relative humidity error is PL, OR

the temperature error is PS AND the relative humidity error is PL, OR

the temperature error is Z AND the relative humidity error is PL, OR

the temperature error is NS AND the relative humidity error is PL, OR

the temperature error is PL AND the relative humidity error is PS, OR

the temperature error is PS AND the relative humidity error is PS, OR

the temperature error is Z AND the relative humidity error is PS, OR

the temperature error is NS AND the relative humidity error is PS, OR

the temperature error is PL AND the relative humidity error is Z, OR

the temperature error is PS AND the relative humidity error is Z, OR

the temperature error is NS AND the relative humidity error is Z, OR

the temperature error is PL AND the relative humidity error is NS, OR

the temperature error is PS AND the relative humidity error is NS, OR

the temperature error is Z AND the relative humidity error is NS, OR

the temperature error is PL AND the relative humidity error is NL, OR

the temperature error is PS AND the relative humidity error is NL.

Rule R5: *The cooler increment, dC, is Zero if*

the temperature error is NL AND the relative humidity error is PL, OR

the temperature error is NL AND the relative humidity error is PS, OR

the temperature error is Z AND the relative humidity error is Z, OR

the temperature error is NL AND the relative humidity error is Z, OR

the temperature error is NS AND the relative humidity error is NS, OR

the temperature error is Z AND the relative humidity error is NL.

Rule R6: *The cooler increment, dC, is Positive if*

the temperature error is NL AND the relative humidity error is NS, OR

the temperature error is NS AND the relative humidity error is NL, OR

the temperature error is NL AND the relative humidity error is NL.

Rule R7: *The humidifier increment, dH, is Negative if*

the temperature error is PL AND the relative humidity error is PS, OR

the temperature error is PL AND the relative humidity error is Z, OR

the temperature error is PS AND the relative humidity error is Z, OR

the temperature error is NS AND the relative humidity error is Z, OR

the temperature error is NL AND the relative humidity error is Z, OR

the temperature error is PL AND the relative humidity error is NS, OR

the temperature error is PS AND the relative humidity error is NS, OR

the temperature error is Z AND the relative humidity error is NS, OR

the temperature error is NS AND the relative humidity error is NS, OR

the temperature error is NL AND the relative humidity error is NS, OR

the temperature error is PL AND the relative humidity error is NL, OR

the temperature error is PS AND the relative humidity error is NL, OR

the temperature error is Z AND the relative humidity error is NL, OR

the temperature error is NS AND the relative humidity error is NL, OR

the temperature error is NL AND the relative humidity error is NL.

Rule R8: *The humidifier increment, dH, is Zero if*

the temperature error is PS AND the relative humidity error is PS, OR

the temperature error is Z AND the relative humidity error is PS, OR

the temperature error is NS AND the relative humidity error is PS, OR

the temperature error is NL AND the relative humidity error is PS, OR

the temperature error is Z AND the relative humidity error is Z.

Rule R9: *The humidifier increment, dH, is Positive if*

the temperature error is PL AND the relative humidity error is PL, OR

the temperature error is PS AND the relative humidity error is PL, OR

the temperature error is Z AND the relative humidity error is PL, OR

the temperature error is NS AND the relative humidity error is PL, OR

the temperature error is NL AND the relative humidity error is PL.

Note that, Rules R1, R2 and R3 are established because the effects of increasing the heater are to increase the temperature and reduce the relative humidity. Rules R4, R5 and R6 are established since the immediate effects of increasing the cooler are to reduce both the temperature and relative humidity. Similarly, rules R7, R8 and R9 are true because, the humidifier input has a negligible effect on the temperature variation (from the step response).

Rules R1 - R9 can be translated into mathematical format by using fuzzy set theory (Zadeh, 1965), and the AND and OR operations are defined by

$$\mu_A \text{ AND } \mu_B = \min\{ \mu_A, \mu_B \} \tag{6.4}$$

and

$$\mu_A \text{ OR } \mu_B = \max\{\mu_A, \mu_B\} \tag{6.5}$$

for any two membership functions μ_A and μ_B on fuzzy subsets A and B respectively. For our case, this theory can be interpreted as follows: for each fuzzy output membership function, the minimum value of the rule strength, μ, from each pair of the fuzzy input membership functions of e_T and e_H, as indicated in the fuzzy rules with the statement 'AND' is first obtained, and then these minimum values are sorted to get the largest value amongst them via the statement 'OR' in the rule. Therefore, this value is the rule strength or the degree of membership for that particular fuzzy output membership function.

6.1.2. FLC based on P + I control

In this design, both the output errors $e_T(t)$ and $e_H(t)$ and the integration errors $I_T(t)$ and $I_H(t)$ are fed into the FLC as shown in Figure 6.3.

The integration terms in discrete form are defined by equations (3.4) and (3.5); a well known method to avoid these terms from growing excessively is to apply upper and lower limits, namely $\pm I_{TM}$ and $\pm I_{HM}$ for the room temperature and relative humidity respectively. These limits are incorporated into the fuzzy input scaling factors where I_{TM} (°C_h) and I_{HM} (%rh_h) respectively are both set equal to l_1 (Figure 6.2 a)).

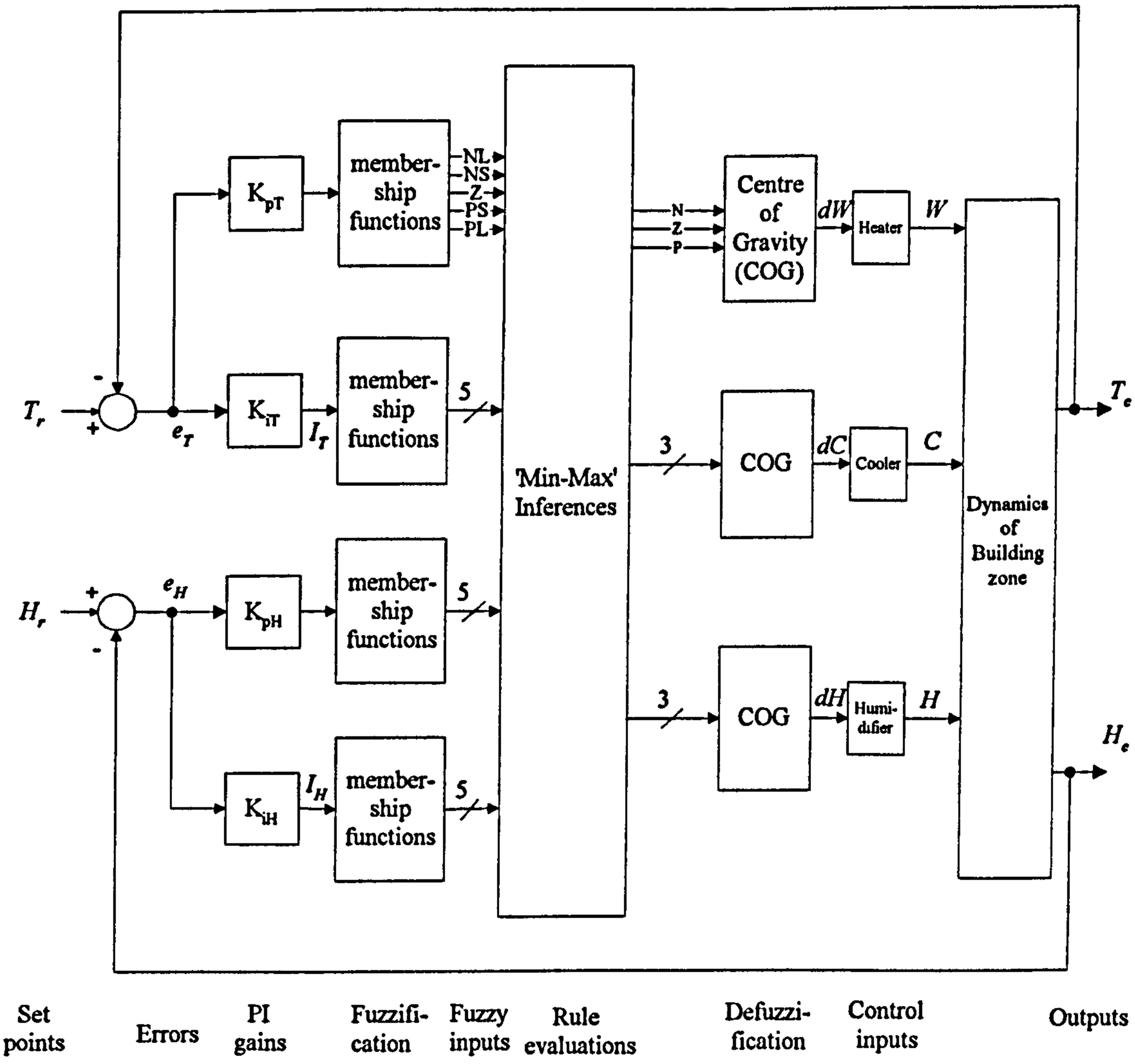

Figure 6.3: Block diagram of a FLC based on P+I control

A similar definition as in Figure 6.2 a) can be used for the fuzzy input membership functions of the integral terms to simplify the FLC design of this type. Furthermore, we can tune both the PI gains and the scaling factors of the fuzzy input and output membership functions because these parameters are important for the FLC tunings in order to obtain a good system performance. For our system, we simplify the overall design by setting the proportional gains K_{pT} and K_{pH}, and the integration gains K_{iT} and K_{iH} to unity.

The fuzzy rules on the integral term that we used are summarized in Table 6.2; the reason for establishing these rules are based on knowledge of the input step responses and the effects of the heater, cooler and humidifier on the room temperature and relative humidity. In this design therefore, the overall fuzzy rules are the combined rules from Tables 6.1 and 6.2. Since we have three membership functions of fuzzy output for each control signal, then the required fuzzy rules are as follows: Rules R10, R11 and R12 are for determining whether the fuzzy heater increment is *dW* Negative (N), Zero (Z) and Positive (P) respectively. Similarly, Rules R13, R14 and R15 are for assessing whether the cooler increments *dC* is N, Z and P respectively, and Rules R16, R17 and R18 are for if the humidifier increment *dH* is N, Z and P respectively. A similar way of writing these rules can be presented here, but we present only Rule R11 as an example.

Rule R11: *The heater increment, dW, is approximately zero if*

the temperature error is PS AND the relative humidity error is PL, OR

the temperature error is Z AND the relative humidity error is PS, OR

the temperature error is Z AND the relative humidity error is PS, OR

the temperature error is Z AND the relative humidity error is Z, OR

the temperature error is Z AND the relative humidity error is NS, OR

the temperature error is Z AND the relative humidity error is NL, OR

the temperature int error is PL AND the RH int error is PL, OR

the temperature int error is PL AND the RH int error is PS, OR

the temperature int error is PL AND the RH int error is NS.

Table 6.2: Fuzzy control rule based on the integration errors

I_H \ I_T	PL	PS	Z	NS	NL
PL	dW = Z	N	N	N	N
	dC = N	N	N	N	Z
	dH = P	P	P	P	P
PS	Z	N	N	N	N
	N	Z	N	N	P
	N	N	N	N	N
Z	N	N	N	N	N
	N	N	N	N	N
	N	N	N	N	N
NS	Z	N	N	N	N
	N	N	N	N	Z
	Z	Z	Z	Z	Z
NL	P	N	N	N	N
	N	Z	N	N	P
	N	N	N	N	N

P = Positive, Z = Zero, N = Negative

A similar calculation using the fuzzy set equations (6.4) and (6.5) can be applied to for this design to obtain the degree of membership for the fuzzy settings for *dW*, *dC* and *dH*.

6.2. Defuzzification process

After the control rules of the fuzzy controller design have been determined and the membership of the incremental fuzzy set of each controlling input has been calculated, then the final stage of the design is the defuzzification process where the fuzzy output membership function is converted into it's crisp or singleton value. This incremental value is then applied to modify the input settings of the HVAC plant in order to maintain

the air temperature and relative humidity in the room at the prescribed setpoints. One of the most commonly used defuzzification techniques is called the centre of gravity (COG) or centroid method; here each output membership function above the value indicated by it respective fuzzy output is truncated. The resulting "clipped" membership functions are then combined and the overall centre of gravity (COG) is calculated. Figure 6.4 illustrates this method where the output memberships of the heater increment Negative (N), Zero (Z) and Positive (P) are 0.1, 0.5 and 0 respectively. The COG of the shaded area is given by (see for example White and Sofge, 1992)

$$\text{COG} = \frac{\int_a^b \mu(x)x\,dx}{\int_a^b \mu(x)\,dx} \tag{6.6}$$

where μ is the rule strength of the fuzzy output, and a and b are the lower and upper limits of the shaded area respectively.

In our case, the control input signals to the HVAC plant such as the heater W, cooler C and humidifier H have limits of 0 - 5.0, 0 - 2.7 and 0 - 2.6 kilowatts respectively. These limits are then incorporated into the FLC design in order to calculate the control inputs to the HVAC plant by applying equations (6.1), (6.2) and (6.3).

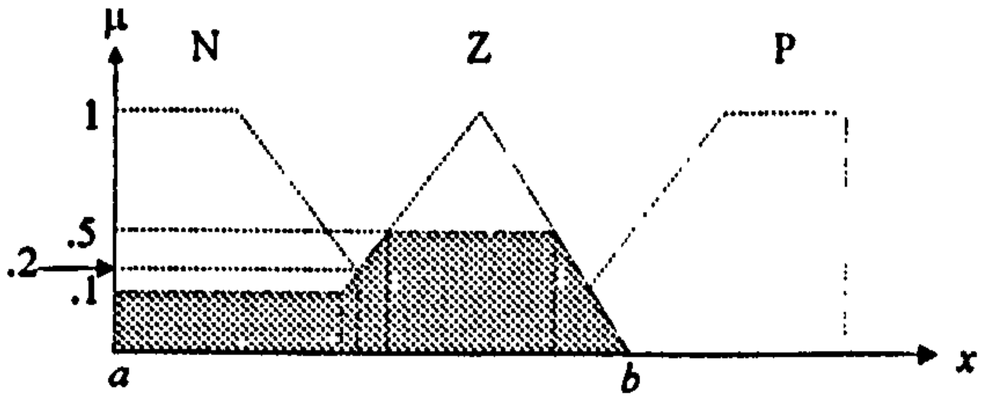

Figure 6.4: Overall area of fuzzy sets

6.2.1. Calculation of the FLC outputs

In general, the control performance of the FLC design depends on the number of fuzzy input and output membership functions, the domain and shape of each membership function, and the way the control rule is evaluated. There are many ways of combining the above considerations, but let us consider that for our system, the room temperature error range of -0.5°C to 0.5°C corresponds to the fuzzy membership Z, between 0°C to 2°C is PS, 0°C to -2°C is NS, and an error greater than 1°C is PL and lower than -1°C is NL. Similarly, these conditions are also applied to the relative humidity error. For these definitions, the chosen membership functions used in the design are shown in Table 6.3. Moreover, the domains of the fuzzy output membership functions: Negative, Zero and Positive are given in Table 6.4. Note that the dimension for the values in Table 6.3 can be either °C or %rh, as explained in Section 6.1.

In the tuning of the presented controllers, we used the actual output and integral errors for fuzzification process and therefore the proportional and integration gains for these designs are unity. We can improve these designs for other gains as well since the P and I terms in P+I controllers linearly correspond to the output and integral errors respectively.

Table 6.3: Scaling factor of fuzzy input membership functions

Fuzzy input	NL and PL			NS and PS			Z	
scaling factor	l_1	l_2	l_3	s_1	s_2	s_3	z_1	z_2
Range	100.0	2.0	1.0	2.0	1.0	0	0.5	0

Table 6.4: Scaling factors for the fuzzy output membership functions

Fuzzy controller output (kW)	Negative (N)			Zero (Z)			Positive (P)		
	x_l	n_m	n_r	z_l	z_m	z_r	p_l	p_m	x_u
dW	-0.20	-0.14	0	-0.14	0	0.14	0	0.14	0.20
dC	-0.20	-0.14	0	-0.14	0	0.14	0	0.14	0.20
dH	-0.20	-0.14	0	-0.14	0	0.18	0	0.18	0.25

As an example, let us assume that the output errors, $e_T(t)$ and $e_H(t)$ at time t are -0.2°C and 0.64%rh respectively. From the fuzzification process and using the scaling factors in Table 6.3 for Figure 6.2, we can calculate the degree of membership, μ, for each fuzzy input. We found that for this value of e_T; PL, PS, Z, NS and NL have values of 0, 0, 0.6, 0.2 and 0 respectively. Similarly, for e_H equal to 0.64%rh the corresponding values are 0, 0.64, 0, 0 and 0. By applying the fuzzy rules R1, R2, ..., R9 and the min-max inferences of equations (6.4) and (6.5) to these fuzzy inputs, we can obtain the degree of membership for all our fuzzy output incremental settings: N, Z and P of each controller's output. The details of the calculations are as follows:

i). Heater increment, *dW*

$$\begin{aligned}\mu_n = {} & \max\{\min\{0.2, 0\}, \min\{0, 0\}, \min\{0.2, 0.64\}, \min\{0, 0.64\}, \min\{0.2, 0\}, \\ & \min\{0, 0\}, \min\{0.2, 0\}, \min\{0, 0\}, \min\{0.2, 0\}, \min\{0, 0\}\} \\ = {} & \max\{0, 0, 0.2, 0, 0, 0, 0, 0, 0, 0\} = 0.2\end{aligned}$$

$$\begin{aligned}\mu_z = {} & \max\{\min\{0, 0\}, \min\{0.6, 0\}, \min\{0.6, 0.64\}, \min\{0.6, 0\}, \min\{0.6, 0\}, \\ & \min\{0.6, 0\}\} \\ = {} & \max\{0, 0, 0.6, 0, 0, 0\} = 0.6\end{aligned}$$

$$\begin{aligned}\mu_p = {} & \max\{\min\{0, 0\}, \min\{0, 0.64\}, \min\{0, 0.64\}, \min\{0.6, 0\}, \min\{0, 0\}, \\ & \min\{0, 0.2\}, \min\{0, 0\}, \min\{0, 0\}, \min\{0, 0.64\}\} \\ = {} & \max\{0, 0, 0, 0, 0, 0, 0, 0, 0\} = 0\end{aligned}$$

ii). Cooler increment, *dC*

μ_n = max{min{0, 0}, min{0, 0}, min{0.6, 0}, min{0.2, 0}, min{0, 0.64}, min{0, 0.64}, min{0.6, 0.64}, min{0.2, 0.64}, min{0, 0}, min{0, 0}, min{0.2, 0}, min{0, 0}, min{0, 0}, min{0.6, 0}, min{0, 0}, min{0, 0}}
= max{0, 0, 0, 0, 0, 0, 0.6, 0.2, 0, 0, 0, 0, 0, 0, 0, 0} = 0.6

μ_z = max{min{0, 0}, min{0, 0.64}, min{0.6, 0}, min{0, 0}, min{0.2, 0}, min{0.6, 0}}
= max{0, 0, 0, 0, 0, 0} = 0

μ_p = max{min{0, 0}, min{0.2, 0}, min{0, 0}}
= max{0, 0, 0} = 0

iii). Humidifier increment, *dH*

μ_n = max{min{0, 0.64}, min{0, 0}, min{0, 0}, min{0.2, 0}, min{0, 0}, min{0, 0}, min{0, 0}, min{0.6, 0}, min{0.2, 0} min{0, 0}, min{0, 0}, min{0, 0}, min{0.6, 0}, min{0.2, 0}, min{0, 0}}
= max {0, 0, 0, 0, 0, 0, 0, 0, 0, 0, 0, 0, 0, 0, 0, 0} = 0

μ_z = max{ min{0, 0.64}, min{0.6, 0.64}, min{0.2, 0.64}, min{0, 0.64}, min{0.6, 0}}
= max {0, 0.6, 0.2, 0, 0} = 0.6

μ_p = max{min{0, 0}, min{0, 0}, min{0.6, 0}, min{0.2, 0}, min{0, 0}}
= max {0, 0, 0, 0, 0} = 0

Now, we can calculate the physical values of *dW*, *dC* and *dH* via the defuzzification process. By using the scaling factors in Table 6.4, we find that *dW*, *dC* and *dH* are -0.018, -0.116 and 0.095 kW respectively. If the previous control inputs *W*, *C*, *H* to the plant are 4.936, 0.478 and 0.076 kW respectively, then using equations (6.1), (6.2) and (6.3), their present values become 4.918, 0.362 and 0.171 kW respectively.

6.3. Simulation results

In this section, we present some simulation results using the FLC developed in Section 6.1. In these simulations, the system performance for step reference inputs is studied. As before, our objectives of the design are:

1) to obtain minimal output errors at steady state conditions,

2) to minimise the overall energy consumption of the HVAC plant, and

3) possess fast settling time i.e. the time required to reach the setpoints from an initial condition should be as fast as possible.

A simulation program was developed by applying the fuzzy design procedures presented in Section 6.1 and the scaling factors in Tables 6.2, 6.3 and 6.4. In the simulation, we assume that the air dynamics of the room follows equations (2.1) and (2.2). Moreover, the climatic disturbances such as the laboratory temperature, T_l, outside air temperature, T_o, outside relative humidity, H_o, and total solar irradiance, S, are assumed to be constant at 20°C, 15°C, 80%rh and 0.1Wm^{-2} respectively, and the white noise processes, V_1 and V_2, and the constants, k_1 and k_2, are zero. Note that the fuzzy input domains as presented in Table 6.3 are arbitrarily chosen as discussed in Section 6.2.1 but the fuzzy output domains in Table 6.4 were obtained after several simulations trials carried out for the above conditions so that the desired overall control performances can be achieved.

The system performances can be judged by calculating the magnitude of the errors of the actual room temperature and relative humidity from the setpoints as well as deducing the energies consumed by the system. Let us consider the system under the setpoints of 25°C and 50%rh for the room temperature and relative humidity

respectively, and their initial values are assumed to be at 15°C and 80%rh respectively. Moreover, all the three control inputs to the plant have not been used initially. The simulated results are shown in Figure 6.5; the control performance calculated over the last 100 data points after steady state had been reached and the following results are obtained:

- the required control input energies are 22.3, 0 and 5.4 kWh for the heater, cooler and humidifier respectively;
- the output squared errors are $0.2°C^2$ and $2.8\%rh^2$ for the temperature and relative humidity respectively; and
- the required times to reach the temperature and relative humidity setpoints are 5.8 and 5.0 hours respectively.

We can see that excellent control regulation has been achieved from this type of FLC. We found that the heater consumed more power and the cooler was not used in all the simulation periods; this is reasonable since the temperature setpoint of 25°C is much higher than the ambient temperature (equal to 9.9°C as discussed in Section 2.3.1).

Figure 6.6 shows that the good regulation performance of the system is maintained even when climatic disturbances (see section 4.2.1) and white noise processes are included in the analysis. The disturbances for the noise terms were inserted in the form of pseudo random binary sequences (PRBS) generated using 6 bits shift register (Godfrey, 1980) with 10% of magnitude, i.e. their values were ±0.1. The control performance at steady state conditions for these situations are calculated over the last 100 data points and found to be as follows:

- the required control input energies are 28.2, 0 and 6.8 kWh for the heater, cooler and humidifier respectively; and

- the output squared errors are $2.2°C^2$ and $4.2\%rh^2$ for the temperature and relative humidity respectively.

Clearly, these increased output squared errors are due to the noise present in the system. We can also see that the total required energy of the FLC for this condition is bigger as compared to the system without noise but the cooler was not used in both conditions. This is due to the heater and humidifier fighting each other to reduce the output errors.

The above results also show that the superiority of the fuzzy logic controller based on output errors over the conventional multi PI-loop controller (Chapter 3) as the FLC output regulations remain small even when disturbances are present in the system.

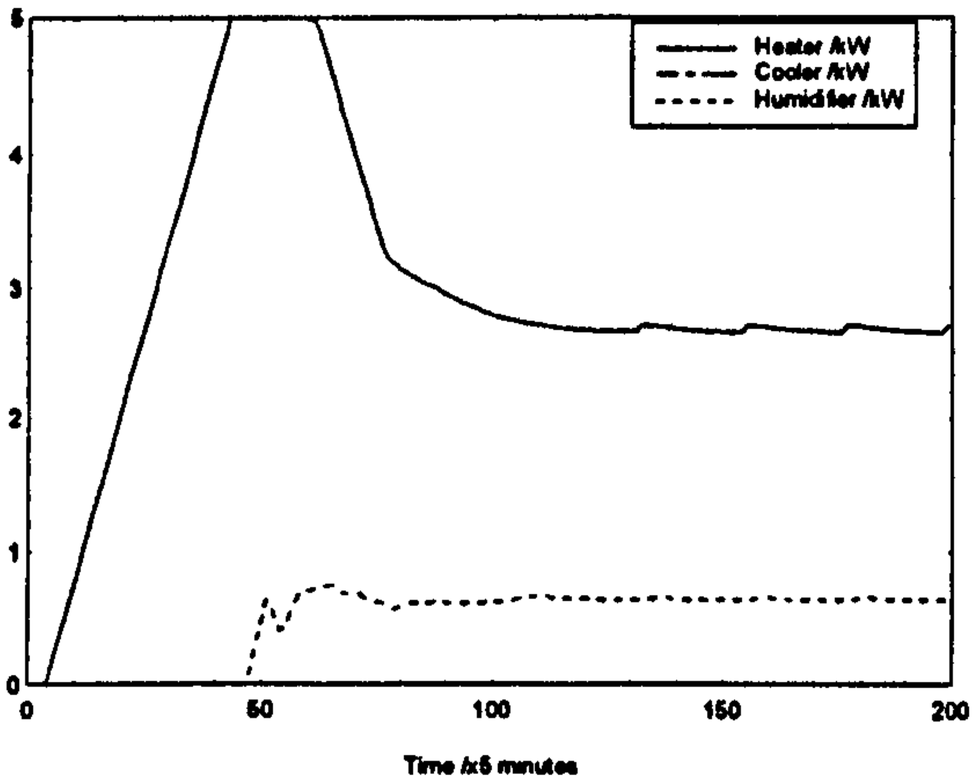

a) Control inputs

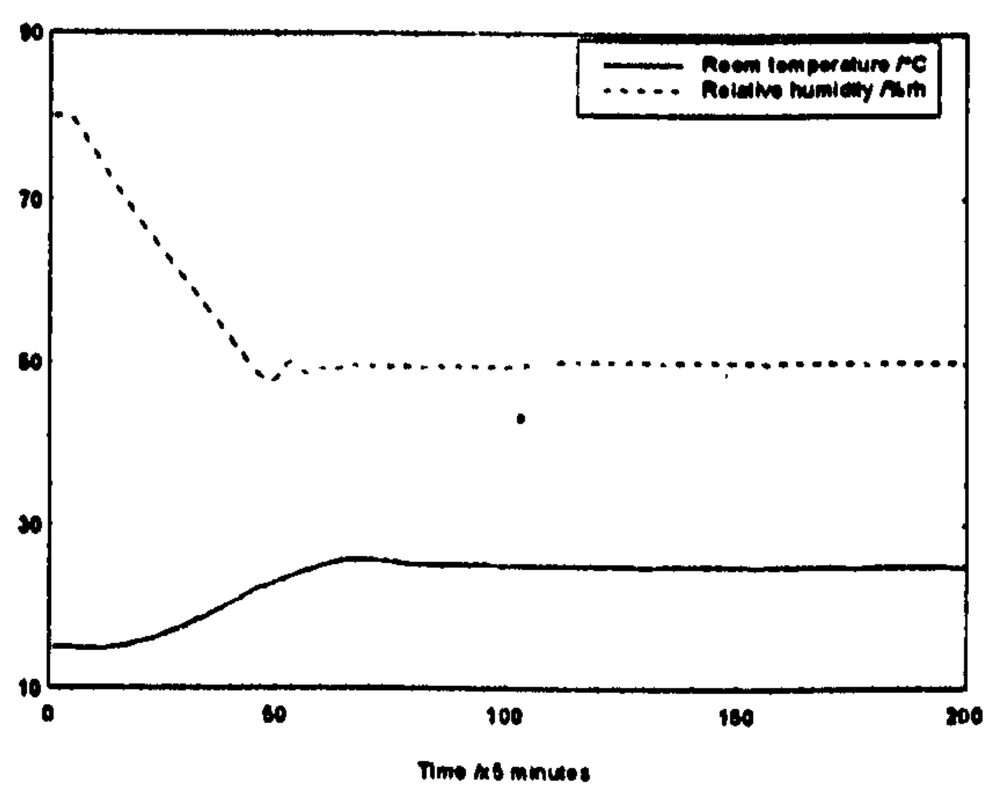

b) System outputs

Figure 6.5: Control performance of the proportional FLC

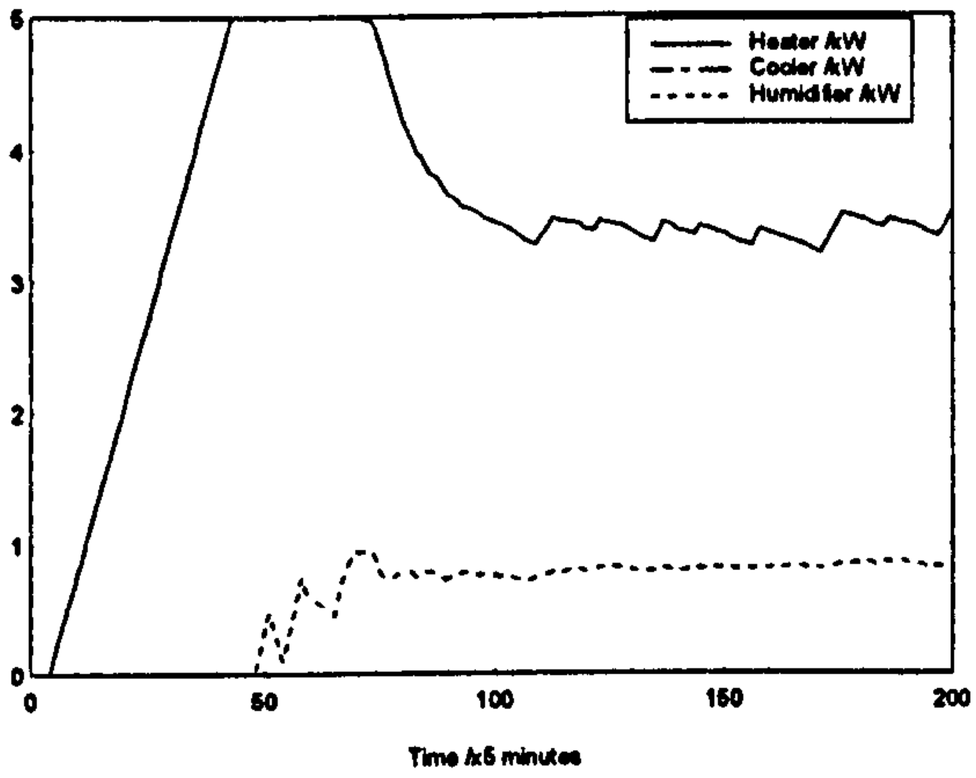

a) Control inputs

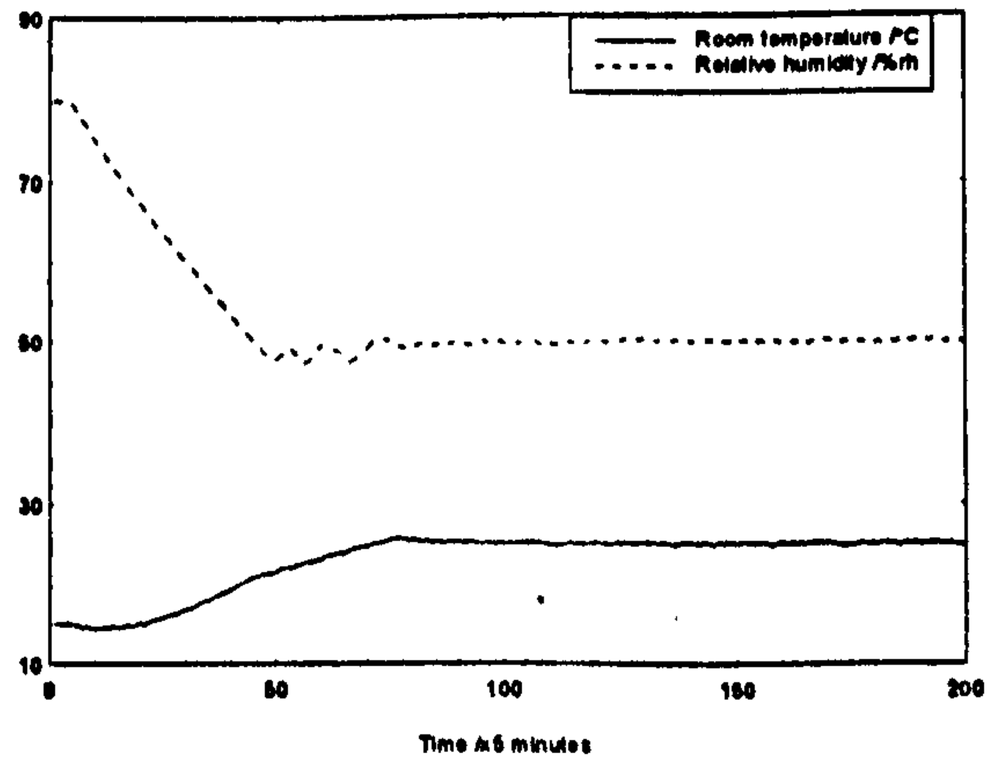

b) System outputs

Figure 6.6: Control performance of the proportional FLC with disturbances present

In this study, we also investigated the regulation performance of the system for other setpoints by using the tuning procedures as described in sections 6.1 and 6.2. When the setpoints of the above FLC design are changed to 20°C and 40%rh for the temperature and relative humidity respectively, we found that the control performances are significantly deteriorated as the relative humidity is always above the setpoint at steady state conditions and this is shown in Figure 6.7. For these setpoints, the control performance over the last 100 sampling intervals was found to be as follows:

- the required control input energies are 19.4, 3.5 and 0 kWh for the heater, cooler and humidifier respectively; and
- the output squared errors are 4.2°C^2 and 320.7%rh^2 for the temperature and the relative humidity loops respectively.

The relative humidity error increase is due to a larger effect on the RH for a set cooler decrement at this lower setpoint than for the setpoint of 50%rh. Therefore, we could reduce the relative humidity error at steady state conditions by selecting a new set of

fuzzy output scaling factors as shown in Table 6.5 where only the fuzzy output membership functions of the cooler, namely z_r, p_m and x_u are increased to 0.21, 0.21 and 0.3 kW.

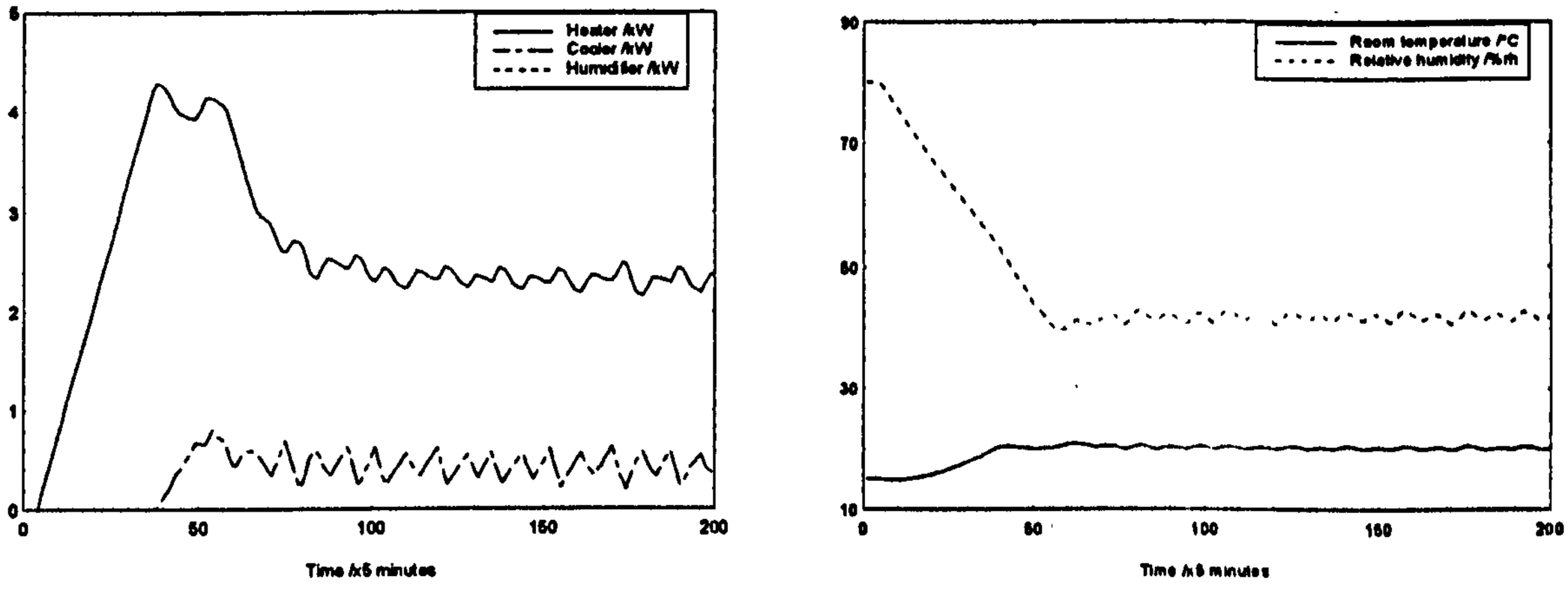

a) Control inputs

b) System outputs

Figure 6.7: Control performance of the proportional FLC (setpoints change)

Table 6.5: Scaling factors for the fuzzy output membership functions

Fuzzy controller output (kW)	Negative (N)			Zero (Z)			Positive (P)		
	x_l	n_m	n_r	z_l	z_m	z_r	p_l	p_m	x_u
dW	-0.20	-0.14	0	-0.14	0	0.14	0	0.14	0.20
dC	-0.20	-0.14	0	-0.14	0	0.21	0	0.21	0.30
dH	-0.20	-0.10	0	-0.10	0	0.18	0	0.18	0.25

The simulated result for this redesigned FLC is shown in Figure 6.8 where we can see that all the three signals are required to regulate the system outputs. The control performance of the controller was calculated for the last 100 iterations of the simulation trial; the value of the squared errors were found to be $0.4°C^2$ and $3.9\%rh^2$ for the

temperature and relative humidity respectively which is almost similar to the result obtained from the previous fuzzy settings, but the energies consumed by the heater, cooler and humidifier were relatively large at 24.5, 8.0 and 3.5 kWh respectively. We can see that the three control inputs are fighting one another in order to regulate the two outputs.

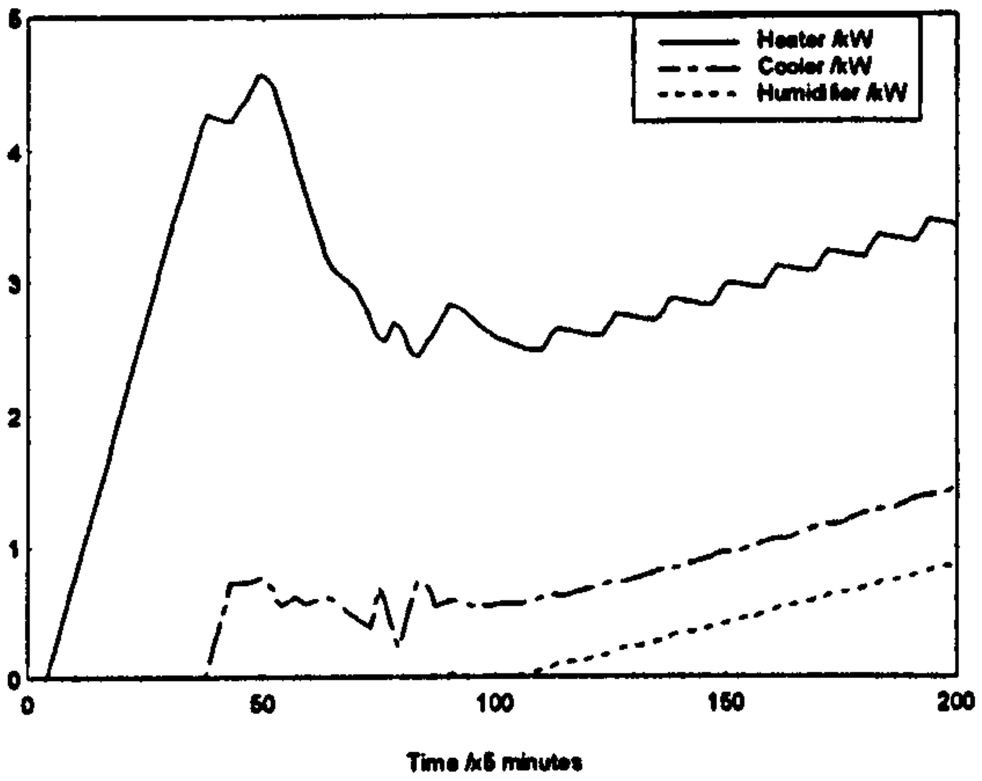

a) Control inputs

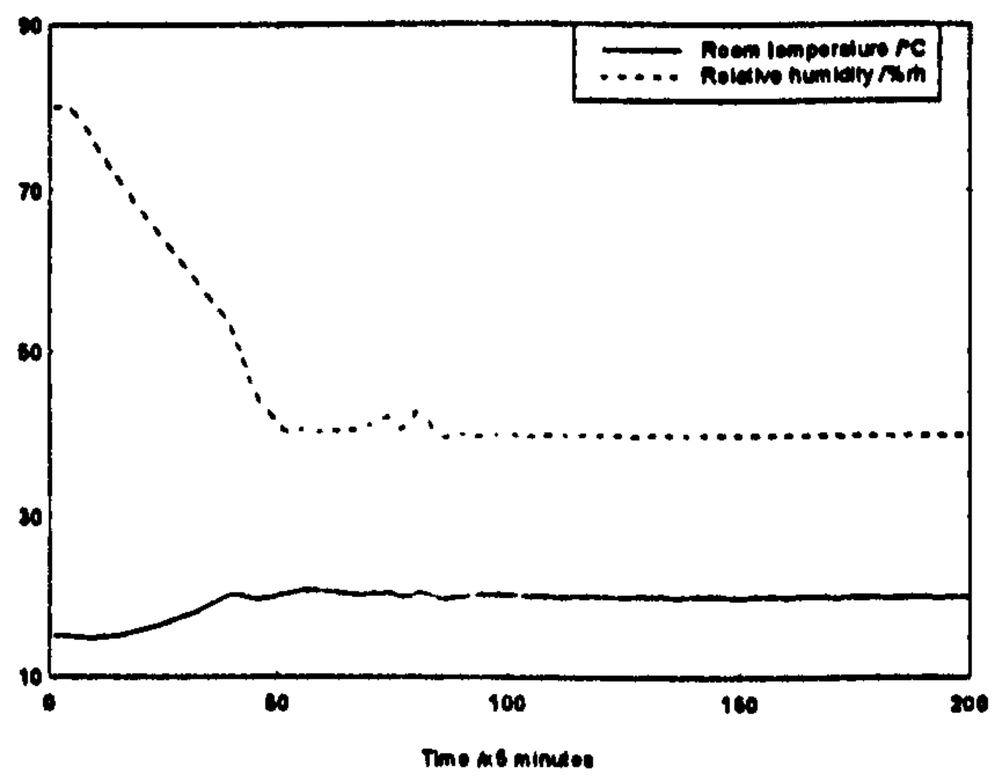

b) System outputs

Figure 6.8: Control performance of the proportional FLC with redesigned fuzzy membership functions

For the FLC based on a P+I design, the control performance is shown in Figure 6.9 where identical climatic disturbances and white noise processes as earlier are applied. The scaling factors for the P+I terms (as indicated in Tables 6.3 and 6.6) are used in this design. Again, the fuzzy input domains of the integral terms I_T and I_H as presented in Table 6.6 were obtained after several simulation trials so that the desired output regulations can be achieved.

The steady state performance over the last 100 data points was calculated and it found to be as follows:

- the required control input energies are 27.8, 0.1 and 6.7 kWh for the heater, cooler and humidifier respectively, and
- the output squared errors are 5.9°C^2 and 84.6%rh^2 for the temperature and relative humidity respectively.

Table 6.6: Scaling factors for the fuzzy input membership functions for the integration term

Fuzzy input	NL and PL			NS and PS			Z	
Scaling factor	l_1	l_2	l_3	s_1	s_2	s_3	z_1	z_2
Room temperature, °C_h	0.010	0.008	0.005	0.008	0.004	0	0.003	0
Relative humidity, %rh_h	0.010	0.008	0.005	0.008	0.004	0	0.003	0

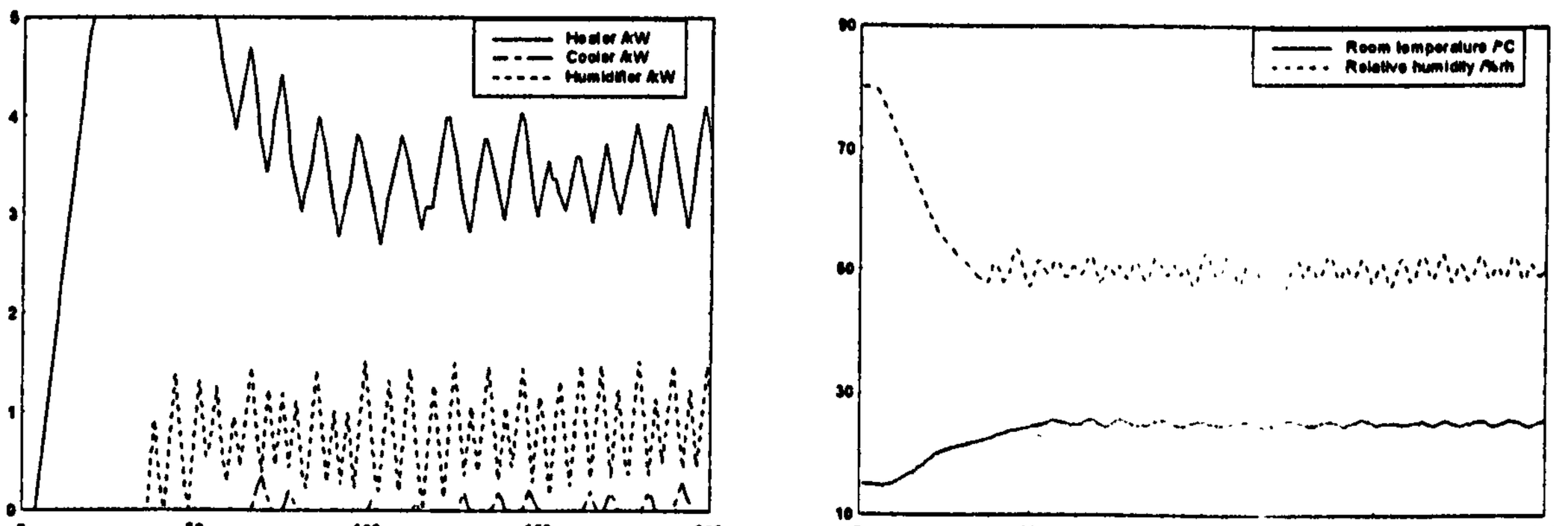

a) Control inputs b) System outputs

Figure 6.9: Control performance of the P+I FLC with disturbances present

We can see that the output regulation at steady state conditions is acceptable but degraded as compared to that obtained through the proportional FLC. This is because the proportional FLC in fact also contains integral action as it is implemented with incremental control. If it was a true proportional only FLC the performance would be inferior with steady-state error due to the zero type number of the system and controller configuration. Both results for the proportional and P+I FLCs can be improved further by modifying the overall fuzzy rules as well as the scaling factors for the fuzzy input and output membership functions.

We have also designed other types of FLC based on the PID controller, such as employing P+D or P+I+D terms, and found that the required FLC tunings are more difficult to achieve and extensive simulation trials are needed in order to achieve a good design. This problem is due to our system being multivariable, and many parameters are involved in the tuning process which are quite difficult to carry out in practice.

From the results presented here, we have faced a difficulty of obtaining the appropriate values of the fuzzy membership functions where extensive simulation trials are needed to achieve the desired FLC control performance. To improve the situation, we propose the use of genetic algorithm (GA) optimisation techniques to automatically search these functions, and this is discussed in Chapter 7.

6.4. Conclusions

This chapter has shown that good control performances can be achieved by using fuzzy logic controllers (FLC) based on proportional techniques with incremental control, when applied to a HVAC plant /office zone system having three inputs and two outputs. These

good results have also been obtained using a P+I FLC but P+D and P+I+D controllers require more effort in tuning them in order to achieve a good result. These practical aspects are considered in Chapter 7.

Chapter 7

Genetic Algorithms for BEMS

The genetic algorithm based method (GA) is a global search technique which uses natural selection and genetics. It searches from a population of solutions, by using random choice as a selection tool to obtain the best solution. The first thorough treatment of the use of genetic algorithms was given by Holland (1975) but a more upto date description of the theory and application of GA methods may be found in Goldberg (1989). Examples of the use of GAs in control applications are given in Waddicor (1993), McGregor et al (1992) and Etter et al (1992).

These algorithms operate on a population of character strings in much the same way as genetic action operates on chromosomes in a population of organisms. GAs enforces a Darwinian "survival of the fittest" strategy among a population of strings. In every generation, a new set of strings is created using parts of the fittest individuals from the previous generation. The algorithms use past information efficiently to explore new regions of decision space with a high probability of finding improved performances.

GAs are different from typical search methods in three primary ways, namely,

1. they work with a coding of the parameter set rather than with the actual parameters,

2. they search from a population of solutions, and

3. they use probabilistic transition rules.

Several parameter coding schemes have been developed. The most commonly used is binary and grey coded population strings consisting of the characters {0, 1, *} where * symbols indicate "don't care" positions. In GA terminology, these strings are called chromosomes and each chromosome represents a set of physical parameters. It is assumed that a fitness value can be evaluated for each chromosome, where this fitness is defined as a nonnegative value of merit to be optimised and corresponds to the objective function in classical optimisation theory.

7.1. GA methodology

One way to solve an optimisation problem is to generate a number of solutions and then by following certain procedures, all these solutions can be tested so that the "best" one is chosen. If the best solution does not comply to the required specifications, then another set of solutions is generated and this process is repeated until the answer is obtained. This explains how the genetic algorithm is operated to solve the problem. The general operation of a GA is shown in Figure 7.1 where the algorithm initialises a number of solutions, which is called the initial population, and selects the best solution from this population via a reproduction process. New solutions are then created by the methods called crossover and mutation, and this routine is repeated until the optimal solution is found. The details of the GA method are described next for completeness.

7.1.1. Initialisation

The initial population of solutions, i.e. the parameter sets can be generated in two main ways; the first of these is to guess in a random manner and the second is to use directed search methods such as employing standard optimisation algorithms.

7.1.2. Encoding

In order for the genetic operators to be applied to a population, each solution must be represented as a chromosome. The procedure of converting a solution into a chromosome is known as encoding.

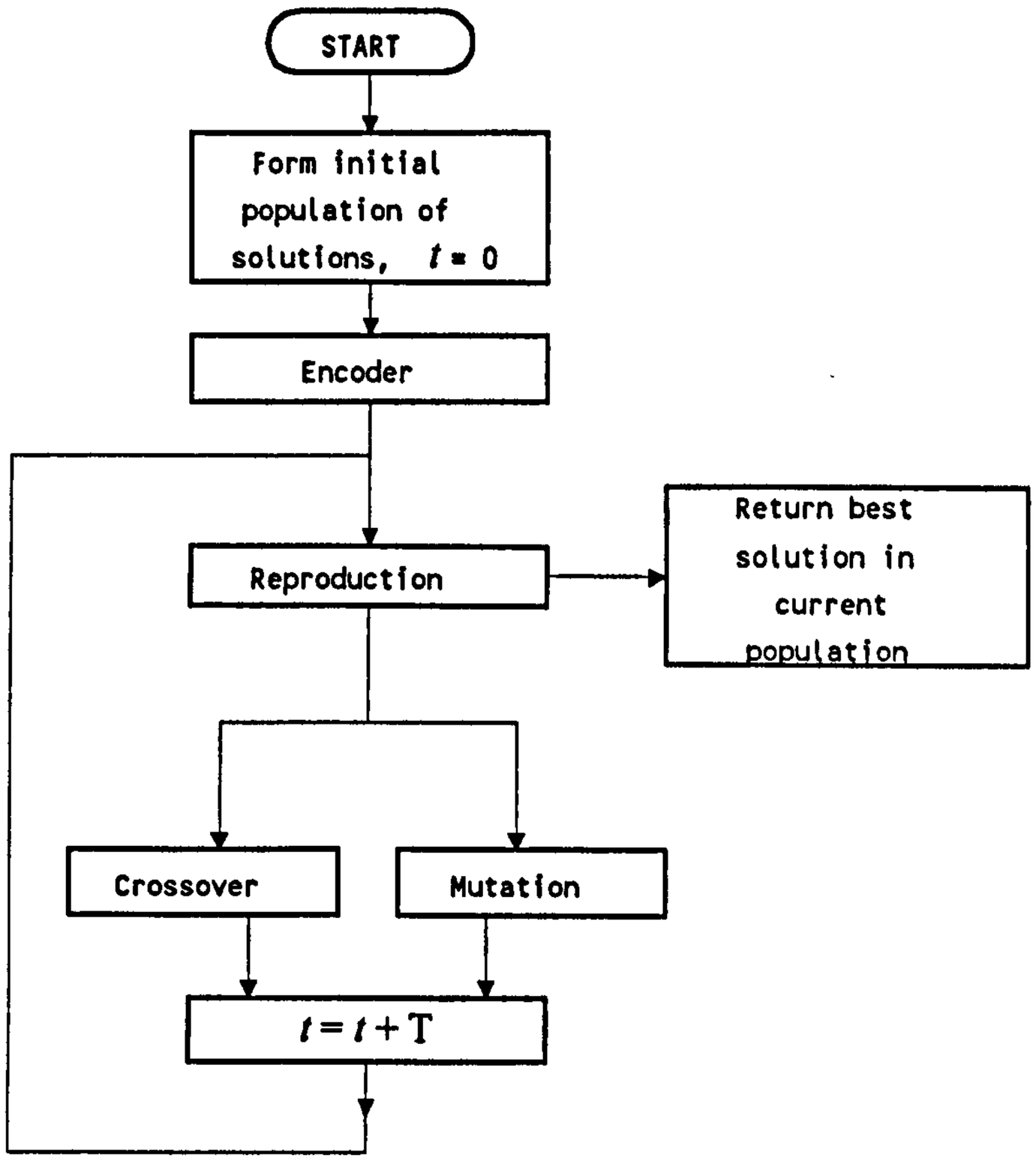

Figure 7.1: Flowchart of Genetic Algorithm

The encoding procedure varies according to the type of problem being considered and nature of the solution being sought; for a solution which is specified as a set of parameters expressed as floating point numbers, the following procedure may be used. However before encoding can take place, it is necessary to determine the minimum and maximum values for each parameter as well as the number of possible values it may take. This corresponds to the resolution R and is set to 2^n-1, where n is a positive integer. Each parameter value may then be normalised to a value in the range 0 - R, by using

$$NormalisedValue = \frac{OriginalValue - MinimumValue}{MaximumValue - MinimumValue} \times R \qquad (7.1)$$

This normalised value is rounded to the nearest integer, which is then expressed in binary logic or base 2 arithmetic. The result is a chromosome with a word length (number of bits) equal to $\log_2(R+1)$; Figure 7.2 shows this procedure more clearly where the integer n = 4, i.e. 4 bit string of each of the three parameters, namely x_1, x_2 and x_3, and their resolution, R, are calculated to equal 15. The normalised values can be calculated from equation (7.1) where the maximum values are 5.0, 2.7 and 2.6 for x_1, x_2 and x_3 respectively and their minimum values are zero. When all the parameters within a set of solutions have been converted to strings, the strings are concatenated to produce the chromosome of length S, where S represents the number in the parameter set, and for this example, S =12.

7.1.3. Evaluation

The performance for each chromosome is evaluated by calculating the fitness function for its parameter set which is obtained by performing the reverse of the above encoding process.

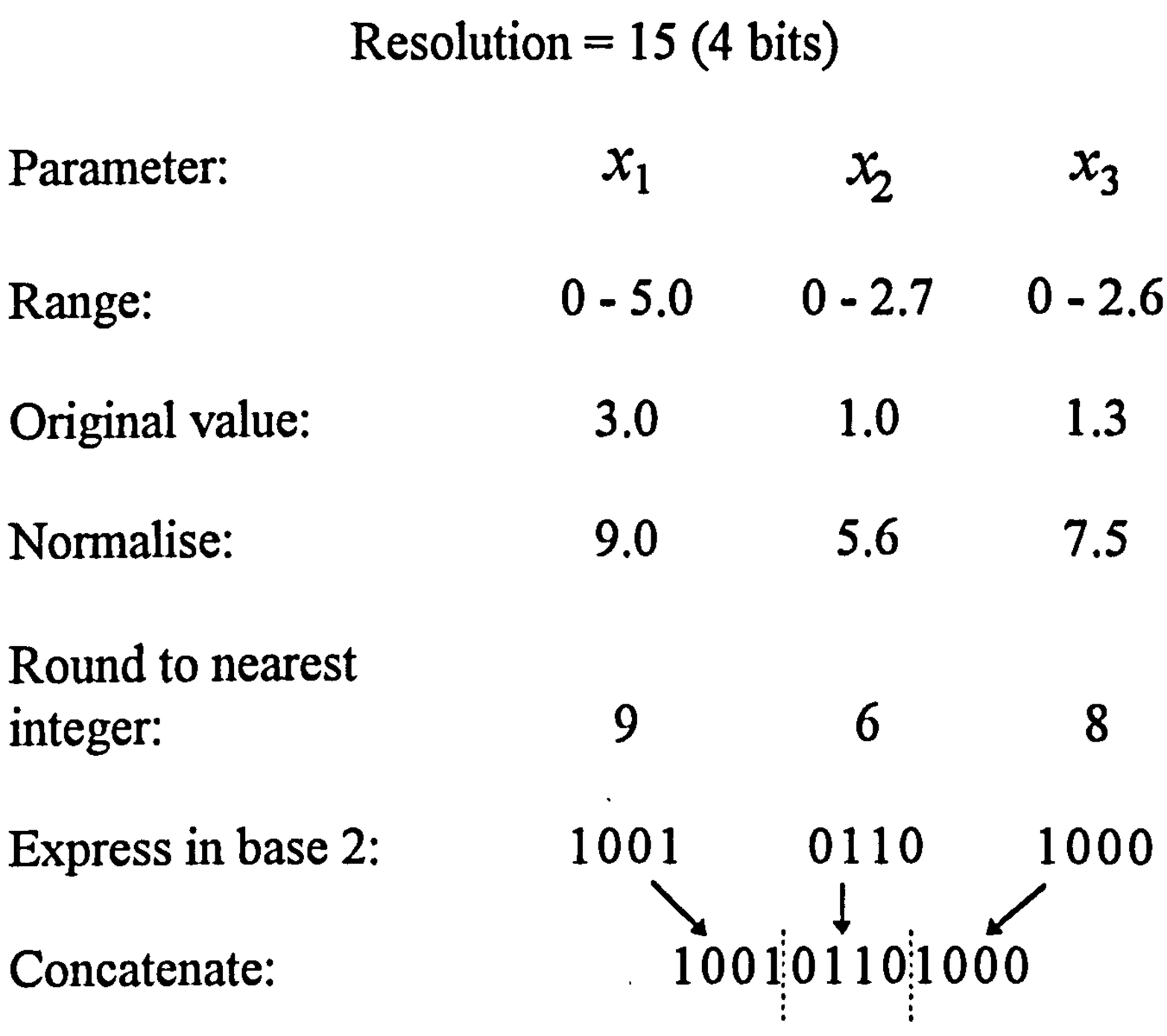

Figure 7.2: An example of Binary encoding

7.1.4. Genetic operators

There are three well known genetic operators, namely reproduction, crossover and mutation. Here, we briefly explain their operations for the GA methodology.

Reproduction is a process in which individual chromosomes are copied into the next generation of solution according to their fitness, i.e. the 'better" chromosomes survive to reproduce and the less fit ones "die" out. In the reproduction process, two chromosomes are randomly chosen from the previous population, and the 'best" one is copied into the next population. This process continues until all members of the next population have been generated.

After reproduction, simple crossover of the genes occurs in two steps. First, the members of the newly reproduced chromosomes are "mated" randomly and crossover is then accomplished by

(i). randomly selecting a number of positions in the chromosome (usually over half of the bits in a chromosome); and

(ii). swapping all the succeeded positions, thus creating two new chromosomes.

Figure 7.3: Crossover and Mutation operators

In the mutation process, we randomly change the value of a specific chromosome (bit); this is usually applied to only a few positions in the chromosomes of the new population, for example, a ratio of the order 1 in every 1000 is normally applied. A randomly selected bit is flipped, i.e., if its value is 0, it becomes 1, and vice versa. This operation, when used sparingly, ensures that potentially useful information in a string position is not lost forever.

The crossover and mutation operators in a binary code are shown in Figure 3 where we can see that the crossover rate is 5 out of 8 bits (60%) and takes place at bit positions 2, 3, 5, 7 and 8 and the mutation is at position 6 from the left.

7.1.5. Convergence

All GAs eventually produce a population in which the best chromosome is identical to that obtained from the previous generations. At this point, the GA is said to have converged, and this chromosome represents the optimal solution to the problem.

7.2. Controller based on GA

In the control of a HVAC plant/office zone system, we require that the room temperature T_c and relative humidity H_c track their respective setpoints T_r and H_r and the output errors, namely e_T and e_H should be as small as possible at steady state conditions. Therefore, the objective is to simultaneously minimise e_T and e_H, which are defined by equations (3.3) and (3.6).

There are other ways to define the objective function for the above HVAC plant. For example, to minimise the total energy consumption in applying the controlling inputs, namely, the heater W, cooler C and humidifier H while maintaining the output errors to within an acceptable limit. The objective function for this definition may be difficult to formulate due to the plant being multivariable in nature and optimisation of many parameters would be required. Thus, we restrict our discussion to the earlier definition for simplicity and investigate the system performance of different fitness functions, and different setpoints.

In this chapter, we present the use of GA techniques to solve the problem of determining the three strategies for calculating the control inputs to drive the HVAC

plant/office zone system. The first type is to apply the structure of a multi-proportional loop controller where the GA is used to tune the proportional gains. The second type will be to search the best combination of fuzzy membership functions so that the control performance of the FLC based on output errors is improved and the third type minimises the predicted system output errors at time t+T and the GA is used to obtain the best combination of the three control inputs at each time step t. This adaptive type of controller is further improved by the use of hybrid GA techniques to reduce the control input switching problems encountered earlier in our research.

7.3. Multi-proportional loop controller

In this type of controller, the requirement is to tune the proportional gains so that the system output closely tracks the desired setpoint. For our application, the block diagram of the overall control system as shown in Figure 3.3 can be used to solve this problem where all the PI controllers are replaced by simple proportional controllers. For this configuration, the control inputs $W(t)$, $C(t)$ and $H(t)$ can be calculated by summing the proportional terms obtained from the temperature and relative humidity loops limited by their respective input constraints, namely,

$$W(t) = K_{P1} e_T(t) + K_{P2} e_H(t), \quad 0 \le W(t) \le 5.0 \tag{7.2}$$

$$C(t) = K_{P3} e_T(t) + K_{P4} e_H(t), \quad 0 \le C(t) \le 2.7 \tag{7.3}$$

$$H(t) = K_{P5} e_T(t) + K_{P6} e_H(t), \quad 0 \le C(t) \le 2.6 \tag{7.4}$$

where K_{P1}, K_{P2}, .., K_{P6} are the proportional gains for the controllers #1, #2, .., #6 respectively.

The design problem here is to tune these gains by the GA method so that the output errors are as small as possible at steady state conditions. This can be done by first applying the main information about the input step responses as discussed in chapters 2 and 3; note the sign of gains K_{P1}, K_{P5} and K_{P6} should be positive and those of K_{P2}, K_{P3} and K_{P4} negative in order to reduce the errors. Moreover, since the majority of the modified Ziegler-Nichols proportional gains, as presented in Chapter 3 fall in the range between 0 and 1, we assume that these gains lie in this range. Then, the GA optimisation technique described in section 7.1 can be adopted for this case by introducing a set of individual chromosomes p_j, j = 1, 2, ..., M which belong to the population $P(i)$ at generation i and the following steps are implemented in order to determine the gains:

Proportional GA algorithm

Step 1. Select a random initial population $P(i)$ comprising M solutions satisfying the above assumption, i.e. $0 \leq |K_l| \leq 1$, l =$P1$, $P2$, .., $P6$. Set the encoding resolution R for each gain, and the crossover and the mutation rates. Initialise the generation $i = 0$.

Step 2. **Encoding:** Perform the encoding procedure for each solution, i.e. the parameter set $\{K_{P1}, K_{P2}, K_{P3}, K_{P4}, K_{P5}, K_{P6}\}$ is converted into a chromosome, as shown in Figure 7.2.

Step 3. Calculate the parameter set for each chromosome by performing the reverse of the encoding process.

Step 4. **Reproduction:** Calculate the fitness function for each chromosome and generate the population $P(i+1)$ of M chromosomes according to the reproduction procedure.

Step 5. Go to Step 6 or Step 7 randomly.

Step 6. **Crossover:** Mate the members of $P(i)$ at random, and carry out the crossover operation at random for each pair of chromosomes. We then have 2M chromosomes for population $P(i+1)$, that is M chromosomes belong to the parent and M chromosomes belonging to the offspring. Go to Step 8.

Step 7. **Mutation:** Select at random a chromosome from the population $P(i)$. Carry out the mutation operation for that chromosome, we then have an offspring chromosome and the population $P(i+1)$ contains M+1 chromosomes.

Step 8. Set $i = i + 1$ and Goto Step 3.

The above steps are iterated until the fitness function of the best chromosome at generation i converges to a minimal value. The details of each step in the algorithm are explained next.

7.3.1. Initial population

The initial population is generated by using a random selection method. In our application, the multi-proportional loop controller requires 6 gains in the range between 0 and 1, then using the MATLAB language, this population can be generated using the "rand" function; hence $P(0)$ = rand(6, M); this generates random numbers between 0 - 1 of equal opportunity. Thus, we have a population of P of dimension 6xM and p_j is the jth. column vector of P for the jth. parameter set $\{K_{P1}^j, K_{P2}^j, .., K_{P6}^j\}$ where $j = 1, 2, ...,$ M. In the genetic algorithm, the physical value of the parameter set is encoded into a chromosome. If the encoding resolution is 15, then we have a 4 bit string for each input

(see Figure 7.2) and these strings are concatenated to produce a chromosome of length 24 bits with the first, second, third, fourth, fifth and sixth four bits represent the gains K_{P1}, K_{P2}, K_{P3}, K_{P4}, K_{P5} and K_{P6} respectively. If the required encoding resolution is 255, i.e. 8 bit words, then each chromosome will be 48 bits long.

The size of the population M is normally set between 20 to 80 in order to obtain "enough variety" of chromosomes and ensuring that the computational requirements do not become excessive; it is obvious that, the larger the M the longer the simulation period.

7.3.2. Reproduction

In the reproduction process, two chromosomes are selected at random from the population $P(i)$ and these compete through a fitness function for survival to the next generation. The fitter chromosome will be selected and the weaker one will die. This process is repeated for other pairs of chromosomes until we obtain a total number of M chromosomes for the population $P(i+1)$.

The fitness function (normally known as the objective function in the field of optimisation) plays an important factor for the system to converge, it has to be formulated in such a way that both the system outputs should converge to the required setpoints at steady state conditions. A sensible choice for the fitness function, f_j, for the chromosome p_j is the summation of the absolute room temperature and relative humidity errors. In this way larger values will indicate a poor solution and smaller errors a good one. A convenient way of combining the temperature and humidity errors is as follows:

$$f_j(i) = E_T^j(i) + \alpha E_H^j(i), \text{ for } i = 1, 2, 3, \ldots$$

$$j = 1, 2, 3, \ldots, 2M \text{ for crossover}$$

$$j = 1, 2, 3, \ldots, M+1 \text{ for mutation} \qquad (7.5)$$

where α is a weighting term to allow us to vary the relative importance to the temperature and / or relative humidity, and j is the chromosome number. E_T^j and E_H^j are defined as

$$E_T^j = \sum_k |e_T^j(kT)| \text{ and } E_H^j = \sum_k |e_H^j(kT)| \qquad (7.6)$$

respectively. The summation for the total absolute errors was chosen to begin at iteration $k = 50$ because the system normally reaches steady state condition (as seen from the figures presented in this thesis) after about 50 iterations of the simulation start; in addition a total of 150 iterations ($k = 50$ to 200) was selected to get a clear picture of the system's behaviour at steady state conditions.

At each generation, e_T^j and e_H^j are obtained by calculating the system outputs T_c and H_c from equations (2.1) and (2.2) where the constrained control inputs W, C and H are obtained from equations (7.2), (7.3) and (7.4) respectively with the gains K_{P1}^j, K_{P2}^j, .., K_{P6}^j for the jth. chromosome. These outputs are then substituted into equations (3.3) and (3.6) respectively and E_T^j and E_H^j are obtained after the system has been simulated for 200 iterations. The fitness function f_j is next calculated via equations (7.5) and (7.6) for each chromosome j of the population $P(i)$. The temperature and relative humidity setpoints T_r and H_r for this fitness function were chosen at 25°C and 50%rh respectively for the comfort of the occupants in the room.

In the reproduction process, all the chromosomes at generation *i* compete for survival and the M chromosomes with the smallest values of fitness functions are selected to win the competition and survive for the next generation.

7.3.3. Crossover

The crossover operation is performed through the example in Figure 7.3, where two offspring chromosomes are produced from any pair of parent chromosomes of population $P(i)$ after being crossovered. It is normally over half of the number of bits in a chromosome which take part in the crossover operation. For example, if the resolution for each gain is 15, and the crossover rate, *cr*, is $^{15}/_{24}$, then there are 15 out of 24 bits of each chromosome to be involved in this operation. The actual bit positions which crossover in each pair of the parent chromosomes are randomly chosen.

7.3.4. Mutation

The mutation operation is usually selected at a very low rate of occurrence in most applications because otherwise the method reduces to a random search; normally at one in a thousand bit positions of the parent chromosomes are chosen to mutate in this way. As an example, for our case, if the number of population M is 20, and the chromosome length is 24 bits, then the chances of a bit in a chromosome, b_{jk} , $j = 1, 2, ..., 20$; $k = 1, 2, ..., 24$, to alter it's value is $1/480$. This probability is also called the mutation rate, *mr*. If the mutation rate is $1/1000$, that is about half of $1/480$, an average possibility for mutation to occur in Step 6 of the algorithm is in every other iteration.

7.3.5. Convergence

For the fitness function described in section 7.3.2, the GA is assumed to have converged when the lowest value of the fitness function f_s at generation i reduces to a minimum. It is clear that the fitness function is monotone decreasing, that is $f_s(i) \leq f_s(i-1)$ for all i. The number of generations after which the GA should be terminated is determined by the value of the fitness function and when an acceptable level for the output errors has been reached.

7.3.6. Tuning of the proportional gains

In the GA tuning process, we assume that the initial conditions of the room temperature, $T_c(0)$, and relative humidity, $H_c(0)$, are at 15°C and 60%rh respectively, and all the three control inputs to the plant are zero. For convenience, the climatic disturbances such as the laboratory temperature, T_l, outside air temperature, T_o, outside relative humidity, H_o, total solar irradiance, S, are assumed to be constant at 20°C, 15°C, 70%rh and 0.1 Wm^{-2} respectively, and the unmodelled stochastic influences, V_1 and V_2 are not present. The desired setpoints T_r and H_r are assumed to be 25°C and 50%rh respectively. The weighting term α in the fitness function from equation (7.5) is normally less than 1 because the temperature is normally more important from an occupant comfort viewpoint than the relative humidity.

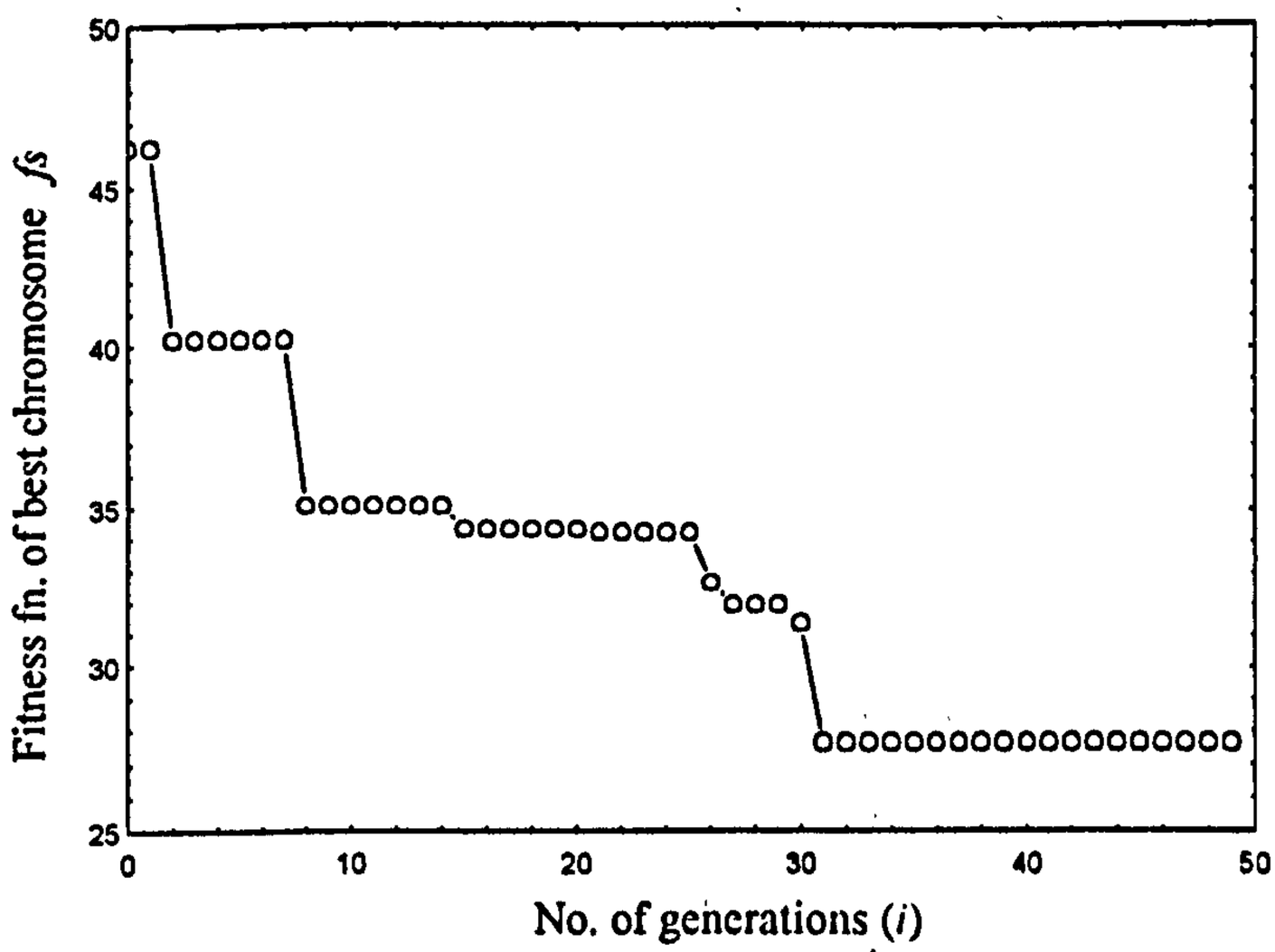

Figure 7.4: Convergence of the GA

In our research, the simulation trials were carried for different magnitudes of GA's generation and population, M, as well as the fitness function's weighting term, α, and found that a good result was normally obtained when we simulated the GA trials for 50 generations with M = 30 and $\alpha = 0.3$; hence we use these values for our results. The encoding resolution R used is 15, i.e. 4 bits for each proportional gain, thus producing a total of 24 bits for a chromosome of 6 gains. The crossover and mutation rates are $^{15}/_{24}$ and $^{1}/_{1000}$ respectively. The result is shown in Figure 7.4 where f_s converges to 27.6 after 31 generations. The chromosome for this solution is converted into it's physical value, that is to the proportional gains K_{P1}, K_{P2}, K_{P3}, K_{P4}, K_{P5} and K_{P6}; these equal 1.00, -0.47, -0.87, -0.067, 0 and 0.27 respectively. These GA tuned gains for the multi-proportional loop controller are then applied to control the HVAC plant/office zone system by assuming that the air dynamics of the test room obeys equations (2.1) and

(2.2), and the three control inputs can be calculated via equations (7.2), (7.3) and (7.4) using these gains. The simulation results are presented next.

7.3.7. Simulation results

The performance indexes such as the output error, the energy consumption and the settling period, of this multi-proportional loop controller is investigated via simulation studies where the setpoints, the climatic disturbances and other stochastic effects are identical to those described in section 7.3.6. A simulated result is shown in Figure 7.5 where we can see that a good control performance is achieved for the setpoints $\{T_r, H_r\}$ at {25°C, 50%rh}, and the system has small steady state errors as shown in Table 7.1.

It is worthwhile to compare this GA tuned controller with the conventional Ziegler-Nichols (1942) method for this multivariable system. For the open-loop step responses as discussed in Chapter 3, the proportional gains for this method is given by $K_P = \frac{U_s}{NL}$ where U_s, N and L are as previously defined; these gains are calculated for the six proportional controllers and found to equal 5.34, -7.53 and 15.26 kW/°C for K_{P1}, K_{P3} and K_{P5}, and -6.57, -1.17 and 1.48 kW/%rh for K_{P2}, K_{P4} and K_{P6} respectively. A simulation result for this method is shown in Figure 7.6 where the control performance is poor as compared to the results obtained via the GA tuned controller. We can see that the room temperature and the relative humidity have large fluctuations around the set-point of 25°C and 50%rh respectively and the control inputs are switching excessively between the on and off states.

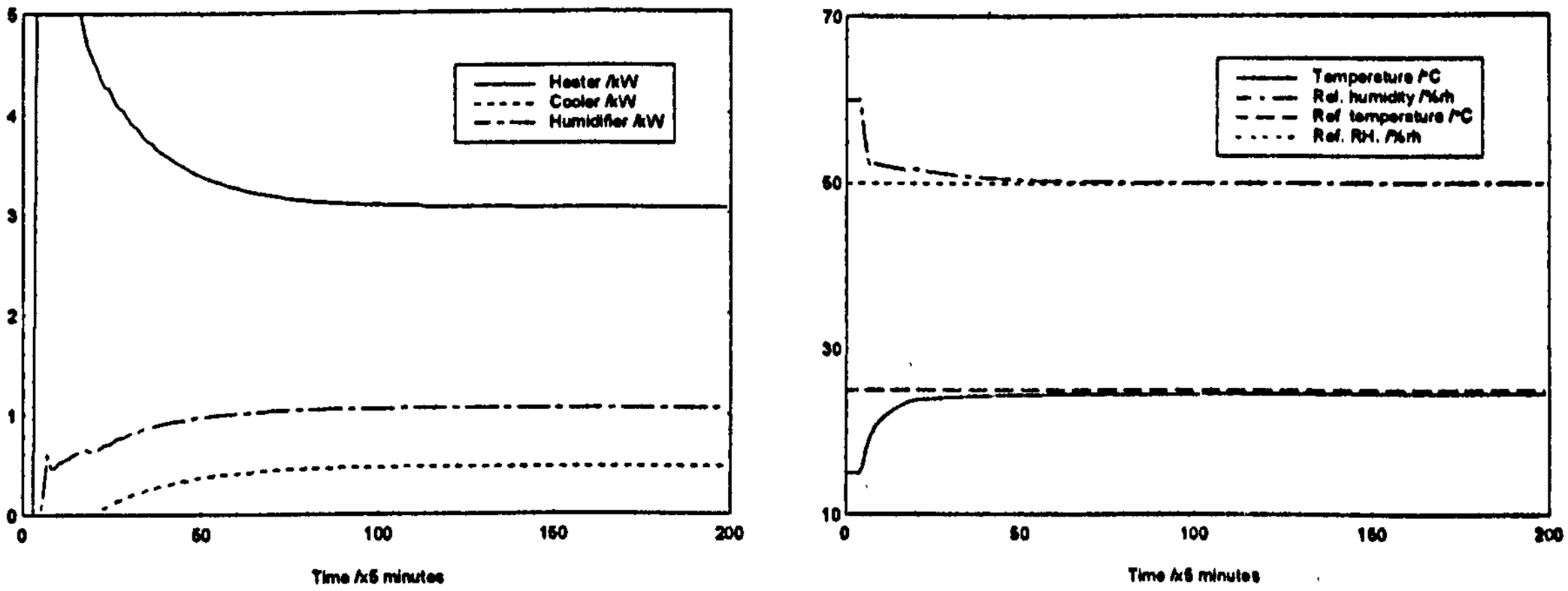

a) Control inputs b) System outputs

Figure 7.5: Proportional GA tuned controller for $T_r = 25°C$; $H_r = 50\%rh$

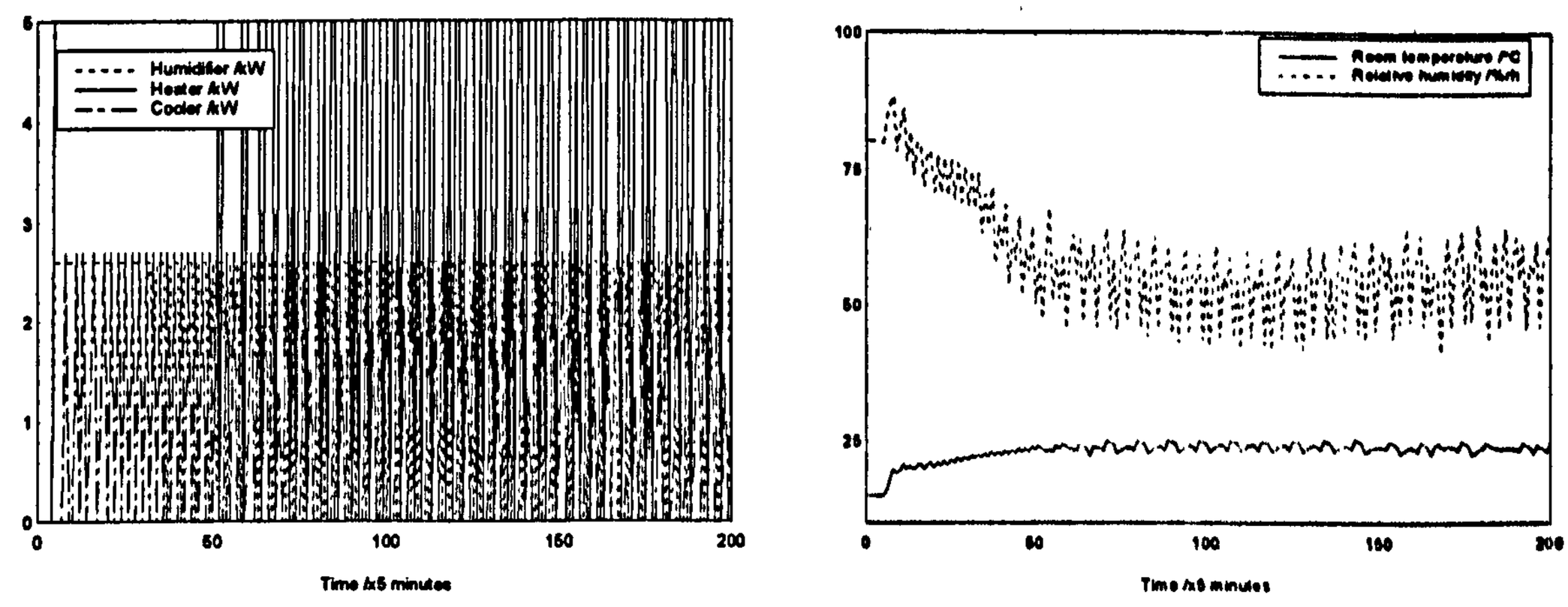

a) Control inputs b) System outputs

Figure 7.6: Performance of multi-proportional controller via Ziegler-Nichols tuned gains

As discussed in Chapter 3, this poor performance can be improved by modifying the Ziegler-Nichols tuned gains. When these are carried out, we found that the modified proportional gains, K_{PM}, equal 0.45, -0.418 and 0.51 kW/°C for controllers #1, #3 and #5, and -0.047, -0.047 and 0.049 kW/%rh for controllers #2, #4 and #6 respectively. A simulated result for this case is shown in Figure 7.7 where the control performance is still

poor as compared to that obtained using the GA tuned method. The steady state performance over the last 100 data points are calculated and found to be as follows:

- the required control input energies are 25.2, 5.8 and 11.5 kWh for the heater, cooler and humidifier respectively; and
- the output squared errors are 73.9°C^2 and 943.0%rh^2 for the temperature and relative humidity respectively.

From these results, we can conclude that the control performance of the GA proportional controller is superior than the proposed tuning method presented in Chapter 3 where its output errors at steady state conditions (Table 7.1) are relatively small.

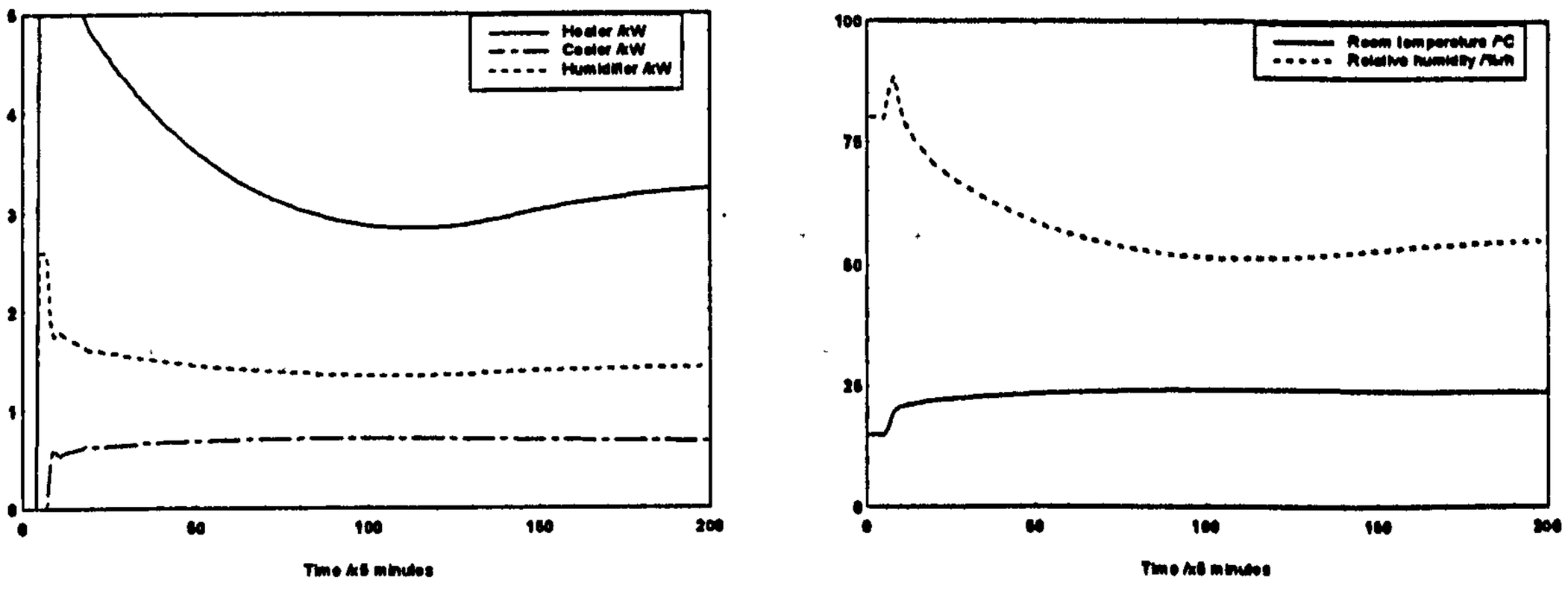

a) Control inputs

b) System outputs

Figure 7.7: Performance of multi-proportional controller via modified Ziegler-Nichols gains

Now we study the effects of changing the setpoints for the proportional GA controller. When the setpoints $\{T_r, H_r\}$ are changed to {20°C, 40%rh} at the 200th. iteration, the system outputs oscillate during their transient period and the output errors after settling are bigger for the RH loop although the temperature errors are far superior

and this is shown in Figure 7.8. The gains are obviously no longer tuned for this setpoints and hence, the GA needs to be simulated for the setpoints of {20°C, 40%rh} and the temperature and relative humidity weightings in the fitness function need modifying.

Table 7.1: Proportional GA controller results

Performance at steady state conditions for 100 iterations		$\{T_r, H_r\}$ = {25°C, 50%rh}	$\{T_r, H_r\}$ = {20°C, 40%rh}
Error^2	Temp. (°C^2)	25.6	2.1
	Rel. H. (%rh^2)	0.9	224.2
Energy (kWh)	Heater	25.5	25.6
	Cooler	4.0	9.5
	Humidifier	8.8	5.7
	Total	38.3	40.8
Settling time (hours)	Temperature	2.5	0.8
	Rel. Humidity	4.2	2.5

From the table, we can see that although the temperature setpoint is reduced by 5°C, the heater energy remains, the cooler is double its energy and the humidifier energy reduced. This situation clearly shows that the cooler and humidifier energies are fighting one into another to reduce the output errors.

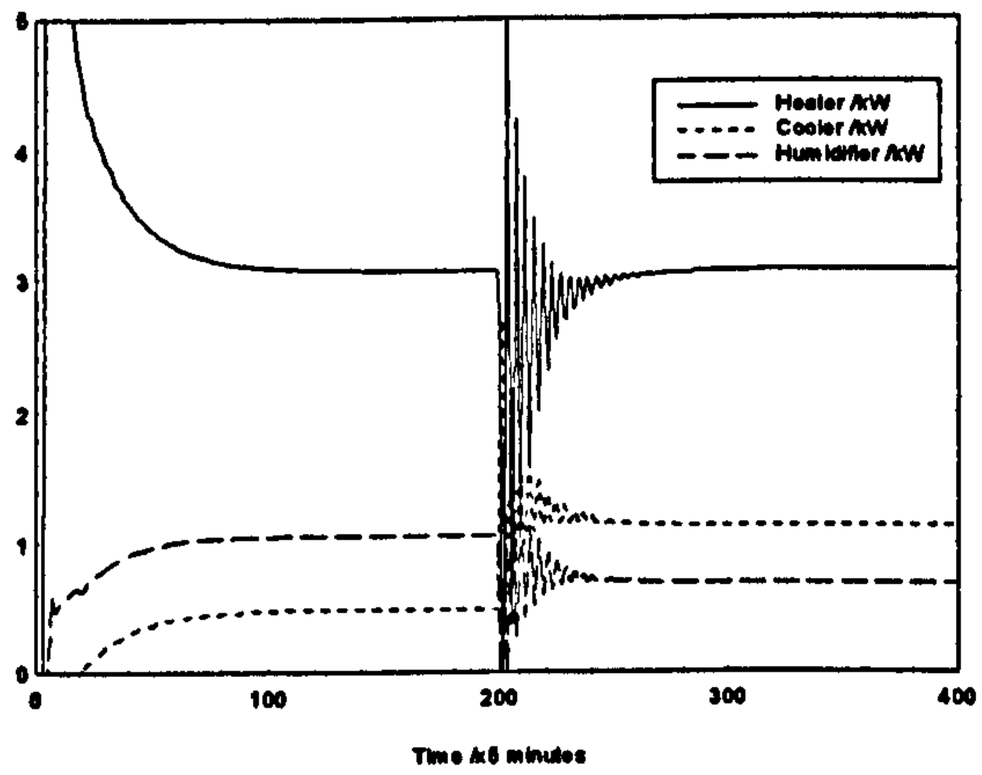

a) Control inputs

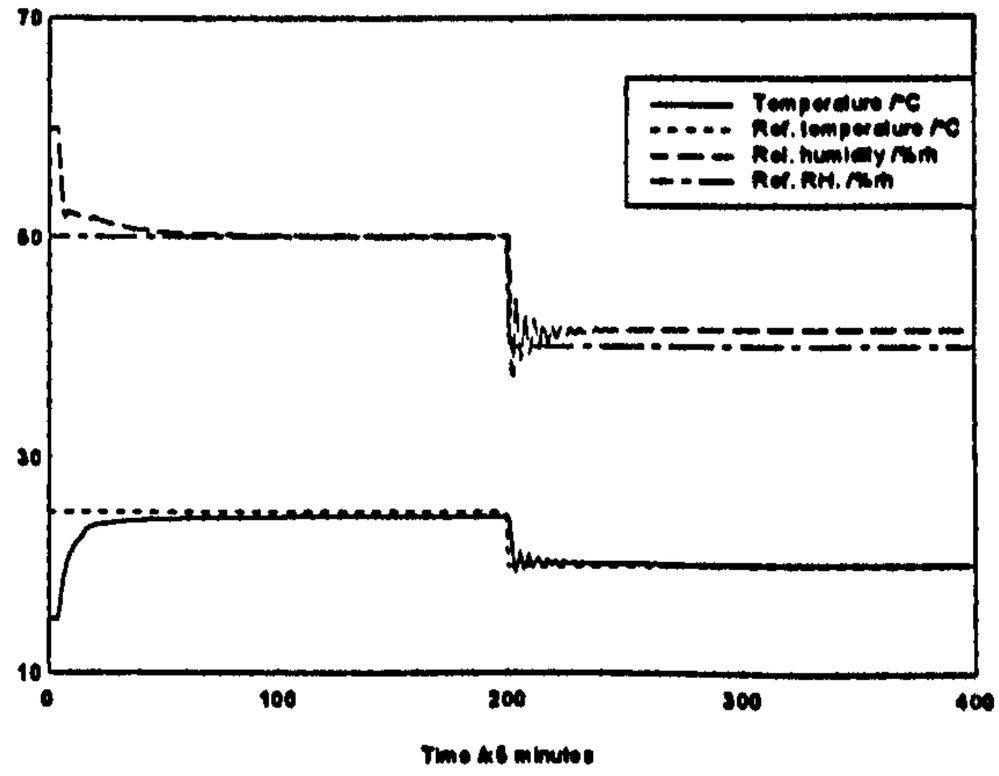

b) System outputs

Figure 7.8: Effects of change in setpoint T_r: 25°C → 20°C, H_r: 50%rh → 40%rh

Simulation trials were also carried out for the weighting terms $\alpha = 1$ and 2 and the setpoints $T_r = 25°C$ and $H_r = 50\%rh$; the obtained results are summarised as follows:

$\alpha = 1$: K_{P1}, K_{P2}, K_{P3}, K_{P4}, K_{P5} and K_{P6} equal 1.00, -0.60, -0.67, -0.07, 0 and 0.13 respectively after twentieth generation; and

$\alpha = 2$: K_{P1}, K_{P2}, K_{P3}, K_{P4}, K_{P5} and K_{P6} equal 0.93, -0.47, -0.80, -0.13, 0 and 0.07 respectively after twenty eightieth generation.

For $\alpha = 1$, the steady state performance over the last 100 data points are calculated and found to be as follows:

- the required control input energies are 25.4, 4.3 and 9.0 kWh for the heater, cooler and humidifier respectively; and
- the output squared errors are $33.0°C^2$ and $0.0\%rh^2$ for the temperature and relative humidity respectively.

Similarly for $\alpha = 2$, the steady state performance over the last 100 data points are found to be as follows:

- the required control input energies are 25.7, 4.2 and 9.0 kWh for the heater, cooler and humidifier respectively; and
- the output squared errors are 27.8°C^2 and 1.0%rh^2 for the temperature and relative humidity respectively.

We can see that the three weighting terms, namely α = 1, 2 and 0.3, give relatively large temperature errors at steady state conditions. This drawback could be improved by selecting a larger GA resolution, R and this is demonstrated in Section 7.5. The results also show that the control performances for the proportional GA controllers for the three selected αs are similar although the gain combinations are different. This demonstrates the randomisation of the GA approaches where a number of optimal solutions can be obtained.

The parameter set $\{K_{P1}, K_{P2}, K_{P3}, K_{P4}, K_{P5}, K_{P6}\}$ for several setpoints are searched for by this GA methodology and the results are presented in Table 7.2. We can use this table to set the proportional gains for the desired setpoints or to re-tune the controller when a new setpoint is required. Furthermore, we can interpolate these gains for intermediate setpoints. For example, if the required references T_r and H_r are 22°C and 40%rh respectively, then we could use the gains for the setpoints $\{T_r, H_r\}$ = {20°C, 40%rh} with K_{P1} could be slightly greater than 1, say, 1.2°C/kW to increase the heating signal due to increased sensitivity of controller #1 so that the temperature could track its setpoint at steady state conditions.

Table 7.2: Look up table for the multi-proportional controller

T_r °C	H_r %rh	K_{P1} °C/kW	K_{P2} %rh/kW	K_{P3} °C/kW	K_{P4} %rh/kW	K_{P5} °C/kW	K_{P6} %rh/kW
15	30	0.80	-0.80	-0.73	-1.00	0.67	0
15	40	0.93	0	-0.27	-0.20	1.00	1.00
15	50	0.47	-0.33	-0.87	-0.07	1.00	0.20
20	30	0.80	-0.40	0	-0.07	0.27	1.00
20	40	1.00	-0.27	-0.53	0	0.47	0.53
20	50	0.40	-0.67	-0.27	-0.07	0.67	0.20
25	30	0.73	-0.93	-0.53	-0.13	0	0.20
25	40	1.00	-1.00	-0.53	-0.13	0.07	0
25	50	1.00	-0.47	-0.87	-0.07	0	0.27

In an actual system, the office zone/HVAC plant will have climatic disturbances, and unmodelled stochastic influences such as internal light intensity, the number of occupants in the room and the opening of doors and windows. A set of actual climatic disturbances presented in section 4.2.1, and for convenience, pseudo random binary sequences (PRBS) of 6 shift registers (Godfrey, 1980) and values ±0.25 were used as the stochastic influences applied to our simulation of the office zone. A simulation trial with setpoints T_r = 25°C and H_r = 50%rh was carried out with these effects included and the results are shown in Figure 7.9. The steady state performance over the last 100 data points is calculated and the results are found to be as follows:

- the required control input energies are 29.2, 2.3 and 8.1 kWh for the heater, cooler and humidifier respectively; and
- the output squared errors are 78.0°C^2 and 111.7%rh^2 for the temperature and relative humidity respectively.

This result shows that the control performance has deteriorated as expected. Looking at the control inputs we can observe excessive switching which is highly undesirable and commonly encounted in systems subject to stochastic influences. There are several method for handling this problem; these range from inserting a weighting term into the fitness function to penalise excessive controller switching or simply inserting a smoothing filter.

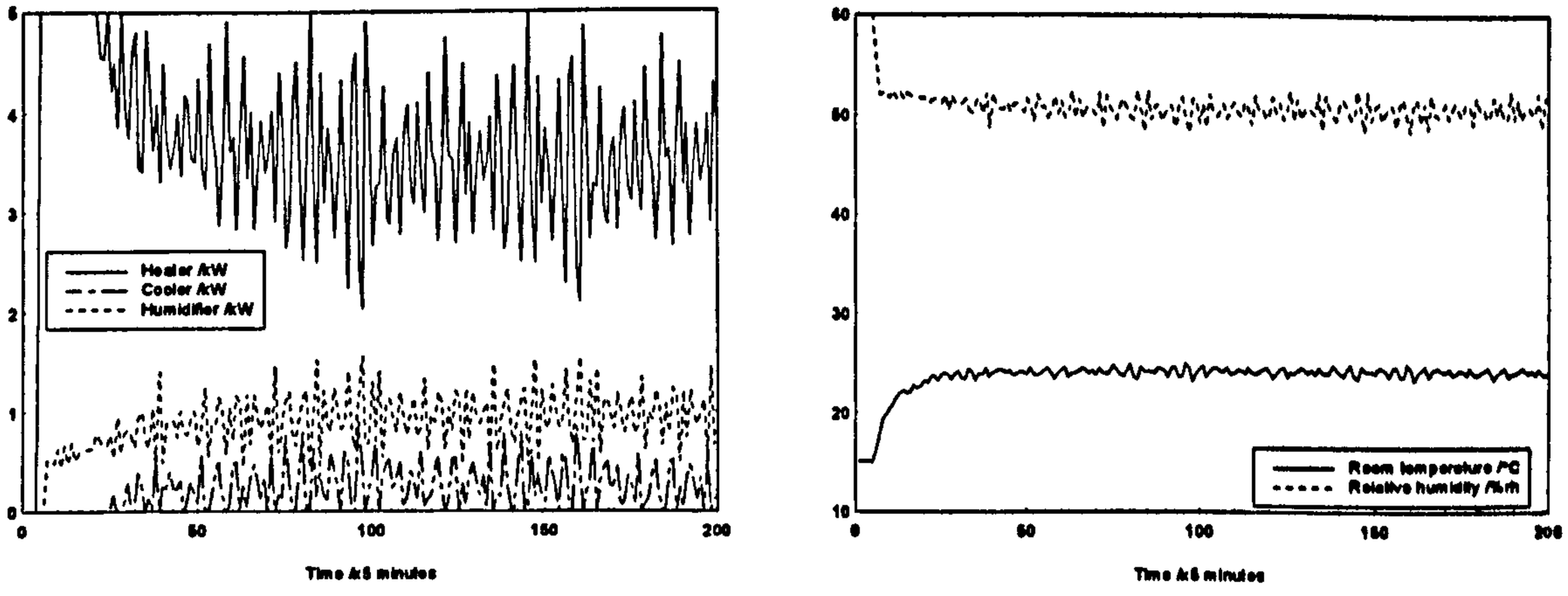

a) Control inputs

b) System outputs

Figure 7.9: Proportional GA controller with climatic and stochastic disturbances

We introduce two different low-pass filters for performing the smoothing, namely,

Filter I. $$u_f(t) = \{u(t) + u(t - \mathrm{T})\}/2$$

Filter II. $$u_f(t) = \{u(t) + 2u(t - \mathrm{T}) + u(t - 2\mathrm{T})\}/4$$

where u_f is the filtered input and u is the control input vector consisting of W, C and H which is calculated from equations (7.2), (7.3) and (7.4) respectively. Here Filter I assumes a simple averaging over two consecutive control values whereas Filter II does this over three inputs. Simulation trials were carried out for this controller by using the filtered input, u_f, and for the gains chosen for the setpoints $\{T_r, H_r\} = \{25°C, 50\%rh\}$ with the prescribed conditions; the results show that both filters reduce the excessive switching of the control inputs as well as the output regulations and this is shown in Figure 7.10. For the controller with Filter I, the steady state performance over the last 100 data points are found to be as follows:

- the required control input energies are 29.1, 2.2 and 8.0 kWh for the heater, cooler and humidifier respectively; and
- the output squared errors are $71.9°C^2$ and $73.2\%rh^2$ for the temperature and relative humidity respectively,

and for the controller with Filter II, the steady state performance over the last 100 data points are found to be as follows:

- the required control input energies are 30.3, 3.6 and 9.0 kWh for the heater, cooler and humidifier respectively; and
- the output squared errors are $126.5°C^2$ and $12.4\%rh^2$ for the temperature and relative humidity respectively.

When the steady state performances of these controllers are compared, we found that the proportional GA controller with Filter I is better since it consumed lower energy as well as improved regulation.

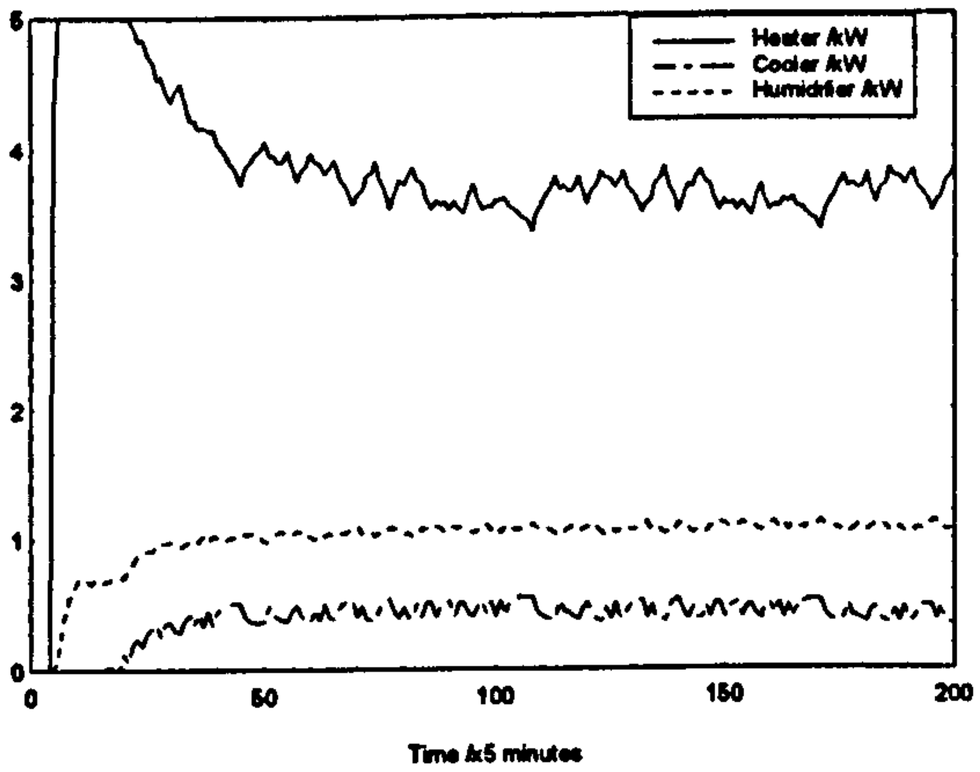

a) Control inputs

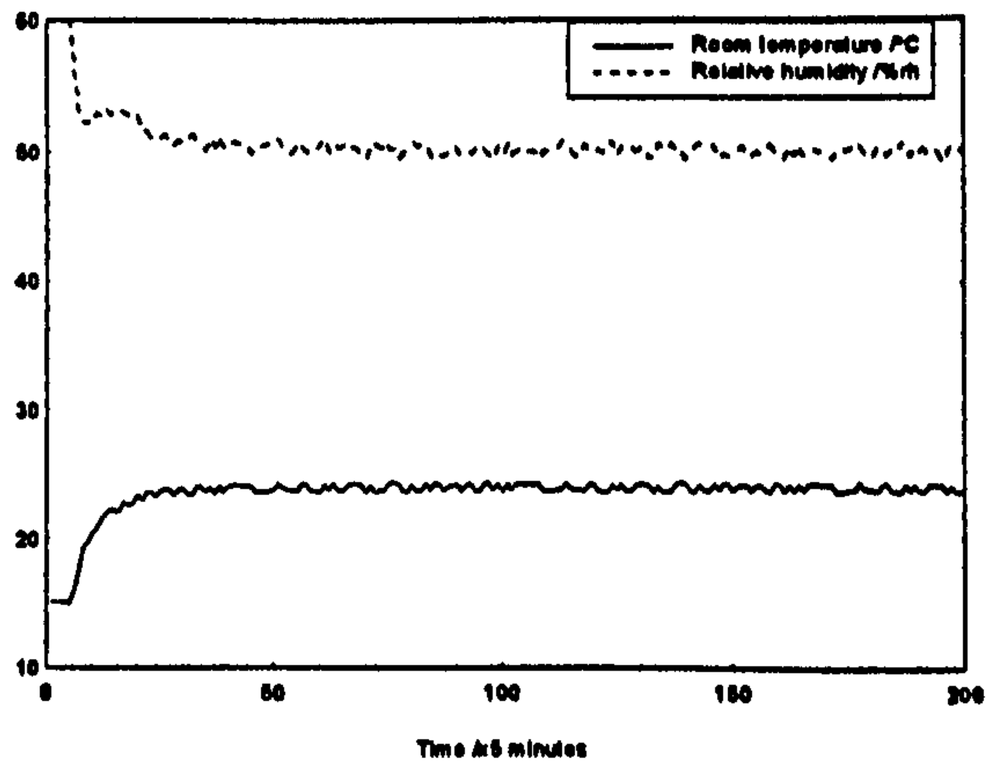

b) System outputs

Figure 7.10: Improving the proportional GA controller by Filter II

The results in Table 7.1 and Figure 7.6 show that the proportional GA tuned controller gives a good control performance only for the setpoint at which the GA was used to calculate the gains. The control performance deteriorates when the setpoints are changed. This demonstrates the main disadvantage in using the structure of proportional controller where the values are only accurate for the tuned setpoints and some modification needs to be made to remedy this shortcoming.

7.4. Improved FLC using GA technique

There are many methods of improving the basic GA procedure presented in Section 7.3, for example we could extend the work to PID controllers, consider a state-space GA solution or integrate GAs with neural networks for advanced intelligent BEMS control. This opens up a vast area of research in itself and could be worthy of a whole project; instead we consider integrating the fuzzy logic approach presented in Chapter 6 with the genetic algorithm method to access whether an improved solution can be realised. In

particular we will use the GA optimisation techniques to adjust the fuzzy membership functions so that the control performance of the FLC can be improved (see for example Genshe and Xinhai, 1993). In our case, we implement the GA method to adjust the tuning parameters of the FLC based on output errors as described in chapter 6. Recall that this controller has 5 fuzzy input membership functions for each of the 2 output errors and 3 fuzzy output membership functions for each of the 3 incremental control signals as shown in Figure 6.1 to make a total of 19 fuzzy membership functions. These functions need to be optimised so that the required FLC's performance is as good as it can be to reduce the output errors, consume minimal energy and have fast settling periods as compared to the ordinary FLC.

We now consider the example shown in Figure 6.5 where a good performance has been achieved but we assume that it could be further improved by using the GA method. Therefore, most of the scale factor settings in the fuzzy membership functions can be fixed as they are in order to reduce the complexity of designing the GA operators. For this reason we have chosen the 10 fuzzy input membership functions to be fixed at the values shown in Table 6.3, and the fuzzy output membership functions in Figure 6.2b) for each incremental control signal are defined by

i) $z_l = n_m$, $n_r = z_m = p_l = 0$ and $x_u = p_m$;

ii) $n_m = 0.7x_l$ and $p_m = 0.7x_u$; and

iii) the incremental control limits are $0.1 \le x_l \le 0.5$ and $0.1 \le x_u \le 0.5$.

The objective here is to obtain the best set of x_l and x_u for the three incremental control signals, i.e. dW, dC and dH so that the controller's performance is optimised. This can be done by concatenating them into a parameter set $\{x_{lW}, x_{uW}, x_{lC}, x_{uC}, x_{lH}, x_{uH}\}$ where x_{lW}, x_{lC} and x_{lH} are the lower limits, and x_{uW}, x_{uC} and x_{uH} are the upper limits of the

heater, cooler and humidifier increments respectively. This situation with six unknown parameters is identical to that described in section 7.3. Therefore, the parameter set $\{K_{P1}, K_{P2}, K_{P3}, K_{P4}, K_{P5}, K_{P6}\}$ can be replaced by $\{x_{lW}, x_{uW}, x_{lC}, x_{uC}, x_{lH}, x_{uH}\}$ and by applying all the relevent prescribed parameters and conditions for the GA operators, we can simulate the GA to search the best combination of fuzzy output membership functions so that the control performance is optimised. We can also use the fitness function as defined in equation (7.6) with the constant α chosen to equal 0.3 for convenience. The initial population $P(0)$ for the above fuzzy output constraints is given by $P(0) = 0.1 + 0.4$*rand(6,M) so that the magnitudes of x_{lW}, x_{uW}, x_{lC}, x_{uC}, x_{lH} and x_{uH} will be limited to the range of 0.1kW to 0.5kW for all generations.

At each generation i, the fitness function, $f_j(i)$, for chromosomes $j = 1, ..., M$, is calculated using equations (7.5) and (7.6) by decoding them into their physical values, i.e., the parameter set $\{x_{lW}, x_{uW}, x_{lC}, x_{uC}, x_{lH}, x_{uH}\}$ and using the GA reproduction operator to perform a simulation over 200 iterations for each chromosome. As previously mentioned, the fittest chromosome in each generation is the one which has the smallest fitness function and this chromosome is selected to represent the best combination of fuzzy output membership functions for the FLC.

7.4.1. Simulation results

In the simulation trials, the GA is simulated for 50 generations with 30 populations in each generation and the setpoints T_r and H_r were set to 25°C and 50%rh respectively. It was found that $f_s(i)$ converges to 3.2 after the fourteenth generation with the resulting best chromosome $\{x_{lW}, x_{rW}, x_{lC}, x_{rC}, x_{lH}, x_{rH}\}$ is {0.45, 0.31, 0.31, 0.31, 0.13, 0.15}.

By using the definition of the fuzzy outputs for this FLC design we can calculate n_m and p_m for each incremental control input and the results are shown diagrammatically in Figure 7.11. Analysis of this diagram as well as comparison to the ordinary FLC's output membership functions as presented Table 6.4 is difficult to perform here since many tuning parameters and rules are involved, and the GA only presents one of many minimal solutions. If the conditions are maintained as before and the GA simulation trial is carried out for the second attempt, we could obtain a new set $\{x_{lW}, x_{rW}, x_{lC}, x_{rC}, x_{lH}, x_{rH}\}$ of minimal solution which would also give a good control performance. Therefore, we could have more than one 'best" combination of the FLC tuning parameters to give similar control performances by using the GA method.

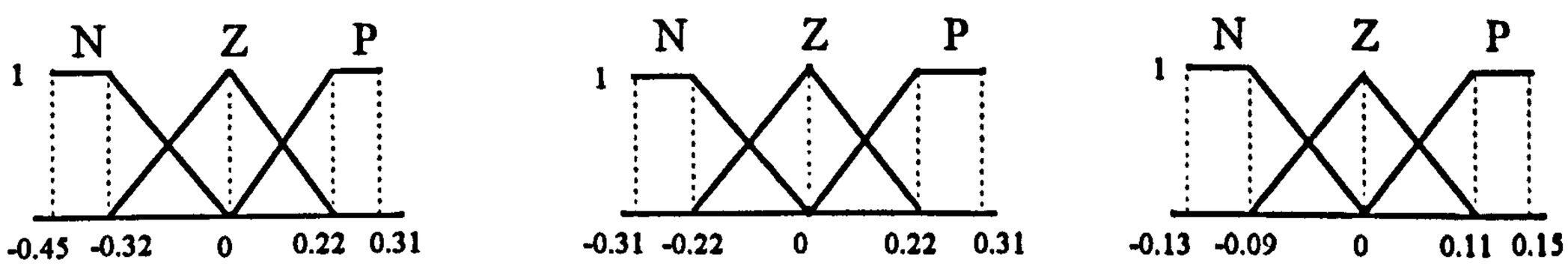

a) Heater (kW) b) Cooler (kW) c) Humidifier (kW)

Figure 7.11: Incremental fuzzy output membership functions via GA

The GA solution was utilised in the FLC and the simulated results are shown in Figure 7.12; the control performance calculated over the last 100 data points after steady state had been reached gives the following results:

- the required control input energies are 22.3, 0 and 5.3 kWh for the heater, cooler and humidifier respectively; and
- the output squared errors are $0.1°C^2$ and $2.1\%rh^2$ for the temperature and relative humidity respectively.

These results are slightly better than those obtained from the ordinary FLC discussed in Chapter 6. Clearly, the GA optimisation could be introduced to several stages within the fuzzification and defuzzification processes and potentially further improvements could be made.

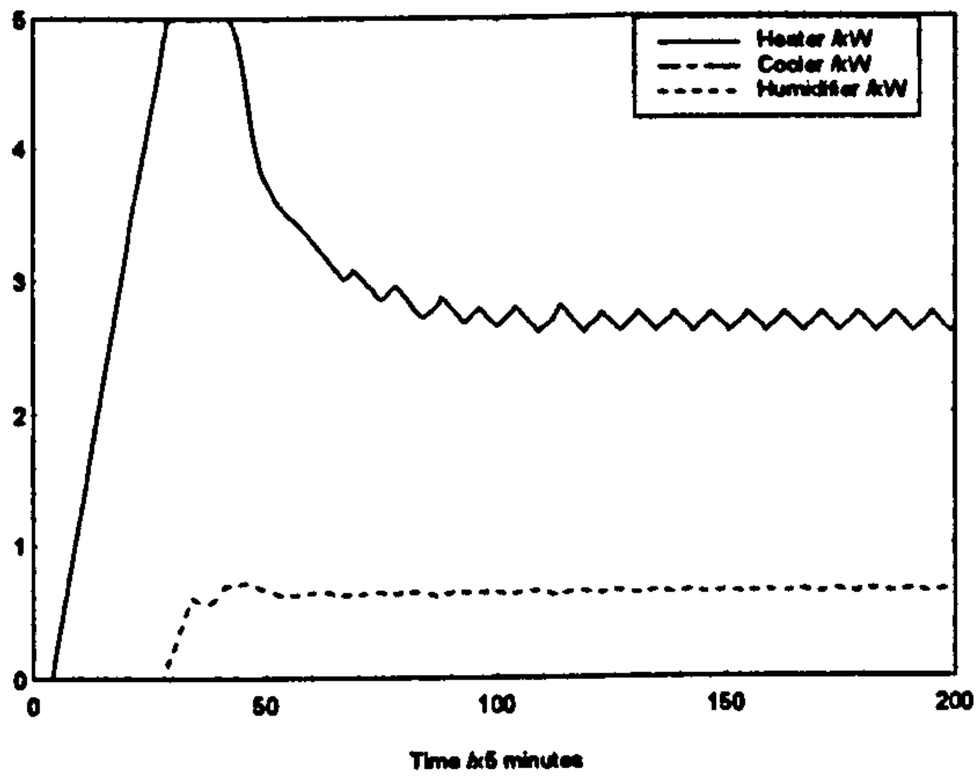

a) Control inputs

b) System outputs

Figure 7.12: FLC + GA based controller performance

When the setpoints T_r and H_r are changed to 20°C and 40%rh respectively, the GA produces the best parameter set equal to {0.10, 0.50, 0.45, 0.45, 0.10, 0.45} after twenty three generations; this is shown diagrammatically in Figure 7.13. For this situation, the control performance over the last 100 data points after settling is as follows:

- the required control input energies are 19.9, 3.6 and 0 kWh for the heater, cooler and humidifier respectively; and
- the output squared errors are 24.9°C^2 and 62.2%rh^2 for the temperature and relative humidity respectively.

The results have clearly degraded as before and some modification to the procedure needs to be made so that setpoint changes can be accommodated. A better result could

be achieved if the encoding resolution is increased and this is demonstrated in section 7.5.

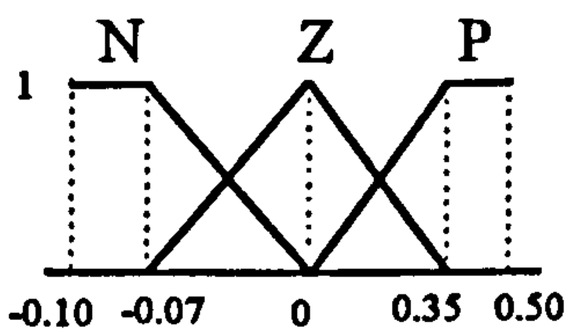

a) Heater (kW)

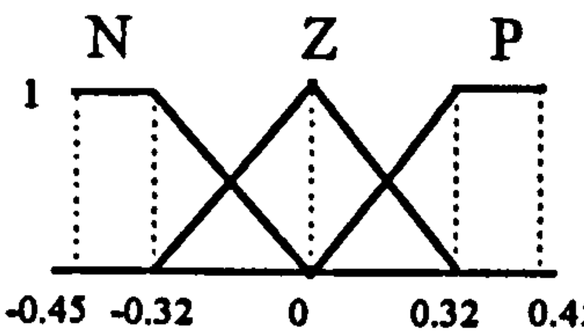

b) Cooler (kW)

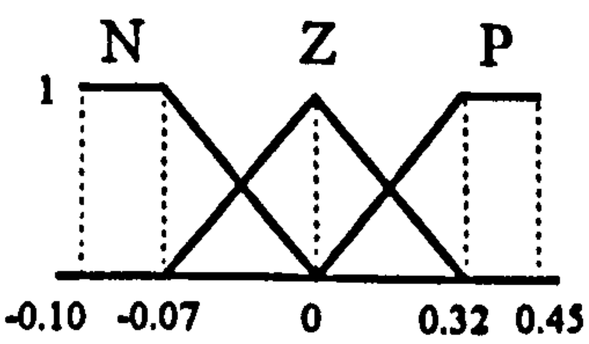

c) Humidifier (kW)

Figure 7.13: Incremental fuzzy output membership functions via GA

($T_r = 20°C$; $H_r = 40\%rh$)

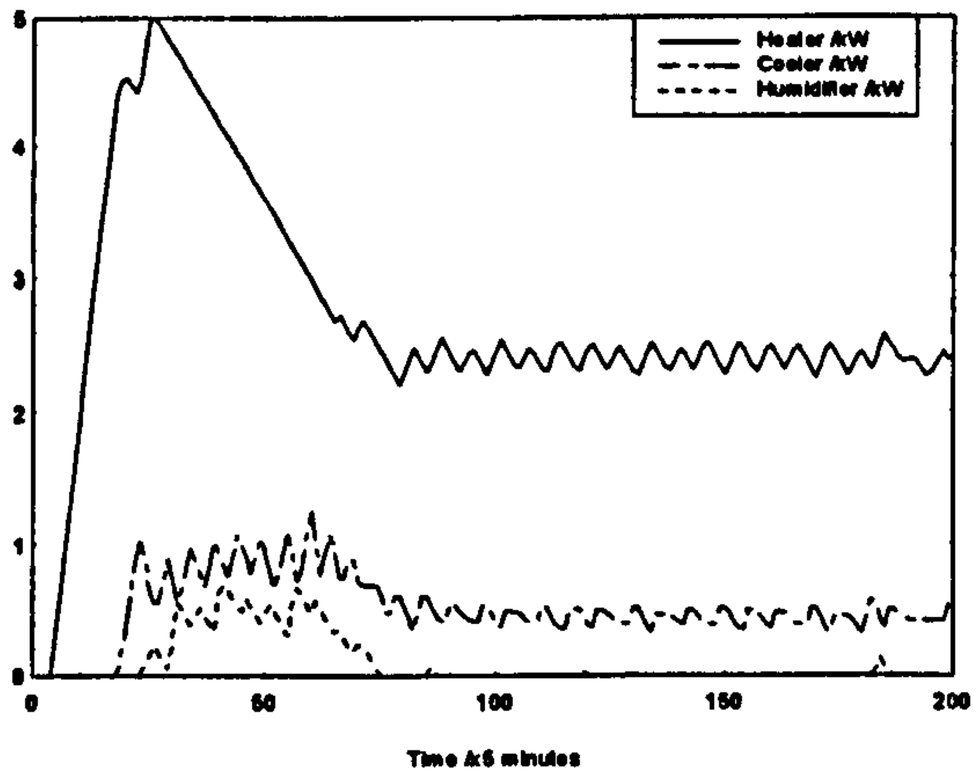

a) Control inputs

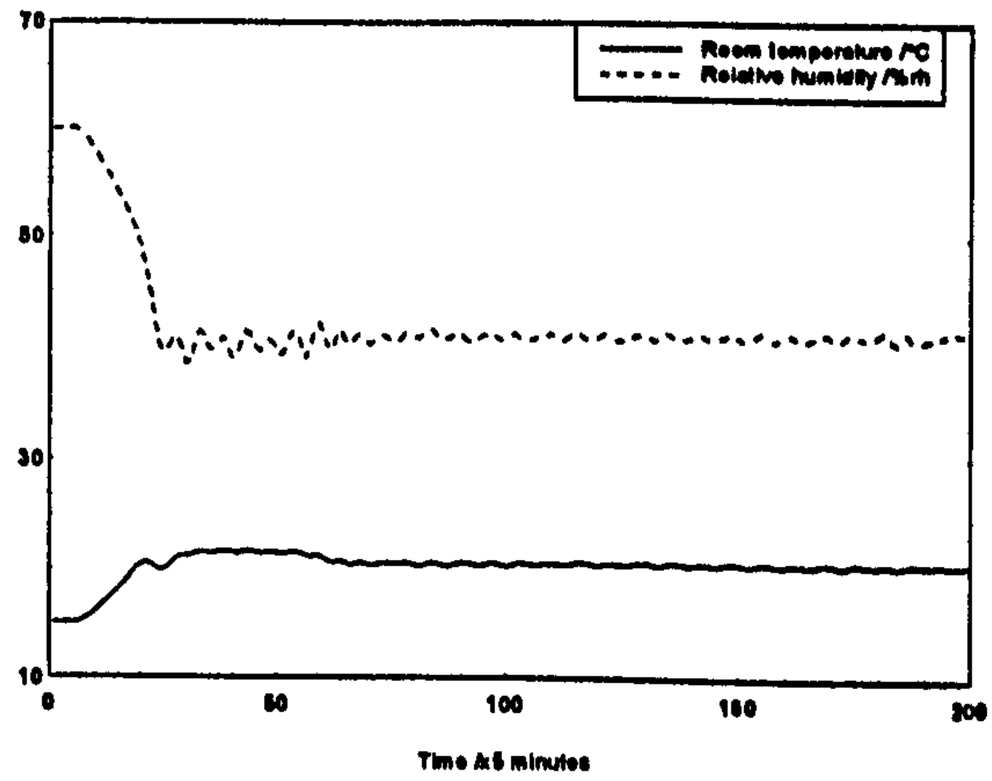

b) System outputs

Figure 7.14: FLC + GA based controller performance for $T_r = 20°C$; $H_r = 40\%rh$

We can see that the major advantage of using this approach is that the search of the best fuzzy membership functions is carried out automatically via the genetic operator from one generation to another, rather than using manually repeated simulation trials which is normally implemented by a FLC design.

7.5. GA for adaptive control

In this application, we will use the advantage of one-step ahead predictions from the mathematical model (2.1) and (2.2) to forecast the air temperature and relative humidity in the test room if certain inputs are applied. To implement this using GAs, we present M solutions for the control inputs W, C, and H at time t (each one represents an individual chromosome p_j , $j = 1, 2, ..., M$ which belongs to the population $P(t)$). The GA operators are then applied to the population $P(t)$ to generate new population $P(t+T)$ at time $t+T$. We summarise the GA algorithm as follows:

Step 1. Select a random initial population $P(t)$ of solutions satisfying the input constraints, i.e. W, C and H have limits of 5.0, 2.7 and 2.6 kilowatts respectively. Set the resolution, R, the crossover, the mutation rates, the sample time T, and set $t = 0$.

Step 2. Encoding: Encode the control inputs $\{W, C, H\}$ into a chromosome.

Step 3. Calculate the controls $\{W, C, H\}$ for individual chromosomes by reversing the encoding process.

Step 4. Reproduction: Calculate the fitness function for individual chromosomes and generate the population $P(t+T)$ according to the reproduction procedure. The controls $\{W, C, H\}$ having the fittest chromosome from population $P(t+T)$ is selected and applied to the HVAC plant at time t.

Step 5. Go to Step 6 or Step 7 randomly.

Step 6. Crossover: Mate the members of $P(t)$ at random, and carry out the crossover operation randomly for each pair of chromosomes to generate 2M chromosomes for population $P(t+T)$. Go to step 8.

Step 7. Mutation: Select at random a chromosome from the population $P(t)$ and carry out the mutation operation for that chromosome.

Step 8. Set $t = t + \mathrm{T}$ and Goto Step 3.

The initial population is generated by using a random method; for our application we require 3 control inputs of different ranges and using the MATLAB language, the initial population can be generated using $P(0)$ = [5*rand(1, M); 2.7*rand(1, M); 2.6*rand(1, M). Thus, P is a 3xM matrix and p_j is the jth. column vector of P, and we represent the jth. parameter set by $\{W^j, C^j, H^j\}$, $j = 1, 2, ..., \mathrm{M}$. If the encoding resolution is 15, then we have a 4 bit string for each input and then these strings are concatenated to produce a chromosome of length 12 bits. If the required encoding resolution is 255, i.e. an 8 bit word length then the chromosome will have a length of 24 bits.

As before, the reproduction process selects two solutions as potential parents which compete for survival; this is repeated until we obtain M chromosomes in the population $P(t+\mathrm{T})$. The best chromosome amongst them is selected and decoded into $\{W, C, H\}$ before being applied to the HVAC plant at time t.

The fitness function is again formulated so that both the room temperature and relative humidity track the setpoints as the GA is advancing from a generation $P(t)$ to the next generation $P(t+\mathrm{T})$. As before we propose the fitness function, f_j, for the chromosome p_j by

$$f_j(t) = \left| e_T^j(t+\mathrm{T}) \right| + \alpha \left| e_H^j(t+\mathrm{T}) \right|, \quad t = 0, \mathrm{T}, 2\mathrm{T}, 3\mathrm{T}, \ldots$$

$$j = 1, 2, 3, \ldots, 2\mathrm{M} \text{ for crossover}$$

$$j = 1, 2, 3, \ldots, \mathrm{M}+1 \text{ for mutation} \qquad (7.7)$$

where e_T^j and e_H^j are the predicted output errors at time t+T and can be obtained from equations (2.1), (2.2), (3.2) and (3.5), and α is a weighting factor as before. The controls $\{W^j(t), C^j(t), H^j(t)\}$ for chromosome j can be used to calculate their fitness functions via equation (7.7); the chromosome having the lowest fitness function f_j is selected for applying to the HVAC plant at time t. Note each time step is now a generation within this GA setting.

7.5.1. Convergence

The GA is assumed to have converged when the output errors e_T and e_H become zero and steady state conditions have been reached; this can be written as:

$$\lim_{t\to\infty} e(t) = 0 \qquad (7.8)$$

where $e = \begin{bmatrix} e_T \\ e_H \end{bmatrix}$. Ideally, the controlling inputs W, C and H are constant at steady state conditions, so that the system outputs remain at their setpoints and the best chromosomes in any generation within this period are identical to each other, i.e. the GA operators will not produce any better solutions; this situation is identical to that shown in Figure 7.4 where the best fitness function, $f_s(t)$, at generation t remains constant at this minimal condition.

When the climatic and stochastic disturbances are present in the system, the GA operator will produce a better chromosome even at the steady state condition; here the method is reacting to noise to reduce the error.

7.5.2. Simulation results

Let us consider the system under the setpoints T_r and H_r and calculate the performances for the last 100 generations (sampling periods) of the simulation trials. We assume that the initial conditions for the room temperature, $T_c(0)$, and relative humidity, $H_c(0)$, are known and all the three controlling inputs to the plant are zero.

A number of simulation trials were carried out to get the best value of α in the fitness function and it was found that an appropriate value of α is between 0.13 to 0.14. Values beyond this range lead to the system going out of control where the output errors are very large at steady state conditions. This value is also tested for the system with other pairs of $\{T_r, H_r\}$, such as {20°C, 40%rh}, {15°C, 60%rh} and {15°C, 30%rh}, as well as for different initial conditions such as $T_c(0) = 35$°C and $H_c(0) = 100$%rh.

The simulation results showed that the control performance for all the trials were acceptable and the system outputs converged to the desired setpoints. We can conclude that this α value can be used for any set of $\{T_r, H_r, T_c(0), H_c(0)\}$ within the ranges of 5°C to 35°C for room temperature and 10%rh to 100%rh for relative humidity. An example of the system performance is shown in Figure 7.15 where the corresponding values for $\{T_r, H_r, T_c(0), H_c(0)\}$ are{15°C, 30%rh, 35°C, 100%rh}. From this figure, we can see that although the system outputs are quite smooth at steady state conditions, all three control inputs have large fluctuations and excessive controller switching is again seen. This can be tackled as discussed in Section 7.6.

All the above simulation trials were carried out by setting the resolution R to 15, the crossover rate $cr = 7/12$ and the population size M = 20. Furthermore, we assume that the climatic disturbances such as T_i, T_o, H_o and S, are constant at 20°C, 10°C, 100%rh and

0.1 Wm^{-2} respectively, and the unmodelled stochastic influences, V_1 and V_2 were absent.

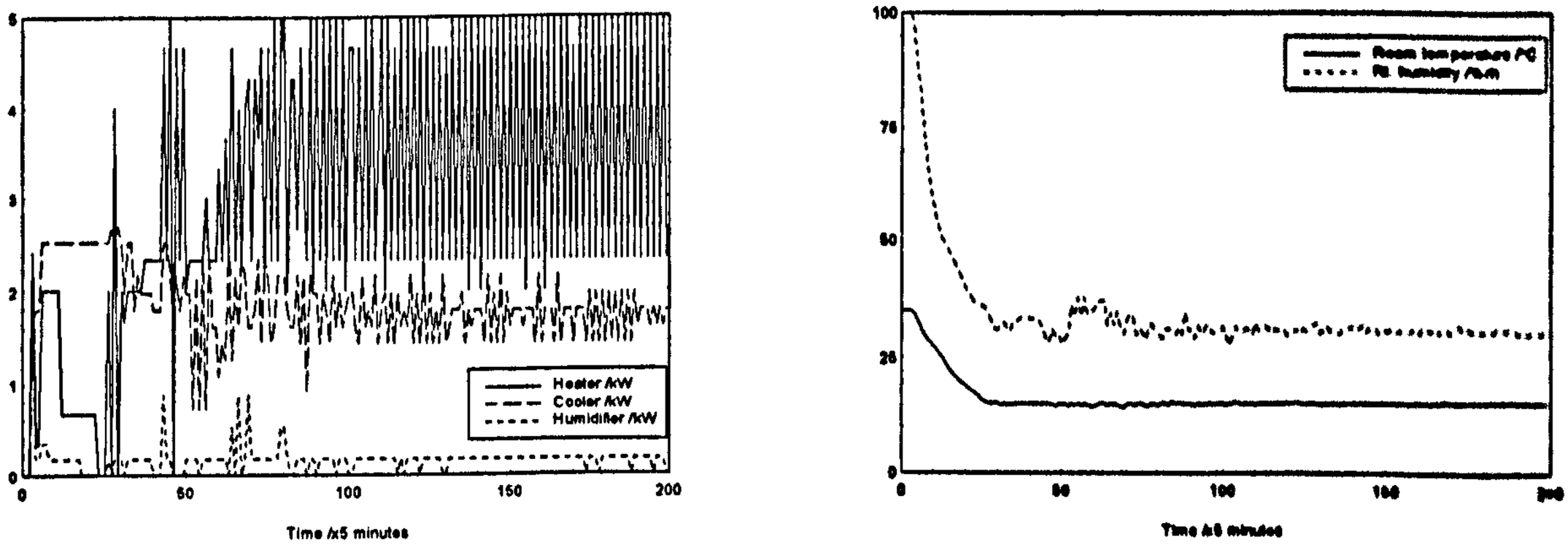

a) Control inputs b) System outputs

Figure 7.15: Adaptive GA controller performance

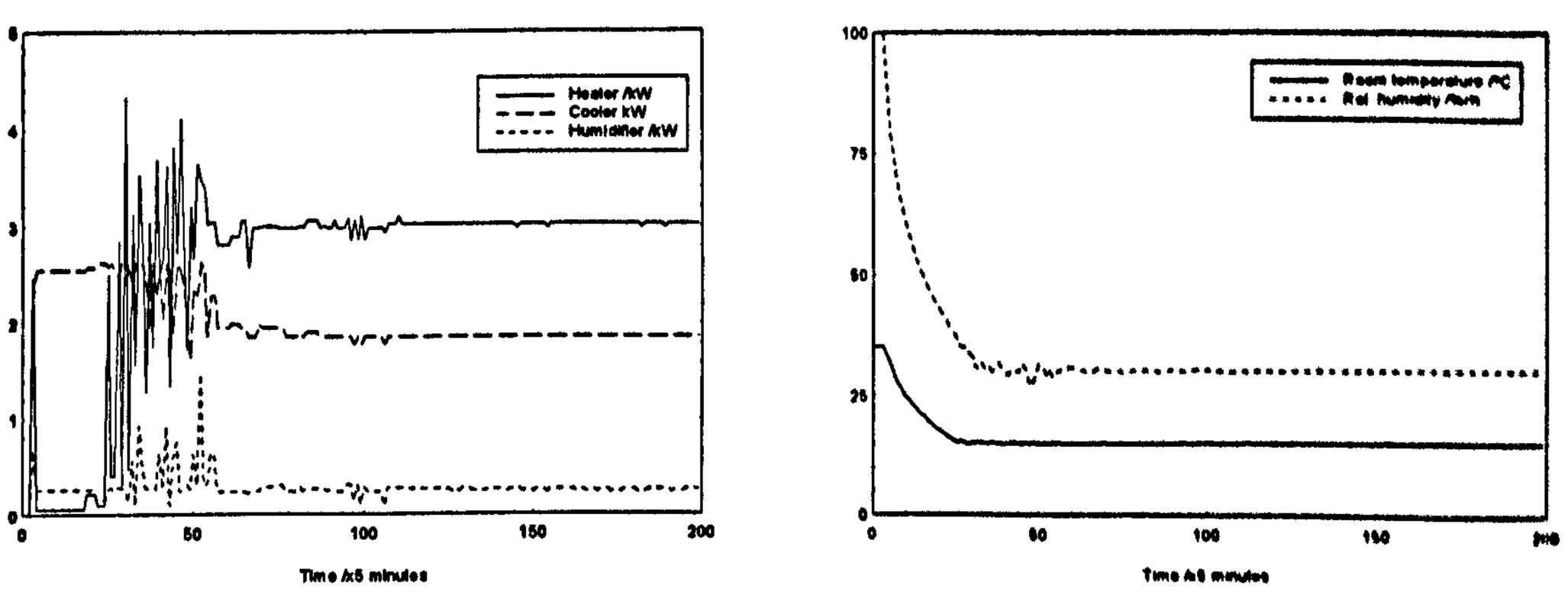

a) Control inputs b) System outputs

Figure 7.16: Adaptive GA controller with enhanced resolution

An improvement to the GA design can be made by increasing the resolution, R. By selecting R = 255 for each control input, and applying the above procedure and conditions, a simulation trial was carried out and the result is shown in Figure 7.16. We

can see that all the three control input variations are significantly reduced and the system outputs at steady state conditions are improved; this result shown is for $\{T_r, H_r, T_e(0), H_e(0)\} = \{15°C, 30\%rh, 35°C, 100\%rh\}$, and $cr = {}^{15}\!/_{24}$. For this case, the control performance over the last 100 data points after settling is as follows:

- the required control input energies are 25.2, 18.3 and 1.8 kWh for the heater, cooler and humidifier respectively; and
- the output squared errors are $0.1°C^2$ and $0.9\%rh^2$ for the temperature and relative humidity respectively.

The results show that an excellent output regulation has been achieved by this controller but it wastes a lot of energy from the heater and cooler in order to maintain the setpoints.

When the same climatic disturbances as in section 4.2.1 are present in the system, the performance is as shown in Figure 7.17 the control inputs are switching more but the system output responses appear unchanged.

In a real system, the HVAC plant will have climatic disturbances, and unmodelled stochastic influences such as people in the room and the opening and closing of doors and windows. For convenience, these influences are included here in the form of pseudo random binary sequences (PRBS) of 6 shift registers and values ± 0.1. For this situation, a simulation trial was carried out and the results are shown in Figure 7.18 where the control performance over the last 100 data points after settling is as follows:

- the required control input energies are 34.0, 17.4 and 3.4 kWh for the heater, cooler and humidifier respectively; and
- the output squared errors are $0.3°C^2$ and $1.9\%rh^2$ for the temperature and relative humidity respectively.

We can see that both the heating and humidifying energies are increased but the cooler remains roughly unchanged, and the output errors remain very small. Therefore, the heater and humidifier are fighting between themselves to reduce the output errors due to the disturbances. Although the GA operators can produce the best control inputs {*W*, *C*, *H*} at each sampling period, as seen from the system output responses (Figure 7.18 b)), the control inputs (Figure 7.18 a)) have excessive switching and some filtering or weight to this in the fitness function needs to be given within the design method.

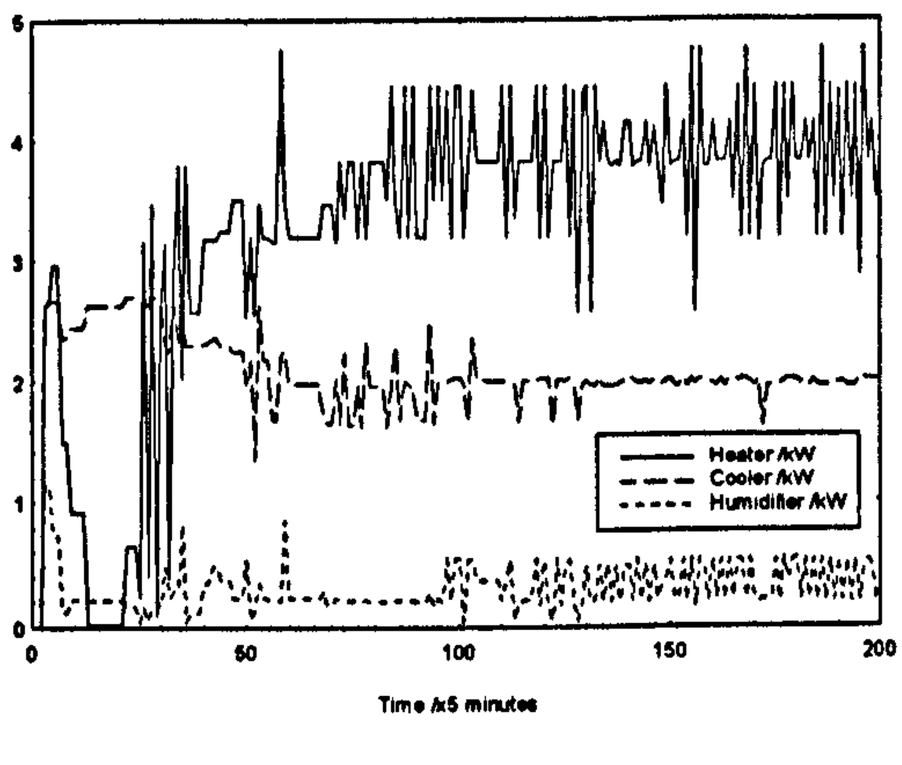

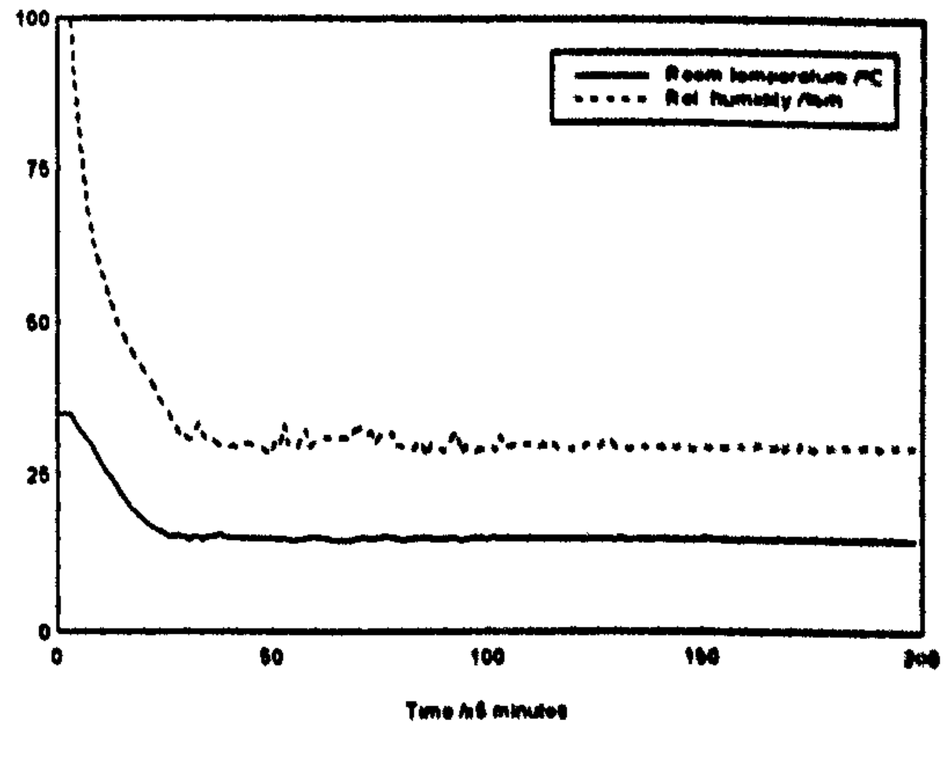

a) Control inputs b) System outputs

Figure 7.17: Adaptive GA controller with climatic disturbances

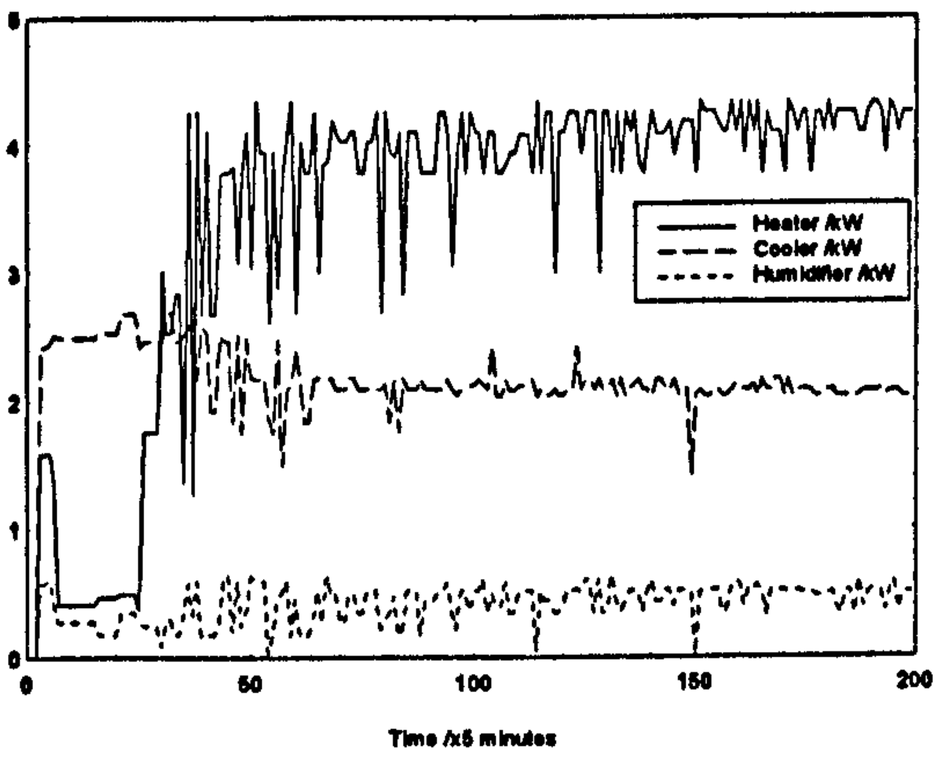

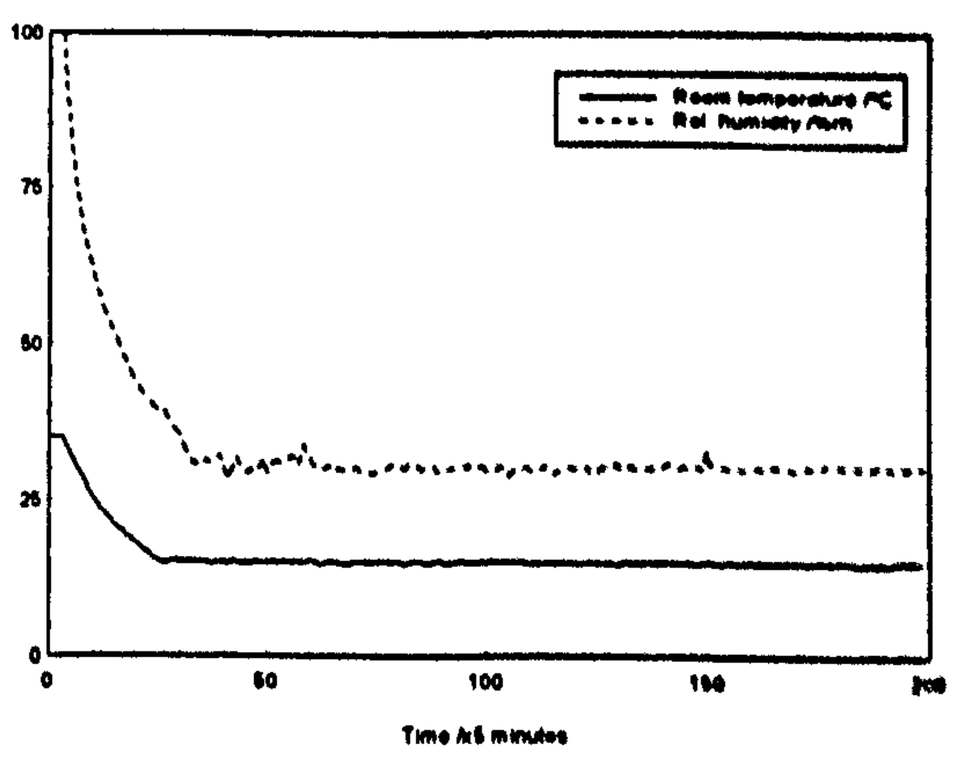

a) Control inputs b) System outputs

Figure 7.18: Adaptive GA controller with climatic and 10% stochastic disturbances

Figure 7.19 shows another good regulation result of this type of adaptive controller where the setpoints have changed from {25°C, 50%rh} to {20°C, 40%rh} after the two hundreth generation. For this case the initial conditions for $T_c(0)$ and $H_c(0)$ were set at 15°C and 60%rh respectively, and the climatic and 25% stochastic disturbances are assumed to be present. We can see that the system outputs follow the setpoints quite quickly but the control switching remains a problem. This is due to the fact that the control strategy is always searching for the best solution to minimise the output errors and no emphasis to control switching is assumed. This needs to be remedied in any practical solution based on GAs.

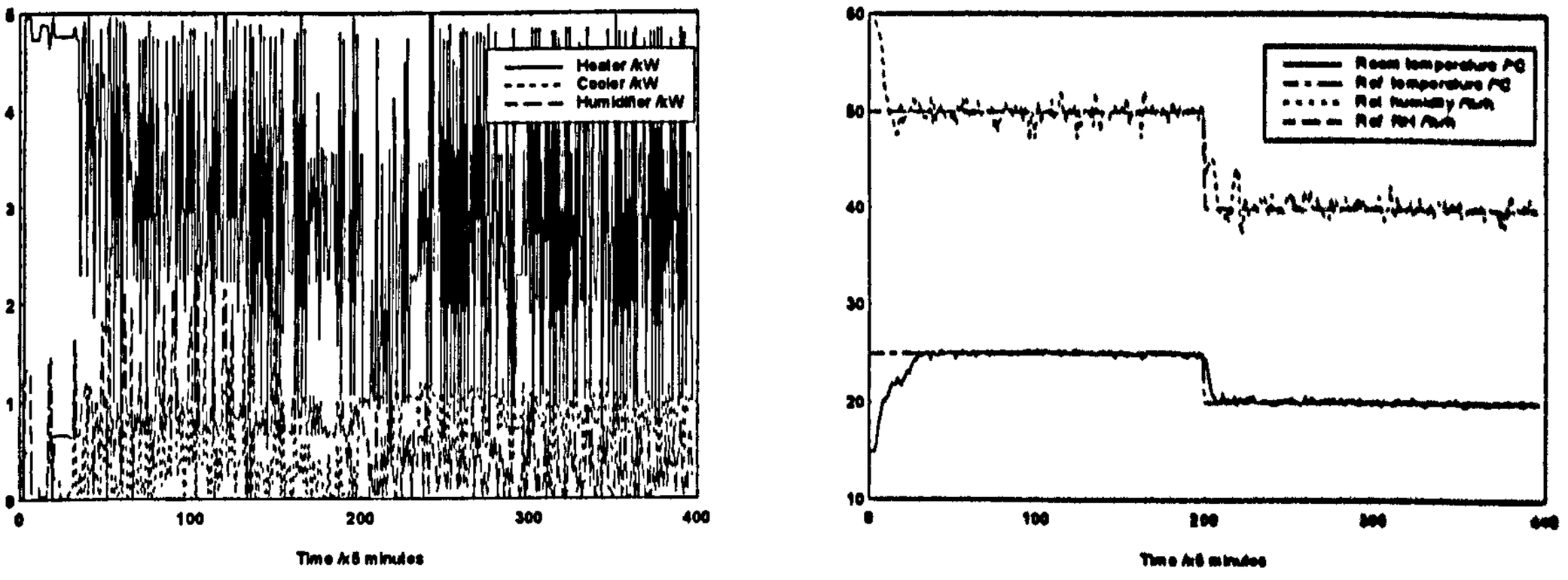

a) Control inputs

b) System outputs

Figure 7.19: Adaptive GA controller with setpoint change

The control performance at steady state conditions for the setpoints $\{T_r, H_r\}$ = {25°C, 50%rh} over 100 data points after settling is as follows:

- the required control input energies are 25.4, 2.9 and 7.9 kWh for the heater, cooler and humidifier respectively; and

- the output squared errors are 2.7°C^2 and 71.9%rh^2 for the temperature and relative humidity respectively.

We can see that this performance is similar to that obtained from the control strategies presented earlier in this thesis; the multi PI-loop controllers (Chapter 3), Constrained inputs MIMO adaptive control (Chapter 5) and fuzzy logic controller (Chapter 6); hence there is potential for the GA approach.

7.6. Smoothing of GA solutions

As presented in section 7.5, GAs can be used to regulate the system outputs at the desired setpoints to within acceptable limits at steady state conditions, but the variation of the control inputs with respect to time is excessive. This problem is due to the GA working on the basis of randomly generated solutions where the designed fitness function does not relate between one generation to the next. This causes large variations in the control inputs which are not recommended in practice because this will reduce the life span of the control actuators. To overcome this problem, we propose the introduction of a smoothing routine within the GA presented in Section 7.5 (Davis, 1991); one way of achieving this smoothing is to use a digital filter. The smoothing is introduced to the control strategy whenever appropriate to suppress the switching of control signal when it exceeds beyond the permissible limits. The low pass filter is designed by defining two different values of the control input, namely Δu and $\Delta u'$ where

$$\Delta u = |u_{ga}(t) - u(t\text{-T})| \tag{7.9}$$

$$\Delta u' = |u(t\text{-T}) - u(t\text{-2T})| \tag{7.10}$$

where $u_{ga} = W_{ga}, C_{ga}, H_{ga}$ is the control input vector which is obtained by the GA and u is the required control input vector consisting of W, C and H. The requirement of the system is that if Δu is less than $\Delta u'$ by a certain amount then $u_{ga}(t)$ is applied at time t, otherwise the filtered control input, u_f, will be used. In a mathematical form, this can be written as

$$u(t) = u_{ga}(t), \quad \Delta u < \beta \, \Delta u'$$

$$= u_f(t), \text{ otherwise.} \tag{7.11}$$

where $0 < \beta < 1$ defines the permitted level of input switching (this could be different value for each control input). Let β_1, β_2 and β_3 be the levels for the heater, cooler and humidifier respectively, then we have

$$W(t) = W_{ga}(t), \quad \Delta W < \beta_1 \Delta W'$$

$$= W_f(t), \quad \text{otherwise.} \tag{7.12}$$

$$C(t) = C_{ga}(t), \quad \Delta C < \beta_2 \Delta C'$$

$$= C_f(t), \quad \text{otherwise.} \tag{7.13}$$

$$H(t) = H_{ga}(t), \quad \Delta H < \beta_3 \Delta H'$$

$$= H_f(t), \quad \text{otherwise.} \tag{7.14}$$

and the system outputs $T_c(t+\mathrm{T})$ and $H_c(t+\mathrm{T})$ are re-calculated by applying the mathematical model equations (2.1) and (2.2). These β-values will also indirectly increase the output errors since the GA control inputs, W_{ga}, C_{ga} and H_{ga} are supposedly the best solutions to regulate the system outputs optimally.

Now, we define the filtering control inputs, W_f, C_f and H_f. It is important to decide the level of suppression which is needed so that good overall control performance is

maintained. For example, if the suppression is very large then the system output regulation becomes poor and the system may even go out of control. Here, we use Filters I and II as described in Section 7.3.7 with slightly different notations as follows:

Filter I. $$u_f(t) = \{u_{ga}(t) + u(t - \mathrm{T})\}/2$$

Filter II. $$u_f(t) = \{u_{ga}(t) + 2u(t - \mathrm{T}) + u(t - 2\mathrm{T})\}/4$$

The control performances for the adaptive controllers using Filters I and II with identical β-values are shown in Figures 7.20 and 7.21 respectively where their output regulations as well as the magnitudes of the control input fluctuations were found to be similar; therefore, the comparison of performances between the two adaptive GA controllers are difficult to analyse here due to the GA method operating on the basis of randomly minimal solutions. To present them quantitatively, we calculate the performances for Figure 7.20 at steady state conditions where the setpoints $\{T_r, H_r\}$ equal {20°C, 40%rh}; the performances over the last 100 data points were found to be as follows:

- the required control input energies are 29.4, 10.9 and 6.9 kWh for the heater, cooler and humidifier respectively; and
- the output squared errors are $0.4°C^2$ and $41.9\%rh^2$ for the temperature and relative humidity respectively.

We can see that the switching of the control inputs have been significantly reduced but the output errors at steady state error are slightly degraded as compared to the original GA controller. Nevertheless, these errors are still acceptable and overall we conclude that the solutions have been enhanced due to the filtering.

When the level of permitted input switchings, namely, β_1, β_2 and β_3 were increased to 0.6, 0.7 and 0.8 respectively and simulation trials were carried out for the GA adaptive controllers with Filters I and II, we found that the output regulations are similar but the input switchings are slightly worse as compared to Figures 7.20 and 7.21; the results are shown in Figures 7.22 and 7.23 respectively. These effects are due to increased chances of choosing the GA control input, u_{ga}, (which is randomly produced by the GA operators) rather than the filtered input, u_f at time t. As before, the control performances for Figure 7.23 were calculated for over 100 data points after settling; they were found to be as follows:

- the required control input energies are 25.4, 5.9 and 1.9 kWh for the heater, cooler and humidifier respectively; and
- the output squared errors are 0.1°C^2 and 33.1%rh^2 for the temperature and relative humidity respectively.

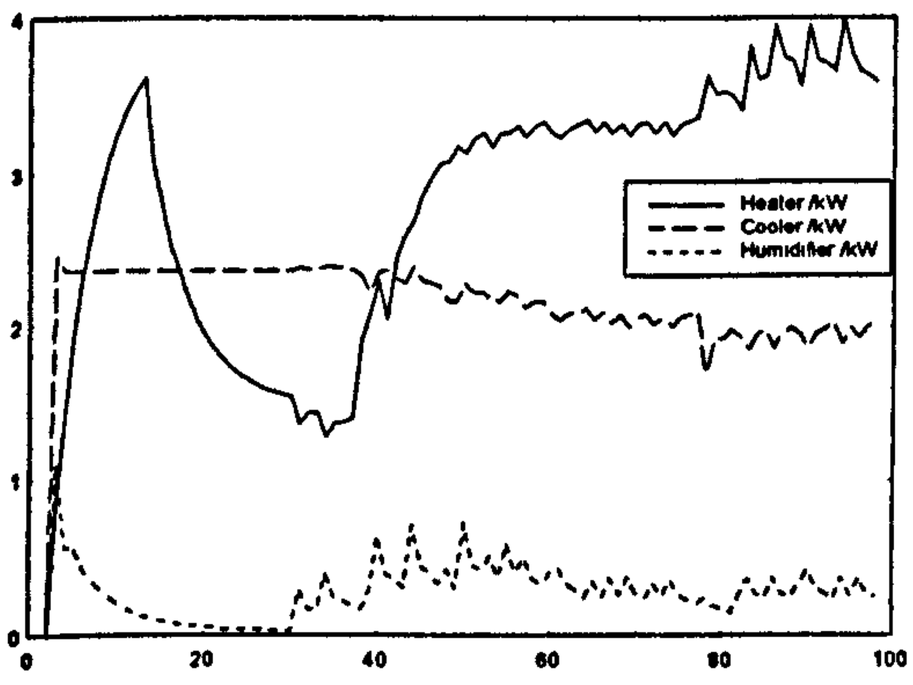

a) Control inputs

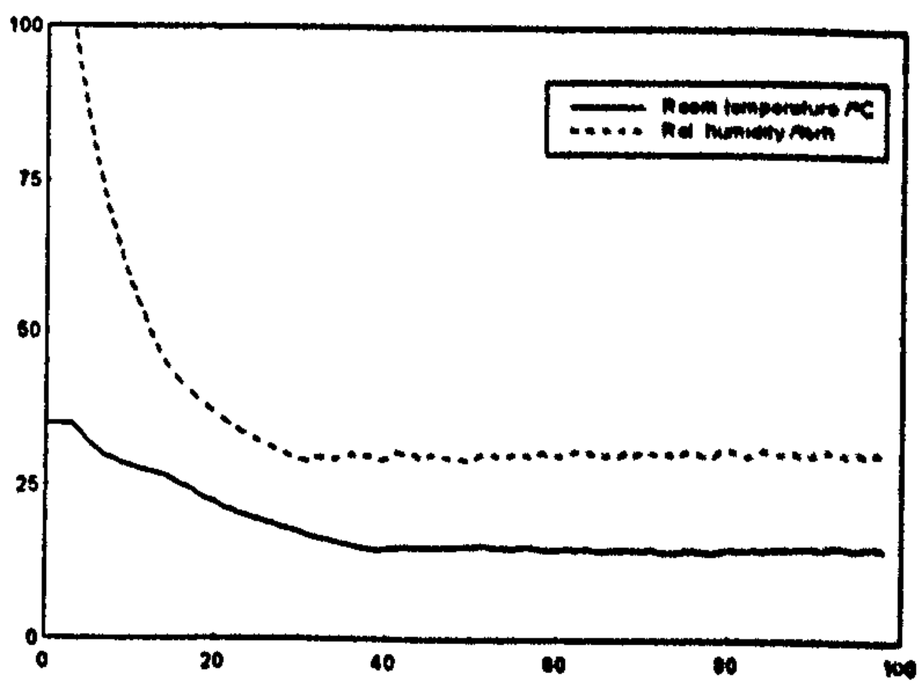

b) System outputs

Figure 7.20: GA controller with noise (Filter I): $\beta_1 = 0.5$, $\beta_2 = 0.5$, $\beta_3 = 0.7$

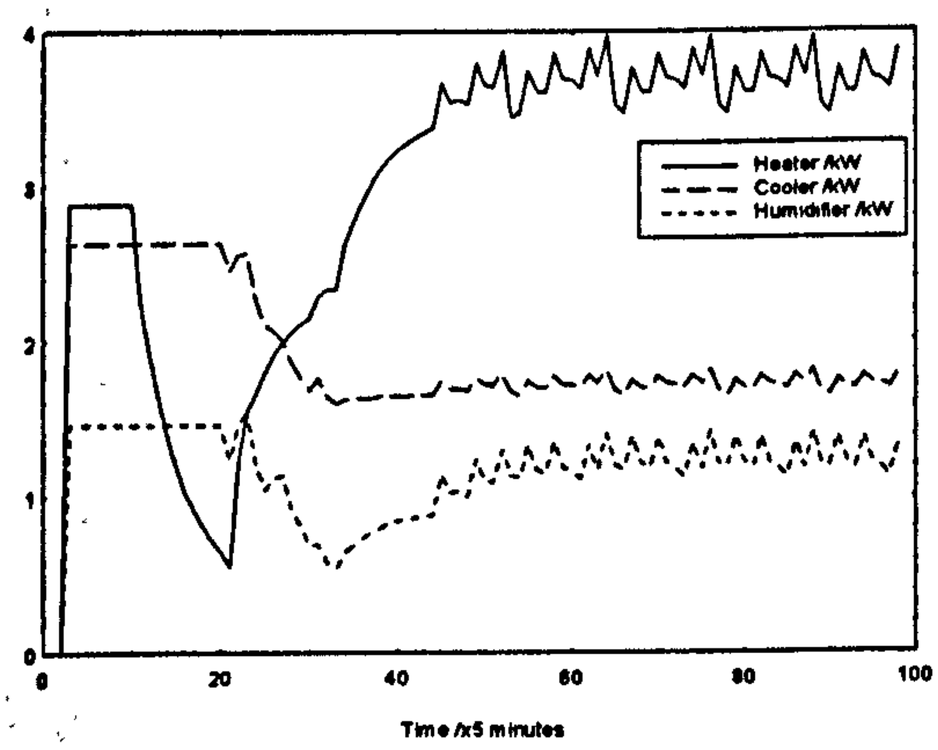

a) Control inputs

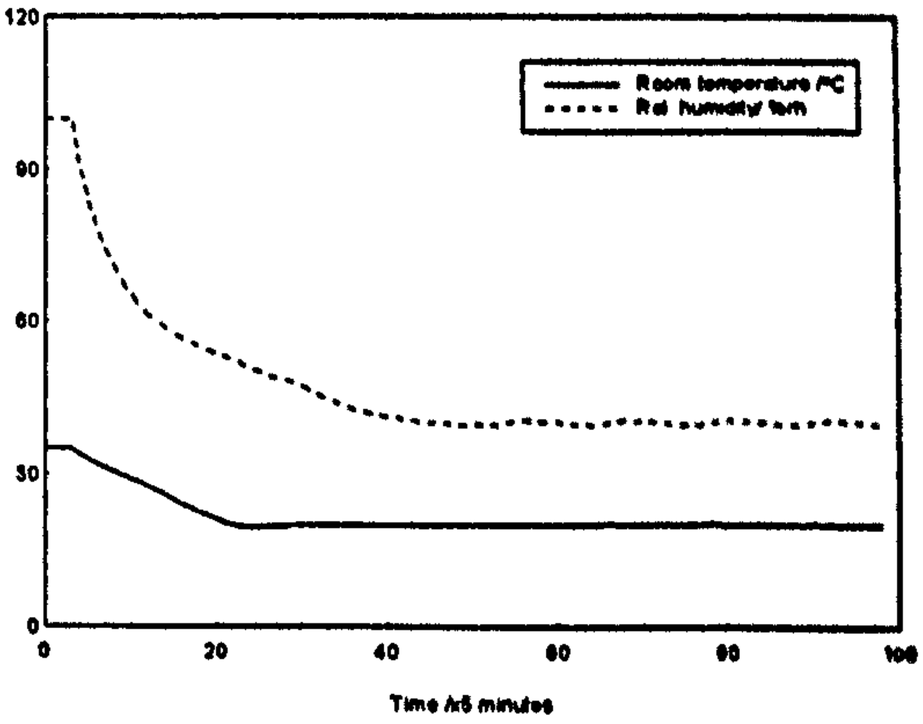

b) System outputs

Figure 7.21: GA controller with noise (Filter II): $\beta_1 = 0.5$, $\beta_2 = 0.5$, $\beta_3 = 0.7$

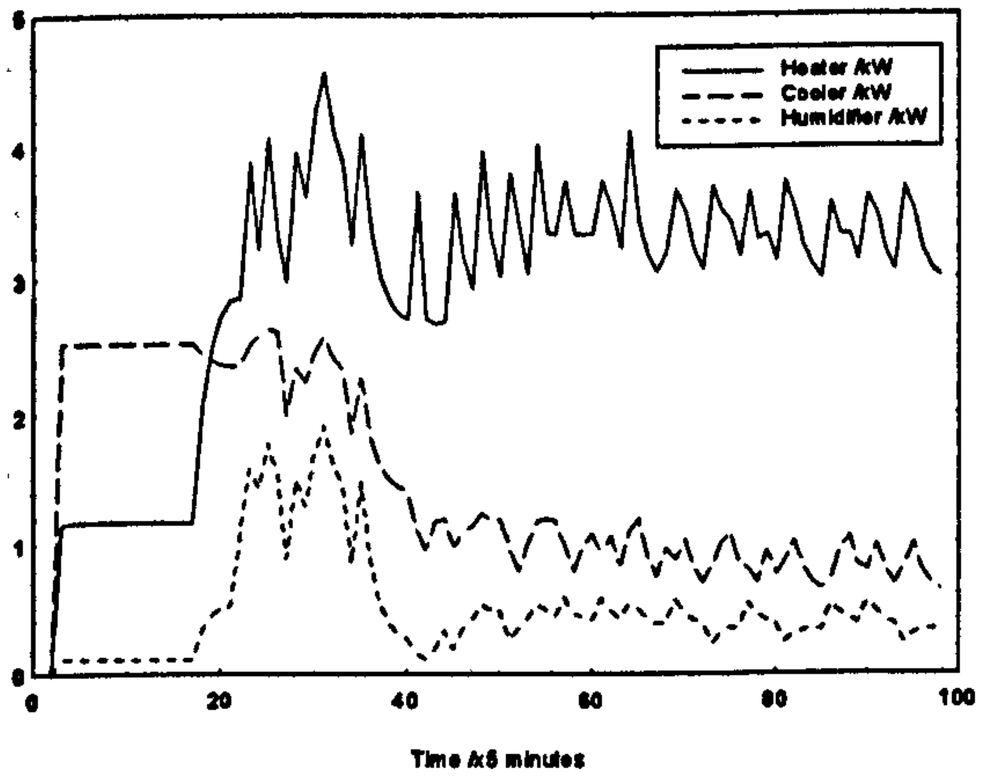

a) Control inputs

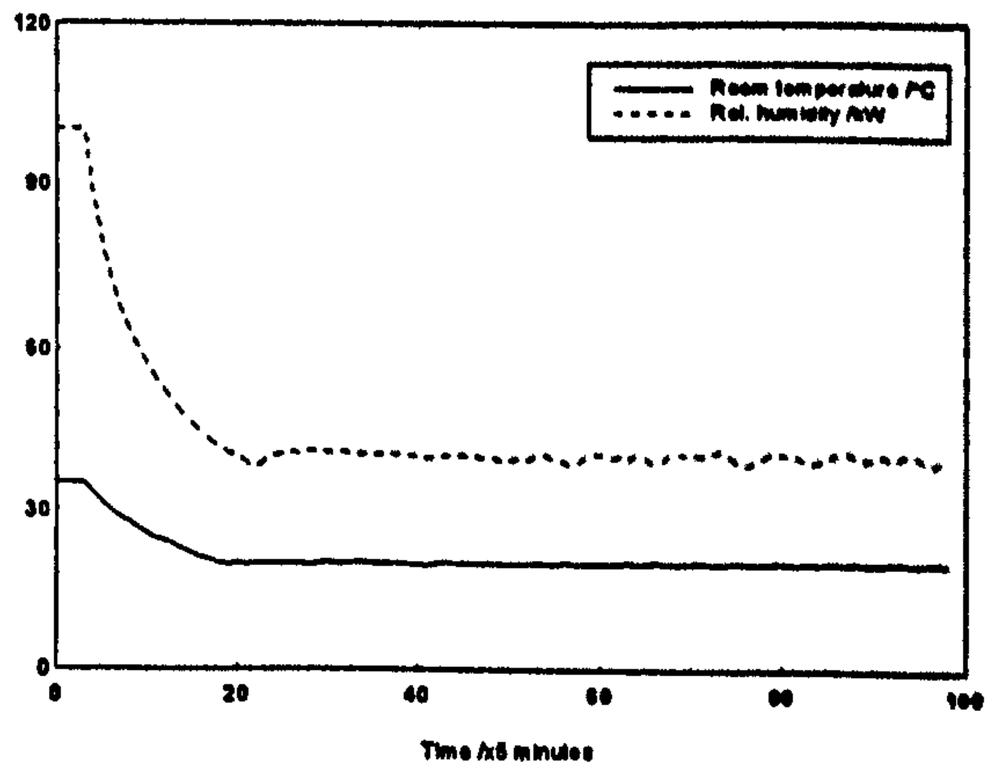

b) System outputs

Figure 7.22: GA controller with noise (Filter I): Increased switching allowed

($\beta_1 = 0.6$; $\beta_2 = 0.7$; $\beta_3 = 0.8$)

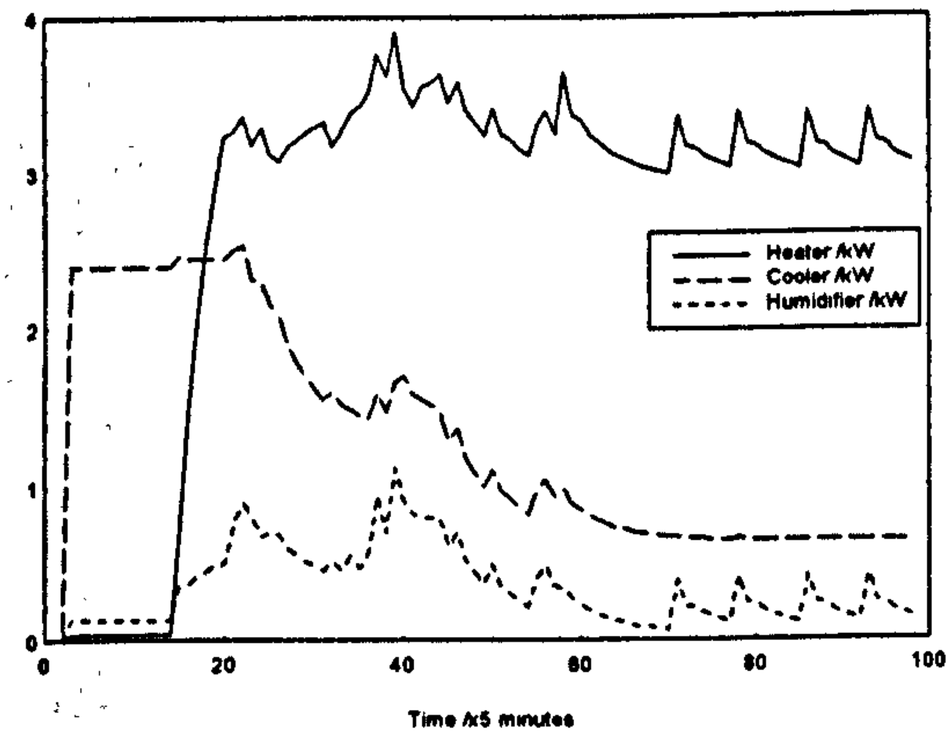

a) Control inputs

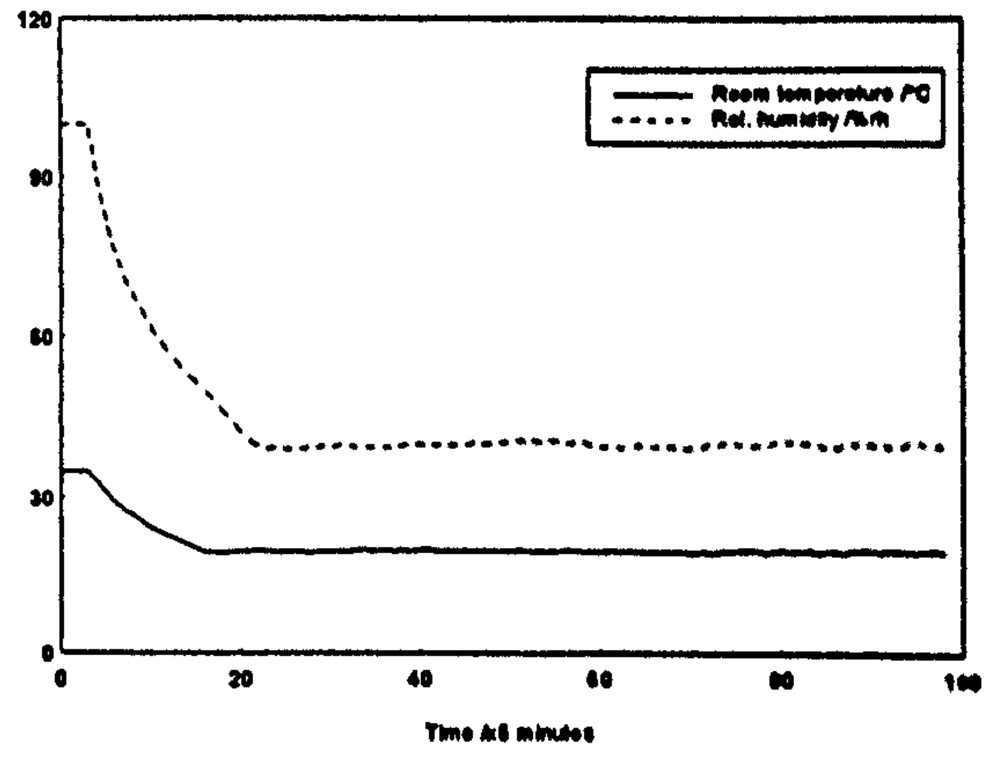

b) System outputs

Figure 7.23: GA controller with noise (Filter II): Increased switching allowed

$(\beta_1 = 0.6;\ \beta_2 = 0.7:\ \beta_3 = 0.8)$

7.7. Conclusions

In this chapter, the use of GA techniques to solve the problem of determining the three control inputs for the HVAC plant/office zone system are presented. The first solution presented uses a multi-proportional loop controller where the GA method is used to tune the six proportional gains. The second solution uses GAs to search the best combination of fuzzy membership functions so that the control performance of a FLC based on output errors is improved. The third GA-based solution minimises the predicted system output errors at the next time instant t+T. This adaptive type controller is further improved by employing a smoothing technique.

The GA proportional controller gives good results when regulating to the setpoints used in the tuning but the performance deteriorates as the setpoints are changed. This demonstrates a weakness in using the conventional controller such as a PID structure

where retuning is necessary. This difficulty can be overcome by using interpolation techniques to modify the controller gains as the setpoints are changed.

It is found that the performance of the fuzzy logic controller presented in Chapter 6 is improved when the membership functions are chosen using a genetic search procedure.

The adaptive GA controller gives good results even when the setpoints are changed. The excessive switching of the inputs is shown to be reduced by applying a smoothing technique using digital filters.

Chapter 8

Real-time Controls

The control systems described in the previous chapters are further investigated for their performances within in a real-time control situation, namely on the newly commissioned BEMS laboratory at the University of Bradford. The facility comprises a full-scale three roomed office set up with its own variable air volume (VAV) HVAC plant. The detailed specifications of the laboratory are presented in Appendix A, and the task here is to regulate the air temperature and relative humidity in Room 1 at their desired setpoints by controlling the main heater, W_m, cooler, C, and humidifier, H; the performances of the multi PI-loop controller, the constrained input and output adaptive controller, the fuzzy logic controller and the GA-based controllers are assessed here. For this purpose, a minor modification needs to be made to the respective simulation software presented earlier, namely that the computer needs to be interfaced to sensors and actuator drivers. The sampling interval T was chosen to be 5 minutes for all experiments to allow reasonable changes in the outputs due to a change in the three control inputs. During the experiments, all the three reheaters were switched off, the fresh air intake and the discharge dampers were fully open and the return damper was closed to allow significant climatic disturbances to the room via the fresh intake. Moreover, the VAV 1 damper,

D_1, was arbitrarily chosen to be 70% opened. The air pressure in the room was assumed to be constant due to the automatic control of the fresh air intake and discharge fans by the Caradon Trend equipment. Moreover, the laboratory activities in the three rooms were like those found in ordinary office buildings where occupants move around and go in and out from the room, and the light intensity varies due to occupancy. These disturbances are treated as stochastic effects to the system in the following discussions.

8.1. Multi PI-loop controller

For tuning the PI controller parameters, open loop step responses were carried out on the test room where the control inputs were increased from 50% to 75% of their maximum power to give the required parameters N and L for PI#1, PI#2, - PI#6; these parameters are given in Table 8.1 and the PI gains K_P and K_I are then calculated via the Zeigler-Nichols equations (3.1) and (3.2) for each controller. An experimental testing of the multi PI-loop controller was then carried out for a duration when steady state conditions were reached, say after 5 hours; this allows us to graphically estimate the average output swings and gives the modified PI gains K_{PM} and K_{IM} as discussed in Chapter 3. The results are summarised in Table 8.1.

A number of experiments to assess the controller's performance were carried out by using the modified PI gains K_{PM} and K_{IM}, and a sample trial is presented in Figure 8.1; this experiment began at 5 p.m. on 24th. February, 1996 and logging lasted for a period of 24 hours with setpoints of 22°C and 40%rh for the temperature and relative humidity respectively. We can see that an acceptable regulation has been achieved by this

controller and the performance over the last 100 sampling intervals is calculated to be as follows:

- the required control input energies are 27.0, 0 and 37.5 kWh for the heater, cooler and humidifier respectively; and
- the output squared errors are 247.3°C^2 and 400.8%rh^2 for the temperature and the relative humidity respectively.

Table 8.1: Ziegler-Nichols and modified PI gains via open loop step responses

Temperature loop									
PI #	N (°C/h)	L (h)	U_s (kW)	K_P (kW/°C)	K_I (kW/°C_h)	Ave. output swing (kW)	Reduct. factor	K_{PM} (kW/°C)	K_{IM} (kW/°C_h)
1	0.66	0.025	1.13	61.4	736.8	420	0.0107	0.657	7.88
3	-0.99	0.017	0.75	-40.1	-707.8	400	0.0075	-0.301	-5.31
5	0.21	0.033	1.13	146.1	1328.2	800	0.0056	0.818	7.44

Relative humidity loop									
PI #	N (%rh/h)	L (h)	U_s (kW)	K_P (kW/%rh)	K_I (kW/%rh_h)	Ave. output swing (kW)	Reduct. factor	K_{PM} (kW/%rh)	K_{IM} (kW/%rh_h)
2	-4.47	0.025	1.13	-9.1	-108.7	330	0.0136	-0.124	-1.48
4	-4.60	0.017	0.75	-8.6	-152.3	400	0.0075	-0.065	-1.14
6	13.0	0.033	1.13	2.4	21.5	70	0.0643	0.154	1.38

We can see that the humidifier was used at its maximum power to fight the heating energy; the result was that the energy was wasted and clearly this is not recommended from the user viewpoint. Moreover, the cooler was not used in this trial because the desired room temperature was higher than the outside temperature which was on average at approximately 6°C .

This result shows that the proposed multi PI-loop tuning methodology to modify the Ziegler-Nichols PI gains as described in Chapter 3 is practically applicable for the actual control of HVAC systems and may be useful for controlling other multivariable systems as well.

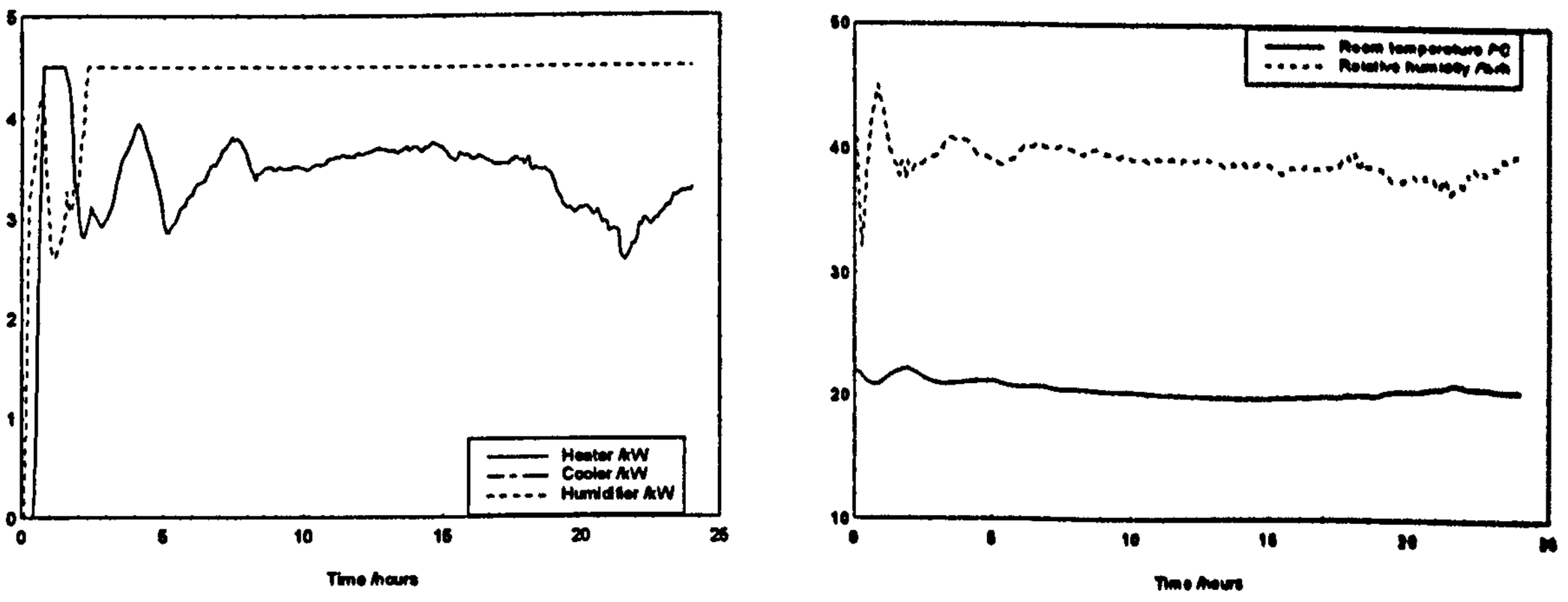

a) Control inputs

b) System outputs

Figure 8.1: Performance of the multi PI-loop controller with 6 PI units

We notice that the maximum slopes of the step responses, *N*, for this system are less than the values obtained for the Loughborough BEMS system (Table 3.1). This is due to the fact that although the heating, cooling and humidifying powers for both facilities are similar the total air volume of the three rooms (Appendix A) is much larger in

comparison to that in the test room at Loughborough and also the thermal structure of the two offices are quite different.

8.2. Constrained input MIMO adaptive controller

The constrained input MIMO adaptive controller described in sections 5.1 - 5.4 was next implemented for real-time control of the test room. In this implementation, it is assumed that the on-line process model with observability indices $n = 1$ and 2 are adequate to describe the conditions in the room.

The experimental results for $n = 1$ are shown in Figures 8.2 and 8.3 where we can see that this type of controller is capable of controlling the air temperature and relative humidity within the room. Figure 8.2 represents the result of a trial using the controller with a prediction horizon $N = 5$, and the maximum permissible change in the control inputs, $\boldsymbol{D}_u = \begin{bmatrix} 0.5 & 0.5 & 0.5 \end{bmatrix}^T$ kW. The trial began at 6 p.m. on 14th. October, 1995 and logging lasted for a period of 12 hours with the room temperature and relative humidity setpoints chosen at 22°C and 45%rh respectively. The control performance over the last 100 sampling intervals are found to be as follows:

- the required control input energies are 18.0, 15.6 and 28.1 kWh for the heater, cooler and humidifier respectively; and
- the output squared errors are $6.0°C^2$ and $134.8\%rh^2$ for the temperature and relative humidity respectively.

Figure 8.3 represents the result of an experiment using the controller with a prediction horizon $N = 2$, and the maximum permissible change in the control inputs $\boldsymbol{D}_u$

$= [1 \quad 2 \quad 1]^T$ kW. The experiment began at 6 p.m. on 4th. September, 1995 and a logging period of 15 hours was used with the room temperature and relative humidity setpoints chosen to be 22°C and 50%rh respectively. The control performance over the last 100 sampling intervals are found to be as follows:

- the required control input energies are 22.7, 3.8 and 22.6 kWh for the heater, cooler and humidifier respectively; and
- the output squared errors are 38.0 $°C^2$ and 177.7 $\%rh^2$ for the temperature and the relative humidity respectively.

The large output fluctuations are due to the larger changes allowed here with those used for Figure 8.2.

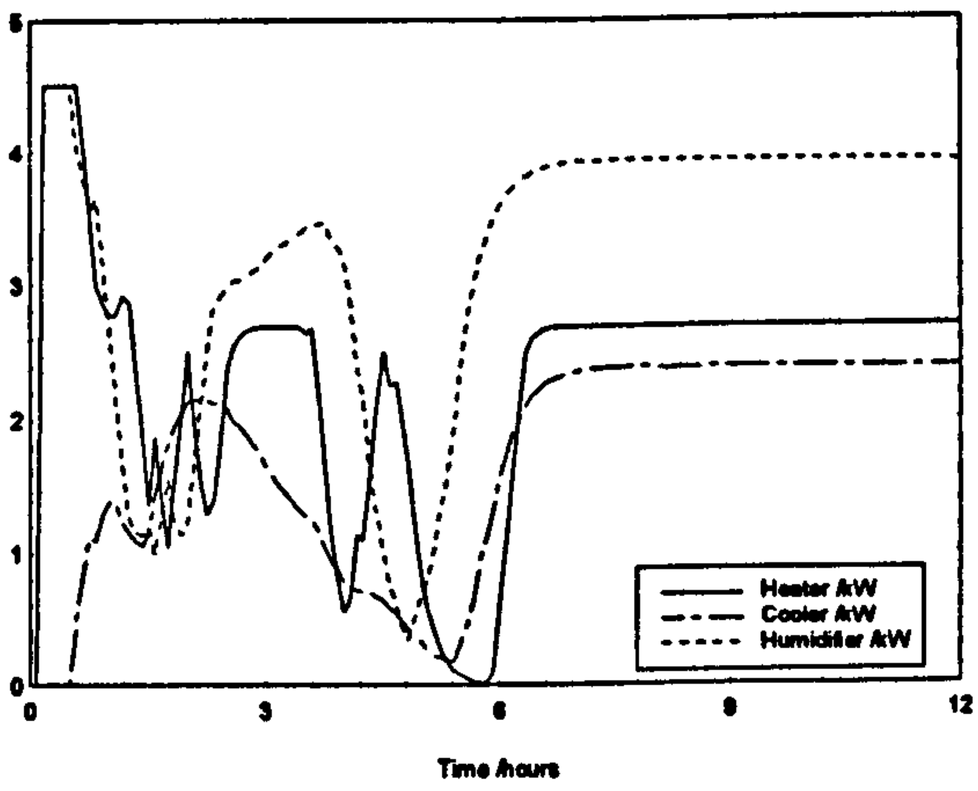

a) Control inputs

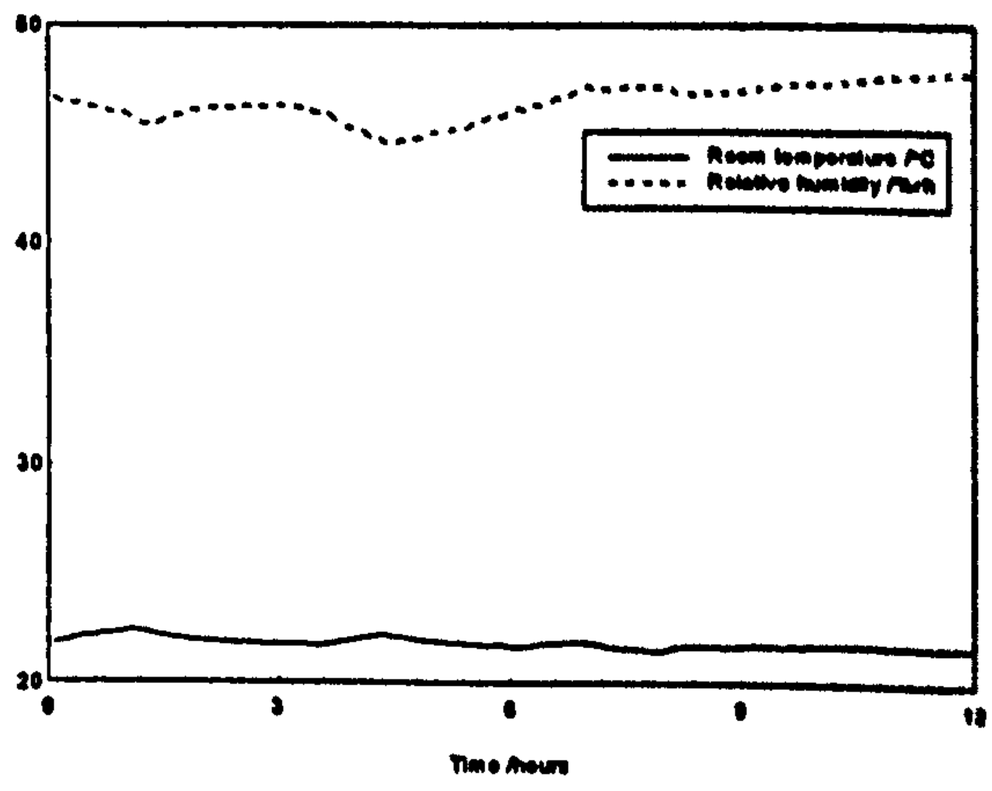

b) System outputs

Figure 8.2: Constrained input MIMO controller results ($n = 1$; $N = 5$; $\boldsymbol{D}_u = [0.5 \quad 0.5 \quad 0.5]^T$)

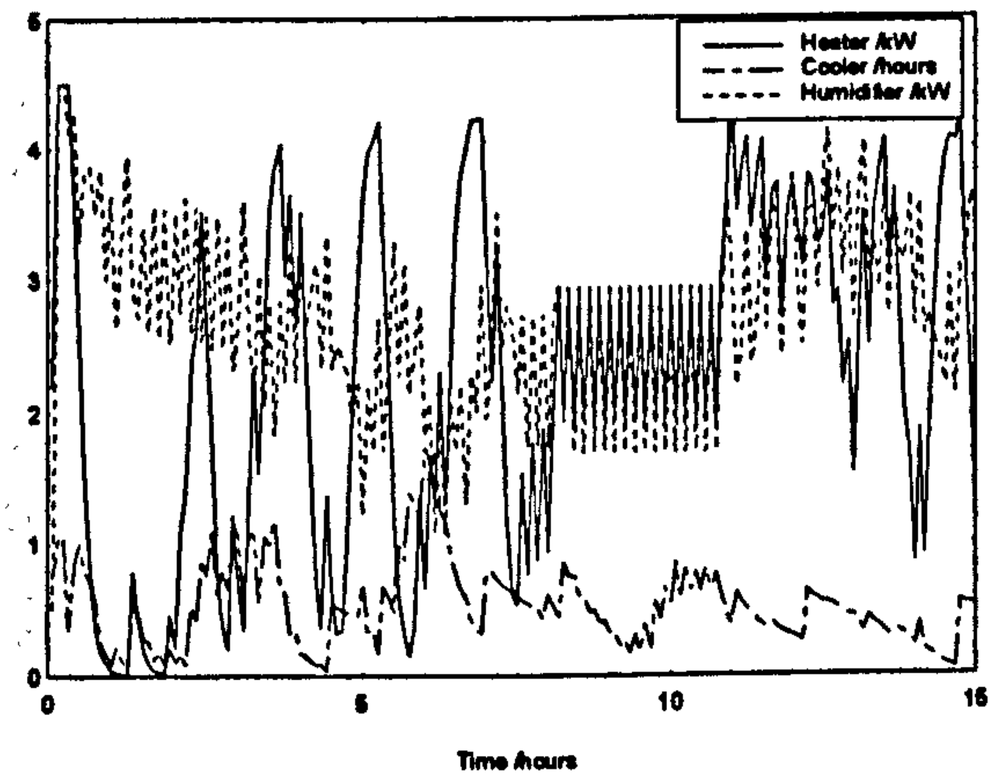

a) Control inputs

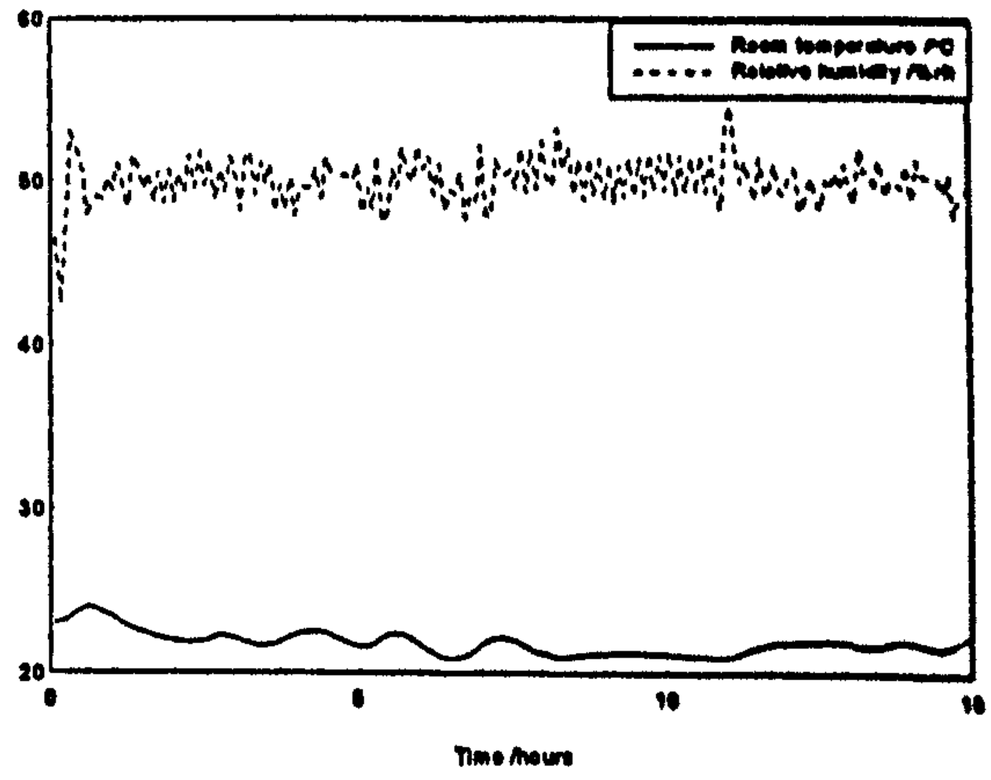

b) System outputs

Figure 8.3: Constrained input MIMO controller results ($n = 1; N = 2;\ D_u = \begin{bmatrix} 1 & 2 & 1 \end{bmatrix}^T$)

The experiments were also carried out for the on-line process model of observability index, $n = 2$ and a prediction horizon, $N = 2$. One of the experiment began at 5 p.m. on 23rd. February, 1996 and a logging period of 24 hours was used with the room temperature and relative humidity setpoints chosen to be 22°C and 40%rh respectivcly. The result is shown in Figure 8.4 where the control performance over the last 100 sampling intervals are found to be as follows:

- the required control input energies are 19.0, 1.5 and 29.7 kWh for the heater, cooler and humidifier respectively; and
- the output squared errors are 10.4 $°C^2$ and 50.2 $\%rh^2$ for the temperature and relative humidity respectively.

We can see in this experimental trial that during the transient period, the heater is switched on to its maximum power to increase the temperature and followed by the humidifier which increases the relative humidity that was initially at 16.1%rh. The controller took 3 hours to reach the relative humidity setpoint of 40%rh.

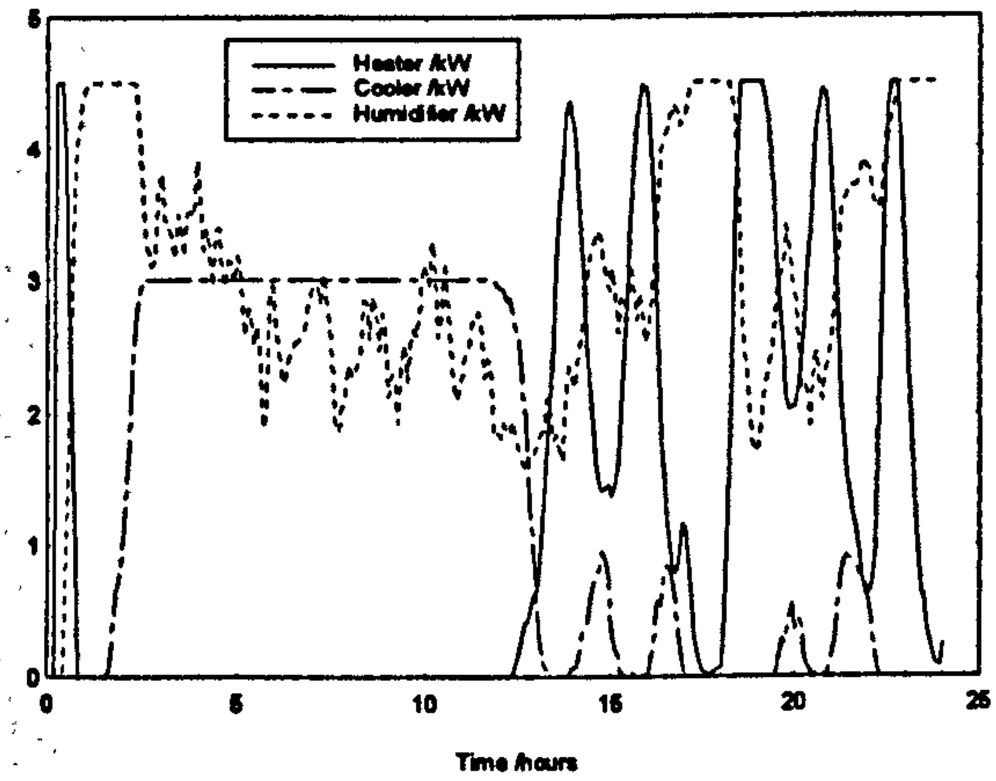

a) Control inputs

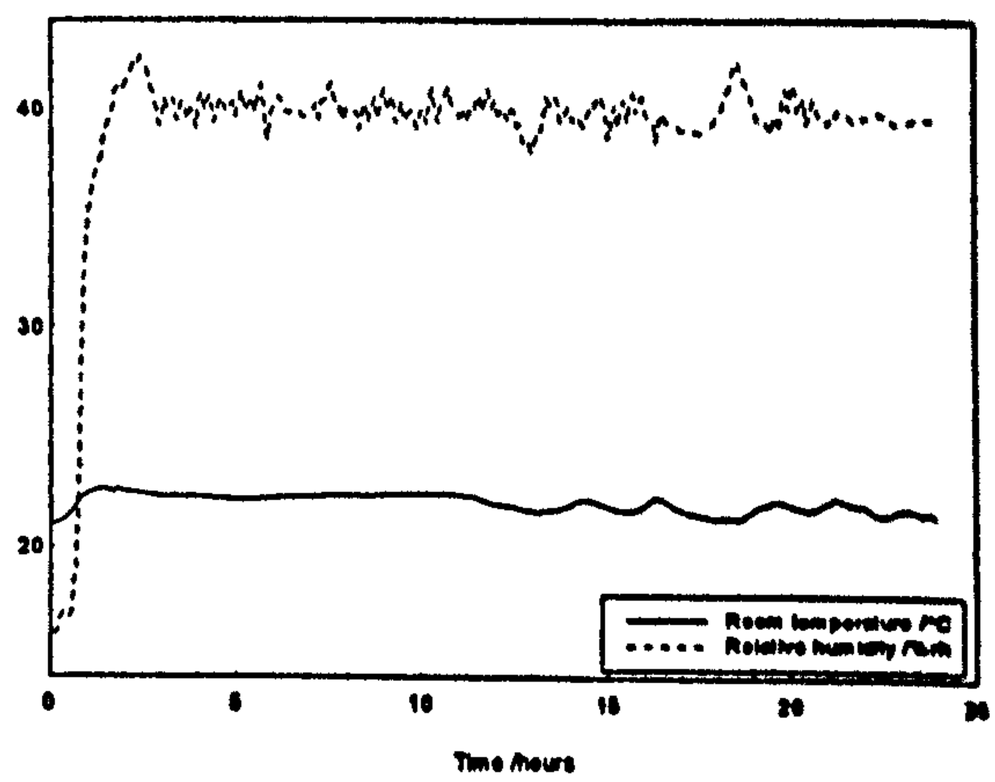

b) System outputs

Figure 8.4: Constrained input MIMO controller results ($n = 2$; $N = 2$; $D_u = [1 \quad 1 \quad 1]^T$)

8.3. Fuzzy logic controller

In the implementation of the fuzzy logic design for real-time control of the conditions within the room, we only require the knowledge of each control input's step response to estimate the outputs at the next time step. This knowledge is then applied to design the fuzzy evaluation rules for this system; the step test experiments were carried out for Room 1 and it was found that the responses were similar to those obtained using the Loughborough model equations (2.1) and (2.2) as presented in Chapter 2. Since the physical structure and air volume in Room 1 of the Bradford facility is quite different from the test room in Lougborough, it was felt necessary to construct new fuzzy input and output membership functions.

A number of experiments were carried out on the room by using the FLC design based on the proportional fuzzy logic controller where the fuzzy rules in Table 6.1, the fuzzy input and output membership functions in Tables 8.2 and 8.3 respectively are

applied into the Bradford system (details concerning the FL controller have already been discussed in length in Chapter 6).

Table 8.2: Scaling factor for the fuzzy input membership functions

Fuzzy input scaling factor	NL and PL			NS and PS			Z	
	l_1	l_2	l_3	s_1	s_2	s_3	z_1	z_2
Temperature,°C	50.0	1.0	0.5	1.0	0.5	0	0.5	0
Rel. Humidity, %rh	50.0	3.0	1.0	3.0	1.0	0	1.0	0

Table 8.3: Scaling factor for the fuzzy output membership functions

Fuzzy controller output (kW)	Negative (N)			Approx. Zero (Z)			Positive (P)		
	x_l	n_m	n_r	z_l	z_m	z_r	p_l	p_m	x_r
dW	-0.22	-0.16	0	-0.16	0	0.16	0	0.16	0.22
dC	-0.22	-0.16	0	-0.16	0	0.16	0	0.16	0.22
dH	-0.22	-0.11	0	-0.11	0	0.25	0	0.25	0. 40

One of the experiments began at 6 p.m. on 10th. October, 1995 and a logging period of 15 hours was used with setpoints chosen at 22°C and 45%rh for the room temperature and relative humidity respectively. The controlled results are shown in Figure 8.5 where the regulation performance over the last 100 sampling intervals are found to be as follows:

- the required control input energies are 35.8, 0 and 21.4 kWh for the heater, cooler and humidifier respectively; and

- the output squared errors are $2.0°C^2$ and $34.6\%rh^2$ for the temperature and relative humidity respectively.

The controller investigations were also carried out for the PI-based FLC using the design presented in Section 6.1.2 where the fuzzy membership functions from Tables 6.7, 8.2 and 8.3, and the combined fuzzy rules from Tables 6.1 and 6.2 were applied. A trial began at 6 p.m. on 15th. October, 1995 and logging lasted for a period of 23 hours with the setpoints chosen at 22°C and 45%rh for the room temperature and relative humidity respectively. The experimental results are shown in Figure 8.6 where the control performance over the last 100 sampling intervals are found to be as follows:

- the required control input energies are 33.0, 0 and 5.3 kWh for the heater, cooler and humidifier respectively; and
- the output squared errors are $3.0°C^2$ and $33.4\%rh^2$ for the temperature and relative humidity respectively.

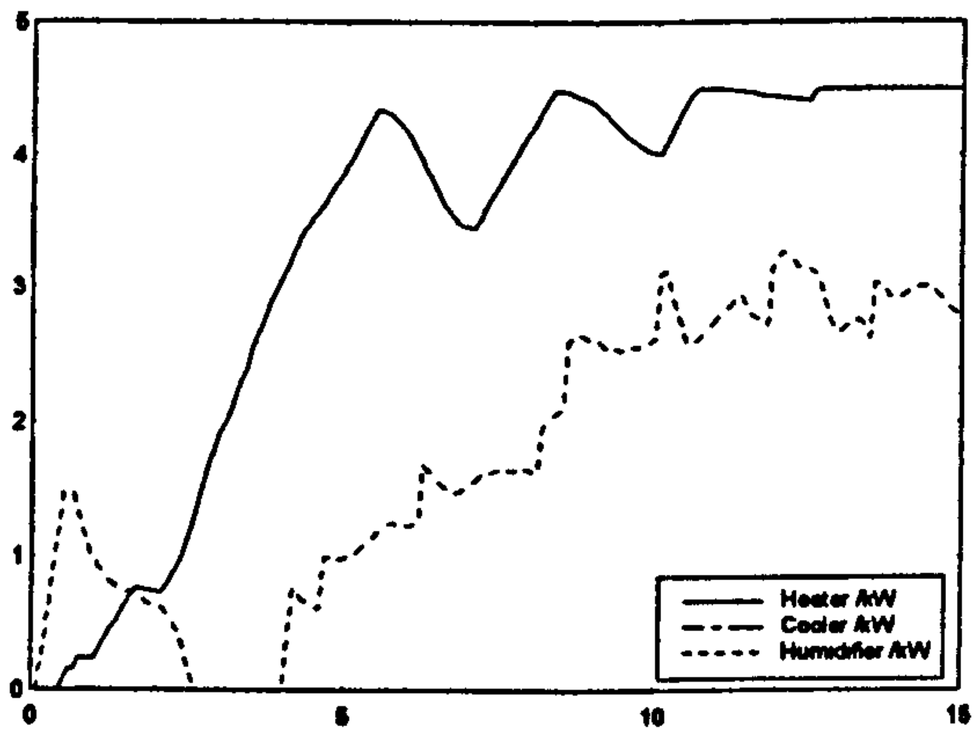

a) Control inputs

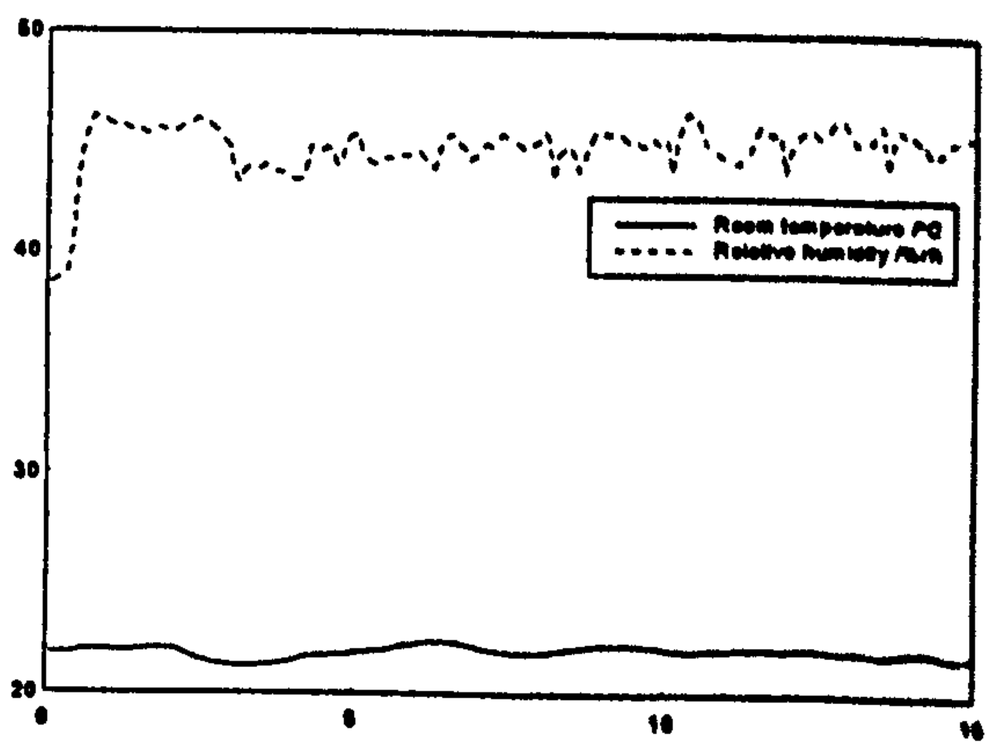

b) System outputs

Figure 8.5: Performance of the proportional fuzzy logic controller

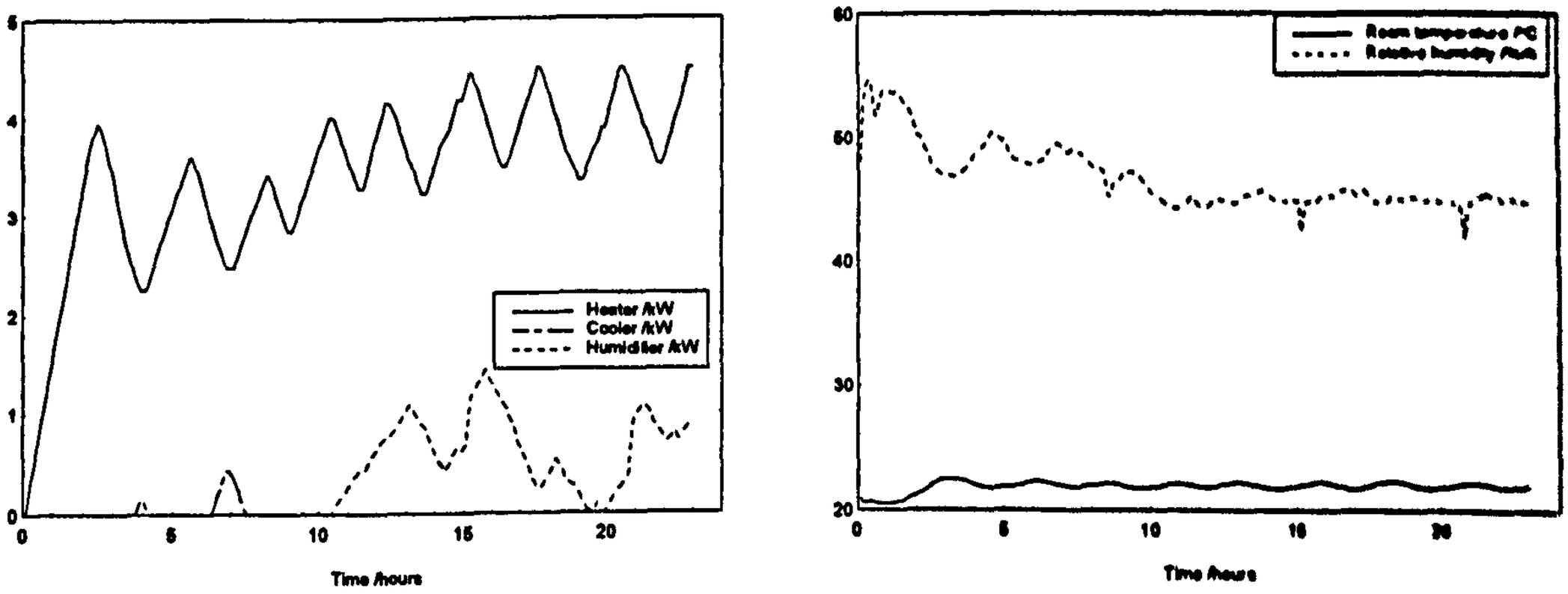

a) Control inputs b) System outputs

Figure 8.6: Performance of the PI-based FLC

8.4. Genetic algorithm

The adaptive GA controller presented in Section 7.4 can not be implemented here in an on-line because it requires an accurate mathematical model to predict the conditions within the test room. In other words, the GA is required to forecast the room temperature and relative humidity at the next time step t+T for all population of the three control inputs in order to select the best solution at the current time t via the fitness function. This forecasting can only be done via the model or through thermo-physical analysis of the input-output relationships within this multivariable system - this is not easy to formulate. Research to develop a suitable mathematical model to describe the conditions in this Bradford BEMS facility is currently being carried out but no suitable model exists at present.

Nevertheless, this problem is tackled here simply by using simple step response knowledge to predict the system outputs at the next time step t+T; this will work to a first approximation because these three control inputs are significantly dominant in

comparison to the other effects such as climatic and stochastic disturbances. When the control input step test experiments were carried out it was found that all the open-loop response had the form of a first order differential equation (as shown in Figure 3.1); it is well known that such a response can be represented by

$$\Delta Y(s) = \frac{e^{-Ls}}{1+s\mathrm{T}_1} k\,\Delta U(s) \qquad (8.1)$$

where $Y = T_c,\ H_c$; $U = W,\ C,\ H$; k is individual output/input coefficient and s is the Laplace operator. The time constants L and T_1 are as previously defined in Figure 3.1 and their magnitudes depend on individual input/output relations.

Equation (8.1) can be used as a crude model to predict the changes in the room temperature and relative humidity at the next time step, t+T due to incremental changes to the three control inputs at the current time t. Since this system has a relatively slow response (as shown in Table 8.1), we can assume that the output change is directly dependent on the change in the control input for a short period of time. Thus, equation (8.1) can be written in the time domain as $\Delta Y(t) \cong k\,\Delta U(t)$ for $0 \le t \le \mathrm{T}$. Therefore, the predicted output changes can be approximated by the summation of these input changes if the effects of the climatic and other stochastic disturbances are ignored by:

$$\Delta T_c^j(t+\mathrm{T}) \cong k_{wt}\ \ \Delta W^j(t) + k_{ct}\,\Delta C^j(t) + k_{ht}\,\Delta H^j(t) \qquad (8.2)$$

$$\Delta H_c^j(t+\mathrm{T}) \cong k_{wh}\ \ \Delta W^j(t) + k_{ch}\,\Delta C^j(t) + k_{hh}\,\Delta H^j(t) \qquad (8.3)$$

where

$$\Delta T_c^j(t+\mathrm{T}) = T_c^j(t+\mathrm{T}) - T_c(t), \qquad \Delta H_c^j(t+\mathrm{T}) = H_c^j(t+\mathrm{T}) - H_c(t), \qquad (8.4)$$

and

$$\Delta W^j(t) = W^j(t) - W(t-\mathrm{T}), \qquad \Delta C^j(t) = C^j(t) - C(t-\mathrm{T}),$$

$$\Delta H^j(t) = H^j(t) - H(t\text{-T}), \tag{8.5}$$

Here, j is the 'label number" of the chromosome in the GA, and $W^j(t)$, $C^j(t)$ and $H^j(t)$ are the physical values of jth chromosome at generation t. We can assume that the coefficients to control input changes $k = k_{wt}, \ldots, k_{hh}$ are constant for a period between one sampling instant and the next, t to t+T. For our applications, we propose to calculate these coefficients by using the results from the mid-range step responses (50% to 75% of the maximum power) as described in section 8.1; the values were found to be:

$k_{wt} = 0.126, \quad k_{ct} = -0.028, \quad k_{ht} = 0.015$ (°C/kW).

$k_{wh} = -0.60, \quad k_{ch} = -0.127, \quad k_{hh} = 0.956$ (%rh/kW).

The predicted room temperature $T_c^j(t+\text{T})$ and relative humidity $H_c^j(t+\text{T})$ are then calculated for all the chromosomes p_j via equation (8.4) and the fitness function evaluated using equation (7.3) with α equals 0.13 since this value is suitable for the simulation environment (Chapter 7). The best control input setting at generation t is then chosen and applied into the Bradford HVAC system.

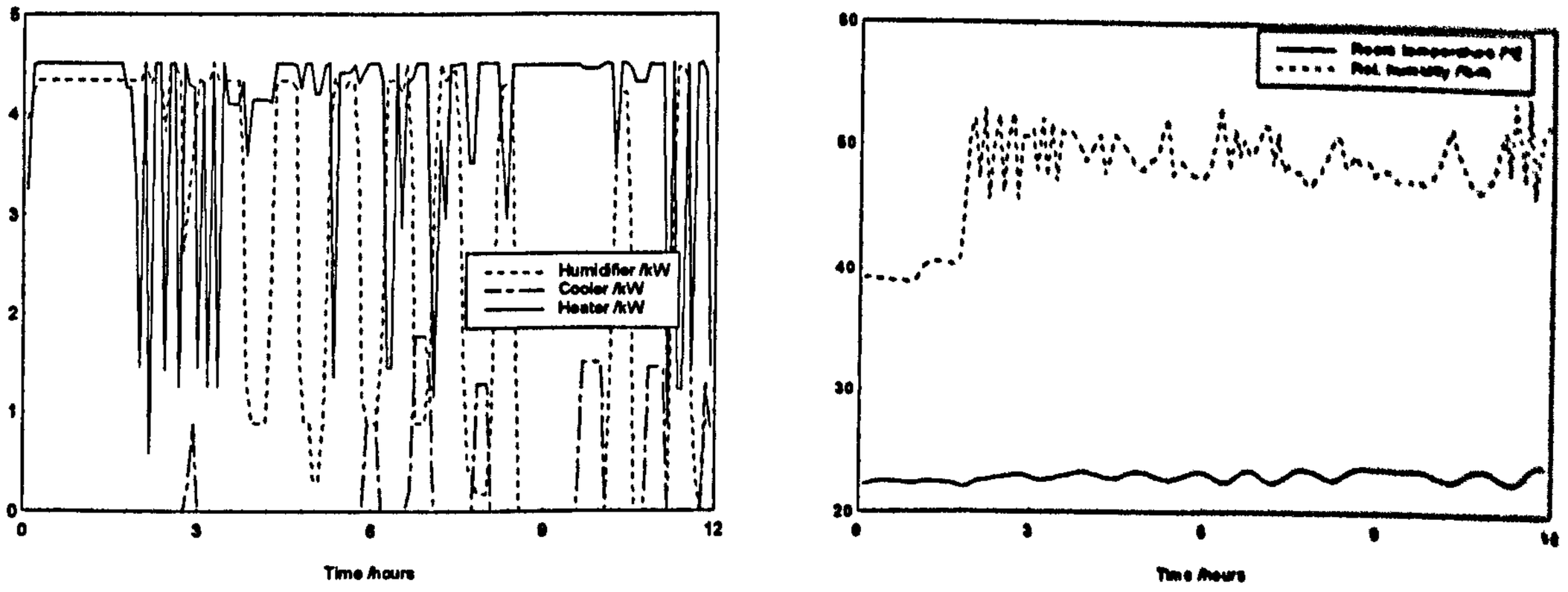

a) Control inputs

b) System outputs

Figure 8.7: Performance of the adaptive GA controller

By using this approximation, experimental trials were carried out and one sample run is shown in Figure 8.7 where we can see that the GA controller is capable of regulating the air temperature and relative humidity of the main room. The experiment began at 6 p.m. on 4th. September, 1995 and logging lasted for a period of 12 hours and the desired setpoints were chosen at 22°C and 50%rh for the temperature and humidity respectively. The control performance over the last 100 sampling intervals are found to be as follows:

- the required control input energies are 15.7, 2.4 and 33.6 kWh for the heater, cooler and humidifier respectively; and
- the output squared errors are 16.7°C^2 and 387.8%rh^2 for the temperature and relative humidity respectively.

8.5. Commercial controller

It is worthwhile to compare the advanced controllers designed here with a commercial controller which was installed for the Bradford BEMS Laboratory when it was commissioned. The control strategy of the commercial controller is divided into two parts; the first part is to regulate the AHU supply air temperature, T_s, and the return relative humidity, RH_r by controlling the main heater, W_m, cooler, C, humidifier, H, fresh air damper, D_f, return damper, D_r, and discharge damper, D_d; the second part is for the individual office rooms, that is, to maintain the air temperature and relative humidities at their setpoints by controlling the reheater and damper in the VAV Box for each room.

The aim of the control strategy is to regulate the room temperature and the humidity to within required comfort levels. The air pressure in this system is kept constant via the AHU supply fan, Fs, and the extract fan, Fe, which correspond to controlling the dampers D_f, D_r and D_d. The setpoints were chosen as 17°C and 40%rh for the AHU supply air temperature and return relative humidity, and 22°C and 45%rh for the air temperature and humidity respectively of the three rooms (such values are typical for offices). The experiment was carried out on 21st. November, 1995 and the result is shown in Figure 8.8. We can see that the room temperature is regulated at the desired value but the relative humidity does not reach its setpoint, this could be due to poor tuning of the PI controllers at the commissioning stage of the system. The control performance over the last 100 sampling intervals are found to be as follows:

- the required control input energies are 0, 0, 2.5 and 8.8 kWh for the main heater, cooler, humidifier and the reheater #1 (in VAV Box 1) respectively; and
- the output squared errors are 26.8°C^2 and 7567.3%rh^2 for the temperature and relative humidity respectively.

Note that the control system is designed in such a way that the amount of intake and discharge dampers (in %) are identical but the return damper is (100% - intake damper). For this experiment, the average intake and discharge dampers opening were found to be at 40% and the return damper at 60%, and the average damper opening in VAV Box 1 was 40%.

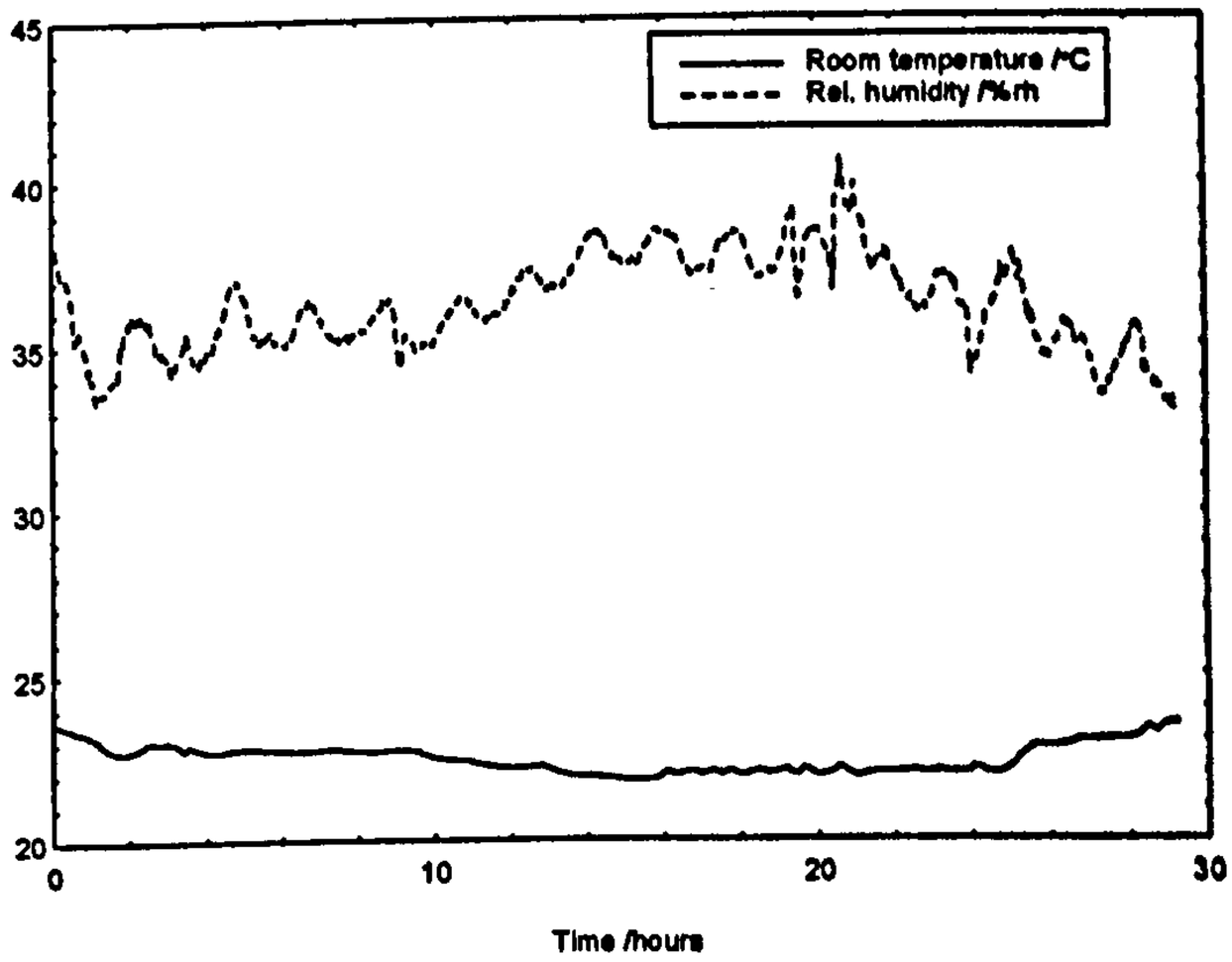

Figure 8.8: Control performance of the Concord PI controller

8.6. Discussion of Results

The experimental results of all the controllers as presented earlier need to be compared in order to choose the best one. The results such as the errors squared of the system's output and its energy consumption are summarised in Table 8.4 so that the control performances can easily be analysed.

We can see that the Proportional and PI-based fuzzy logic controllers give smallest output errors as compared to the other controllers. This is followed by the constrained input MIMO adaptive controllers and then the adaptive GA-based controller. The multi PI-loop controller is the worst amongst the designed controllers since it gives the greatest output errors and the temperature is mostly slightly below the setpoint but it is still better than the commercial PI controller in term of the relative humidity error.

Table 8.4: Controller's performance over the last 100 sampling intervals

No	Controller	Output error squared		Energy consumption (kWh)			Total energy (kWh)
		Temp, $°C^2$	RH, $\%rh^2$	Heater	Cooler	Humidifier	
1	Multi PI-loop	247.3	400.8	27.0	0	37.5	64.5
2	Adapt ($n = 1, N = 5$)	6.0	134.8	18.0	15.6	28.1	61.7
3	Adapt ($n = 1, N = 2$)	38.0	177.7	22.7	3.8	22.6	49.1
4	Adapt ($n = 2, N = 2$)	10.4	50.2	19.1	1.5	29.7	50.3
5	Proportional FLC	2.0	34.6	35.8	0	21.4	57.2
6	PI-based FLC	3.0	33.4	33.0	0	5.3	38.3
7	Adaptive GA	16.7	387.8	15.7	2.4	33.6	51.7
8	Commercial PI	26.8	7567.3	0	0	2.5	2.5

We can also see that for all the controllers, the control inputs such as the heater, cooler and humidifier are fighting between one another in order to regulate the temperature and relative humidity. For example in the proportional FLC, a more humidifying energy is needed in order to compensate for the effect of the heating energy so that the relative humidity can be maintained at the desired value and the cooler is not required here since the desired room temperature is higher than the outside temperature. This type of situation is a normal case in multivariable systems.

The energy consumptions between the various trials is not easy to compare here due to the different periods of the experiments which means that different magnitude of the uncontrolled parameters such as the climatic disturbances to the system are present. Moreover, the control strategy for the commercial PI controller is different for the other controllers presented here as dissussed in Section 8.5. Nevertheless, a fair energy

comparison can be estimated by looking at the energy requirement for the fresh air intake. For our case, we propose to calculate the energy spent to condition one litre per second (ls^{-1}) of fresh air intake order to achieve the required temperature and RH setpoints by monitoring the fresh air temperature, T_o, the AHU supply temperature, T_s, and the air flow rate into the test room via VAV 1 damper, D_1, in each experimental trial. It is well known that the effective energy rate in an air flow, E_f (in $^{kJ}/_{s}$) can be calculated from the relation (see for example Legg, 1991):

$$E_f = \Delta T_{so}\, a_f\, C_p\, K \qquad (8.6)$$

where in our system,

ΔT_{so} is the temperature difference of the fresh air from the AHU supply, i.e.

$\Delta T_{so} = T_s - T_o$ (in °C), and

a_f is the air flow rate into the test room via VAV 1 damper, D_1 (in $^{m^3}/_{s}$);

and $C_p = 1.048\ ^{kJ}/_{kg\ °C}$ and $K = 1.29\ ^{kg}/_{m^3}$ are constant.

For the Bradford BMS facility, the air flow rates, a_f, were measured to equal 62 ls^{-1} and 126 ls^{-1} for 40% and 70% of damper D_1 openings respectively.

For the commercial controller's experimental trial, we calculate the total energy supplied by the return air to the fresh air intake by applying equation (8.6) where a_f = 62 ls^{-1} (or 0.62 m^3s^{-1}) and the average temperatures of T_s and T_o were found to be 17.2°C and 8.0°C respectively; the effective energy rate, E_f, was calculated to equal 7.7 $^{kJ}/_{s}$ and for the last 100 sampling intervals (500 minutes), the total energy of the return air was found to be 64.2 kWh. Since the fresh air intake was at an average of 60% damper

energy consumed by the system is the summation of the main heater, cooler, humidifier, reheater #1 and the return air energies and this is equal to 49.8 kWh.

For the other designed controllers, the effective energy provided by the return air was assumed to be 0 kWh since the return damper was closed during experimental trials and the total energy consumed by the system is only the summation of the main heater, cooler and humidifier energies.

Now, we can calculate the energy spent to condition 1 ls^{-1} of fresh air simply by dividing the total energy consumption into the air flow rates, a_f, for each controller where a_f equals 62 $ls^{-1}$and 126 ls^{-1} for the commercial and other controllers respectively. In order to obtain a sensible comparison of energy consumption between these controllers, we shall normalise the energy spent to condition 1 ls^{-1} of the fresh air in term of the average temperature different between the fresh air and the AHU supply air, namely, ΔT_{so} and the results are summarised in Table 8.5.

From Tables 8.4 and 8.5, we can see that in term of energy consumption normalised in this way the constrained input MIMO adaptive controller with a process model of $n = 2$ and a prediction horizon, $N = 2$ is the best one because it gives the smallest magnitude of the normalised energy spent to condition 1 ls^{-1} of the fresh air over ΔT_{so} as compared to the other controllers and the worst is the commercial PI controller. These results also show the superiority of the advanced controllers designed here for this multivariable system over a commercial PI controller in the aspects of overall control performances.

Table 8.5: Normalised energy spent to condition 1 ls^{-1} of the fresh air over ΔT_{so}

Controller No. (from Table 8.4)	Total energy, kWh	Energy / fresh air, kWh/ $1s^{-1}$	T_o, °C	T_s, °C	ΔT_{so}, °C	Energy / fresh air + ΔT_{so}, kWh/ $1s^{-1}$/°C
1	64.5	0.51	6.0	21.9	15.9	0.032
2	61.7	0.49	11.2	21.8	10.6	0.046
3	49.1	0.39	12.1	21.9	9.8	0.040
4	50.3	0.40	5.6	22.0	16.4	0.024
5	57.2	0.45	11.9	22.1	10.2	0.044
6	38.3	0.30	12.1	21.9	9.8	0.031
7	51.7	0.41	12.2	22.2	10.0	0.041
8	49.8	0.80	8.0	17.2	9.2	0.087

8.7. Conclusions

This chapter has presented the control performances of several advanced controllers to regulate the conditions within the Bradford plant/office zone system; in particular the multi PI-loop controller, the constrained input MIMO adaptive control, the fuzzy logic controller and the genetic algorithm-based controllers which have been discussed in previous chapters have been experimentally verified. The results show that the multi PI-loop controller with 6 PI units, the fuzzy logic controller and the constrained input adaptive controller can achieve good regulation control performances. The adaptive GA-

based controller is also capable of regulating the system outputs at their desired setpoints, but it is felt that its performance could be improved if a more accurate mathematical model which can describe the conditions in the room is available.

Chapter 9

Conclusions and Future Work

The main objectives of the research presented in this thesis have been to investigate the design of advanced controllers which are suitable for building energy management systems (BEMS). These include the multi PI-loop controller, state feedback in the state-space, the constrained input MIMO adaptive controller, the fuzzy logic-based controller and the genetic algorithm optimisation technique. The control performances based on the system's output errors squared, the energy consumptions and the settling period have been investigated for different parameters and rules to assess their effect on the performances.

In this research, the BEMS under study is presented as a 3 input/2 output system subject to external disturbances and effects. The three inputs are the heater, cooler and humidifier, and the two outputs are the test room's air temperature and relative humidity. The external disturbances consist of climatic effects, incidental gains due to occupancy and other stochastic influences. The study is carried out within a simulation environment using the mathematical model which describes the conditions within the BMS test room facility at the University of Loughborough; some of the controllers developed are also tested in a real-time situation to control the experimental BEMS Laboratory at the

University of Bradford. The aim of the control strategy is to regulate the room temperature and humidity to stay as close to desired setpoints as possible.

The thesis begins with an introduction to the BMS research area which is discussed in Chapter 1 and this is followed in Chapter 2, by describing the research environment in which our studies are carried out; the research findings in the remaining chapters are presented here as the conclusions from our studies.

In Chapter 3, it has been shown that the control performance of a multi PI-loop controller based upon the traditional Zeigler-Nichols tuning rules is unable to adequately control this multivariable system. A new simple tuning methodology for this situation is developed by applying the knowledge of the control input step responses and reducing the magnitude of the Zeigler-Nichols suggested PI gains so that the output swing of each PI output falls into the constraints of the control inputs. It has been demonstrated that good control regulation is achieved when this tuning methodology is used. A methodology to reduce the total number of PI controllers required for regulation about specific setpoints is also presented in this chapter.

In Chapter 4, a standard format of state-space equation for describing the conditions within the test room is derived from it's discrete transfer function model. The closed-loop set up with state and output feedback strategies are then developed for this system and the pole-placement designs as well as modal-based controllers are used to obtain the feedback matrix and the final value theorem for calculating the feedforward matrix. It has been demonstrated that these methods are unable to give a good result due to the system having constraints on the control inputs and the desired pole locations cannot be chosen to lie at any arbitrary location.

In Chapter 5, a new multivariable adaptive control algorithm based on generalised predictive control techniques which explicitly take into account natural constraints on the input and output signals is presented. The process model with observatory indices n = 1 and 2 are chosen for this system. It has been demonstrated that the chosen process models together with the designed control law and the selected constraints are adequate for controlling the overall system. It has been found that the controller's performance can be improved by reducing the maximum permissible control input changes, D_u, and suitable combinations of the weighting factors, R, Q_1 and Q_2 in the quadratic criterion, $J(t)$, as well as the predictive horizon, N.

In Chapter 6, it has been demonstrated that good control regulation is achieved by using the fuzzy logic controller based on the proportional (P) controller. This result was obtained by well constructed five fuzzy input membership functions for each output error and three fuzzy output membership functions for each incremental control input as well as the rule evaluations between these fuzzy levels. A good control performance was also achieved by using the PI-based fuzzy logic controller.

In Chapter 7, it has been demonstrated that the new GA-based controller for HVAC plant/office zone systems has considerable potential and is capable of producing an excellent regulation to desired setpoints. We present three methods for solving the control problem in this multivariable system using the GA technique. The first method is to apply the structure of a multi proportional-loop controller where the GA is used to tune the proportional gains. The second method is to search the best combination of the fuzzy membership functions of the FLC presented in Chapter 6 and the third method is to use an adaptive type of controller where the objective is to minimise the predicted system output errors at the next time step t+T and the GA is used to obtain the best control

inputs at the current time *t*. It has been found that all these three GA-based methods have produced good control results. The third method has an advantage in the sense that it can adapt to the changing of the setpoints as well as to the external disturbances effecting the system without deteriorating the control performance. This approach is further improved by applying a smoothing operation by using a moving average digital filter to suppress the excessive control input fluctuation whenever these grow beyond maximum permissible limits at each sampling instant.

The advanced controllers presented in this thesis are further verified by testing them within a real-time control situation where experimental trials were carried out on the full-scale Bradford BEMS Laboratory. For this system, the HVAC plant/office zone system was configured to have an identical number of inputs and outputs as used in the simulation environment and the actual climatic disturbances and other influences present in the system. It has been demonstrated that the developed controllers, except the state-space-based ones, are capable of regulating the air temperature and relative humidity of the test room by simultaneously controlling the main heater, cooler and humidifier. Note that the state-space method was not experimentally tested on the Bradford BMS due to the lack of a suitable mathematical model for the Bradford BMS test facility.

9.1. Future work

An important aspect of this work is that the research was started with a known dynamical model of a test room and the main objective of the selected control systems was to minimise the closed-loop system output errors. With this model, we can study many other control objectives; for example to minimise the energy consumption as well

as the output errors by modifying the FLC rule evaluations as well as designing a suitable fitness function of the GA controller presented in Section 7.4.

There are many other advanced methods that are suitable for solving the control regulation problem within this multivariable system. Such methods are the improved fuzzy logic controller using genetic algorithm, see for example Genshe and Xinhai (1993); neural network (NN) and neuro-fuzzy controllers, see for example White and Sofge (1992). Fuzzy logic controllers for BEMS could also be based on commercial controller strategies. For example, the strategy of the one installed at the Bradford test facility as explained in Section 8.5 where the fuzzy logic methods decision can be used to obtain the fresh air intake and the three main control inputs as well as the damper's opening and the reheater for individual office rooms.

The method of obtaining the feedback matrix in a closed-loop system with constrained control inputs should be developed so that the outputs are critically tracking the setpoints. It has been found that this can be achieved by making some of the closed-loop poles ρ_i, $i = 1, 2, .., 6$ lie on the real-imaginary axis with $|\rho_i| \leq 1$ (Virk and Ghazali, 1994).

Another important research area needing attention is to design a fault diagnosis system for BEMS applications via a simulation environment since the air dynamics in rooms can be known from mathematical models. A possible way of implementing this could be to apply a set of input and output related data from a normally operating system as a reference and then training a neural network using faulty input/output data. This trained NN can accurately predict the system outputs under normal and failed conditions, and hence can be used to detect a variety of faults. This can be further extended to

designing a control reconfiguration system in the case of system failure so that the over system remains functional.

BIBLIOGRAPHIES

ASTROM, K. J., C. C. HANG, P. PERSSON, AND W. K. HO (1992). Towards Intelligent PID Control. *Automatica*, Vol. 28, No. 1, pp. 1-9.

ATHIENITIS, A. K. (1988). A predictive control algorithm for massive buildings. *ASHRAE Transactions*, Vol. 94, pt. 2, pp. 1050-1068.

BORRISON, U. (1979). Self-tuning regulators for a class of multivariable systems. *Automatica*, vol. 15, pp. 209-215.

CHEN, C. T. (1984). Linear System Theory and Design. Holt, Rinehart and Winston Series, pp. 372-373.

CLARKE, D. W. (1984). Self-tuning control of nonminimum-phase systems. *Automatica*, Vol. 20, No. 5, pp. 501-517.

CLARKE, D. W., C. MOHTADI AND P. S. TUFFS (1987). Generalized predictive control - part I: The basic algorithm; part II: extension and interpretation. *Automatica*, 23, pp. 137-160.

COLEY, D. A. AND J. M. PENKAN (1992). Second order system identification in the thermal response of real buildings. Paper II: Recursive formulation for on-line building energy management and control, *Building and Environment*, Vol. 27, No. 3, pp. 169-277.

CULP, C., J. HEBERL, L. NORTORD, P. BROTHERS AND J. D. HALL (1990). The impact of AI technology within the HVAC industry. *ASHRAE* 32.12, pp. 12-22.

CUTLER, C. R. AND B. L. RAMAKER (1980). Dynamic matrix control - a computer control algorithm. J.A.C.C.: Joint Automatic Control Conference, San Francisco, paper WP5-B.

DAVIS, L. (ed.) (1991). Handbook of genetic algorithms. Van Nostrand Reinhold.

DEXTER, A. L., G. GENG AND P. HAVES (1990). The application of self-tuning PID control to HVAC systems. *IEE Colloquium on Control in Building Energy Management Systems*, IEE Digest 1990 093 May, 1990.

DEXTER, A. L. AND D. W. TREWHELLA (1990). Building control systems: fuzzy rule-based approach to performance assessment. *Building Serv. Eng. Res. Technol.*, 11(4), 115-124.

DION, J. M., L. DUGARD, A. FRANCO, N. M. TRI AND D. REY (1991). 'MIMO adaptive constrained predictive control case study: An environmental test chamber. *Automatica*, Vol. 27, No. 4, pp.611-626.

ELLIOTT, H., W. A. WOLOVICH AND M. DAS (1984). Arbitrary adaptive pole placement for linear multivariable systems. *IEEE Trans. Automatic Control*, Vol. AC-29, No. 3.

ETTER, D. M., M. J. HICKS AND K. H. CHO (1992). Recursive adaptive filter design using an adaptive genetic algorithm. in *Proc. IEEE Int. Conf. Acoustics, Speech, and Signal Processing, 1992*, Vol. 2, pp. 635-638.

FIELDEN, C. J. AND T. I. EDE (1982). Computer based energy management in buildings. West Bvrleet: Pitman Abba Consultants Automation.

FLETCHER, R. (1981). Practical methods of optimization, Vol. 2: Constrained optimization. Wiley, Chichester.

FRIEDLAND, B. (1986). Control system design: An introduction to state space methods. McGraw Hill, Inc.

GENSHE, C AND C. XINHAI (1993). Improved fuzzy logic controller using genetic algorithm and its application to spacecraft rendezvous. *IEEE TENCON'93*, Beijing.

GHAZALI, A. B. (1994). Advanced Intelligent Control and Fault Diagnosis in Building Energy Management Systems (BEMS). PhD Proposal, Dept. of Electrical Engineering, Univ. of Bradford.

GODFREY, K. R. (1980). Correlation Methods. *Automatica*, Vol. 16, pp. 527-534, Pergamon Press Ltd.

GOLDBERG, D. E. (1989). Genetic algorithms in search, optimization and machine learning. Reading, M. A.: Addison-Wesley.

HAMBLIN, J. (1995). Why control your buildings? *Energy Efficiency Yearbook 1995, Energy Systems Trade Association (ESTA)*, Gloucestershire, UK. pp. 28-29.

HAVES, P. AND A. L. DEXTER (1991). Use of a building emulator to evaluate control strategies implemented in commercial BEMS. *Proc. Building Environmental Performance BEP '91, University of Kent, Canterbury*, pp. 31-41.

HE, S. Z, S. TAN, F. L. XU AND P. Z. WANG (1993). Fuzzy self-tuning of PID controllers. *Fuzzy Sets and Systems*, 56, pp. 37-46, North Holland.

HOLLAND, J. H. (1975). Adaptation in natural and artificial systems. Ann Arbor, MI: Univ. of Michigan Press.

ISERMANN, R., K. H. LACHMANN AND D. MATCO (1992). *Adaptive control systems*. Prentice Hall Ltd.

JACKSON, T. B. (1971). The theory and economics and optimum start programming of heating plant. *Inst. of Heating and Ventilating Engineers Journal*, 39, A24-38.

KAUTSKY, J., N. K. NICHOLS AND P. V. DOOREN (1985). Robust Pole Assignment in Linear State Feedback. *Int. J. Control*, Vol. 41, no. 5, pp. 1129-1155.

KOIVO, H. N. AND S. POHJOLAINEN (1985). Tuning of multivariable PI-controllers for unknown systems with input delay. Automatica, Vol. 21, No. 1, pp. 81-91.

KOO, D. (1977). Element of optimization: with application in economic and business. Heidelberg Science Library.

KUO, B. C. (1992). Digital Control systems, 2nd ed. Saunder College Publishing, pp. 556-563.

KUCERA, V. (1979). Discrete Linear Control; the Polynomial Equation Approach. John Wiley & Sons.

LEGG, R. C. (1991). Air Conditioning Systems. BT Batsford.

LEIGH, J. R. (1985). Applied Digital Control: Theory, Design and Implementation. Prentice/Hall International.

LETHERMAN, K. M. (1981). Automatic Controls for Heating and Air-Conditioning. Pergamon Press, Oxford.

LING, K. V. AND A. L. DEXTER (1994). Expert control of air-conditioning plant. *Automatica*, Vol. 30, No. 5, pp. 761-773.

LJUNG, L. (1987). System Identification: Theory for the User. Prentice Hall, Englewood Cliffs, New Jersey.

LOVEDAY, D. L., J. Y. M. CHEUNG AND G. S. VIRK (1990). Building Energy Management Using Advanced Mathematical Models. Proc. 'Facilities Management International", Building Performance Volume, 'Building as Energy Systems", paper 2.33, Glasgow.

LOVEDAY, D. L. AND G. S. VIRK (1992a). Artificial Intelligence for Buildings. *Journal of App. Energy*, Vol. 41, No. 3, pp. 201-221.

LOVEDAY, D. L. AND G. S. VIRK (1992b). Final Report to the Science and Engineering Research Council, Research Contract GR/F/02014: The Effectiveness of Predictive Control Applied to Warm Air Heating Systems For Commercial Building. August 1989 - August 1992.

MACLAY, D. AND R. DOREY (1993). Applying genetic search techniques to drive train modeling. IEEE Control System, pp. 50-55.

MATLAB User Guide (1994). The MathWorks Inc., 24 Prime Park Way, Natick, MA.

MCHALE, A. (1995). Major changes ahead in the controls industry. *Energy Efficiency Yearbook 1995, Energy Systems Trade Association (ESTA)*, Gloucestershire, UK. p. 4.

MCGREGOR, D. R., M. O. ODETAYO AND D. DASGUPTA (1992). Adaptive control of a dynamic system using genetic-based methods. *in Proc. IEEE Int. Symp. Intelligent Control 1992*, pp. 521-525.

MIKLES, J. (1990). A multivariable self-tuning controller based on pole-placement design. *Automatica*, Vol. 26, No. 2, pp. 293-302.

MIKLES, J. AND A. MESZOROS (1991). A decoupling pole-placement controller for a class of multivariable systems. *Problem of control and Information Theory*, Vol. 20(4), pp. 291-298.

MOHTADI, C., S. L. SHAH AND D. W. CLARKE (1986). Generalized predictive control of multivariable systems. Report no. OUEL 1640/86, Dept. Eng. Science, Univ. of Oxford, U. K.

MURDOCH, N., J. M. PENMAN AND G. I. LIVERMORE (1990). Emperical and theoretical optimum start algorithms. Building Serv. Eng. Res. Technol, 11(3), 97-103.

NISHIKAWA, Y., N. SANNOMIYA, T. OHTA AND H. TANAKA (1984). A Method for Auto-tuning of PID Control Parameters. *Automatica*, Vol. 20, No. 3, pp.321-332.

NORTON, J. P. (1986). An Introduction to Identification. Academic Press, London.

OGATA, K. (1987). Discrete-Time Control Systems. Prentice/Hall International, p. 668.

OHKAWA, F. AND Y. YONEZAWA (1982). A discrete model reference adaptive control system for a plant with input amplitude constraints. *Int. J. Control.* **36**, 747-753.

ORTEGA, R., M. M'SAAD AND C. CANUDAS (1984). Practical requirements and theoritical results in robust adaptive control. Preprints *IFAC 9th World Congr.*, Budapest, Vol. VII, 189-195.

PATERKA, V. (1975). A square root filter for real-time multivariable regression. *Kybernetica*, **11**, 55-67.

PAYNE, A. N. (1986). Adaptive one-step-ahead control subject to an input amplitude constraints. *Int. J. Control.* **43**, 1257.

PENKAN, J. M. (1990). Second order system identification in the thermal response of a working school. *Building and Environment*, Vol. 25, pp. 105-110.

PENMAN, I. M. (1990). Real time thermal modelling and the control of buildings. *Proc. Congress International de Domonique*, Rennes, 27-29 June.

PENTTINEN, J. AND H. N. KOIVO (1980). Multivariable tuning regulators for unknown systems. *Automatica*, Vol. 16, pp. 393-398.

PIKE AND PENNYCOOK (1992). Commissioning of BEMs - A Code of Practice; Application Handbook AH 2/92. *Building Services Research and Information Association*, Brockwell.

PORTER, B. AND R. CROSSLEY (1972). Modal Control, Theory and Applications. Taylor and Francis Ltd.

ROUSE, K. (1990). Future trends in building energy management. Energy World, 176(3), 11-13.

SHAW, M. R. (1987). Applying Expert Systems to Environmental Management and Control Problems. *Building Research Establishment, U. K.*, pp. 113-125.

SONNOMIYA, N. AND H. IIMA (1992). Genetic algorithm approach to a production ordering problem in an assembly process with buffers. *IFAC Information control problems in Manufacturing Technology*, Toranto, Canada.

VIRK, G. S., J. Y. M. CHEUNG AND D. L. LOVEDAY (1990). The Role of Control Technology for Energy Savings in Buildings. *IEE Colloquium "SCADA and Energy Management Systems"*, Digest No. 1990/173, pp. 3/1 - 3/7.

VIRK, G. S., J. Y. M. CHEUNG AND D. L. LOVEDAY (1992). Advanced controllers for the built environment. *Proc. Canadian Conf. on Industrial Automation*, Vol. 2, pp. 34.17-34.21, Montreal, June.

VIRK, G. S. AND A. B. GHAZALI (1994). State Space Methods in Building Systems Control. Research Report No. 529, Department of Electronic and Electrical Engineering, University of Bradford, U. K, January.

VIRK, G. S., D. L. LOVEDAY AND J. Y. M. CHEUNG (1995). Practical stochastic multivariable identification for buildings. *J. Applied Mathematical Modelling*, Vol. 19, October.

WADDICOR, I. (1993). A genetic algorithm for PID controller tuning. M.Sc dessertation, Dept. of Control Engineering, Univ. of Bradford.

WELLSTEAD, P. E. AND M. B. ZARROP (1991). Self-tuning Systems: Control and Signal Processing. John Wiley & Sons, Chichester. pp. 80-81, 150.

WHITE, D. A. AND D. A. SOFGE (Ed.) (1992). Handbook of Intelligent Control: Neural, Fuzzy and Adaptive Approaches. Van Nostrand Reinhold, N. Y.

YING, H., W. SILER AND J. J. BUCKLEY (1990). Fuzzy control theory: a nonlinear case. *Automatica*. Vol. 26, No. 3, pp. 513-520.

ZADEH, L. A. (1965). Fuzzy Sets. *Inf. Control*. 8, 338.

ZADEH, L. A. (1975). The concept of a linguistic variable and its applications to approximate reasoning. *Information Sciences*, Vol. 8, pp. 199-249.

ZAHEER-UDDIN, M. (1990). Combined energy balance and recursive least squares method for identification of system parameters. *ASHRAE Transactions*, Vol. 96, pt. 2, pp. 239-244.

ZIEGLER, J. G. AND N. B. NICHOLS (1942). Optimum settings for automatic controllers. *ASME Trans.*, 64, 759-768.

Appendix A: BMS Research Laboratory (Room D1.02, University of Bradford)

The laboratory comprises three office rooms with its own dedicated HVAC plant. The rooms consist of Room 1 having dimensions of 7.42 metres in length, 2.92 metres in width and 2.80 metres in height, Room 2 having dimensions of 4.12 metres in length, 2.92 metres in width and 3.12 metres in height and Room 3 having dimensions of 3.14 metres in length, 2.92 metres in width and 3.12 metres in height. The plant, of VAV (Variable Air Volume) type, comprise a main heater having 4.5kW rating, a cooler/dehumidifier of 3kW rating and a humidifier of 4.5kW (6kg steam/hr) rating and they are driven by a control module where the input signals are given in percentage of maximum power rating. In addition, Each room is serviced by a VAV box which consists of an air damper and a reheater. Reheaters of 3kW capacity are installed for Room 1 and Room 2, and Room 3 has a reheater of 2kW capacity. The air handling unit (AHU) is located in the false ceiling of the main room and data monitoring and control functions are performed using Caradon Trend BMS equipment.

The control of each of the VAV boxes and the AHU is carried out by a separate IQ module and the strategy implemented at commissioning consists of using the AHU to regulate the temperature of the air supplied to VAV boxes and the moisture content of the return air from all three rooms. Each VAV box controller will use the reheater and the damper to increase or reduce, respectively, the room temperature as required. The block diagram of the BEMS Research laboratory is shown in Figure A1 and the symbols in the diagram are explained below.

System inputs

W_i control input to heating device (i = m, 1, 2, 3 = main heater, reheaters 1, 2, 3).

H control input to humidifier.

C control input to cooler/dehumidifier.

D_i control input to damper (i = 1, 2, 3, f, r, d = VAV1, VAV2, VAV3, fresh air, return, discharge).

F_s control input to supply fan.

F_e control input to extract fan.

System outputs

T_i space temperature (i = 1, 2, 3, o, p, r, s, si = Rooms 1, 2, 3, outside, re-heat, return, AHU supply, supply to VAV i).

RH_i space relative humidity (i = 1, 2, 3, o, r, s = Rooms 1, 2, 3, outside, return, AHU supply).

L_i light level (i = outside, inside).

S_i sensor (i = p, vi = duct pressure, velocity VAV i).

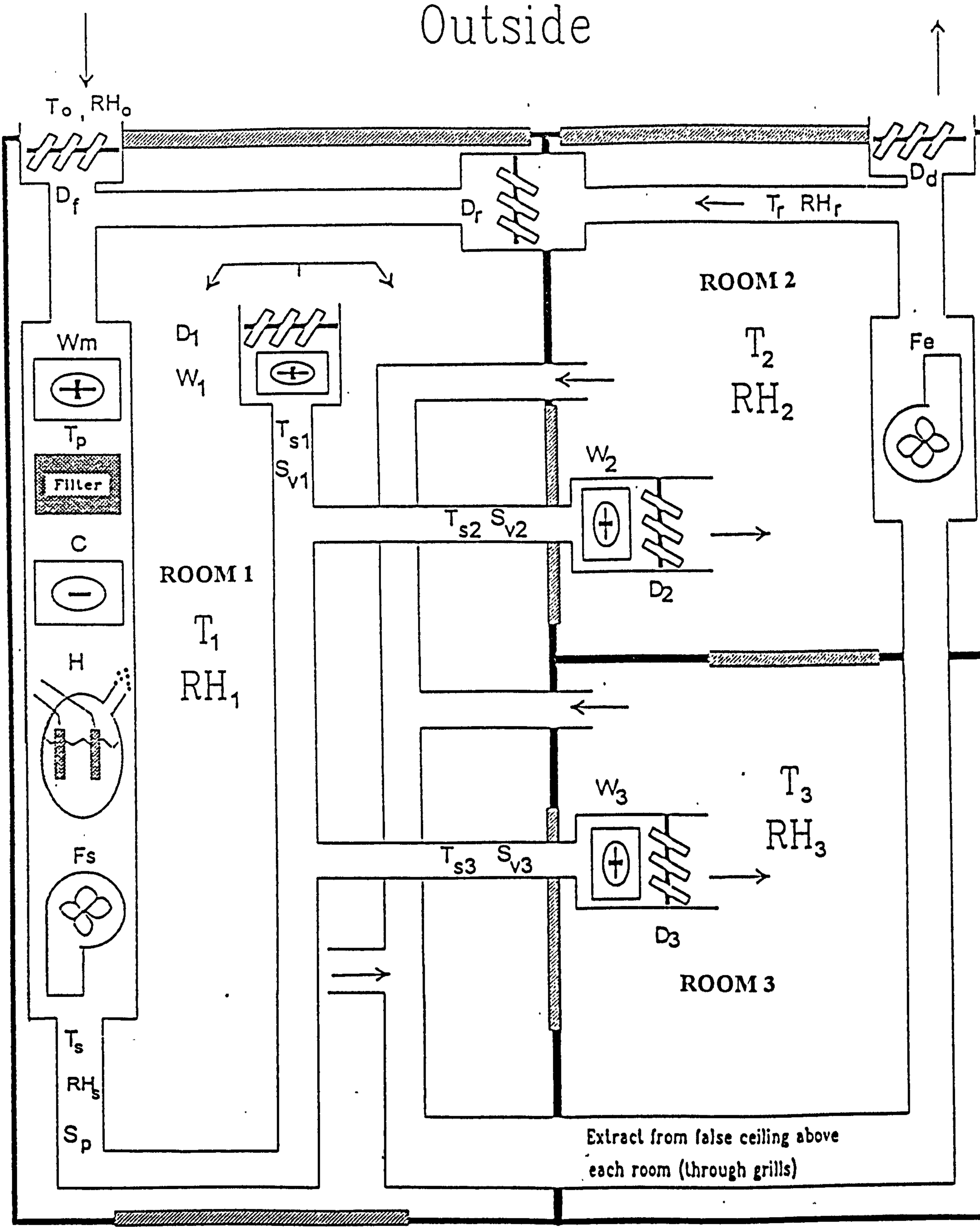

Figure A1: Block diagram of Bradford BMS research facility